Dimethylsulphoniopropionate (DMSP) metabolism within the coral holobiont

by

Felicity W.I. Kuek

June 2021

A thesis submitted in partial fulfilment of the requirements for the degree of

Doctor of Philosophy

(Natural and Physical Sciences)

ARC Centre of Excellence for Coral Reef Studies,

College of Public Health, Medical and Veterinary Sciences,

James Cook University

and

AIMS@JCU, Australian Institute of Marine Science,

Townsville, Queensland, Australia

Dedicated to my grandmother, Margaret Ngansa.

Dum spiro spero.

Declaration

I hereby declare that this research entitled “Dimethylsulphoniopropionate (DMSP) metabolism within the coral holobiont” is original and contains no material which has been accepted for the award to the candidate of any other degree or diploma, except where due reference is made in the text of the examinable outcome; to the best of my knowledge contains no material previously published or written by another person except where due reference is made in the text of the examinable outcome; and where work is based on joint research or publications, discloses the relative contributions of the respective workers or authors. Every reasonable effort has been made to gain permission and acknowledge the owners of copyright material. I would be pleased to hear from any copyright owner who has been omitted or incorrectly acknowledged.

Felicity W.I. Kuek

Acknowledgements

I would like to acknowledge the Australian Aboriginal and Torres Strait Islander peoples as the first inhabitants of the nation, and acknowledge the Bindal and Wulgurukaba peoples as Traditional Owners of the land and waters on where much of the research for this thesis was conducted. I pay respect to Elders past, present, and future, and value the traditions, cultures, and aspirations of the First Australians of this land.

This entire thesis would not have been possible without **Assoc. Prof. David Bourne** who kindly replied to my first email and subsequently assisted in assembling the 'dream team' supervisory panel **Prof. David Miller**, **Dr. Cherie Motti**, and **Dr. Jean-Baptiste Raina**. I am profoundly grateful that everyone gamely took a chance on me, a wild card from a non-pedigree background, and with much patience and support have guided me to be the scientist I am today. In particular, I do not think I would have completed this thesis without David B's encouragement to keep going when everything seemed to be falling apart. I appreciate David M's guidance with all things molecular, and for his support and generosity with funds needed for the work in this thesis. Cherie's morning tea sessions were always the highlight of the day at AIMS – I will forever appreciate your help in overcoming my fear of all things chemistry and always treasure your insightful advice for the future. Much of this work is also attributed to JB's rock star mentoring, always available and willing to discuss anything I was unsure of, even while away travelling.

It would be remiss of me if I do not mention **Libby Evans-Illidge** who has gone above and beyond in ensuring that I had adequate financial and moral support. Thank you so much for the kindness you have shown me especially in the second half of my candidature. It has been an honour and privilege to be an AIMS@JCU student, and most of this work would not exist without this strategic partnership.

Thank you, **Dr. Ira Cooke**, for stepping in with the nifty MinION and rescuing part of this thesis. While it may seem like a small thing, without the combined (and generous!) expertise of Ira and **Jia Zhang**, this thesis may not be finished.

Although it was a short stint, I am grateful to **Assoc. Prof. Peta Clode** who 'adopted' me while I was at Perth, making sure that I had everything I needed and was comfortable at UWA, and for connecting me with **Dr. Thomas Becker** who has been immensely helpful with the Raman. Thank you for sticking with me throughout the (admittedly) slow process.

This journey would also not be possible without the guidance and assistance by **Dr. Aurelie Moya** and **Dr. Alanna Sorenson** at the JCU labs, and **Dr. Sara Bell**, **Dr. Brett Baillie**, **Dr. Lone Høj**, **Lesa Peplow**, and **Peter Thomas-Hall** at the AIMS labs. Without their approachable and friendly presence, I would have been very lost in the labs. Not forgetting **the Negri lab** and **staff at SeaSIM** who helped me out every year with coral spawning. And also, **Merle Schlawinsky** and **Geoffrey Yau**, who provided additional hands during coral settlements, chemical syntheses, and NMR measurements.

A quick shoutout also to friends and colleagues in Townsville who, at different points through the years, have welcomed me and made my time here memorable: **Olivia Lee**, **Kessia Virah-Sawmy**, **Ashleigh Smith**, **John Nguyen**, **Leela Chakravarti**, **Michael Jarrold, Bettina Glasl**, **Katarina Damjanovic**, **Danielle Asson-Batzel**, **Natalia Andrade**, **Casey Whalen**, **Christopher and Ramona Brunner**, **Bruna Luz**, **Beatriz Diaz-Guijarro**, **Sieara Claytor**, **Marites Canto**, **Marina Santana**, **Refilwe Kgoadi**, and **Maria Andersen**. I am *really* glad to have met you all here.

Also not forgetting **Benjamin Moh**, **Doria Abdullah**, **Adam Lim**, and **Emma Elvidge** – all of whom while not in Townsville, have checked in on me and were always willing to lend an ear. Special thanks to **Rachel Goh** who made my time in Perth so much better simply by accompanying me during the weekends and whenever we had spare time.

Finally, I am eternally grateful for the financial, mental, and moral support from my family back home in Malaysia, especially my parents, **Frank Kuek** and **Pauline Lim**. It has been difficult being away, especially when the pandemic hit, but their unconditional love and support have never wavered. Thank you for letting me to take this leap of faith and allowing me to leave home to pursue my dreams. I also appreciate the support and prayers of my extended family members: aunties **Pauline** and **Florence** in Australia, and aunties **Irene** and **Tina** in Malaysia.

Statement of the contribution of others

Research and travel funding:

- James Cook University (JCU)
- ARC Centre of Excellence for Coral Reef Studies (ARC CoE)
- Australian Institute of Marine Science (AIMS)
- AIMS@JCU
- Robert Logan Memorial Bursary

Supervision:

- Prof. David J. Miller (JCU, ARC CoE)
- Assoc. Prof. David G. Bourne (JCU, AIMS)
- Dr. Cherie A. Motti (AIMS)
- Dr. Jean-Baptiste Raina (University of Technology, Sydney)

Experimental set-up and instrumentation:

- Prof. Jonathan D. Todd, Dr. Andrew R.J. Curson, and Dr. Beth T. Williams (University of East Anglia; Chapter 2)
- Assoc. Prof. David G. Bourne (JCU, AIMS; Chapters 2 and 4)
- Dr. Cherie A. Motti (AIMS; Chapters 2, 4, and 5)
- Dr. Jean-Baptiste Raina (UTS; Chapters 2, 4, and 5)
- Dr. Ira Cooke (JCU; Chapter 3)
- Dr. Nahshon Siboni (UTS ; Chapter 4)
- The Negri lab (Dr. Andrew Negri) and staff of the National Sea Simulator (SeaSIM, AIMS; Chapter 5)
- Assoc. Prof. Peta Clode, Dr. Hua Li, and Dr. Paul Guagliardo (University of Western Australia; Chapter 5)
- Dr. Thomas Becker (Curtin University; Chapter 5)

Biostatistics and bioinformatics analyses:

- Dr. Ira Cooke and Jia Zhang (JCU; Chapter 3)
- Dr. Jean-Baptiste Raina (UTS; Chapter 4)

Illustrations:

- Hillary Smith (JCU; Figure 1.7 and parts of Figure 6.1)

Editorial assistance:

- Prof. David J. Miller, Assoc. Prof. David G. Bourne, Dr. Cherie A. Motti, and Dr. Jean-Baptiste Raina (whole thesis)
- Dr. Ira Cooke (JCU; Chapter 3)
- Assoc. Prof. Peta Clode (UWA; Chapter 5)
- Dr. Thomas Becker (Curtin University; Chapter 5)

Thesis abstract

Dimethylsulphoniopropionate (DMSP) is a key molecule in the marine sulphur cycle. It is an abundant nutrient for bacteria, a foraging cue attracting zooplankton, fish and seabirds, and also the precursor of dimethyl sulphide (DMS), a gas involved in cloud formation. Extremely high DMSP concentrations are produced by corals and their dinoflagellate endosymbionts, Symbiodiniaceae. Although corals are known to harbour bacteria capable of using DMSP as a nutrient source, it was only recently discovered that prokaryotes are also capable of synthesising DMSP. Reviewed in Chapter 1 is the biochemistry of DMSP metabolism in the ocean, with a focus on the coral holobiont. It also discusses the potential role of coral-associated bacteria in the production of DMSP and the possible functions of its catabolic product, acrylate. The aims of this thesis are (i) to determine if coral-associated bacteria can produce DMSP, (ii) to identify the environmental factors influencing DMSP production, and (iii) to elucidate the functional role of acrylate, a breakdown product of DMSP, in corals.

Within the coral holobiont, DMSP production has been attributed to both the coral animal and their algal partner Symbiodiniaceae, however, their diverse associated bacteria could potentially be a cryptic source of DMSP. In Chapter 2, bacteria associated with corals were isolated and screened for potential DMSP-producing ability by targeting the bacterial DMSP synthesis gene, *dsyB*. Of the 240 bacteria strains obtained, 6% of the isolates harboured *dsyB*. All the *dsyB*-harbouring bacteria belonged to the Alphaproteobacteria class and their capability to produce DMSP was confirmed through liquid chromatography-mass spectrometry (LC-MS) and nuclear magnetic resonance (NMR) measurements. These results show that coral-associated bacteria can produce DMSP and have the ability to contribute to the large DMSP pool produced by the coral holobiont.

The functional capabilities of coral-associated DMSP-producing bacteria are unknown. In Chapter 3, the genome of *Shimia aestuarii* AMM-P-2, a DMSP-producing bacterium associated with *Acropora millepora*, was analysed to characterise its sulphur cycling capabilities. Specifically, this bacterium was confirmed to have the genetic machinery to assimilate sulphate and synthesise the DMSP precursors, cysteine and methionine, to catabolise DMSP to methanethiol, DMS, and acrylate, and to utilise or detoxify acrylate. These findings provide the basis for understanding the involvement of *S. aestuarii* AMM-P-2 in sulphur metabolism within the coral holobiont.

DMSP production is impacted by environmental stressors experienced by coral reefs in the Anthropocene. The discovery that coral-associated bacteria can also produce DMSP has

introduced an additional factor influencing DMSP dynamics within the coral holobiont. In Chapter 4, cultures of *S. aestuarii* AMM-P-2 were exposed to variation in both temperature and salinity, high UV radiation, and complete darkness, and DMSP concentrations monitored. Intracellular DMSP concentrations increased almost two-fold under both hypersaline conditions (40 PSU) and following UV exposure. Meanwhile, conditions that are stressful for the coral host but not necessarily for the bacteria, such as fluctuations beyond the average temperature range (22 and 32°C), did not induce significant changes in intracellular DMSP concentrations. DMSP production in response to variable salinity and UV suggests that under stress, *S. aestuarii* AMM-P-2 favoured the DMSP cleavage pathways, which in addition to acrylate, produce the antioxidant DMS. Overall, these results indicate that DMSP biosynthesis by *S. aestuarii AMM-P-2* is impacted by specific environmental conditions which are not necessarily tied to coral stress.

Acrylate is directly derived from DMSP catabolism and is produced in high concentrations by fast-growing, reef-building corals, including *A. millepora*, constituting a substantial carbon source in the coral holobiont. While possible functions of acrylate in corals have been hypothesized, the reason for its accumulation in these organisms is still unknown. In industrial applications, its polymerised form, polyacrylate, can produce a stable scaffold for the precipitation of calcium carbonate ($CaCO_3$), which is the major component of coral skeleton. In Chapter 5, the potential role of acrylate in coral skeleton formation was investigated. One-week old aposymbiotic *A. millepora* juvenile corals were supplemented with ^{13}C-labelled acrylate and the coral skeleton examined using nanoscale secondary ion mass spectrometry (NanoSIMS) and confocal Raman spectroscopy, for the presence of polyacrylate. Although the NanoSIMS results were inconclusive, polyacrylate was detected by Raman at the growing edge of the skeleton, suggesting a role in the biomineralization of $CaCO_3$ and growth of the skeleton. These results suggest the presence of an alternate biomineralization mechanism that can be adopted by acrylate-producing corals, potentially contributing to the fast accretion rate of these coral genera.

In summary, this thesis applied an interdisciplinary strategy to investigate the production of DMSP by coral-associated bacteria, and revealed a novel link between the DMSP breakdown product acrylate and the mechanism of calcification of coral skeleton in fast-growing coral species. It demonstrates that specific coral-associated bacteria can produce DMSP, adding this trait to the functional repertoire of prokaryotes within the coral holobiont. In addition, this work revealed a novel link between the DMSP breakdown product acrylate and the mechanism of calcification of coral skeleton in fast-growing coral species.

Table of contents

List of figures

List of tables

Chapter 1:
General introduction

1.1 The marine sulphur cycle

Sulphur is an essential element for life, and it can be found in large quantities in the ocean in the forms of dissolved organic and inorganic sulphate and sedimentary minerals (Sievert et al., 2007). This element makes up approximately 1% of the dry weight of all organisms on Earth through its incorporation in proteins, organosulphur compounds, coenzymes, and bridging ligands (Sievert et al., 2007). The essential steps in the sulphur cycle include the assimilatory uptake of sulphate by phytoplankton at the ocean's surface waters, which is used to form sulphated polysaccharides, methionine, and cysteine (Sievert et al., 2007). Methionine then acts as a precursor in the synthesis of dimethylsulphoniopropionate (DMSP), an extremely stable yet soluble form of reduced sulphur (Gage et al., 1997).

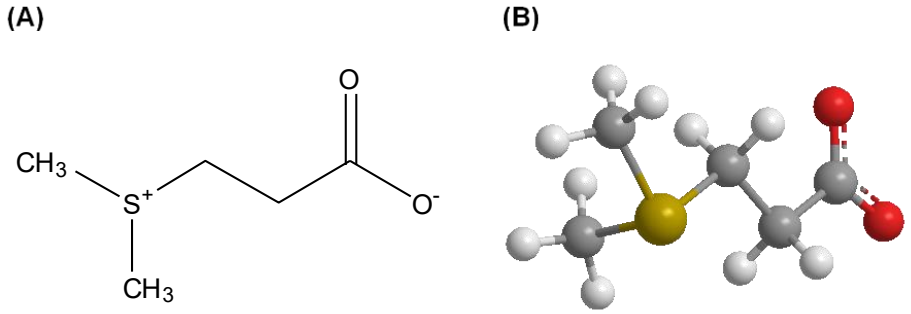

Figure 1.1. (A) Chemical structure and (B) 3D ball and stick model of DMSP. Colour code: grey, carbon; white, hydrogen; red, oxygen; yellow, sulphur.

Challenger and Simpson (1948) first discovered DMSP in the red algae *Polysiphonia fastigiata* and *Polysiphonia nigrescens*. We now know that this compound is ubiquitous in marine surface waters (van Duyl et al., 1998; Stefels et al., 2007) with more than a billion tons of DMSP produced in the marine environment every year (Kettle and Andreae, 2000; Kiene et al., 2000). DMSP contains five carbon atoms [$(CH_3)_2S^+CH_2CH_2COO^-$, Figure 1.1; also expressed as five units of carbon], making its metabolism a crucial process in the marine carbon cycle (Sievert et al., 2007): the biosynthesis (anabolism) of DMSP represents approximately 3-10% of the carbon fixed by primary producers in the ocean (Kiene et al., 2000; Archer et al., 2001; Simó et al., 2002),

and through its degradation (catabolism), DMSP supplies up to 10% of the total carbon demand (including C3 products) of heterotrophic bacteria in surface waters (Simó et al., 2002).

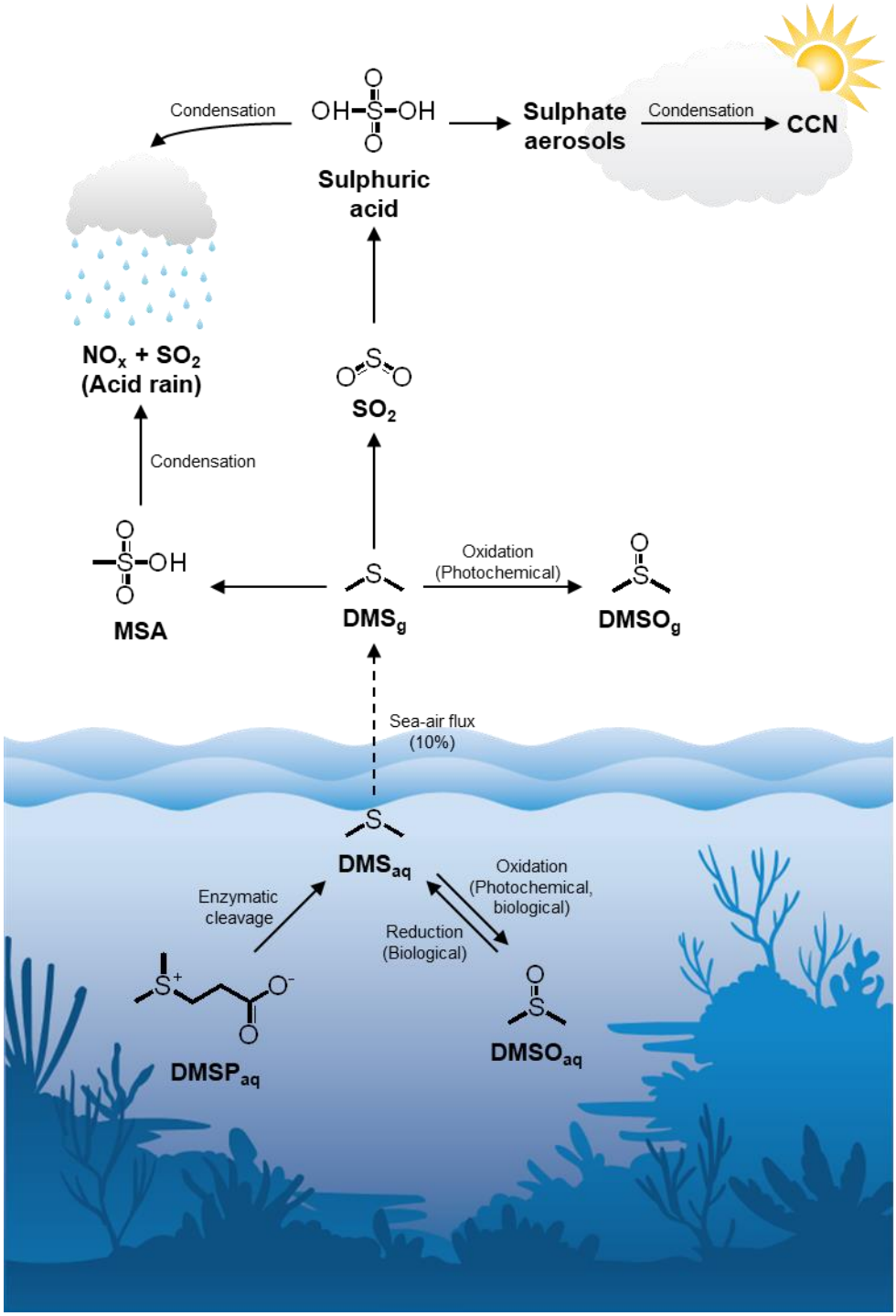

Figure 1.2. The dimethylsulphoniopropionate (DMSP) cycle in marine environments, illustrating the chemistry of sea-to-air dimethyl sulphide (DMS) fluxes and the production of sulphate aerosol particles. Dimethyl sulphoxide (DMSO); sulphur dioxide (SO_2); methanesulphonic acid (MSA); cloud condensation nuclei (CCN).

DMSP is zwitterionic in nature, having a positive and a negative charge on different parts of the same molecule. This prevents passive diffusion through cell membranes, making DMSP an ideal osmolyte for phytoplankton (Stefels, 2000; Yoch, 2002). It also acts as a chemo-attractant for several marine micro- and macro-organisms (DeBose and Nevitt, 2007; Seymour et al., 2010) and has been hypothesized to act as an antioxidant in marine algae and corals (Sunda et al., 2002; Deschaseaux et al., 2014b; Gardner et al., 2016), or as a cryoprotectant in polar organisms (Karsten et al., 1996). Lastly, DMSP is well known as the precursor of dimethyl sulphide (DMS), a volatile gas and a crucial link between the oceanic and atmospheric reservoirs in the sulphur cycle (Figure 1.2) (Stefels et al., 2007).

DMS accounts for the majority of the sulphur transferred from the ocean to the atmosphere and is therefore a crucial link in the global sulphur cycle (Stefels et al., 2007). In the marine environment it is a product of DMSP cleavage mediated by enzymes (i.e., DMSP lyases), but it may also be generated either through photochemical or biological reduction of dimethyl sulphoxide (DMSO), the latter via a poorly understood reduction pathway that depends on DMSO-reductases (Fuse et al., 1995; Spiese et al., 2009; Asher et al., 2011). Oceanic (or dissolved) DMS_{aq} can be subsequently oxidised into DMSO either chemically or biologically, a reaction again mediated by marine bacteria (Zeyer et al., 1987; Zhang et al., 1991).

On average, approximately 10% of the dissolved pool of oceanic DMS_{aq} (or 1-2% of the sulphur originating from DMSP) diffuses to the atmosphere where it is photochemically oxidised to DMSO (Deschaseaux et al., 2016). It can also be converted to methanesulphonic acid (MSA) or SO_2 (Shon et al., 2001), followed by sulphuric acid, and subsequently condensed into sulphate aerosols (Andreae et al., 1985; Malin et al., 1992; McGillis et al., 2000). This conversion is comparable in magnitude to the formation of anthropogenic sulphur dioxide (SO_2) from fossil fuel emissions (Bullock et al., 2017). The oxidation of atmospheric DMS_g to SO_2 is critical for the evaluation of the relative contribution of DMS into the atmosphere, as its conversion efficiency is used to estimate new particle formation of precursor gases (von Glasow and Crutzen, 2004). Furthermore, organic sulphur displays a longer residence time in the atmosphere, thus playing a greater role in the global sulphur budget (Lovelock et al., 1972; Chin and Jacob, 1996) with natural fluxes comprising 25% of the total gaseous sulphur fluxes to the atmosphere (Lana et al., 2011) and ultimately to land.

1.2 DMSP production

Estimates based on biogeochemical approaches have indicated that as much as 10% of primary production in the marine environment is channelled towards the synthesis of DMSP, suggesting a major flow of sea surface carbon and sulphur through this single compound (Howard et al., 2008). An increasing number of taxa are being recognised as DMSP producers: historically, the main producers were phytoplankton from the classes Dinophyceae (dinoflagellates) and Prymnesiophycaea (coccolithophores) (Keller et al., 1989). Other DMSP producers include coastal angiosperms (*Spartina alterniflora*) and grasses (*Wollastonia biflora*) (Hanson et al., 1994; Kocsis et al., 1998), diatoms and marine algae (*Ulva intestinalis*) (Gage et al., 1997), the coral animal (Raina et al., 2013), and most recently, several bacteria from the Alphaproteobacteria class (Curson et al., 2017). DMSP occurrence also appears to be increasingly widespread within the plant kingdom, with detectable levels of the compound measured in the shoots and roots of monocots and dicots from both freshwater and saline environments (Ausma et al., 2017).

Three DMSP biosynthetic pathways have been identified (Figure 1.3): the methionine transamination pathway in marine algae (Gage et al., 1997), the methionine methylation pathway in coastal plants (Rhodes et al., 1997) and the decarboxylation pathway in marine cordgrass and a dinoflagellate (Uchida et al., 1996; Kocsis et al., 1998). All these pathways use methionine as a precursor. Plants and microorganisms such as Symbiodiniaceae, bacteria and fungi have the metabolic machinery required for de novo synthesis of cysteine and methionine (Giovanelli and Harvey Mudd, 1967; Giovanelli, 1987; Ravanel et al., 1998; Wirtz and Droux, 2005). Methionine is produced through methionine synthase (MetH), the enzyme responsible for the regeneration of methionine from homocysteine (Croft et al., 2005). Although all three DMSP synthesis pathways start with methionine, the subsequent steps leading to DMSP differ.

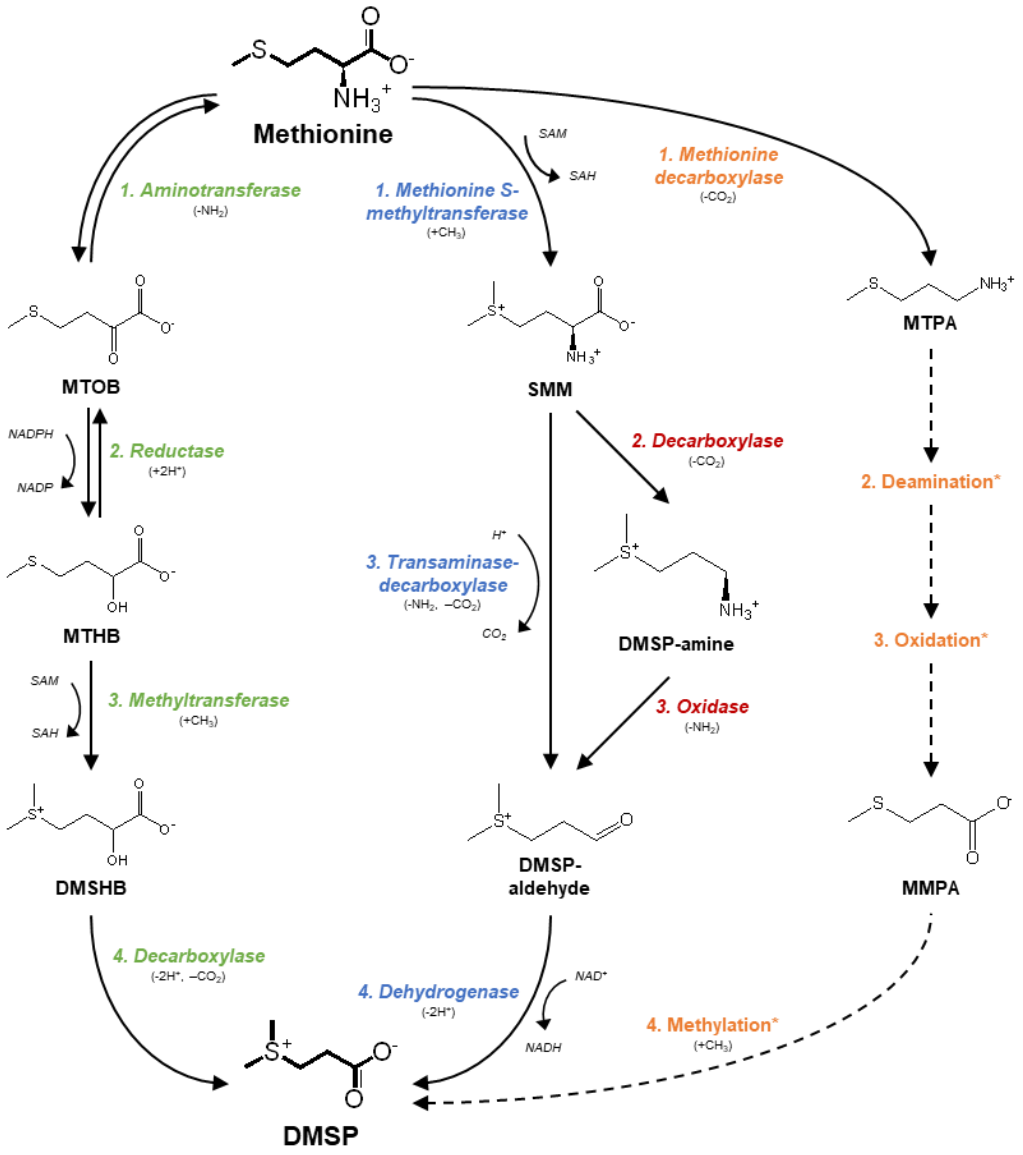

Figure 1.3. Proposed DMSP biosynthetic pathways adapted from Bullock et al. (2017) and Aguilar et al. (2017). The methionine transamination pathway (in green), methylation pathway (in blue), and decarboxylation pathway (in red) have been well-described in marine algae, coastal plants, and marine cordgrass respectively. An alternate decarboxylation pathway has been hypothesised in dinoflagellates (in orange). Dimethylsulphonio-2-hydroxybutyrate (DMSHB); dimethylsulphoniopropionate (DMSP); 4-methylthio-2-hydroxybutyrate (MTHB); 2-oxo-4-methylthiobutanoate (MTOB); S-adenosylhomocysteine (SAH); S-adenosylmethione (SAM); S-methylmethionine (SMM). Enzyme types and associated cofactors are shown in italics.

1.2.1 The methionine transamination pathway

Up to 90% of the reduced sulphur found in algal cells is in the form of DMSP (Gage et al., 1997). Resultantly, the biosynthetic pathway for DMSP was initially identified in marine algae, although much about its metabolism is still not well understood. The transamination pathway begins with catabolism of methionine by aminotransferase to produce 4-methylthio-2-

oxobutyrate (MTOB), followed by a NADPH-linked reductase, a methyltransferase, and an oxidative decarboxylase (Gage et al., 1997; Summers et al., 1998). The third step of this pathway, which is specific to DMSP producers, is hypothesised to be the key step: the methylation of 4-methylthio-2-hydroxybutyrate (MTHB) to 4-dimethylsulphonio-2-hydroxybutyrate (DMSHB) is catalysed by MTHB methyltransferase (MHM) (Gage et al., 1997; Summers et al., 1998; Ito et al., 2011). DMSHB has been subsequently found in *Ulva pertusa*, *Emiliania huxleyi*, *Tetraselmis* sp., and *Melosira nummuliodes*, indicating this pathway is present in a range of marine algae and phytoplankton (Gage et al., 1997; Summers et al., 1998; Ito et al., 2011)

Recently, it has been proposed that bacteria from the Alphaproteobacteria class use the transamination pathway to synthesise DMSP. Although they are more commonly known as prolific DMSP degraders, the first DMSP biosynthesis gene to be identified in any organism, *dsyB*, was discovered in the heterotrophic bacterium *Labrenzia aggregata* LZB033 (Curson et al., 2017). The gene encodes a methyltransferase-like protein that mediates the key step of the DMSP production pathway. The bacterial strain has been demonstrated to grow in the presence of all transamination pathway intermediates, and exhibit MHM activity, converting MTHB to DMSHB and ultimately, DMSP (Curson et al., 2017). *dsyB* has also been found in various other Alphaproteobacteria (*Oceanicola batsensis* HTCC2597, *Pelagibaca bermudensis* HTCC2601, *Sediminimonas qiaohouensis* DSM21189, *Amorphus coralli* DSM18348, *Sagittula stellata* E-37, *Labrenzia aggregata* IAM12614, and *Thalassobaculum salexigens* DSM19539). The *dsyB* genes from these bacteria strains were successfully cloned in the non-DMSP producer *Rhizobium leguminosarum*, and their ability to synthesize DMSP was confirmed. This gene was estimated to be present in 0.5% of bacteria sampled in the Tara Oceans and Global Ocean Sampling (GOS) marine metagenomes (Curson et al., 2017).

Functional *dsyB* homologues, termed *DSYB*, have also been identified in many phytoplankton and corals genomes (Curson et al., 2018). These homologous enzymes are localised in the chloroplast and mitochondria of *Prymnesium parvum* (Curson et al., 2018), two energy powerhouses that can sustain the energy-demanding process of DMSP biosynthesis (Matrai and Keller, 1994). Phylogenetic analyses suggest the ability to produce DMSP may have originated in prokaryotes before being transferred to eukaryotes through endosymbiosis at the time of mitochondrial origin, or via horizontal gene transfer (HGT) (Curson et al., 2018).

1.2.2 The methionine methylation pathway

The methionine methylation pathway is found in angiosperms from the family Compositae and is best studied in *W. biflora* (Hanson et al., 1994). The intermediates of this

biosynthetic pathway are very different from marine algae (Dickschat et al., 2015). The pathway starts with the methylation of methionine to S-methyl-L-methionine (SMM) (Hanson et al., 1994; Kocsis et al., 1998), followed by a transamination-decarboxylation sequence yielding 3-(dimethylsulphonio)propionaldehyde (DMSP-aldehyde) (Rhodes et al. 1997). Although many flowering plants have the enzymes to mediate the methylation of methionine and the oxidation of DMSP-aldehyde, it is the conversion of SMM to DMSP-aldehyde in DMSP producers that is specific for DMSP biosynthesis (Stefels, 2000). The final step of this pathway involves a dehydrogenase that rapidly oxidises DMSP-aldehyde to DMSP at very high rates (James et al., 1995). This difference between the methylation and transamination pathways suggests the ability to synthesise DMSP in plants and algae evolved independently from each other, which in turn indicates separate responses to selective environmental pressures (Bullock et al., 2017).

Recently, specific bacteria belonging to the Alphaproteobacteria, Gammaproteobacteria, and Actinobacteria have been shown to produce DMSP using pathways independent of *dsyB* (Williams et al., 2019). The *mmtN* gene was identified in these bacteria, and all were shown to produce SMM, an intermediate which is unique to the methionine methylation pathway (Figure 1.3, in blue). In the cell extracts of the Alphaproteobacteria *Novosphingobium* sp. BW1, two other down-stream intermediaries, DMSP-amine and DMSP-aldehyde, were also detected and were used to confirm the occurrence of this pathway (Williams et al., 2019). The *mmtN* gene shares ≤30% identity with the N-terminal methyltransferase domain of plant methionine methyltransferase suggesting these pathways are ancient, and if any gene transfer occurred between plants and bacteria, the event happened a long time ago (Williams et al., 2019). Bacteria containing *mmtN* were found to be generally less abundant than those with *dsyB* (Williams et al., 2019), but *mmtN* transcripts are present at varied levels in Tara Oceans bacterioplankton databases.

1.2.3 The methionine decarboxylation pathway

This last pathway has been described in *S. alterniflora* and is common in marine grasses belonging to the family Gramineae (Kocsis et al., 1998). The conversion of methionine to SMM is similar to that in the methylation pathway, but the pathway then undergoes two additional catabolism steps involving decarboxylation to produce DMSP-amine as an intermediate, then oxidative deamination which eventually yields DMSP-aldehyde (Kocsis et al., 1998; Kocsis and Hanson, 2000). Although the DMSP biosynthetic pathways of *S. alterniflora* and *W. biflora* both begin and end with the same methylation and oxidation steps (Figure 1.3), it is the production of

DMSP-amine by *S. alterniflora* that revealed the evolution of DMSP production in these two plant families occurred separately from each other (Kocsis et al., 1998; Stefels, 2000).

In the heterotrophic dinoflagellate, *Crypthecodinium cohnii* and the thalli of *Ulva lactuca*, a slightly different decarboxylation pathway was proposed (Greene, 1962; Uchida et al., 1996). A methionine decarboxylase catalyses the first step of the biosynthesis pathway, the conversion of methionine to 3-(methylthio)propylamine (Uchida et al., 1996; Dickschat et al., 2015). Contrary to the pathway in Gramineae, SMM was not observed to be an intermediate (Greene, 1962; Uchida et al., 1996), but the subsequent steps following decarboxylation has been suggested to involve deamination, oxidation, and methylation, forming the intermediate 3-methyl-propionate (MMPA) prior to the synthesis of DMSP (Uchida et al., 1996; Stefels, 2000). Although the experiments exploring this particular pathway were not conclusive (Stefels, 2000), it was postulated that the methionine decarboxylase purified from *C. cohnii* may be a key enzyme in DMSP biosynthesis (Uchida et al., 1996).

While most of the intermediates involved in the aforementioned pathways have been established, the identities of the genes involved in DMSP production are still largely unknown. Candidate genes have emerged from proteomic and gene expression analyses, implicating a number of classes of enzymes based on the increased abundance of DMSP under favourable biosynthesis conditions (Lyon et al., 2011; Kettles et al., 2014; Aguilar et al., 2017). Their involvement in DMSP production, however, still needs to be confirmed.

1.3 DMSP degradation

While DMSP is predominantly synthesised by algae, its catabolism (or degradation) in the ocean is mediated by both bacterial and algal DMSP-degrading enzymes. Studies on DMSP degradation initially focused on DMSP-producing phytoplankton and macroalgae (Curson et al., 2011b). An enzyme believed to be responsible for DMSP cleavage was first isolated from the red algae, *Polysiphonia lanosa* (Cantoni and Anderson, 1956). Similar DMSP lyase activity was also reported in coccolithophores (Steinke et al., 1998) and dinoflagellates (Yost and Mitchelmore, 2009). However, there was a lack of molecular descriptions of the enzyme and its corresponding gene, partly due to the difficulty in obtaining axenic cultures (Curson et al., 2011b). Recently, *Alma1*, a DMSP lyase gene, was identified and characterised in the bloom-forming algae *Emiliania huxleyi* (Alcolombri et al., 2015).

1.3.1 DMSP catabolism in phytoplankton

Alma1 is a nuclear-encoded gene containing two introns, highlighting its eukaryotic origin. *Alma1* also does not share any homology with any of the known bacterial DMSP lyase families (Curson et al., 2011b; Moran et al., 2012), indicating that it must function differently from its bacterial counterparts. Subsequently, paralogs of the *Alma1* gene were also found in other algal species known to possess high DMSP lyase activity such as dinoflagellates, other haptophytes and even in reef-building corals (Alcolombri et al., 2015). Different *E. huxleyi* strains have different baseline levels of DMSP lyase activity which correlates with the amounts of Alma1 protein present (Alcolombri et al., 2015), although the intrinsic or extrinsic signals that affect *Alma1* gene expression are currently unknown.

Although this newly identified algal DMSP lyase allows for increased understanding of the roles methylated sulphur play within *E. huxleyi*, the available sequences of many other phytoplankton which also exhibit DMSP lyase activity (de Souza et al., 1996) do not contain any convincing homologues of *Alma1* (Johnston, 2015). This suggests that these phytoplankton may have other enzymes that encode for DMSP degradation. The green macroalga *Ulva curvata* not only has the ability to lyase DMSP, it is also able to use the transamination pathway to synthesise DMSP (de Souza et al., 1996). While this dual ability raises issues regarding relative contributions of organic sulphur from such organisms and the way in which these processes are affected by environmental parameters (Johnston, 2015), their ability to metabolise DMSP has been hypothesised to play a role in the regulation of the organism's intracellular DMSP in response to changing salinity (de Souza et al., 1996).

1.3.2 Bacterial demethylation and cleavage of DMSP

Bacterioplankton are known to preferentially use DMSP as a source of sulphur for protein synthesis, particularly in the euphotic zone (Kettle et al., 1999; Kiene et al., 2000). Between 50-100% of the sulphur required for heterotrophic bacterial biomass production comes from DMSP (Malmstrom et al., 2004) suggesting it is expended in almost all cellular functions, allowing bacteria to adapt to evolutionary pressures and utilise every possible thermodynamic advantage (Vallino et al., 1996). Marine bacteria degrade DMSP through two main routes (Figure 1.4): the demethylation pathway that converts DMSP to MMPA, and subsequently to 3-mercaptopropionate (MPA) and methanethiol (MeSH) (Kiene et al., 2000; Howard et al., 2006; Todd et al., 2007); and the cleavage pathway whereby DMSP is converted to equal parts DMS and acrylate (Yoch, 2002; Moran et al., 2004; Todd et al., 2007). The overall DMSP turnover in the oceans is large (~130 nM d^{-1} in non-bloom waters; >1000 nM d^{-1} during phytoplankton

blooms) (Kiene, 1996; van Duyl et al., 1998; Kiene and Linn, 2000) with up to 90% catabolised through the demethylation pathway (Kiene and Linn, 2000; Kiene et al., 2000; Moran et al., 2012). This pathway thereby asserts major biological control over DMS formation (González et al., 1999) and is driven by the fact that MeSH is highly reactive and a readily assimilated source of reduced sulphur for microorganisms (Sievert et al., 2007), particularly for the production of methionine (Kiene et al., 2000), whereas DMS is more readily diffused into the atmosphere and lost.

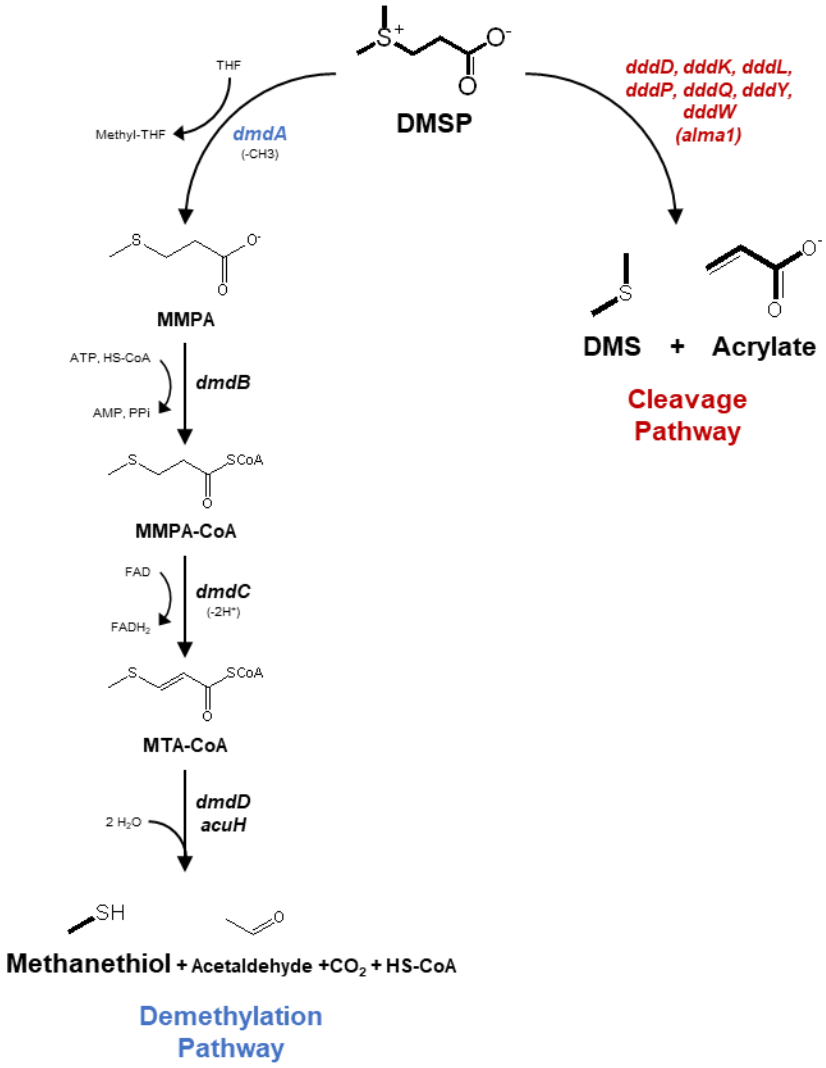

Figure 1.4. Dimethylsulphoniopropionate (DMSP) degradation pathways adapted from (Reisch et al., 2011b), (Reisch et al., 2013), and (Bullock et al., 2017). The demethylation pathway (in blue) is catalysed by the DMSP demethylase (DmdA), MMPA-CoA ligase (DmdB), MMPA-CoA dehydrogenase (DmdC), and either the MTA-CoA hydratase (DmdD) or acrylate utilisation hydratase (AcuH), yielding methanethiol as its main end product. The cleavage pathway (in red) is catalysed by a DMSP lyase (DddP, DddW, DddY, DddQ, DddL, DddK, or the algal Alma1) to produce equal amounts of dimethyl sulphide (DMS) and acrylate.

1.3.2.1 DMSP demethylation: dmdA

The first gene implicated in DMSP degradation, termed *dmdA*, was characterised from *Ruegeria pomeroyi* DSS-3 (Howard et al., 2006). This gene occurs frequently in a wide variety of prokaryotic taxa, particularly within the *Roseobacter* and SAR11 clades of marine bacteria, thus identifying them as primary mediators of DMSP demethylation. Homologues of *dmdA*, which form five distinct clades, are harboured by (i) a third of all bacterioplankton cells in the Sargasso Sea (Venter et al., 2004), (ii) ~three out of five bacterioplankton cells sampled in the 2007 Global Ocean Sampling (GOS) data set (Rusch et al., 2007), and (iii) ~28% of the sampled cells in the Tara Oceans data set (Sunagawa et al., 2015). These homologues were found in samples from the photic zone, confirming that DMSP flux is negligible in deep waters (Miller and Belas, 2004). It is hypothesised that lateral gene transfer (LGT) partially played a role in the extraordinary abundance of *dmdA* in bacteria across several marine habitats (Howard et al., 2008), resulting in the homogenising of the ecological roles of marine bacteria (Ochman et al., 2000). This high frequency of *dmdA* is presumably due to the requirements of these diverse bacteria to reach high cell density under oligotrophic conditions (Tripp et al., 2008). Since the utilisation of a reduced sulphur source like DMSP is energetically less costly compared to sulphate reduction, it is therefore evolutionarily favourable for them to obtain *dmdA* (Tripp et al., 2008; Reisch et al., 2011a).

1.3.2.2 DMSP lysis: dddD, dddL, dddP, dddQ, dddY, dddW, dddK

In contrast to the demethylation pathway, there is a diverse group of genes that mediate the cleavage pathway. Currently, at least seven classes of DMSP-dependent DMS (*ddd*-) bacterial enzymes are known, represented by different polypeptide families:

i. *dddD* (Todd et al., 2007) which converts DMSP to DMS, acetate and 3-hydroxy-propionate (3HP) as its C3 cleavage product, instead of DMS and acrylate like the following *ddd*- genes,
ii. *dddL* (Curson et al., 2008), rare in both cultured and metagenome databases (Reisch et al., 2011a),
iii. *dddP* (Todd et al., 2009), a M24B metalloprotease which cleaves the S-C bond of DMSP, releasing DMS and acrylate (Choi et al., 2015; Wang et al., 2015a) and which is in high abundance in several marine metagenomes (Howard et al., 2008; Varaljay et al., 2012; Carrión et al., 2015; Choi et al., 2015),

iv. *dddQ* (Todd et al., 2011), found exclusively in *Roseobacters* with two adjacent genes (*dddQ1* and *dddQ2*) discovered amongst a 10-gene cluster,
v. *dddY* (Curson et al., 2011a), the only DMSP lyase associated with the bacteria's periplasmic space and often found adjacent to genes encoding various types of cytochromes, some of which resemble those involved in acrylate and/or methacrylate respiration (Mikoulinskaia et al., 1999; Gross et al., 2001),
vi. *dddW* (Todd et al., 2012a), rarest of all *ddd*- genes thus far, and which together with *dddL* and *dddQ*, contains carboxy-terminal domains that form cupin pockets involved in the binding of DMSP (Alcolombri et al., 2014; Li et al., 2014),
vii. *dddK* (Sun et al., 2016), a cupin-like DMSP lyase, only found in Pelagibacterales strains (SAR11), the most numerically abundant heterotrophic bacteria in the ocean, often operating simultaneously with *dmdA*.

The diversity of DMSP lyases is interesting, along with the fact that some bacteria appear to have multiple cleavage pathways within their genome. It is still unclear why these bacteria harbour different genes that carry out the same functions, although it is possible that their physiological functions may be different (Bullock et al., 2017). The relative expression of these different pathways naturally controls the fate of DMSP-derived sulphur into the atmosphere and has led to an often-discussed concept in DMSP biogeochemistry that is referred to as the 'bacterial switch' (Simó, 2001).

1.3.3 The 'bacterial switch' hypothesis (also known as the sulphur demand hypothesis)

All forms of sulphur metabolism can be found within the Proteobacteria (Sievert et al., 2007). While the ability to degrade DMSP to DMS is widespread among bacteria, we are only now beginning to quantify their capacity to produce DMSP. The idea of a 'bacterial switch' that regulates DMS degradation and emission to the atmosphere is not new (Kiene et al., 2000; Simó, 2001). Both reports hypothesised that the two competing bacterial-mediated transformations of DMSP (demethylation vs. cleavage) is driven by bacterial carbon and sulphur demands by DMSP availability. It was postulated that the demethylation pathway (*dmdA*) is favourable when DMSP supply is low relative to bacterial carbon and sulphur demands, while the cleavage pathway (*ddd*-) will be preferred under low bacterial sulphur demand and elevated DMSP supply. It was further suggested that additional factors involving light and temperature may be involved in the regulation of the 'switch' whereby DMSP demethylation occurs under low UV-A dose (UV

radiation up to a wavelength of ~330 nm) while bacterial DMSP cleavage occurs under elevated temperatures and moderate UV-A dose (Levine et al., 2012).

The 'bacterial switch' has significant environmental consequences. It is not only able to modulate the partitioning of fluxes through the demethylation or cleavage pathways (Reisch et al., 2011a), but more importantly, it plays a major role in the regulation of the sulphur cycle from the oceans to land (Todd et al., 2012b). Emerging studies have supported this hypothesis, with strains of *R. pomeroyi* and *Roseobacter* sp. found to regulate both the DMSP demethylation and cleavage pathways in response to changing environmental conditions (Bürgmann et al., 2007; Todd et al., 2012a; Varaljay et al., 2015), and *Pelagibacter* sp. which is able to simultaneously catabolise both DMS and MeSH (Sun et al., 2016). The cellular mechanisms controlling the 'switch', however, remain elusive (Stefels et al., 2007; Moran et al., 2012).

1.4 DMSP metabolism within the coral holobiont

The first measurements of DMS emissions over coral reefs were carried out by Andreae et al. (1983) after they noticed that coral specimens brought on board during their expedition smelled strongly of DMS. Although their results at the time did not show any correlation between the abundance of corals and DMS levels in surrounding water, they found that corals exposed to air increased the average concentration of DMS in the atmosphere (Andreae et al., 1983). Almost a decade later, studies by Jones et al. (1994) established coral reef ecosystems are a major contributor of DMS emissions to the atmosphere by showing levels of both DMSP and DMS increase with proximity to coral reefs. Subsequent expeditions measured elevated levels of atmospheric DMS in the regions of the northern Great Barrier Reef (GBR), Coral Sea, Gulf of Papua, Solomon Sea and Bismarck Sea, showing further correlation with areas of high coral reef biomass (Jones and Trevena, 2005). Specifically, they found that high total particle concentrations in aerosols adjacent to coral reefs are comparable with measured emissions in the past from land surfaces and forest fires (Bigg and Turvey, 1978). *In situ* measurements of atmospheric DMS at the southern GBR further established that coral reefs can be a greater source of DMS compared to temperate marine ecosystems (Swan et al., 2012).

Biologically-derived demethylated sulphur compounds – which include DMSP, DMS and DMSO – are very abundant in coral reefs as they can all be found in most (benthic) organisms within the reef (Jones et al., 1994; Hill et al., 1995; Broadbent et al., 2002; Van Alstyne and Puglisi, 2007; Swan et al., 2012). The highest concentrations of DMSP and DMS recorded in the marine environment were measured from coral mucus, which contained more than 10 times the amount found in sea ice (Broadbent and Jones, 2004). DMSP concentrations in coral tissue can

be up to three orders of magnitude greater than values obtained from benthic macroalgae (Broadbent et al., 2002), suggesting that corals play a major role in the cycling of DMSP and more widely of sulphur. The metabolism of these sulphur compounds was hypothesised to be influenced by a combination of coral growth, grazing of DMS-producing algae by zooplankton or reef fish, phytoplankton growth and benthic microalgae activity (Broadbent and Jones, 2006). However, the relative contribution of the wide variety of reef organisms within the dynamics of DMSP cycling has been difficult to establish (Broadbent et al., 2002; Van Alstyne and Puglisi, 2007; Kamenos et al., 2008).

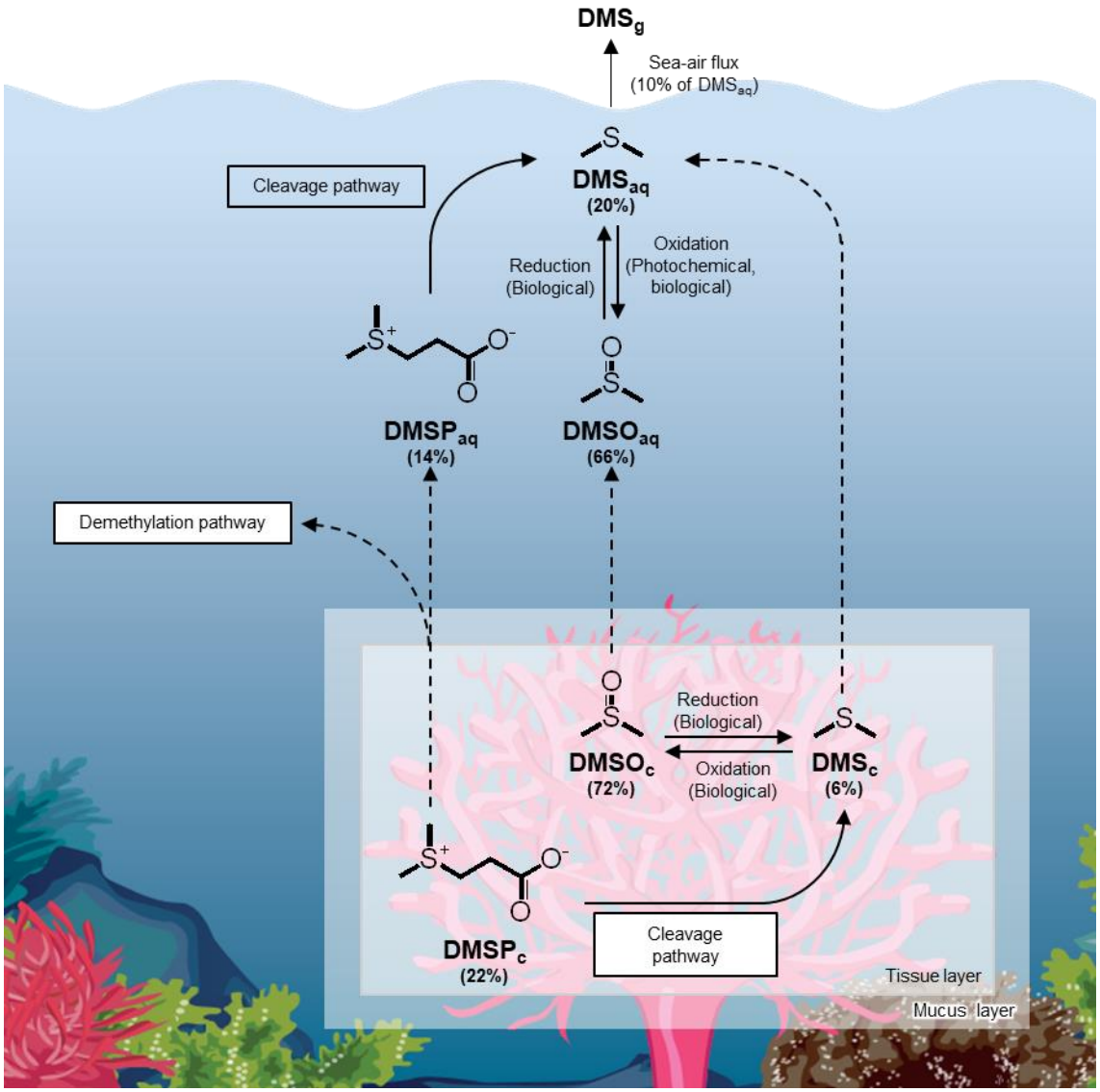

Figure 1.5. Dimethylsulphoniopropionate (DMSP) transformation within the coral holobiont and coral reef waters adapted from Raina et al. (2010) and Deschaseaux et al. (2016). These transformations undergo oxidation and reduction processes on dimethylsulphoniopropionate (DMSP), dimethylsulphide (DMS), and dimethylsulphoxide (DMSO) within Symbiodiniaceae cells, coral tissue, and coral mucus. DMSP can be

degraded by enzymes coral-associated bacteria following two routes, the cleavage pathway or the demethylation pathway. Percentages are estimates of the biochemical budget of each compound in proportion to the total concentrations of demethylated sulphur compounds based on Deschaseaux et al. (2014b) for values within the coral holobiont, and the mean obtained from (Jones et al., 2007) and (Broadbent and Jones, 2006) for values in coral reef waters. Dotted lines indicate the transfer of compounds between coral tissue, coral mucus, and the surrounding waters.

Most intertidal scleractinian corals are hermatypic (reef-building), usually living in symbiosis with photosynthetic dinoflagellates of the family Symbiodiniaceae (Trench, 1979; Douglas, 2003; Harrison and Booth, 2007; Harrison, 2011; LaJeunesse et al., 2018). These algal endosymbionts provide the coral animal primarily with photosynthetically-derived carbon (Muscatine and Porter, 1977; Trench, 1993) in exchange for shelter and nutrients such as ammonium (Trench, 1993; Yellowlees et al., 2008). Corals also host a wide range of bacteria, viruses, fungi, endolithic algae and archaea within their mucus layer, tissue and skeleton (Rohwer et al., 2002; Wegley et al., 2004; Ritchie, 2006; Rosenberg et al., 2007; Marhaver et al., 2008; Bourne and Webster, 2013). Besides providing additional nutrients and occasionally, pathogenic resistance, the coral microbial community are also responsible for the catabolism of DMSP to DMS (Johnston et al., 2008; Raina et al., 2009). Together, these micro- and macro-organisms form a consortium that constitutes the coral holobiont.

Photosynthetic organisms, such as Symbiodiniaceae, bacteria and fungi, can synthesise methionine, which is a precursor of DMSP. Animals usually acquire methionine through symbiosis or their diet (Wirtz and Droux, 2005). Therefore, it was initially assumed that DMSP concentrations measured from corals were the by-product of symbiont activity and thus, were often expressed as per Symbiodiniaceae or per cell biovolume (Deschaseaux et al., 2016). Previous studies have also shown a correlation between symbiont density and measured DMSP production (Van Alstyne et al., 2006). However, the coral animal itself is capable of producing DMSP (Raina et al., 2013), challenging the dogma that DMSP production in the coral holobiont was solely attributed to its endosymbiotic microalgae, and calls into question the relative contribution of the members of the coral holobiont to the sulphur cycle. Even more recently, it has been found that corals have orthologues of the cobalamin-dependent methionine synthase (MetH) present in their transcriptome, indicating that they can synthesise methionine on their own (Aguilar et al., 2017).

It is difficult to determine DMSP flux within the holobiont due to the complex symbiotic relationship the organisms have with each other. When DMSP is measured in isolated free Symbiodiniaceae, concentrations were lower compared to those found within the coral host, suggesting that the polyp may accumulate the compound within its tissue (Jones et al., 1994; Hill

et al., 1995). Different genera of Symbiodiniaceae can also produce different concentrations of DMSP and DMS (Yost and Mitchelmore, 2009; Steinke et al., 2011). The synthesis of DMSP by these endosymbionts correlates with their tolerance towards thermal stress (Deschaseaux et al., 2014a). Coral-associated bacteria can also influence the rate of DMSP degradation to DMS through the action of six different marine bacterial DMSP lyases (*ddd*- families) (Raina et al., 2009; Raina et al., 2010; Alcolombri et al., 2017). Using a mechanism-based inhibitor, 2-bromo-3-(dimethylsulphonio)-propionate (Br-DMSP), that selectively inhibits the Alma enzyme family while avoiding other known DMSP lyase families, Alcolombri et al. (2017) found that more than 90% of DMSP lyase activity was inhibited in the crude extract of *Acropora millepora*. It appears that the eukaryotic components of the holobiont equipped with Alma-like DMSP lyases play a larger role in DMS production than previously thought, although there are other corals (e.g., *Stylophora* sp.) that did not demonstrate any inhibition when Br-DMSP was applied, indicating that their DMS production is of bacterial origin (Alcolombri et al., 2017). With all members of the holobiont heavily implicated in DMSP metabolism, it remains unclear which component dominates these conversions, especially under different environmental conditions. What is currently known of the DMSP cycling within the coral holobiont including predicted budgets is summarised in Figure 1.5.

1.4.1 Factors affecting DMSP metabolism in coral reefs

The range of biological functions that DMSP and DMS play suggests that the production of these compounds may be linked to environmental stress responses, particularly in corals (Deschaseaux et al., 2014b). Previous studies on environmental factors causing oxidative stress found these are accompanied by variations in DMSP and DMS production by the coral holobiont that can amplify physiological stress experienced by the coral host, leading to a potential increase in coral mortality (Van Alstyne et al., 2006; Deschaseaux et al., 2014b; Jones et al., 2014). Studies have shown atmospheric DMS_g to be highest over GBR reef waters at midday in the summer (Broadbent and Jones, 2006). Its production is influenced by biological processes that involve photosynthetic activity, which in turn is affected by light and sea surface temperatures (SST) (Jones et al., 2007). This was confirmed when dissolved oceanic DMSP and DMS_{aq} concentrations measured from the GBR were found to be positively correlated with SST (Jones et al., 2007). The exposure of corals to the atmosphere during low tides at the reef has also resulted in enhanced concentrations of atmospheric DMS_g at the affected local regions (Jones and Trevena, 2005; Jones et al., 2007; Swan et al., 2012).

The exudation of mucus from stressed corals, particularly during low tide exposure or when disturbed, have produced the highest concentrations of DMSP and DMS on record in the marine environment (Broadbent and Jones, 2004). Many marine bacteria that play a central role in the degradation of DMSP are associated with the coral mucus, and their ability to partake in coral DMSP metabolism is implicated in the structuring of healthy resident bacterial communities (Raina et al., 2009; Raina et al., 2010). Coral mucus-associated bacteria are also hypothesised to act as a first line of defence against invasive pathogens, either by dominating coral niches (Ritchie and Smith, 2004) or by the production of antimicrobial compounds that inhibit the growth of invasive microbes (Ritchie, 2006). However, when DMSP concentrations are increased during stress, the compound can act as a kairomone (a chemical signal that favours the receiver), attracting bacterial pathogens that can cause bleaching or tissue-loss (Garren et al., 2014; Tout et al., 2015). Interestingly, some of these pathogens are unable to degrade DMSP (Garren et al., 2014), potentially disrupting the catabolism of the compound when they replace the resident microbial communities in stressed corals.

Since reef-building corals are a major source of DMSP, any decrease in DMS emissions can have significant effects on the regional climate over coral reefs that may intensify mass coral bleaching events (Jones and Ristovski, 2010; Raina et al., 2013). When increased SST and/or tidal exposure exceeds bleaching thresholds, the expulsion of coral symbionts and mucus into the surrounding waters can occur, thus raising DMSP and DMS concentrations on reefs (Broadbent and Jones, 2004; Jones and Trevena, 2005; Hopkins et al., 2016). Given the high abundance and diversity of coral-associated bacteria within coral tissue and mucus (Rohwer et al., 2002; Koren and Rosenberg, 2006; Garren and Azam, 2010; Sunagawa et al., 2010; Daniels et al., 2011; Sweet et al., 2011), it is likely that coral-associated bacteria contribute towards the high levels of DMSP in corals as well. Through the 'bacterial switch' hypothesis and emerging studies that support it (Bürgmann et al., 2007; Todd et al., 2012b; Sun et al., 2016), as well as the discovery of *dsyB* and its homologues, the role of marine bacteria in DMSP metabolism is more important than initially thought. While past studies have investigated the catabolism of DMSP by coral-associated bacteria (Raina et al., 2009; Raina et al., 2010; Raina et al., 2017), there is currently not much known about their capability to produce DMSP, or how their metabolism of DMSP may contribute to the flux of DMS to the atmosphere.

Coral reefs are also comprised of other benthic organisms that play a role in DMSP metabolism (Broadbent et al., 2002; Van Alstyne and Puglisi, 2007; Kamenos et al., 2008). For example, environmental stressors such as ocean acidification and increased temperatures have been shown to affect DMSP production or degradation in the sea anemone *Anemonia viridis* (Borell et al., 2014), coralline algae (Burdett et al., 2014) and the macroalgae *Ulva lactuca*

(Kerrison et al., 2012), indicating that the dynamics between various reef organisms can vary in response to projected future climate conditions. Increased levels of DMSP in macroalgae resulting from exposure to high partial pressure of carbon dioxide (pCO_2) have also been shown to negatively affect grazing behaviour of herbivorous fish and sea urchins (Borell et al., 2013) potentially causing a shift to macroalgal dominance in the reef (Hughes, 1994), ultimately affecting further decline in DMSP production.

1.5 Acrylate – the forgotten story

Concentrations of acrylate, a by-product from the catabolism of DMSP, are exceptionally high in some coral species (Table 1.1) (Tapiolas et al., 2013). However, acrylate is a compound that is relatively understudied in biological systems compared to its precursors. Coral reefs are currently the only known natural environment to contain significant amounts of acrylate (Tapiolas et al., 2010; Tapiolas et al., 2013; Curson et al., 2014). Acrylate is a C3 compound (CH_2=CHCOO$^-$, Figure 1.6) and thus, a substantial carbon source within the coral holobiont (Tapiolas et al., 2010). Its production can be achieved through DMSP lyase: six "*ddd*-" enzymes (*dddK, dddL*, *dddP*, *dddQ*, *dddW*, and *dddY*) are involved in the cleavage of DMSP, subsequently yielding DMS and acrylate (Curson et al., 2014; Sun et al., 2016). The enzymatic lysis of DMSP to acrylate has also been reported in various DMSP-producing organisms including dinoflagellates (Steinke et al., 2002), microalgae (Malin and Erst, 1997; Alcolombri et al., 2015) and chemoheterotrophic bacteria (Todd et al., 2007; Curson et al., 2008). There have also been suggestions that the DMSP demethylation pathway may generate acrylate through the demethiolation of MMPA, resulting in methylthioacryloyl-CoA (MTA-CoA) as a downstream product (Taylor and Gilchrist, 1991; Reisch et al., 2011b; Tan et al., 2013).

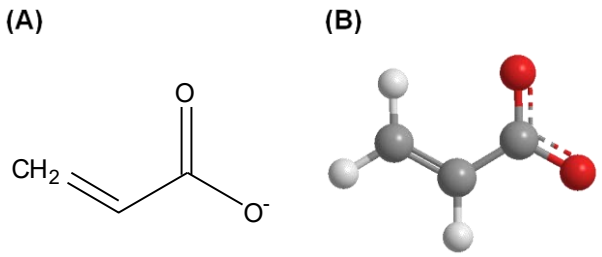

Figure 1.6. (A) Chemical structure and (B) 3D ball and stick model of acrylate. Colour code: grey, carbon; white, hydrogen; red, oxygen.

Table 1.1. Acrylate measurements in 18 hard coral species from the Great Barrier Reef adapted from Tapiolas et al. (2013). ND, not detectable.

Family	Species	Acrylate (nmol mm^{-2})
Acroporidae	*Acropora millepora*	15.223
	Montipora spp.	0.387
Agariciidae	*Pachyseris* spp.	0.803
Euphyllidae	*Physogyra lichtensteini*	0.330
Faviidae	*Diploastrea heliopora*	ND
	Platygyra sinensis	0.936
	Goniastrea aspera	0.253
	Echinopora spp.	8.235
Fungiidae	*Fungia* spp.	ND
Merulinidae	*Merulina ampliata*	2.588
	Hydnophora exesa	0.759
Mussidae	*Symphyllia recta*	0.171
Oculinidae	*Galaxea fascicularis*	1.457
Pocilloporidae	*Seriatopora hystrix*	0.083
	Pocillopora damicornis	0.035
	Stylophora pistillata	0.130
Poritidae	*Porites* spp.	1.083
	Porites cylindrica	2.945

Acrylate, which is more commonly known for its use as an important industrial chemical feedstock for acryloyl polymers in paints and other products of the petrochemical industries (Curson et al., 2014; Tong et al., 2016), is produced in nature. It exhibits high levels of toxicity, for example it is capable of inhibiting photosynthesis in green plants (Swanson and Jacobson, 1955). However, it is non-toxic in dilute concentrations in certain animal tissues such as in the gut of pygoscelid penguins (Sieburth, 1959, 1961). Previously, the only reports of high levels of naturally occurring acrylate were in the epiphytic intertidal alga, *Polysiphonia lanosa*, through investigations of its precursor, DMS (Haas, 1935). In recent years, high levels of acrylate – up to one order of magnitude greater than those of DMSP – have been measured in fast-growing, reef-building corals such as *Acropora* sp. (Tapiolas et al., 2010; Tapiolas et al., 2013). It was suggested that the variations in acrylate levels measured from different coral species may be due to a slower turnover of acrylate compared to DMSP in *Acropora* and several other branching corals, or that acrylate may be stored in these corals (Tapiolas et al., 2013). The reason for its accumulation in corals is currently unknown although it has been correlated to temperature stress (Westmoreland et al., 2017). The dramatic change in acrylate concentrations caused by oxidative stress was also

confirmed in Symbiodiniaceae-free coral tissue, which suggests the metabolite could be of animal origin (Westmoreland et al., 2017).

The intracellular presence of acrylate can inhibit bacterial growth (Sieburth, 1961; Todd et al., 2012b). However, some bacteria can thrive in high concentrations of acrylate (Noordkamp et al., 2000) with some, including Gammaproteobacteria isolated from corals (Raina et al., 2009), using it as a sole carbon source for growth (Yoch, 2002; Todd et al., 2010; Curson et al., 2011a). Coral mucus, the animal's first line of defence against diseases, has a lower pH (~7.7) compared to its surrounding waters (Wild et al., 2005), probably due to the presence of large amounts of acrylate (Broadbent and Jones, 2004). Acrylate carries a negative charge in aqueous environments, enabling the compound to scavenge hydroxyl radicals (Westmoreland et al., 2017) making it a much more effective antioxidant than its precursor, DMSP (Sunda et al., 2002). These properties raise the possibility that acrylate may play an important role – directly or indirectly – in coral defence, particularly against disease-causing pathogens or oxidative stress (Sunda et al., 2002; Reshef et al., 2006; Ritchie, 2006; Raina et al., 2009).

Although there are very few known instances of acrylate accumulation in biological organisms, its presence may have escaped attention due to its rapid flux through a catabolic pathway and its ability to autopolymerise (Sieburth, 1961). Many bacteria can convert exogeneous acrylate to acryloyl-CoA, an active cytotoxic electrophile that attacks sulphhydryl groups (Herrmann et al., 2005; Todd et al., 2012b; Curson et al., 2014). To overcome this, the AcuI enzyme, with widespread distribution in a range of bacterial phyla, plays a primary role in reducing the concentrations of acryloyl-CoA to sub-inhibitory levels (Todd et al., 2012b). The *acuI* gene can be found closely linked to *ddd*- or *dmdA* genes, raising the possibility that this close linkage helps DMSP/DMS-producing bacteria and their host overcome acrylate toxicity (Curson et al., 2014). However, this does not explain why corals, a major producer of DMSP, accumulate high levels of acrylate in its toxic form. In 1960, acrylate was discovered from a green mucilaginous alga, *Phaeocystis pouchetii* (Sieburth, 1960). While it is an acidic volatile substance *in vivo*, it polymerises upon concentration to form inactive residues (Sieburth, 1961). While the polymerisation of acrylate has extensive application in a variety of commercial and industrial uses (Donnet et al., 2005), it is not known whether the coral holobiont can polymerise bioaccumulated acrylate, and if so, whether it is subsequently used for any physiological purpose.

1.6 DMSP metabolism and coral calcification

DMSP metabolism and subsequent acrylate production might play a role in coral calcification. The coral calcification process begins within the skeletal organic matrix (SOM)

(Allemand et al., 1998), an extracellular calcifying medium that is located between the skeleton-forming calicoblastic tissue layer and the growing skeleton (Reggi et al., 2014; Falini et al., 2015). The SOM is a viscous medium composed of macromolecules and ions arranged in a geometric lattice structure of crystallised calcium carbonate ($CaCO_3$) (Figure 1.7) (Michenfelder et al., 2003; Ajikumar et al., 2005; Goffredo et al., 2011; Weiner and Addadi, 2011; Kalmar et al., 2012; Falini et al., 2015; DeCarlo et al., 2018). The arrangement forms a three-dimensional framework, around which $CaCO_3$ is precipitated (Ni and Ratner, 2008; Reggi et al., 2014; Sancho-Tomás et al., 2014). The crystallisation of $CaCO_3$ can result in several structures including calcite and vaterite (Ni and Ratner, 2008), however, modern scleractinian corals primarily form aragonite, a polymorph whose stability is highly sensitive to changes in ocean pCO_2 (Orr et al., 2005; Feely et al., 2009).

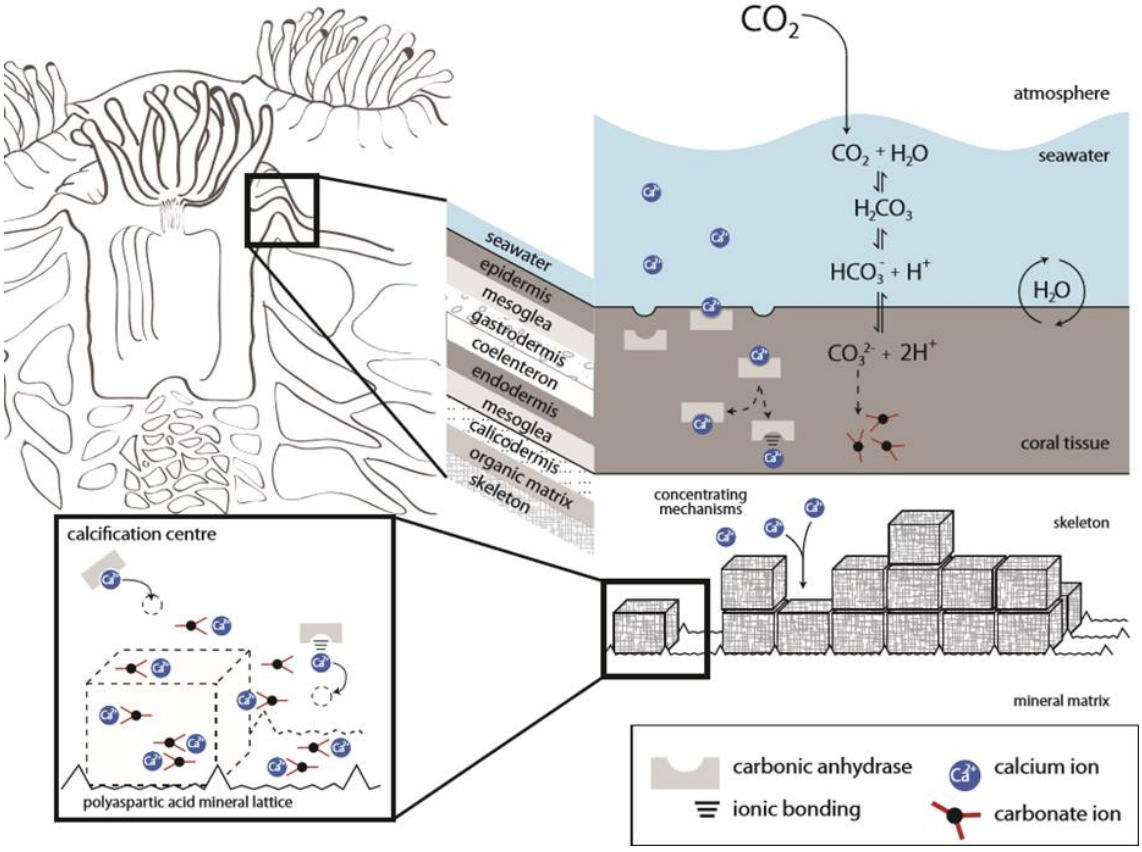

Figure 1.7. Polyp tissues of a scleractinian coral showing the transport mechanisms for calcium (blue) and carbonate (black and red) ions into the organic matrix. Inset shows the calcification centre, where the ions are arranged to form aragonite crystals along the mineral matrix.

High concentrations of aspartate (or aspartic acid) ($C_4H_6NO_4^-$; Figure 1.8a) has been found within the SOM (Reggi et al., 2014). This compound is capable of binding with calcium

ions (Ca^{2+}) (Puverel et al., 2007), making it a very prevalent and functional compound during Ca^{2+} precipitation. The arrangement of Ca^{2+} within the lattice structure is maintained through aspartate-rich proteins during confined mineral formation (Rahman and Oomori, 2008), and in its polymerised form (Figure 1.8b), polyaspartic acid has been hypothesised to be able to influence the orientation of molecules to achieve crystallisation (Taylor and Sigmund, 2010; Cantaert et al., 2013).

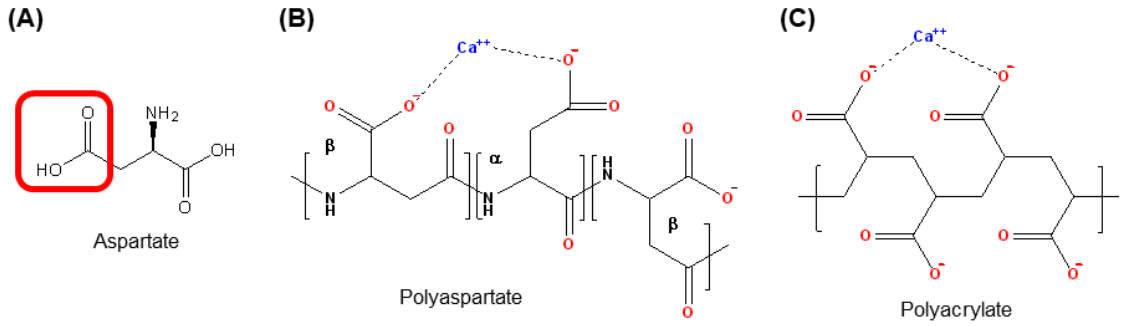

Figure 1.8. (A) Chemical structure of aspartate, with its carboxyl group is highlighted within a red box, (B) polyaspartate and (C) polyacrylate, with their carboxyl groups denoted in red, and dotted lines indicating the chelation of calcium ions (Ca^{2+}).

Acrylate, in its polymerised form, i.e., polyacrylate (Figure 1.8c), bears a strong resemblance to polyaspartate. The high concentration of acrylate in fast-growing corals from the genus *Acropora* suggests that polyacrylate may be utilised by these corals to drive calcification in a similar manner as polyaspartate. If acrylate is used by corals for calcifying purposes, this would explain why vast amounts of acrylate appear to be produced and accumulated in their tissues despite its toxicity.

1.7 Thesis aims and research directions

Coral-associated bacteria are known to utilise DMSP as a nutrient source, with the capability to catabolise this compound through various pathways. However, the recent discovery that prokaryotes are also capable of synthesising DMSP suggests that coral-associated bacteria may have more prominent roles with regards to the sulphur cycle within the coral holobiont. Therefore, the overarching goals of this thesis are (i) to determine if coral-associated bacteria can produce DMSP, (ii) to identify the environmental factors influencing DMSP production, and (iii)

to elucidate the functional role of acrylate, a breakdown product of DMSP, in corals. To accomplish these goals, the following objectives will be addressed:

1. **Determine the occurrence and diversity of DMSP-producing bacteria in corals.** This will be achieved by determining if coral-associated bacteria harbour the key biosynthetic gene, *dsyB*. Production of DMSP in isolates that are *dsyB*-positive will then be confirmed using nuclear magnetic resonance (NMR) and mass spectrometry.

2. **Investigate the metabolic potential of DMSP-producing coral-associated bacteria.** The genome of abundant DMSP-producing bacteria will be fully sequenced to determine their metabolic capabilities and contribution to the sulphur cycling in the coral holobiont.

3. **Quantify how environmental stress affect bacterial DMSP production.** Abundant DMSP-producing bacteria will be subjected to stressors known to affect coral reefs worldwide, such as temperature, UV, and salinity. The effect of these stressors on bacterial production of DMSP will be quantified by NMR and quantitative PCR.

4. **Investigate the influence of acrylate on coral calcification.** Finally, the functional role of acrylate in coral calcification will be investigated using stable isotope tracking, nano-scale secondary ion mass spectrometry (nanoSIMS) and Raman spectroscopy. This unique combination of techniques will aim to follow acrylate incorporation and localisation of its polymer in coral skeleton at high-spatial resolution.

Chapter 2:
Isolation and identification of DMSP-producing bacteria in corals

Abstract

Dimethylsulphoniopropionate (DMSP) is a signature molecule for life at sea. This small sulphur compound is produced in large amounts by marine organisms (more than a billion tons per year globally) and plays a pivotal role in the sulphur cycle. Until recently, DMSP was thought to be synthesized by photosynthetic organisms only, but some corals and heterotrophic bacteria have since been shown to produce it. Within the coral holobiont, DMSP production has been attributed to both the coral animal and their algal partner Symbiodiniaceae, however, their diverse associated bacteria could potentially be a cryptic source of DMSP. Here, bacteria associated with corals were isolated and screened for potential DMSP-producing ability by targeting the bacterial DMSP synthesis gene, *dsyB*. Of the 240 bacteria strains obtained, 6% of the isolates harboured *dsyB*. All the *dsyB*-harbouring bacteria belonged to the Alphaproteobacteria class and their capability to produce DMSP was confirmed through liquid chromatography-mass spectrometry (LC-MS) and nuclear magnetic resonance (NMR) measurements. These results show that coral-associated bacteria can produce DMSP and have the ability to contribute to the large DMSP pool produced by the coral holobiont.

2.1 Introduction

Dimethylsulphoniopropionate (DMSP) is the most abundant organic sulphur compound in the ocean (Johnston et al., 2012) and is central to the marine sulphur cycle (Sievert et al., 2007). This molecule has multiple proposed roles in the marine environment. It is an osmolyte (Kirst, 1996; Stefels, 2000; Yoch, 2002), an antioxidant (Sunda et al., 2002; Deschaseaux et al., 2014b; Gardner et al., 2016), a chemoattractant (Steinke et al., 2002; DeBose and Nevitt, 2007; Seymour et al., 2010) and a cryoprotectant (Karsten et al., 1996) for various marine organisms. DMSP is the precursor of dimethylsulphide (DMS) (Turner et al., 1988), the most abundant biogenic sulphur compound released into the atmosphere. DMS gives the oceans their signature smell and plays a role in the formation of clouds (Andreae et al., 1983; Bates et al., 1987; Kettle and Andreae, 2000; Meskhidze and Nenes, 2006; Lana et al., 2011). Furthermore, DMSP is an essential nutrient source for marine bacteria (Kiene et al., 2000; Wagner-Döbler and Biebl, 2006; Curson et al., 2011b), contributing up to 95% of their sulphur and 15% of their carbon demands (Zubkov et al., 2001; Simó et al., 2002).

DMSP production has long been thought to be restricted to photosynthetic eukaryotes living in or near the marine environment, however, it is now clear that photosynthesis is not a prerequisite for DMSP production. Indeed, marine bacteria found in saltmarshes, seafloor sediments and the water column (Curson et al., 2017; Williams et al., 2019) have recently been shown to produce DMSP. Tropical coral reefs are recognised as DMSP hotspots, particularly when their coral biomass is high (Jones and Trevena, 2005). In reef-building corals, DMSP is produced by the photosynthetic endosymbionts from the family Symbiodiniaceae (Keller et al., 1989; Hill et al., 1995; Broadbent et al., 2002; Van Alstyne et al., 2009; Yost and Mitchelmore, 2009; Steinke et al., 2011), but can also be produced by the coral host itself (Raina et al., 2013; Aguilar et al., 2017). Yet, the potential roles played by coral-associated microorganisms in the production of the exceptionally high DMSP concentrations measured in some reef-building corals has never been investigated.

Bacteria are abundant in and around corals (Ducklow and Mitchell, 1979; Rohwer et al., 2002; Koren and Rosenberg, 2006; Ritchie, 2006; Kooperman et al., 2007; Rosenberg et al., 2007). Together with protists, fungi, archaea, and viruses they form a consortium called the coral holobiont (Rohwer et al., 2002). However, the roles they play within the coral holobiont are still poorly understood. A recent genomic-based assessment of the coral microbiome has indicated that bacteria and archaea potentially support central metabolic processes of the eukaryotic partners through the fixation of carbon, nitrogen cycling through transformation of ammonia, urea and nitrate (Robbins et al., 2019), and supply of essential B-group vitamins. The metabolic pathway of DMSP along with that of another sulphur containing small molecule taurine (or 2-aminoethanesulphonic acid) were also identified within these coral-associated prokaryotic communities (Robbins et al., 2019). These results along with other previous studies have shown that coral-associated bacteria can catabolise DMSP to support their growth (Raina et al., 2009; Raina et al., 2010; Frade et al., 2016). However, it is unknown if coral-associated bacteria can directly produce DMSP.

One of the key genes involved in the DMSP biosynthesis pathway, *dsyB*, was first identified within the Alphaproteobacteria class (Curson et al., 2017). Alphaproteobacteria represents up to 30% of coral-associated microbiota in reef-building corals (Frias-Lopez et al., 2002; Rohwer et al., 2002; Bourne and Munn, 2005; Wilson et al., 2012; Blackall et al., 2015), and have been involved in nitrogen fixation (Lema et al., 2014; Zhang et al., 2016), antimicrobial production (Raina et al., 2016), and maintaining microbial community structure through quorum-sensing (Li et al., 2017). Close homologues of DsyB, a methylthiohydroxybutryate methyltransferase enzyme, exist in the orders Rhodobacterales, Rhizobiales, and Rhodospirillales, which are all abundant in marine environments (Dang et al., 2008; Curson et

al., 2017; Curson et al., 2018). Here, we investigated the bacteria associated with six common species of reef-building corals from the Great Barrier Reef (GBR). We hypothesized that these corals harbour DMSP-producing bacteria, which may contribute towards the overall DMSP pool produced by the holobiont. Bacterial isolates were screened for the presence of the *dsyB* gene, and their capacity to produce DMSP established through chemical analysis.

2.2 Methodology

2.2.1 Sample collection

A total of six scleractinian coral species were sampled opportunistically to isolate coral-associated bacteria. All corals appeared healthy when the samples were collected, with no visual signs of bleaching or disease. One colony each of *Acropora millepora* and *A. tenuis* were sourced from Davies Reef (18°49'03.7"S, 147°38'39.6"E) and transported to the National Sea Simulator (SeaSIM) at the Australian Institute of Marine Science (AIMS) to acclimate for a week before sampling. Long term acclimated SeaSIM corals *Pocillopora acuta* and *Stylophora pistillata* were also sampled to source a wider range of coral-associated isolates.

Corals held in SeaSIM were rinsed in sterile artificial sea water (ASW) and coral mucus collected from five nubbins per colony using sterile 50 ml syringes fitted with 20-gauge hypodermic needles. Mucus samples were kept on ice, transferred to the lab and processed within an hour. In addition, two coral nubbins per colony were sampled using bone cutters and placed in separate Whirl-Pak sterile sample bags (Nasco, Wisconsin, United States). Coral nubbins were immediately air-brushed with 5 ml of sterile ASW to remove coral tissue and their associated microorganisms from the coral skeleton. The tissue slurry was homogenised using sterile Potter-Elvehjem tissue grinders and subsequently transferred into sterile 50 ml centrifuge tubes, placed on ice and processed within an hour. The stripped coral skeletons were then crushed using a sterilised pestle and mortar, applying up to 40 psi of pressure with a French press and the resulting skeletal powder transferred into 50 ml centrifuge tubes which was used immediately.

Additionally, one colony each of *A. millepora*, *A. tenuis*, *A. spathulata*, and *Montipora spumosa* were collected at the Orpheus Island Research Station (OIRS; 18°36'49.7"S, 146°29'21.4"E) and held in flow-through raceway aquaria for up to three days. Mucus swabs were taken from three nubbins per coral colony, using sterile cotton buds stored individually in 15 ml centrifuge tubes. The collected swabs were kept on ice, transferred to the lab and processed within 10 min.

2.2.2 Bacterial isolation

To increase the probability of obtaining DMSP-producing bacteria, a methionine-enriched medium was used thereby providing the isolates with a reduced-sulphur precursor required for DMSP biosynthesis (Curson et al., 2017). Each coral sample type (mucus, tissue slurry and crushed skeleton) was diluted in ASW (2-fold, 10-fold, 100-fold, and 1,000-fold). Aliquots (50 µl) of each dilution were then spread onto Difco Marine Agar 2216 (MA; Becton Dickinson, New Jersey, United States) and modified minimal basal medium (MBM) agar enriched with a mixed carbon source (300 mM; details in Table 2.1), methionine ($C_5H_{11}NO_2S$; 0.5 mM), and ammonium chloride, (NH_4Cl; 20 mM) as nitrogen source. Agar plates were incubated at 28°C in the dark for one week and inspected daily for growth and the formation of morphologically distinct individual colonies. Colonies were picked using sterile 20 µl pipette tips and resuspended in 5 ml of Difco Marine Broth 2216 (MB; Becton Dickinson, New Jersey, United States). The isolates were incubated at 28°C and 180 RPM until growth was visible. These liquid cultures were replated on MA and this procedure repeated until pure isolates were obtained. Isolates were then cultured in liquid MB and aliquots of each isolate stored in 20% v/v glycerol at -80°C.

Table 2.1. Modified minimal basal medium composition used for the isolation of DMSP-producing coral-associated bacteria based on Baumann and Baumann (1981) and Curson et al. (2017).

Solution	Component	Volume or weight per litre
Basal media[a]	1M Tris-HCl (pH 7.5)	300 ml
	Dipotassium phosphate (K_2HPO_4)	0.174 g
	Ammonium chloride (NH_4Cl)	1 g
	Milli-Q water	750 ml
FeEDTA stock[a]	Ethylenediaminetetraacetic acid ferric (FeEDTA) sodium salt ($C_{10}H_{12}N_2NaFeO_8$)	5 g
	Milli-Q water	1,000 ml
Mixed carbon source[b]	Succinate ($C_4H_6O_4$)	54 g
	Glucose ($C_6H_{12}O_6$)	36.3 g
	Sucrose ($C_{12}H_{22}O_{11}$)	68.46 g
	Pyruvate ($C_3H_4O_3$)	17.6 g
	Glycerol ($C_3H_8O_3$)	14.6 ml
	Milli-Q water	985.4 ml
Vitamin supplement[b] (100 ml)	Biotin ($C_{10}H_{16}N_2O_3S$)	2 mg
	Folic acid ($C_{19}H_{19}N_7O_6$)	2 mg
	Pyridoxine-HCl ($C_8H_{12}ClNO_3$)	10 mg
	Riboflavin ($C_{17}H_{20}N_4O_6$)	5 mg
	Thiamine ($C_{12}H_{17}N_4OS^+$)	5 mg
	Nicotinc acid ($C_6H_5NO_2$)	5 mg

	Pantothenic acid ($C_9H_{17}NO_5$)	5 mg
	Cyanocobalamin ($C_{63}H_{88}CoN_{14}O_{14}P$)	0.1 mg
	p-aminobenzoic acid ($C_7H_7NO_2$)	5 mg
	Milli-Q water	100 ml
Mix	Sea salts	35 g
	Basal media	250 ml
	Milli-Q water	394 ml
	FeEDTA†	50 ml
	Mixed carbon source†	300 ml
	Vitamin supplement†	1 ml
	Methionine ($C_5H_{11}NO_2S$) [b†] (optional)	5 ml

[a]Solutions were prepared and autoclaved separately before being combined.
[b]Solutions were prepared and filtered using gamma sterilised 0.22 µm Millex-GP syringe filters (Merck, New Jersey, United States) before being combined.
†Solutions were added post-autoclaving once media had cooled to ~50°C.

2.2.3 DNA extraction and purification

DNA extraction from single strain liquid cultures grown overnight in MB at 28°C was performed using the DNeasy UltraClean Microbial Kit (Qiagen, Hilden, Germany) according to the manufacturer's protocol. The extracted DNA were quantified on a NanoDrop ND-1000 UV-Vis spectrophotometer (Thermo Fisher Scientific, Massachusetts, United States). Aliquots of extracted DNA were diluted with sterile Milli-Q water to 10 ng μl^{-1} and stored at -20°C until required.

2.2.4 PCR amplification of bacterial 16S rRNA and dsyB *genes*

DNA obtained from the isolated coral-associated bacterial strains was screened using the universal primers 27F and 1492R (Lane, 1991), designed to amplify bacterial 16S ribosomal RNA (rRNA) genes, as well as the *dsyB* specific primers dsyB_deg1F and dsyB_deg2R that amplify a 246 bp region of the gene (Williams et al., 2019). Each PCR reaction mixture contained 1× reaction buffer containing NH_4, 2 mM of $MgCl_2$ solution, 1 mM of deoxyribonucleotide triphosphate (dNTP) mix, 0.4 mM of each primer, and 0.5 µl of BIOTAQ DNA Polymerase (Bioline, London, United Kingdom), adjusted to a final volume of 25 µl with UltraPure DNase/RNase-free distilled water (Thermo Fisher Scientific, Massachusetts, United States). Approximately 1 ng μl^{-1} of template DNA was used for each reaction.

Rapid temperature cycling for PCR amplifications was as follows: (i) dsyB_deg1F/ dsyB_deg2R: initial heating at 95°C for 5 min; 30 cycles at 95°C for 30 s, 61°C for 1 min and 72°C for 15 s; and a final extension step at 72°C for 5 min; (ii) 27F/1492R: as described by Bourne

and Munn (2005). PCR products were purified with the Wizard SV Gel and PCR Clean-Up System (Promega, Wisconsin, United States) and visualised via electrophoresis on a 1% agarose gel stained with ethidium bromide. DNA of *Amorphus coralli* DSM19760 and *Oceanicola batsensis* HTCC2597, which harbour *dsyB* (Curson et al., 2017) were used as positive controls.

2.2.5 Sequencing and phylogenetic analysis

PCR products were sent for Sanger sequencing at Macrogen Inc. (Seoul, South Korea). The forward and reverse 16S rRNA and *dsyB* amplicon sequences were paired and the overlapping fragments were merged using Geneious Prime 2019.2.3 (Biomatters, Auckland, New Zealand) where possible. Some *dsyB* amplicon sequences were too short or degraded to be paired and merged, therefore in those instances, only one (either forward or reverse) sequence was used.

Nucleotide BLAST searches (Altschul et al., 1990) were conducted using the 16S rRNA database obtained from the National Center for Biotechnology Information (NCBI) to identify the closest taxonomic-related strains of the isolated coral-associated bacteria. The 16S rRNA sequences were aligned using MAFFT (Multiple Alignment using Fast Fourier Transform) version 7 (Katoh et al., 2002; Katoh and Standley, 2013) using default settings, then trimmed using trimAl version 1.4 (Capella-Gutiérrez et al., 2009) to remove sites with more than 50% missing or degraded data. Following the Bayesian Information Criterion (Schwarz, 1978), the maximum likelihood phylogeny for each sample niche was calculated. The phylogenetic tree was constructed using IQ-TREE version 1.6.12, with 1,000 ultrafast bootstrap replicates (Minh et al., 2013) used to assess node support, and formatted using the ggtree package (Yu et al., 2017) in R (R Core Team, 2020) through RStudio (RStudio Team, 2015).

The *dsyB* amplicon sequences were translated into protein sequences and searches to find regions of local similarity performed using BLASTP. These translated sequences were also aligned with the known DsyB protein from *Labrenzia aggregata* (AOR83342) (Curson et al., 2017) to assess for similarity using the Needleman-Wunsch algorithm (Needleman and Wunsch, 1970). A multiple sequence alignment (MSA) of the prokaryotic DsyB protein sequences was visualised to show conserved residues, conservative mutations, and divergence between the different homologues. The MSA was conducted using T-Coffee version 11.00 (Notredame et al., 2000; Di Tommaso et al., 2011) (available at http://tcoffee.crg.cat/apps/tcoffee/do:regular) with default settings and formatted using Boxshade 3.21 (available at https://embnet.vital-it.ch/software/BOX_form.html).

The bacterial 16S rRNA gene amplicon sequences reported in this study have been deposited in GenBank (https://www.ncbi.nlm.nih.gov) under accession codes MW828351 to MW828582.

2.2.6 Synthesis of DMSP

DMSP was synthesised following the method described by Chambers et al. (1987) and Oduro et al. (2011) with some modifications. All chemicals were sourced from Sigma Aldrich (Missouri, United States). Briefly, sulphuric acid (H_2SO_4) was dripped onto sodium chloride (NaCl) in an airtight flask, producing hydrogen chloride (HCl) gas which was then bubbled slowly through a stirring mixture of dichloromethane (CH_2Cl_2; 20 ml), DMS (5 ml) and acrylic acid (CH_2=CHCOOH; 4 ml distilled over copper wool). The white precipitate was subsequently filtered and recrystallised with ice-cold ethanol to remove any unreacted acrylic acid, then freeze-dried overnight to give DMSP (2.11 g or 27% yield; ~95% purity as determined by ^{1}H-NMR).

2.2.7 Culture of dsyB-*positive bacterial strains*

dsyB-positive bacterial strains were cultured in 500 ml of MB and yeast tryptone sea salts (YTSS; as described in González et al. (1996)) mixed with either unmodified MBM broth or methionine-enriched MBM broth. The cultures were incubated at 28°C and 180 RPM, then harvested after 24 hours by centrifugation (3,000 *g* for 15 min at 4°C). All supernatant was transferred into 50 ml centrifuge tubes, snap-frozen with liquid nitrogen and stored at -20°C until required. The cell pellets were also snap-frozen with liquid nitrogen, lyophilised overnight (Dynavac freeze dryer, Massachusetts, United States; model FD12) and stored at -20°C until required.

2.2.8 Liquid chromatography-mass spectrometry (LC-MS)

Liquid chromatography-mass spectrometry (LC-MS) was used to establish the presence or not of intracellular DMSP in bacterial isolates cultured in liquid MB. Cultures were centrifuged (3,000 *g* for 15 min at 4°C), the supernatant decanted and the residual bacterial cell pellet extracted with CH_3OH:H_2O (2:1), vortexed at maximum speed for 5 min and sonicated for 10 min at room temperature followed by centrifugation (3,000 *g* for 5 min). Extracts were analysed on an Agilent 1100 series high performance liquid chromatograph coupled to a Bruker Esquire

3000 quadrupole ion trap mass spectrometer (LC-MS; Bruker Daltonics, Massachusetts, United States) equipped with an electrospray ionisation interface (ESI). Extracts (5 µl) were separated on a reverse-phase Luna 3µ HILIC column (Phenomenex, California, United States; 150 × 3 mm, with a particle size of 3 µm) maintained at 25°C. Separation was achieved using a programmed step gradient consisting of solvent A: 0.1% formic acid (HCOOH) in Milli-Q water and solvent B: methanol (CH_3OH, HPLC grade OmniSolv), at a flow rate of 0.5 ml min^{-1}. The column was pre-equilibrated at 60% B for 10 min prior to injection. The programmed step gradient was t = 0 min, 60% B; t = 12 min, 10% B; t = 14 min, 10% B; t = 15 min, 60% B; t = 20 min, 60% B; t = 22 min, 60% B. The ESI was operated in positive mode and the target mass of *m/z* 135, corresponding to the $[M+H]^+$ of DMSP, monitored (established from a DMSP standard). Acrylate is a product of DMSP catabolism by some bacteria, and therefore its presence was also monitored for by LC-MS. The target mass of *m/z* 117, corresponding to the $[M+HCOOH]^+$ of acrylate, was monitored in positive mode (established from an acrylate standard).

2.2.9 Nuclear magnetic resonance (NMR)

Dried bacterial pellets were resuspended in 2 ml of deuterated methanol (CD_3OD; Cambridge Isotope Laboratories, Massachusetts, United States), vortexed at maximum speed for 5 min and sonicated for 10 min at room temperature. Deuterium oxide (D_2O, 666 µl; Cambridge Isotope Laboratories, Massachusetts, United States) was added to the mixture and again vortexed at maximum speed for 1 min followed by sonication for 5 min at room temperature. The bacterial extracts were then centrifuged at 3,000 *g* for 5 min to pelletize the debris. A 700 µl aliquot of each particulate-free extract was transferred into a 5 mm Norell 509-UP NMR tube (North Carolina, United States) and analysed immediately by ^1H NMR.

NMR spectra of the bacterial extracts were recorded on a Bruker Avance 600 MHz NMR spectrometer (Bruker BioSpin, Massachusetts, United States) with a triple resonance cryoprobe (TXI), referenced using CD_3OD (δ_H 3.31). ^1H NMR spectra were acquired using the steps outlined in (Tapiolas et al., 2013) using a standard Bruker solvent suppression pulse sequence. 2D NMR spectra were also acquired to confirm assignment of DMSP. All spectra were referenced to residual ^1H and ^{13}C resonances in CD_3OD. In addition, given the zwitterionic nature of DMSP, one extract was spiked with 14 µl of 50 mM DMSP (leading to a 1 mM increase in overall DMSP concentration) to confirm the position of the methyl singlet.

2.3 Results

2.3.1 Isolation of coral-associated bacteria

A total of 240 bacteria belonging to 47 different genera were isolated from mucus swabs (35%), coral mucus (33%) and coral tissue (32%). Attempts to isolate bacteria from the crushed coral skeleton samples were unsuccessful. Based on taxonomic identity established from the 16S rRNA gene data, 44 bacterial strains were isolated multiple times from the different coral niches (i.e., mucus swabs, coral mucus and coral tissue). The most abundant taxon of bacteria isolated from each coral niche was the Gammaproteobacteria class, followed by Alphaproteobacteria and Flavobacteria (Figure 2.1).

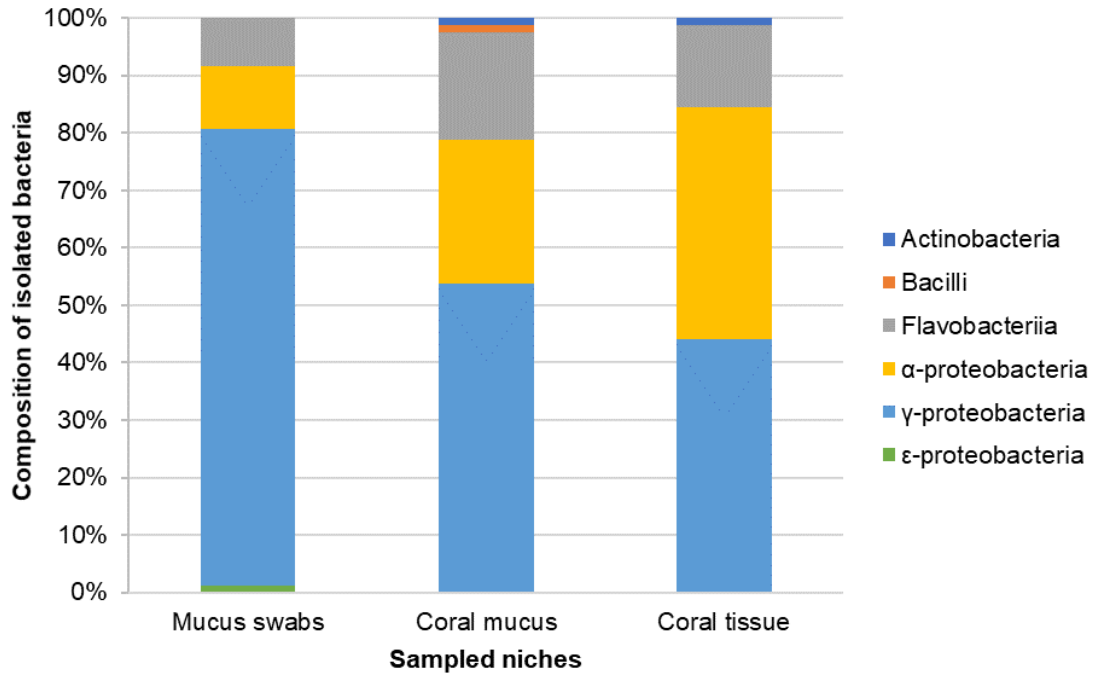

Figure 2.1. Taxonomic composition of isolated coral-associated bacteria, from mucus swabs (83 isolates), coral mucus (80 isolates), and coral tissue (77 isolates).

Table 2.2. Abundance and diversity of coral-associated bacteria isolated from mucus swabs, coral mucus and coral tissue.

Sampled niche	No. of isolates	No. of families	No. of genera	No. of species
Mucus swabs	83	10	17	32
Coral mucus	80	15	30	52
Coral tissue	77	14	29	46

The number of bacteria isolated varied among each sample niche. Isolates obtained from coral mucus and coral tissue belonged to a broader range of phylogenetic groups compared to those from mucus swabs (Table 2.2). This can be attributed to the nature of the mucus swabs which were processed undiluted. Because nutrient-rich growth media favour fast-growing bacterial strains (Stewart, 2012), repeated dilution of the starting samples enabled a wider diversity of slower growing strains to be isolated from coral mucus and coral tissue.

The coral mucus isolates were the most heterogenous across all levels of taxonomy, followed by the coral tissue and mucus swabs isolates. Despite picking approximately the same number of isolates from all three niches, nearly twice as many genera were isolated from the coral mucus and tissue compared to mucus swabs. Although attempts were made to reduce bias when picking colonies, some genera remain over-represented. It is possible that the isolation approaches implemented in this study may preclude the growth of some bacteria species. Maximum-likelihood analyses established the similarity of the bacterial isolates within each niche (Figures 2.2 to 2.4). Many of the isolates grouped together indicating that they are closely related or highly similar strains. This was certainly the case for isolates obtained from mucus swabs (Figure 2.2).

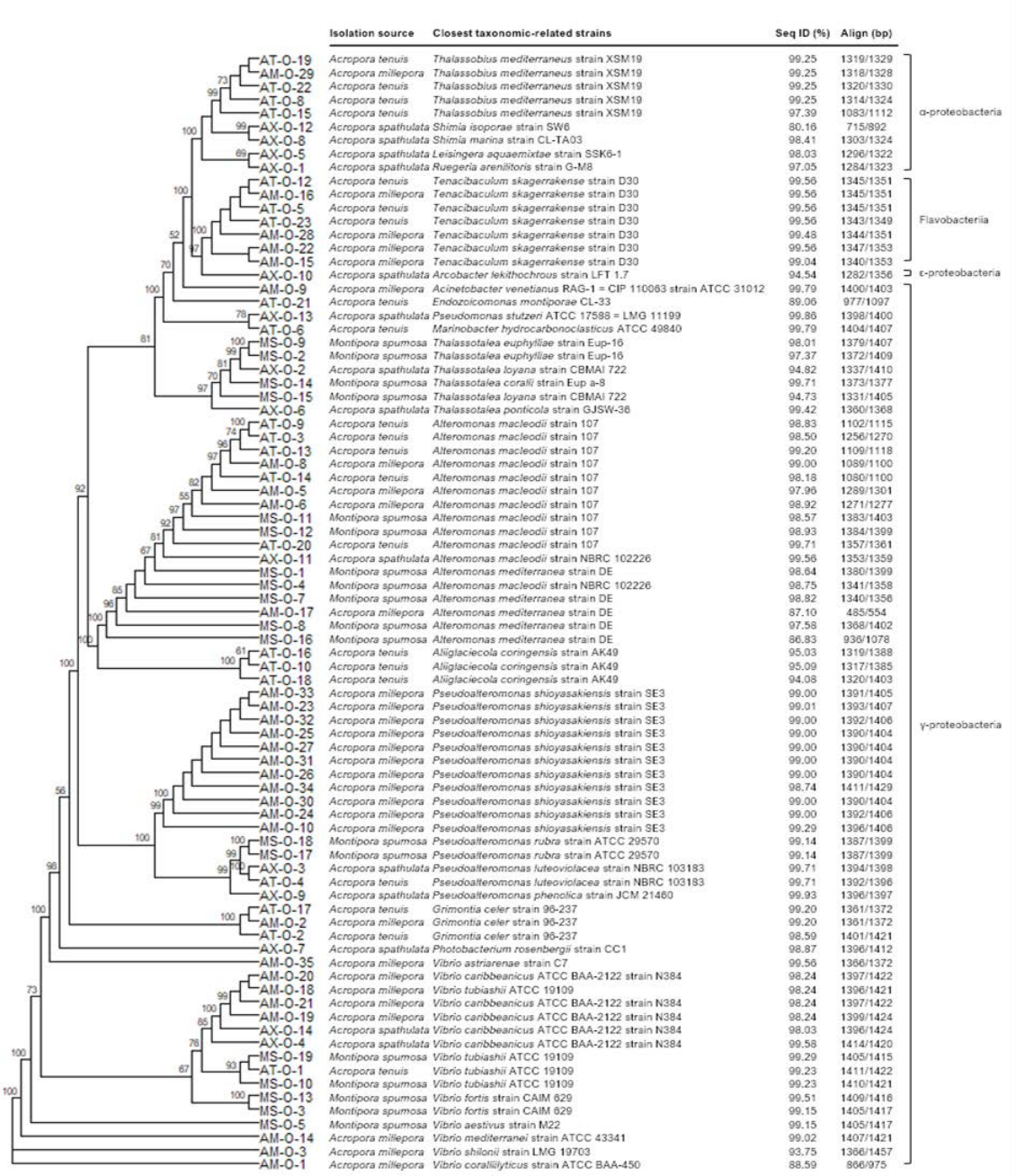

Figure 2.2. Identity of the 83 bacteria isolated from mucus swabs, based on near-complete 16S rRNA sequences. The maximum-likelihood trees were constructed based on MAFFT alignments. Bootstrap support for nodes is indicated with only values of more than 50% indicated.

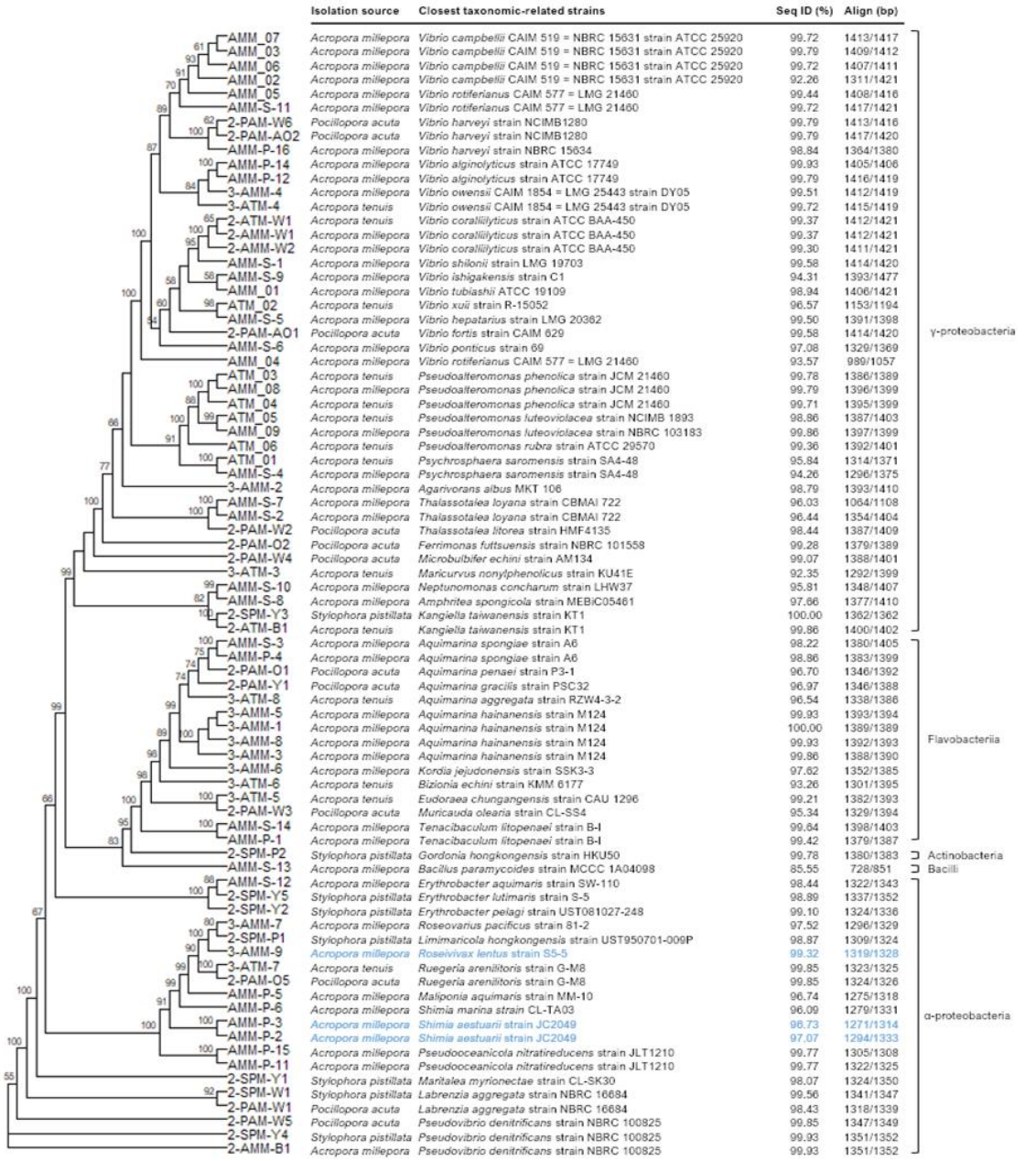

Figure 2.3. Identity of the 80 bacteria isolated from coral mucus, based on near-complete 16S rRNA sequences. The maximum-likelihood trees were constructed based on MAFFT alignments. The isolates in blue are bacteria possessing *dsyB* homologues. Bootstrap support for nodes is indicated with only values of more than 50% indicated.

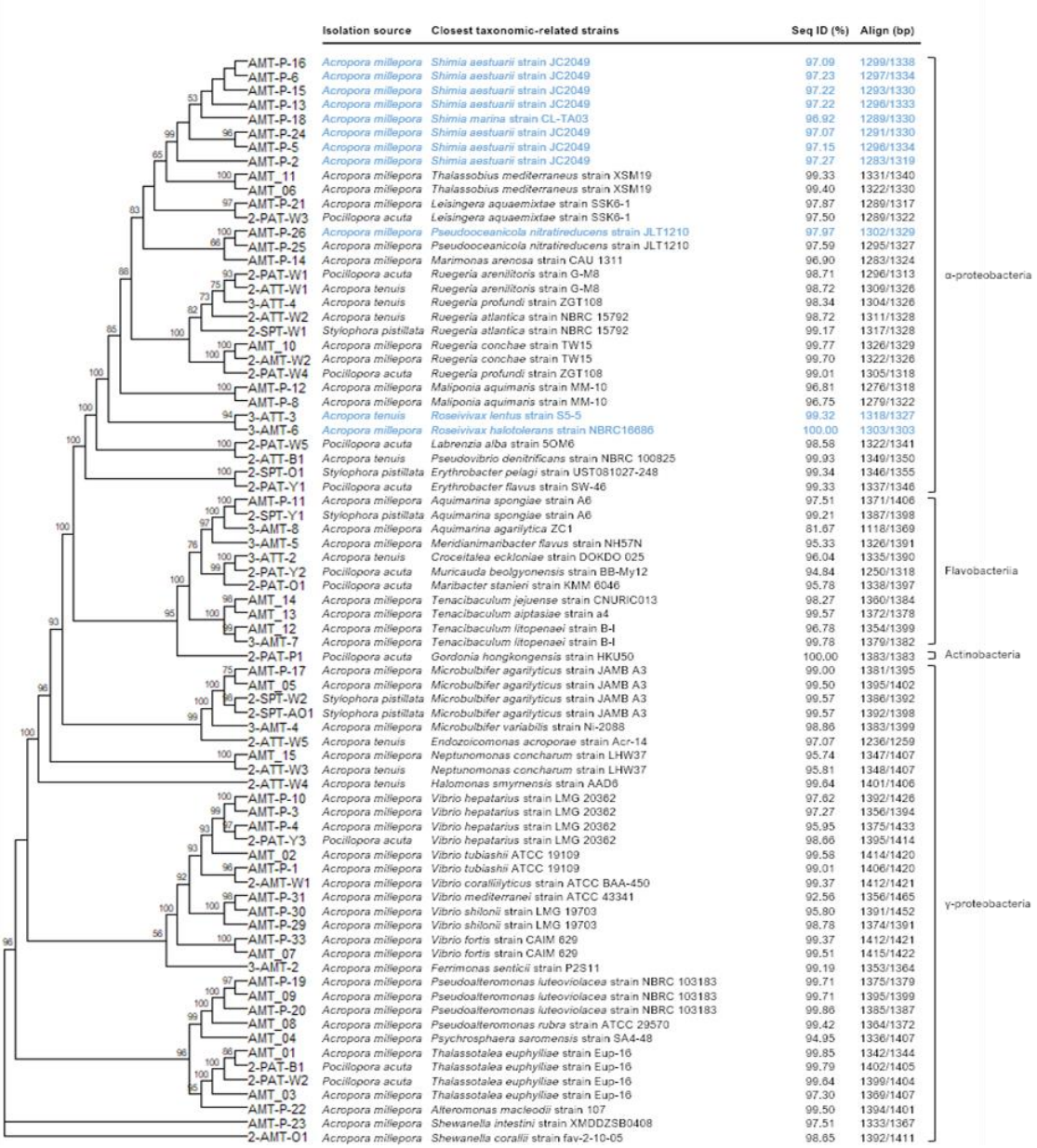

Figure 2.4. Identity of the 77 bacteria isolated from coral tissue, based on near-complete 16S rRNA sequences. The maximum-likelihood trees were constructed based on MAFFT alignments. The isolates in blue are bacteria possessing *dsyB* homologues. Bootstrap support for nodes is indicated with only values of more than 50% indicated.

Of the 48 species isolated, nineteen were common to both the coral mucus and tissue (Figure 2.5), indicating they are true coral associates, potentially occupying the matrix between the coral tissue surface and inner mucus layer, and are unaffected by the surrounding water column. Of these, six genera were also found in mucus swabs: *Pseudoalteromonas* (n = 26 isolates), *Ruegeria* (n = 11 isolates), *Shimia* (n = 13 isolates), *Tenacibaculum* (n = 13 isolates), *Thalassotalea* (n = 13 isolates), and *Vibrio* (n = 52 isolates). Four genera are common between the mucus swabs and coral tissue bacteria composition, including *Alteromonas* (n = 18 isolates),

the ubiquitous *Endozoicomonas* (n = 2 isolates) (Ainsworth et al., 2015; Neave et al., 2017), *Leisingera* (n = 3 isolates), and *Thalassobius* (n = 7 isolates).

Fourteen isolates (6% of the total) were found to harbour the *dsyB* gene. These strains belong to the Alphaproteobacteria class, specifically the family Rhodobacteraceae, and include *Roseivivax* (n = 3), *Shimia* (n = 10), and *Pseudooceanicola* (n = 1) related microorganisms. These *dsyB*-harbouring strains were isolated from the mucus (21%) and tissue (79%) of *Acropora* sp. Preliminary screening also identified a potential match for the gene in a Gammaproteobacterium closely related to *Vibrio hepatarius* (isolate AMT-P-4).

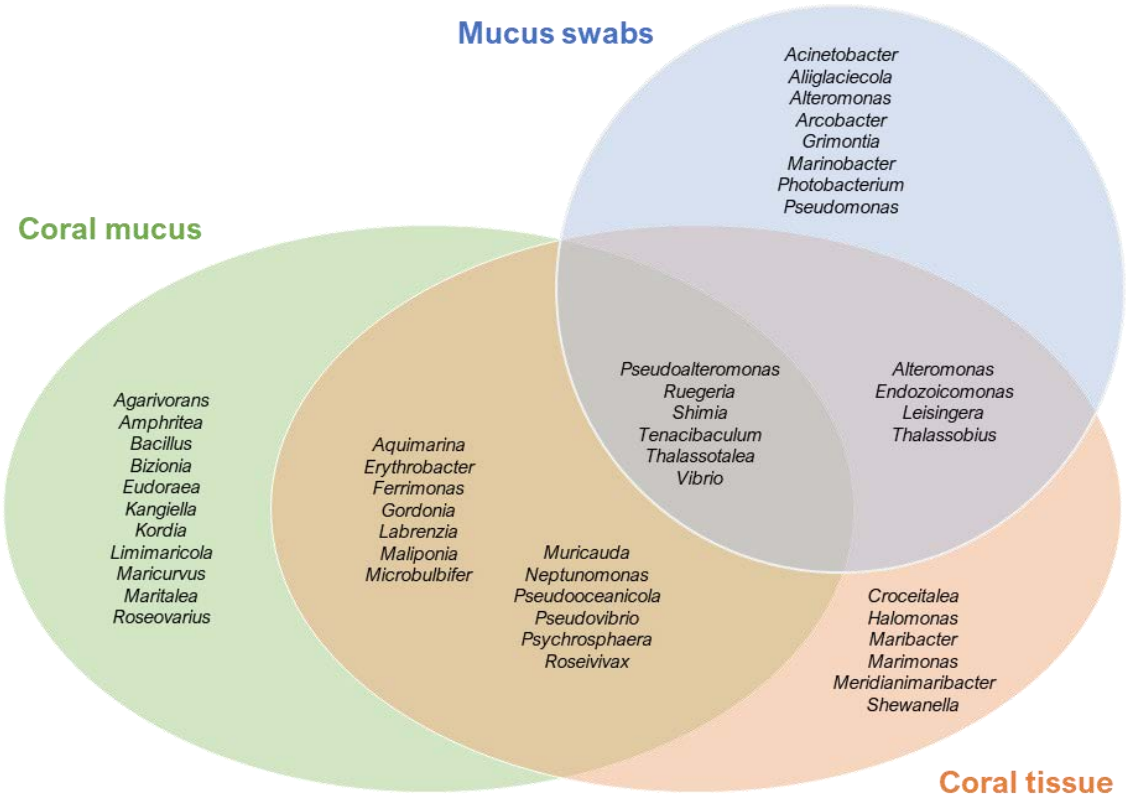

Figure 2.5. Venn diagram showing the bacterial taxa associated with corals (n=48). The three circle Venn diagram shows the distribution of bacteria taxa isolated from coral mucus swabs (blue), mucus (green) and tissue (orange). Nineteen bacterial taxa were common to both the coral mucus and tissue.

2.3.2 Comparative analysis of the dsyB *gene in coral-associated bacteria*

The primers dsyB_deg1F and dsyB_deg2R (Williams et al., 2019) which were used to screen for *dsyB* genes in the isolated bacteria yielded between 150-200 bp of sequence data. The translated amino acid sequences were directly compared to the previously known DsyB protein

obtained from *Labrenzia aggregata* (AOR83342) (Curson et al., 2017). The derived DsyB sequences from the *dsyB*-harbouring isolates showed high sequence identity (see Figure 2.6) with an average of 65% similarity to the described DsyB protein of *L. aggregata* (Curson et al., 2017; Curson et al., 2018). Isolate AMT-P-24 (*Shimia aestuarii*) had the highest sequence identity at 60.3%, while isolate AMT-P-26 (*Pseudooceanicola nitratireducens*) had the lowest sequence identity at 48.1% (Table 2.3).

Figure 2.6. Multiple sequence alignment of DMSP biosynthesis protein DsyB from *Labrenzia aggregata* (Curson et al., 2017) and the DsyB protein amplicons from *dsyB*-positive coral-associated bacteria strains (n=14). The reference protein sequence of *L. aggregata* (AOR83342) is highlighted in blue. Residues that have consensus identity are shaded in black, while conserved substitutions are shaded in grey. Amino acid residues that are conserved across all 15 sequences are marked with asterisks below.

Table 2.3. Selection of protein sequences showing E-values and sequence identity when compared with the *Labrenzia aggregata* DsyB protein sequence.

Accession number	Isolate ID	Closest taxonomic match	E-value	% identity to DsyB
MW828384	3-AMM-9	*Roseivivax lentus*	2e-15	52.63
MW828400	AMM-P-2	*Shimia aestuarii*	2e-12	55.88
MW828401	AMM-P-3	*Shimia aestuarii*	2e-12	55.88
MW828534	3-AMT-6	*Roseivivax halotolerans*	3e-10	51.52
MW828538	3-ATT-3	*Roseivivax lentus*	2e-15	52.63
MW828556	AMT-P-2	*Shimia aestuarii*	2e-12	55.88
MW828559	AMT-P-5	*Shimia aestuarii*	2e-12	55.88
MW828560	AMT-P-6	*Shimia aestuarii*	2e-12	55.88
MW828565	AMT-P-13	*Shimia aestuarii*	3e-11	57.14
MW828567	AMT-P-15	*Shimia aestuarii*	3e-11	57.14
MW828568	AMT-P-16	*Shimia aestuarii*	2e-12	55.88
MW828570	AMT-P-18	*Shimia marina*	2e-12	55.88
MW828576	AMT-P-24	*Shimia aestuarii*	2e-12	55.88
MW828578	AMT-P-26	*Pseudooceanicola nitratireducens*	5e-12	49.02

2.3.3 *DMSP production by coral-associated* dsyB-*positive bacteria*

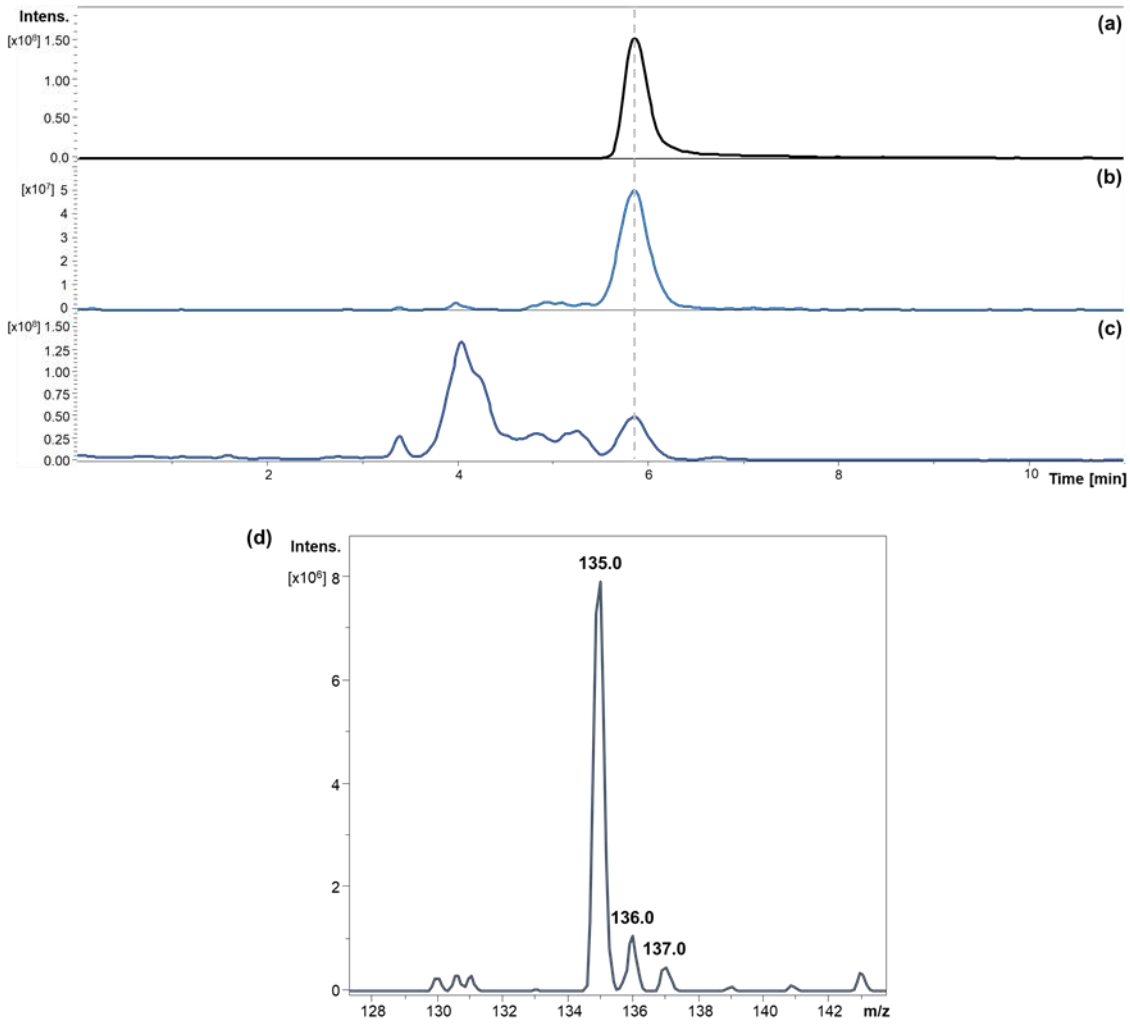

Figure 2.7. Detection of dimethylsulphoniopropionate (DMSP) in the *dsyB*-positive *Shimia* sp. AMM-P-2 (a) DMSP standard ($C_5H_{10}O_2S$; MW=134.197) - extracted ion chromatogram (EIC) of the $[M+H]^+$ ion = 135 *m/z* , and (b) EIC 135 *m/z* of the *Shimia* sp. AMM-P-2 extract, (c) the corresponding base peak chromatogram showing signal resolution, and (d) expanded region of the EIC 135 *m/z* at retention time 5.9 min. LC-MS confirms the production of DMSP by *Shimia* sp.

DsyB-harbouring strains were assessed for their ability to produce DMSP. LC-MS analysis of isolates grown in MBM with methionine enrichment detected a peak at *m/z* 135 and retention time of 5.9 min consistent with DMSP (Figure 2.7). No DMSP was detected in the LC-MS chromatograms of *dsyB*-positive isolates grown in MB and YTSS (Supplementary Data Figure 2.1).

NMR of the bacterial extracts was done to confirm the ion at 135 *m/z* was DMSP. ^{1}H NMR revealed a well-resolved singlet at δ_H 2.95 ppm (2 × CH_3) diagnostic for DMSP (Figure 2.8a and b). Spiking a random sample with DMSP supported the ^{1}H NMR assignment (Tapiolas

et al., 2013) (Figure 2.8c). DMSP was also confirmed to be absent in bacterial extracts of *dsyB*-positive isolates grown in MB and YTSS (Supplementary Data Figure 2.2).

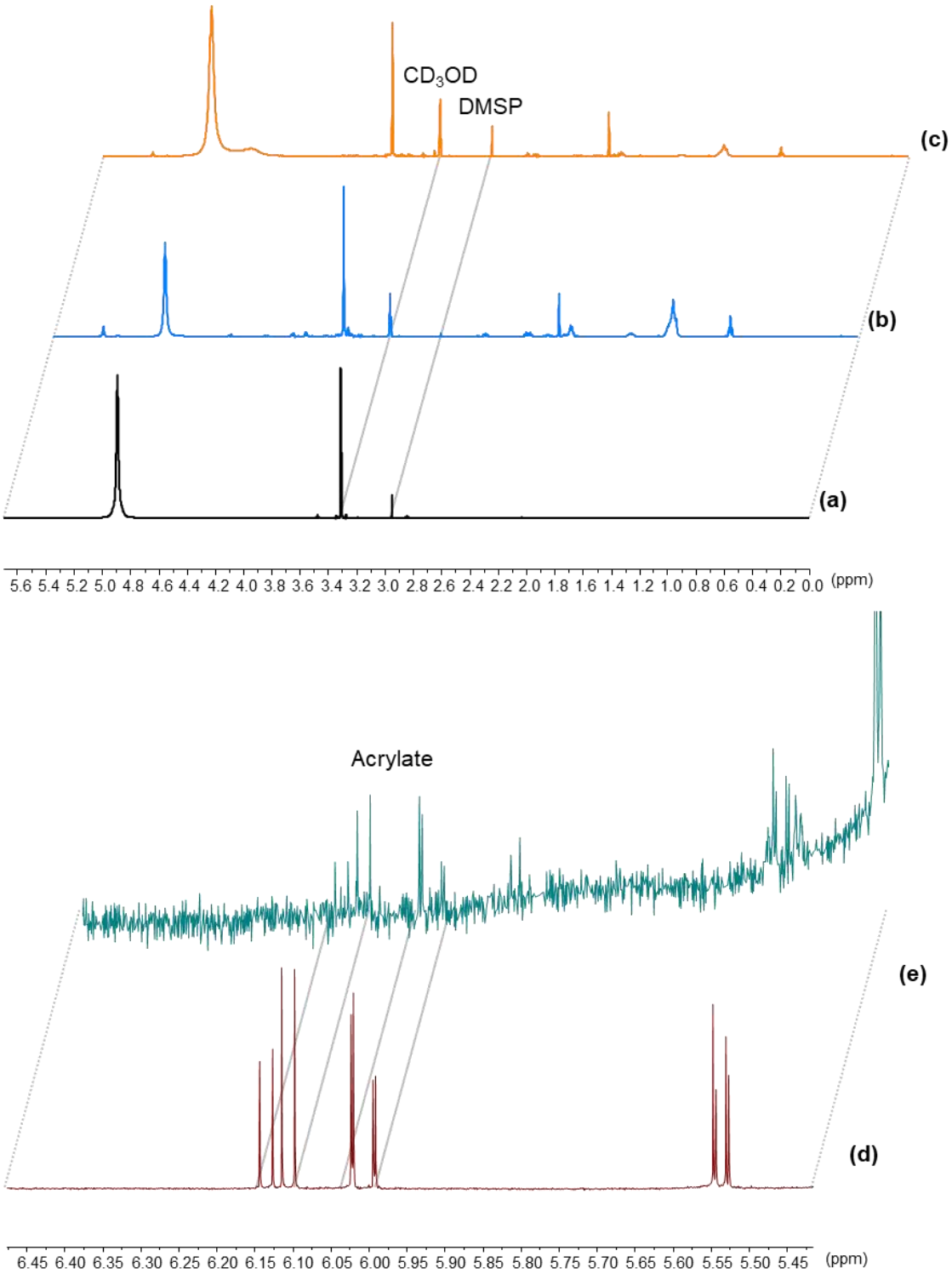

Figure 2.8. ^{1}H NMR spectra of: (a) 1 mM dimethylsulphoniopropionate (DMSP) standard in deuterated methanol (CD_3OD) compared to, (b) extract of a *Shimia* bacterium (isolate AMM-P-2) cultured in methionine enriched minimal basal medium in CD_3OD, (c) the same extracted *Shimia* bacterium spiked

with 10 µl of 1 mM DMSP standard, and (d) 4 mM acrylate standard in CD_3OD compared to (e) extract of AMM-P-2 in CD_3OD.

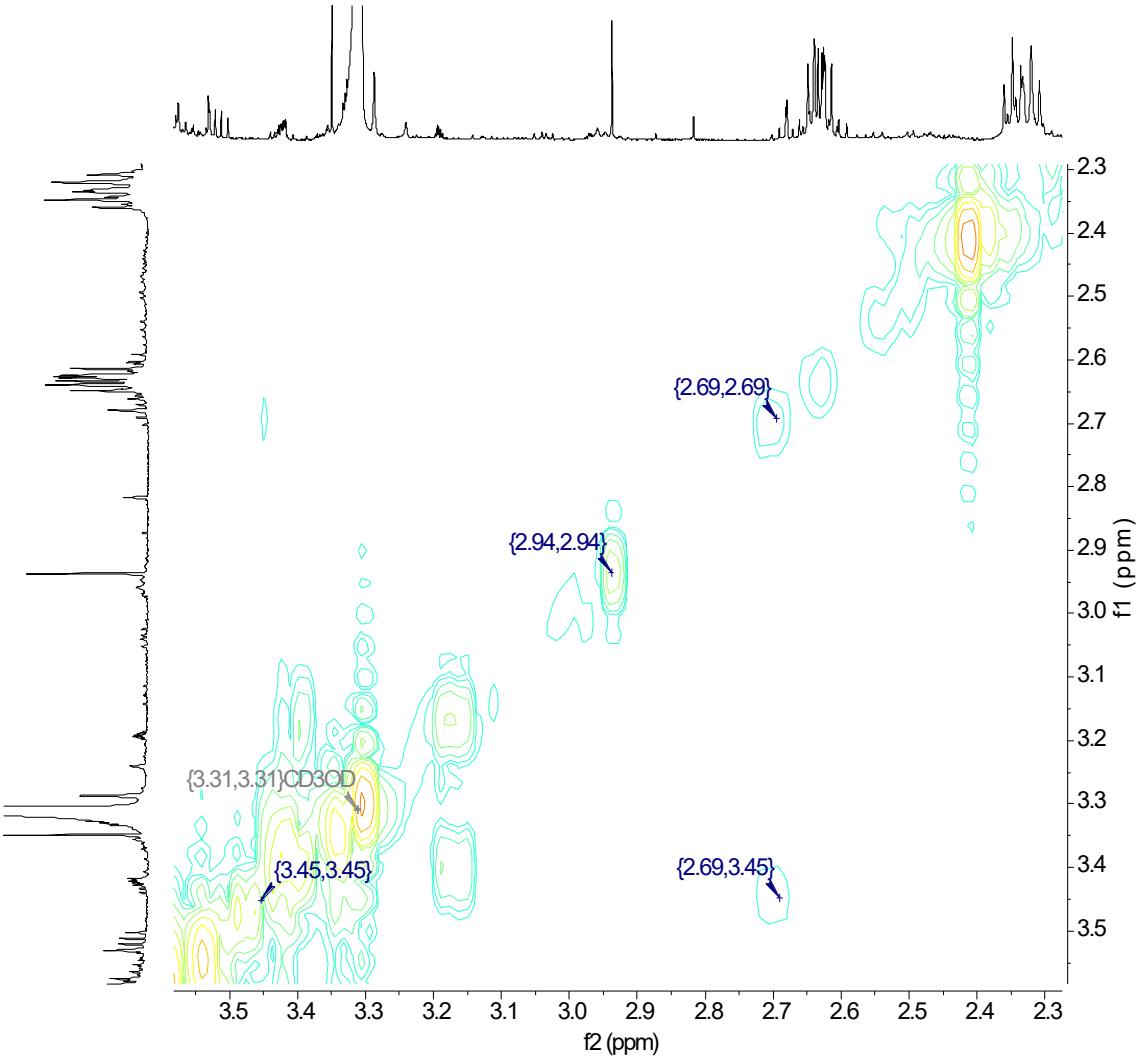

Figure 2.9. ^1H-^1H COSY spectrum of a *Shimia* bacterium (isolate AMM-P-2) extract, cultured in methionine enriched minimal basal medium (MBM), run in CD_3OD. The correlation between the two methylene groups (δ_H 3.45 - δ_H 2.70) is annotated in blue.

A ^1H-^1H correlation spectroscopy (COSY) NMR experiment revealed a correlation between the two methylene groups, S-CH_2- (δ_H 3.45, t) and -CH_2-CO_2H (δ_H 2.70, t) (Figure 2.9). In addition, a ^1H-^{13}C heteronuclear multiple bond correlation (HMBC) NMR experiment (Bax and Summers, 1986; Willker et al., 1993) revealed long-range chemical shift correlations between the protons of the two methyl groups (S-CH_3) and the carbon of the S-methylene group (δ_H 2.94 - δ_C 43.21), and between the carboxyl-methylene protons to the carboxyl carbon (δ_H 2.69 - δ_C 172.03) and the S-methylene carbon (δ_H 2.69 - δ_C 43.21) (Figure 2.10). These correlations observed in the COSY and HMBC spectra established the positions of the methyl and methylene groups in the chemical structure of DMSP, thus verifying the presence of DMSP in the bacteria

extracts. Corroborating the LC-MS data, the methyl signal intensity was low (nearing the detection limit) in isolates grown in MBM but was greatly enhanced in all *dsyB*-harbouring isolates when cultured in methionine enriched MBM (Figure 2.8).

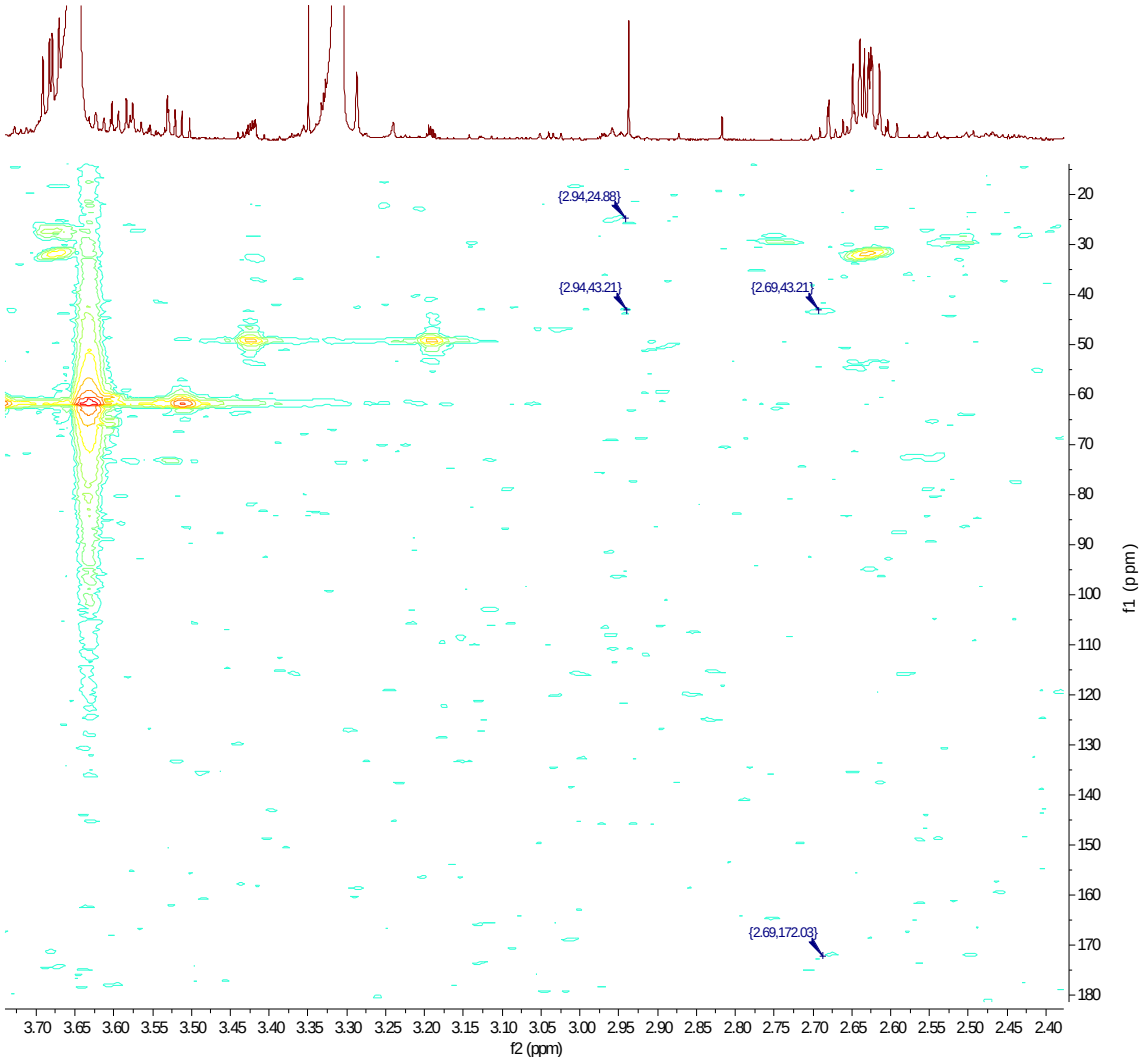

Figure 2.10. ^{1}H-^{13}C HMBC spectrum of a *Shimia* bacterium (isolate AMM-P-2) extract, cultured in methionine enriched minimal basal medium (MBM) run in CD_3OD. Observed correlations for DMSP are annotated in blue.

Ions diagnostic for acrylate were not found in these same bacterial extracts. To confirm this finding, an isolate extract was spiked with acrylate and reanalysed. Acrylate was still not detected indicating a sample matrix effect, hence this method was found unsuitable for the simultaneous detection of DMSP and acrylate. However, acrylate was detected in these bacterial extracts using ^{1}H NMR (Figure 2.8 d and e).

2.4 Discussion

Although the determination of the natural diversity of coral-associated bacteria is informative in the context of coral microbial ecology, the primary goal of this study was to isolate DMSP-producing coral-associated bacteria. Therefore, mucus swabs were obtained from field corals at Orpheus Island and mucus and tissues were sampled from aquarium-adapted corals at the SeaSIM. Aquaria conditions can alter microbiome community profiles (Kooperman et al., 2007; Schöttner et al., 2009; Pratte et al., 2015), which may aid holobiont local acclimatization (Osman et al., 2020). Biological replicates of host colonies were not included in the experimental design as assessing variation in coral microbiome between colonies was not the goal of this work.

DMSP biosynthesis by bacteria was originally identified in *Labrenzia aggregata* LZB033 isolated from the East China Sea (Curson et al., 2017). A gene involved in the production of DMSP, *dsyB* was identified in this bacterium and demonstrated to be a robust reporter gene for the potential of a bacterium to synthesize DMSP (Curson et al., 2017). The production of DMSP by several *dsyB*-harbouring Alphaproteobacteria from the Rhodobacterales order has also been experimentally confirmed, including members of the *Oceanicola*, *Pelagibaca*, *Sediminimonas*, *Amorphus*, *Sagittula*, and *Thalassobaculum* genera (Curson et al., 2017). Reported here for the first time is the presence and identity of DMSP producers among coral-associated bacteria.

2.4.1 Coral-associated bacteria have dsyB

In the present study, approximately 6% of the bacterial strains isolated from six species of corals harboured the *dsyB* gene. All these *dsyB*-harbouring bacteria were isolated from mucus or tissues of *Acropora* sp. corals. As with previous reports (Curson et al., 2017), the *dsyB*-harbouring bacteria belonged to the Rhodobacterales order, with bacteria of the *Shimia* genus being the most commonly isolated. *Shimia* are members of the *Roseobacter* clade (Choi and Cho, 2006), which are metabolically versatile marine bacteria that are abundant in the water column, in marine sediments and are commonly associated with eukaryotic hosts (Lenk et al., 2012; Luo and Moran, 2014). More specifically, members of the *Shimia* genus have been commonly reported in association with phytoplankton (Behringer et al., 2018) and reef-building corals (Chen et al., 2011; Chiu et al., 2012; Séré et al., 2014; Séré et al., 2016). The other isolated *dsyB*-harbouring bacteria belonged to the *Pseudooceanicola* and *Roseivivax* genera. Members of the latter are known to induce settlement in coral larvae (Sharp et al., 2015) and have also been isolated from corals (Chen et al., 2012).

Three strains of *Labrenzia*, the bacterial genus from which the *dsyB* gene was initially identified (Curson et al., 2017), were isolated from the mucus and tissue of *Pocillopora* and *Stylophora* corals, but surprisingly, they did not harbour *dsyB*. While one of the *Labrenzia* strains isolated from coral tissue is of a different species from the one reported (*L. alba*), two of the isolates obtained from coral mucus are closely affiliated (by 16S rRNA gene sequencing) to the model bacteria used by Curson and colleagues (*L. aggregata* LZB033), albeit related to a different strain (*L. aggregata* NBRC 16684). While it is currently unknown if most *Labrenzia* bacteria have *dsyB*, it is probable that only some strains acquire the gene to assist the bacteria in overcoming oxidative stress through the production of DMSP (Curson et al., 2017). *Pocillopora damicornis* and *Stylophora pistillata* have been shown to produce DMSP, but in much lower concentrations than *A. millepora* (Tapiolas 2013). It has been previously suggested that *dsyB* and its homologues have been transferred between prokaryotes, notably of Alphaproteobacterial origin, and eukaryotes multiple times (Curson et al., 2018). It is possible that the lesser production of DMSP in some species of corals could be due to the bacterial community they harbour and the lack of *dsyB* homologues acquired via horizontal gene transfer. Considering that the *dsyB* gene has so far only been identified in Alphaproteobacteria (Curson et al., 2017), further examination of the a potential *dsyB* gene in isolate AMT-P-4, a Gammaproteobacterium closely related to *Vibrio* will have to be done before we can confirm this discovery.

2.4.2 dsyB-*positive coral-associated bacteria are capable of producing DMSP*

DMSP was unambiguously identified in extracts of *dsyB*-harbouring bacteria, but only when the cultures were grown in methionine-enriched MBM. Methionine is the universal precursor of DMSP (Hanson et al., 1994; Uchida et al., 1996; Gage et al., 1997; Rhodes et al., 1997; Kocsis et al., 1998). Supplementation of cultures with methionine increased their DMSP production, indicating that methionine was assimilated by the bacteria. In *dsyB*-harbouring bacteria, methionine is converted successively into 4-methylthio-2-oxobutyrate (MTOB), 4-methylthio-2-hydroxybutyrate (MTHB), 4-dimethylsulphonio-2-hydroxybutyrate (DMSHB) and finally DMSP, with *dsyB* mediating the conversion between MTHB and DMSHB (Curson et al., 2017). Addition of pathway intermediates, including methionine, have been shown to enhance DMSP production, but *dsyB*-harbouring bacteria can produce DMSP through *de novo* production of methionine (presumably from inorganic sulphate present in high concentration in seawater) (Curson et al., 2017).

DMSP concentrations can vary by more than three orders of magnitudes between coral genera. While *Pachyseris* sp. produces tens of picomoles per mm^2, production in the fast-growing

Acropora can reach tens of nanomoles per mm^2 (Raina et al., 2013; Tapiolas et al., 2013; Deschaseaux et al., 2014b). All the DMSP-producing bacteria isolated in the present study originated from *Acropora*, with the majority (78.6%) isolated from coral tissue. This strongly suggests that DMSP-producing bacteria contribute to the large DMSP pool produced by this coral genus. Concomitantly, corals from the genus *Acropora* are also characterised by their high concentrations of the DMSP-breakdown product acrylate (Tapiolas et al., 2010). This compound was detected in the DMSP-producing isolates, suggesting the culture conditions were conducive to the expression of DMSP-degrading genes, and that these bacteria likely possess these genes. Future studies are recommended to identify how much each partner within the coral holobiont (i.e., the host, Symbiodiniaceae and the bacterial communities) contribute to this DMSP pool.

2.4.3 Conclusions and future direction

Bacterial communities associated with corals are highly diverse (Mouchka et al., 2010; Blackall et al., 2015; Hernandez-Agreda et al., 2017; Hernandez-Agreda et al., 2018; van Oppen and Blackall, 2019) but their metabolic capabilities and contributions to the holobiont's nutrient cycling are still poorly characterised. This study demonstrates that coral-associated bacteria can produce the important organosulphur compound DMSP. This result implies that multiple sources of DMSP co-occur within the coral holobiont, with Symbiodiniaceae, coral host and bacterial communities each capable of DMSP production. Quantifying the contribution of each holobiont member to the DMSP pool present in corals and how these contributions are modulated and impacted by extreme events is important given the multifaceted roles of this compound and its involvement in stress response (Sunda et al., 2002). In addition, it has recently been shown that bacteria can also use a second pathway (independent of *dsyB*) to produce DMSP, involving a gene called *mmtN* (Williams et al., 2019). Since this gene is also present in Gammaproteobacteria and Actinobacteria, it is likely that some DMSP-producing bacteria were overlooked by our *dsyB*-centric screening approach. Future studies should therefore aim to characterise the full diversity and abundance of DMSP-producing bacteria associated with corals.

Chapter 3:
Genome analysis of *Shimia aestuarii*, a DMSP-producing bacterium associated with the coral *Acropora millepora*

Abstract

Tropical coral reefs are natural hotspots for the production of dimethylsulphoniopropionate (DMSP), a key component of the marine sulphur cycle and precursor of the climatically-relevant gas dimethylsulphide (DMS). Reef-building corals from the genus *Acropora*, together with their microalgal partner, Symbiodiniaceae, and associated bacteria collectively produce some of the highest DMSP concentrations recorded in the environment. However, the functional capabilities of coral-associated DMSP-producing bacteria are unknown. Here we analysed the genome of *Shimia aestuarii* AMM-P-2, a DMSP-producing bacterium associated with *Acropora millepora*, to characterise its sulphur cycling capabilities. Specifically, this bacterium was confirmed to have the genetic machinery to assimilate sulphate and synthesise the DMSP precursors, cysteine and methionine, to catabolise DMSP to methanethiol, DMS, and acrylate, and to utilise or detoxify acrylate. These findings provide the basis for understanding the involvement of *S. aestuarii* AMM-P-2 in sulphur metabolism within the coral holobiont.

3.1 Introduction

The marine environment is one of the largest reservoirs of bacteria and archaea on Earth. Each litre of seawater contains approximately one billion cells, which account for approximately 70% of the total marine biomass (Bar-On et al., 2018). This abundance encompasses a wide phylogenetic diversity together with a broad range of trophic strategies (Lauro et al., 2009) and the collective metabolic activities of these microorganisms drive marine biogeochemical cycles (Falkowski et al., 2008). Although their roles in the carbon and nitrogen cycles have received much attention to date (Worden et al., 2015), marine microorganisms are also playing a central role in the marine sulphur cycle. Sulphur is present at high concentrations in seawater as inorganic sulphate (~28 mM SO_4^{2-}) (Sievert et al., 2007), which can be assimilated by many marine microorganisms (Cuhel et al., 1982; Gilmore et al., 1989) using *cys*-operons and *PAPSS* or *sat* genes to form sulphide (S_2^-) and subsequently biosynthesise amino acids such as cysteine and homocysteine. However, sulphate is bioenergetically costly to assimilate (Jones-Mortimer, 1968; Kredich, 1971; Sekowska et al., 2000) in comparison to reduced sulphur compounds such as methionine ($C_5H_{11}NO_2S$), methanethiol (MeSH; or CH_3SH) or dimethylsulphoniopropionate

(DMSP; $C_5H_{10}O_2S$). Of these, DMSP represents the most abundant source of organic sulphur in the world's ocean (Johnston et al., 2012), with more than a billion tons produced yearly (Stefels et al., 2007), satisfying up to 95% of the total bacterial sulphur demand (Zubkov et al., 2001).

DMSP can be metabolised by many abundant groups of marine bacteria, such as the *Roseobacter* clade and SAR11 within the Alphaproteobacteria class (Kiene et al., 1999; Tripp et al., 2008). Two competing pathways exist for DMSP degradation, the first is the demethylation/demethiolation pathway and is mediated by the DMSP demethylase genes, *dmdA-D* and is estimated to be present in 60% marine bacteria (Kiene et al., 2000; Venter et al., 2004; Howard et al., 2008). This pathway produces MeSH, which can be used for the biosynthesis of protein amino acids (Kiene, 1996; Kiene and Linn, 2000). The second pathway produces dimethylsulphide (DMS; C_2H_6S) through the *ddd*- [DMSP-dependent DMS] genes and is present in approximately 30% of these microorganisms (Yoch, 2002; Curson et al., 2011b).

Sulphide can also be converted to DMSP following the syntheses of cysteine and methionine. The first DMSP biosynthesis gene (*dsyB*) was identified by Curson et al. (2017) in a marine Alphaproteobacterium *Labrenzia aggregata* LZB033. It encodes a methyltransferase-like protein (SIAM614_21095) and confers DMSP production when expressed in bacteria. A subsequent DMSP biosynthesis gene, coined *mmtN* [methionine methyltransferase], was found in broader groups of bacteria (i.e. Alpha-, Gamma-, and Actinobacteria) from marine surface sediments (Williams et al., 2019). These bacteria have been shown to utilise the methionine methylation pathway, which is *dsyB*-independent, and was formerly only associated with angiosperms. While several reports exploring the functionality of *dsyB* have been published, much of the focus has been on pelagic bacteria or bacteria in sediments (Curson et al., 2017; Curson et al., 2018; Sun et al., 2020; Zheng et al., 2020; McParland et al., 2021). Recently bacteria harbouring the *dsyB* gene have been isolated from reef-building corals and production of DMSP confirmed in culture (see Chapter 2).

To better understand the metabolic capabilities of two coral-associated DMSP-producing bacteria AMM-P-2 and AMT-P-4 from different bacterial classes (Alphaproteobacteria and Gammaproteobacteria, respectively, as isolated in Chapter 2), we sequenced their genomes using the Illumina MiSeq (short reads) and the Oxford Nanopore MinION (long reads) platforms. Using this hybrid assembly pipeline, the complete genomes were constructed, and the sulphur assimilation and degradation repertoire of these bacteria were explored.

3.2 Methodology

3.2.1 DNA extraction

The bacteria were cultured overnight in 5 ml of Marine Broth (based on peptone and yeast extract) at 28°C and 180 RPM. The overnight cultures were then centrifuged for 5 min at 10,000 *g* and the supernatant decanted. To obtain high molecular weight DNA, a modified method based on Wilson (2001) was performed. A combination of 567 µl of tris-ethylenediaminetetraacetic acid buffer, 30 µl of sodium dodecyl sulphate, and 3 µl of proteinase K were added to each sample and the solution was gently mixed using a micropipette. The sample was incubated at 37°C for 1 hour after which sodium chloride (100 µl) was added. Cetyl trimethylammonium bromide buffer (80 µl) was added, the solution again mixed thoroughly, and incubated at 65°C for 10 min. Equal volumes of phenol:chloroform were added to the sample with mixing and then centrifuged at 10,000 *g* for 5 min. The supernatant was carefully transferred into a clean tube followed by addition of chloroform:isoamyl alcohol (1 ml). The solution was mixed gently, centrifuged at 10,000 *g* for 5 min and again the supernatant transferred into a clean tube. To precipitate DNA, an equal volume of chilled (ice cold) isopropanol was added and the sample spun down at 10,000 g for 5 min. The supernatant was decanted, and the DNA gently rinsed with 70% ethanol followed by centrifugation for 10 s. Again, the supernatant was carefully decanted, and the DNA left to air dry for 20 min.

A faster DNA extraction was also performed using the DNeasy UltraClean Microbial Kit (Qiagen, Hilden, Germany) according to the manufacturer's protocol. All extracted DNA was resuspended in 20 µl of UltraPure DNase/RNase-Free Distilled Water (Invitrogen, California, United States) and stored at 4°C until required. DNA that was not used within a week was stored at -80°C until needed. The quality and quantity of the extracted DNA were assessed by spectrophotometry (NanoDrop ND-1000, ThermoFisher, Delaware, United States) and fluorometric quantification (Qubit, ThermoFisher, Delaware, United States).

3.2.2 Genome sequencing

DNA extracted using the phenol:chloroform method was sent to the Ramaciotti Centre for Genomics (Sydney, Australia) for library preparation using the Nextera XT DNA Library Preparation Kit (Illumina, California, United States) and sequenced on the Illumina MiSeq system using V2 with 2×250 bp nano paired end reads.

DNA extracted with the DNeasy UltraClean Microbial kit was sequenced on the Oxford Nanopore MinION system. The library was prepared using the Rapid Sequencing Kit (SQK-RAD004, Oxford Nanopore Technologies, Oxford, United Kingdom) following the manufacturer's protocol. A SpotON Flow Cell with approximately 1200 available pores was flushed, primed, and checked using the MinKNOW software. The library was then loaded onto the flow cell with care to avoid introduction of air bubbles during pipetting. The sequencing run proceeded for 46 hours until the output of high quality (Q>7) reads from the flow cell had dropped below 1000 reads $hour^{-1}$.

3.2.3 Genome assembly and annotation

The MiSeq read set was trimmed, assembled, and error-corrected using Trimmomatic 0.38 (Bolger et al., 2014), SPAdes version 3.13.0 (Bankevich et al., 2012), and Pilon version 1.23 (Walker et al., 2014), respectively. All were implemented through Shovill version 1.0.4 (available at https://github.com/tseemann/shovill) using default settings. Annotation was performed with Prokka version 1.13.3 (Seemann, 2014) using standard databases (i.e. ISfinder, NCBI Bacterial Antimicrobial Resistance Reference Gene Database, and UniProtKB (SwissProt)) and default settings. The MinION read set was assembled using Canu version 1.7 (Koren et al., 2017).

All raw data were used to obtain a draft assembly and to generate trimmed and corrected reads. The draft assembly was then polished using Medaka version 0.7.0 (available at https://nanoporetech.github.io/medaka/index.html) and Racon version 1.3.3 (Vaser et al., 2017). The Canu assembly was first filtered to remove contigs shorter than 100 kB because these cannot be handled by Medaka, and minimap2 version 2.12 (Li, 2018) was used to align the reads to this filtered draft assembly. Racon was then used to correct the raw contigs based on read alignments to produce a corrected assembly. This process was then repeated, mapping reads to the corrected assembly and using Racon a second time to generate an updated assembly before running a final round of polishing with Medaka. The final contigs were subsequently circularised with Circlator version 1.5.5 (Hunt et al., 2015), with a minimum identity percentage of 85% and breaklen set to 1000. Two of the largest contigs from the MinION read set were taxonomically classified using GTDB-Tk version 0.2.2 (Chaumeil et al., 2019). Annotated gene predictions for the assemblies were generated using Prokka version 1.14.6 (Seemann, 2014). The assembly graphs for all genomes were then visualised using Bandage (Wick et al., 2015).

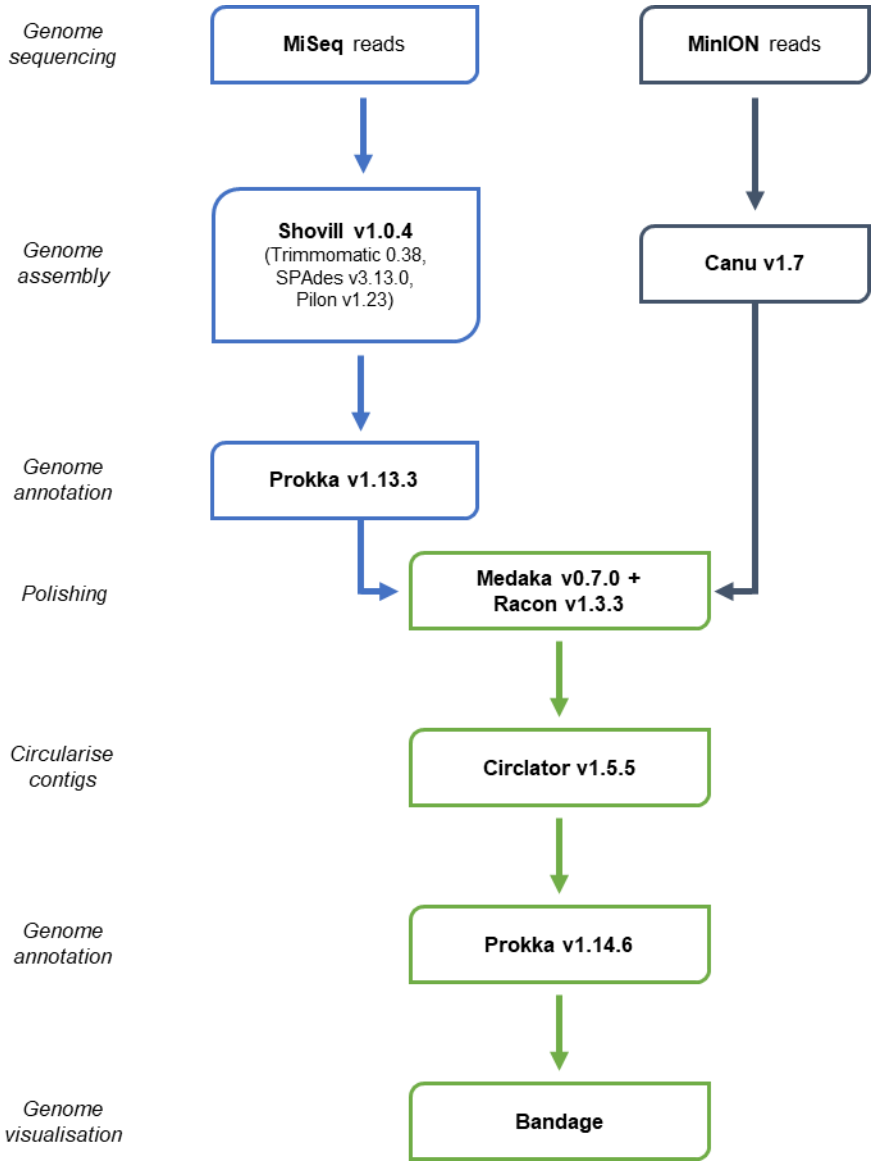

Figure 3.1. A summary of the genome assembly and annotation pipeline. The processing of the MiSeq data is highlighted in blue, while that of the MinION data is highlighted in grey. The steps highlighted in green involved using MiSeq data to polish the MinION assembly.

3.2.4 Bioinformatic analyses

Predicted DsyB protein sequences used in the alignment and maximum likelihood phylogenetic tree were obtained from the shortlisted group (n=47) curated by Curson et al. (2017). Identification of genes involved in sulphur metabolism was performed with BLAST 2.7.1+ (Altschul et al., 1990; Altschul et al., 1997), searching against KEGG (the Kyoto Encyclopedia of Genes and Genomes) (Kanehisa et al., 2004) and UniProtKB (the Universal Protein Resource Knowledgebase) (Consortium, 2018) databases.

The predicted protein sequences including the sequence obtained from *S. aestuarii* AMM-P-2 (n=48) were aligned by MAFFT version 7.394 (Multiple Alignment using Fast Fourier Transform) (Katoh et al., 2002). trimAl version 1.4 (Capella-Gutiérrez et al., 2009) was then used to filter positions with more than 50% gaps. All positions containing gaps and missing data were eliminated, with 337 positions left after trimming. The maximum likelihood tree was inferred using IQ-TREE version 1.6.4 (Nguyen et al., 2014) allowing the best-fitting evolutionary model to be selected automatically using ModelFinder (LG+R4) with 1,000 ultrafast bootstrap. The consensus tree was then visualised in ggtree (Yu et al., 2017; Yu et al., 2018; Yu, 2020).

A multiple sequence alignment (MSA) of the prokaryotic DsyB protein sequences was visualised to show conserved residues, conservative mutations, and divergence between the different homologues. The MSA was conducted using T-Coffee version 11.00 (Notredame et al., 2000; Di Tommaso et al., 2011) (available at http://tcoffee.crg.cat/apps/tcoffee/do:regular) with default settings and formatted using Boxshade 3.21 (available at https://embnet.vital-it.ch/software/BOX_form.html). Conserved domains within the predicted DsyB sequence was detected using CD-Search (Marchler-Bauer and Bryant, 2004) (available at https://www.ncbi.nlm.nih.gov/Structure/cdd/wrpsb.cgi) against the Conserved Domain Database (CDD) version 3.18 (Marchler-Bauer et al., 2010; Marchler-Bauer et al., 2014; Lu et al., 2019).

3.3 Results

3.3.1 Draft de novo *assembly of the genomes of bacterial isolates AMM-P-2 and AMT-P-4*

The genomes derived from bacterial isolates AMM-P-2 and AMT-P-4 assembled from MiSeq reads were unexpectedly similar despite previous 16S rRNA gene Sanger sequencing (see Chapter 2) indicating that the isolates belonged to two different bacterial classes (Alphaproteobacteria and Gammaproteobacteria, respectively). Both genome assemblies were approximately 3.9 Mb, had a GC content of 60.6%, contained nearly equal numbers of genes (3,906 for AMM-P-2; 3,891 for AMT-P-4), and were similarly fragmented (AMT-P-4: 103 contigs, N50 123kb; AMM-P-2: 75 contigs, N50 181kb). The derived 16S rRNA gene from the preliminary genome data was identical for both strains and identified them as Alphaproteobacteria. Isolate AMM-P-2 was confirmed as a *Shimia aestuarii* strain. Visualisation of the assembled genome of isolate AMT-P-4 (Figure 3.2a) clearly indicated fragmentation in the SPAdes assembly of the MiSeq reads (Figure 3.2a), likely due to the fact that short reads obtained from this sequencing method can produce unresolved repeats resulting in ambiguous paths which were difficult to assign.

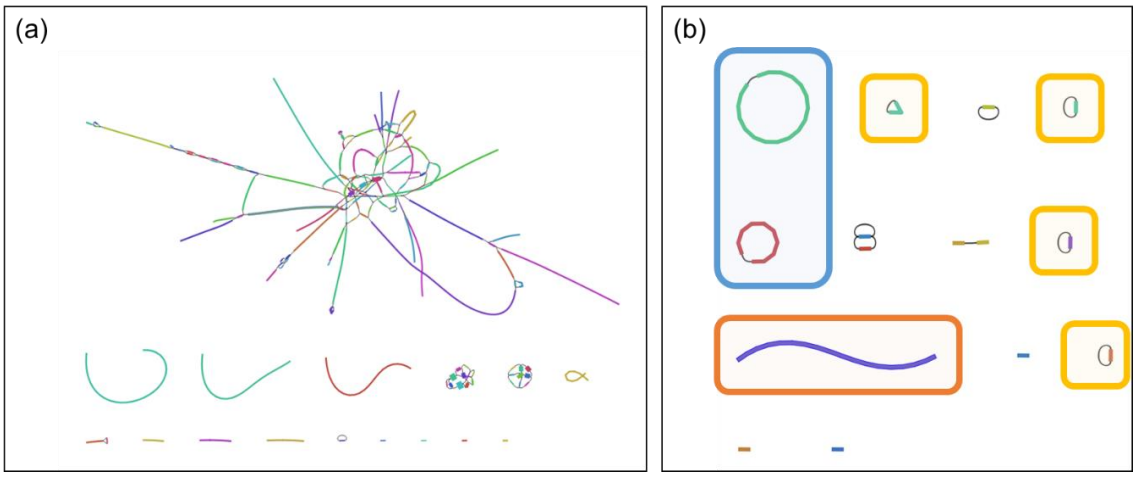

Figure 3.2. Genome assembly of culture AMT-P-4 based on (a) Illumina MiSeq reads using SPAdes and (b) Oxford Nanopore MinION reads using Canu. The colours denote different nodes, and the black connecting lines represent known overlaps. Branching node intersections are caused by multiple potential overlapping nodes. The gammaproteobacterial genome related to *Vibrio hepatarius* is highlighted by the blue rectangle, the alphaproteobacterial genome related to *Shimia aestuarii* is highlighted by the orange rectangle. Plasmids are highlighted by the yellow boxes, but it is unclear which genome they belong to.

To resolve the issues around assembly of the derived genome from the AMT-P-4 culture, further sequencing was carried out on the MinION platform. Assembly of the raw reads derived from this culture resulted in two complete circular chromosomes of 3.4 and 1.8 Mb, which is the typical organisation of the genomes of members of the bacterial genus *Vibrio* (Figure 3.2b) (Okada et al., 2005). Comparative analyses of the 16S rRNA region confirmed that the isolate was closely related to *Vibrio hepatarius*. In addition to the two large, closed chromosomes, a long linear contig was also assembled. The size (3.5 Mb) and much lower read coverage (~8×), when compared with the circular *Vibrio* contigs (both ~150×), suggested that it might correspond to the Alphaproteobacterium genome partially assembled from the previous MiSeq sequencing data. In light of this, the MiSeq reads were used to polish this MinION assembly. As predicted, the 16S region of this genome matched with *Shimia aestuarii* JC2049 (≥97% similarity). Closer inspection of this MinION-assembled *S. aestuarii* genome resulted in the identification of a *dsyB* gene sequence homologous to that reported in *Labrenzia aggregata* LZB033 (Curson et al., 2017). These results confirmed that the initial ambiguity in identification was due to the AMT-P-4 culture being a mixture of two species, a *Shimia aestuarii* strain and a *Vibrio hepatarius* affiliated species. Analysis of the *Vibrio* sp. genome failed to identify genes involved in DMSP biosynthesis (i.e., *dsyB* gene homologues), implying that the positive PCR results obtained for this AMT-P-4 culture were likely due to co-culture of the *Shimia aestuarii* strain. All subsequent analyses therefore focused only on the *dsyB*-harbouring *S. aestuarii* AMM-P-2 strain. The genome statistics for *S. aestuarii* AMM-P-2 are summarised in Table 3.1.

Table 3.1. Genome statistics for *Shimia aestuarii* AMM-P-2.

Attribute	Value
Genome size (bp)	4,151,190
DNA coding (bp)	3,972,669
No. of sequences	75
GC content (%)	60.6
N50	181,193
Gap ratio (%)	0.0
No. of CDSs	3,906
No. of rRNA	3
No. of tRNA	46
No. of CRISPRS	0
Coding ration (%)	89.7

3.3.2 Phylogenetic analysis of the S. aestuarii *AMM-P-2 DsyB protein*

The phylogenetic position of the predicted *S. aestuarii* AMM-P-2 DsyB protein was examined by comparison with the representative range of bacteria included in the Curson et al. (2017) analysis (Figure 3.3), all of which were obtained from either NCBI (the National Center for Biotechnology Information) or JGI (the U.S. Department of Energy Joint Genome Institute) databases. All sequences included in the phylogenetic analysis identified as DsyB orthologues (with ≥39% identity, and E-value of ≤ $1e^{-67}$ in comparison to *L. aggregata* LZB033) are from Alphaproteobacteria; the sequences from Firmicutes (*Bacillus mycoides*) and Actinobacteria (*Streptomyces varsoviensis*) are related (i.e., non-DsyB) proteins that were included in the analysis to act as outgroups. Thus, the phylogenetic analysis confirmed that the predicted *S. aestuarii* AMM-P-2 protein is a typical DsyB family member (sequence data is available in Supplementary Data Table 3.1.)

Overall, the predicted *S. aestuarii* AMM-P-2 DsyB protein had 58.81% identity with the reference sequence from *L. aggregata* LZB033, the E-value for this comparison being ≤1 e^{-136}. The closest match to the *S. aestuarii* AMM-P-2 DsyB protein was from an unidentified member of the Rhodobacteraceae (≥74.78% identity, E-value ≤ 1 e^{-179}). Predictably, the maximum likelihood tree (Figure 3.3) closely resembles that which was previously published in Curson et al. (2017), and broadly reflects the accepted species phylogeny of the Alphaproteobacteria. One inconsistency in the DsyB phylogeny was identified: sequences from members of the Rhodospirillales did not form a monophyletic group. Rather, three sequences from Rhodospirillales formed an early diverging clade, whereas those from two *Nisaea* isolates and from Rhizobiales were embedded in clades dominated by members of the Rhodobacterales.

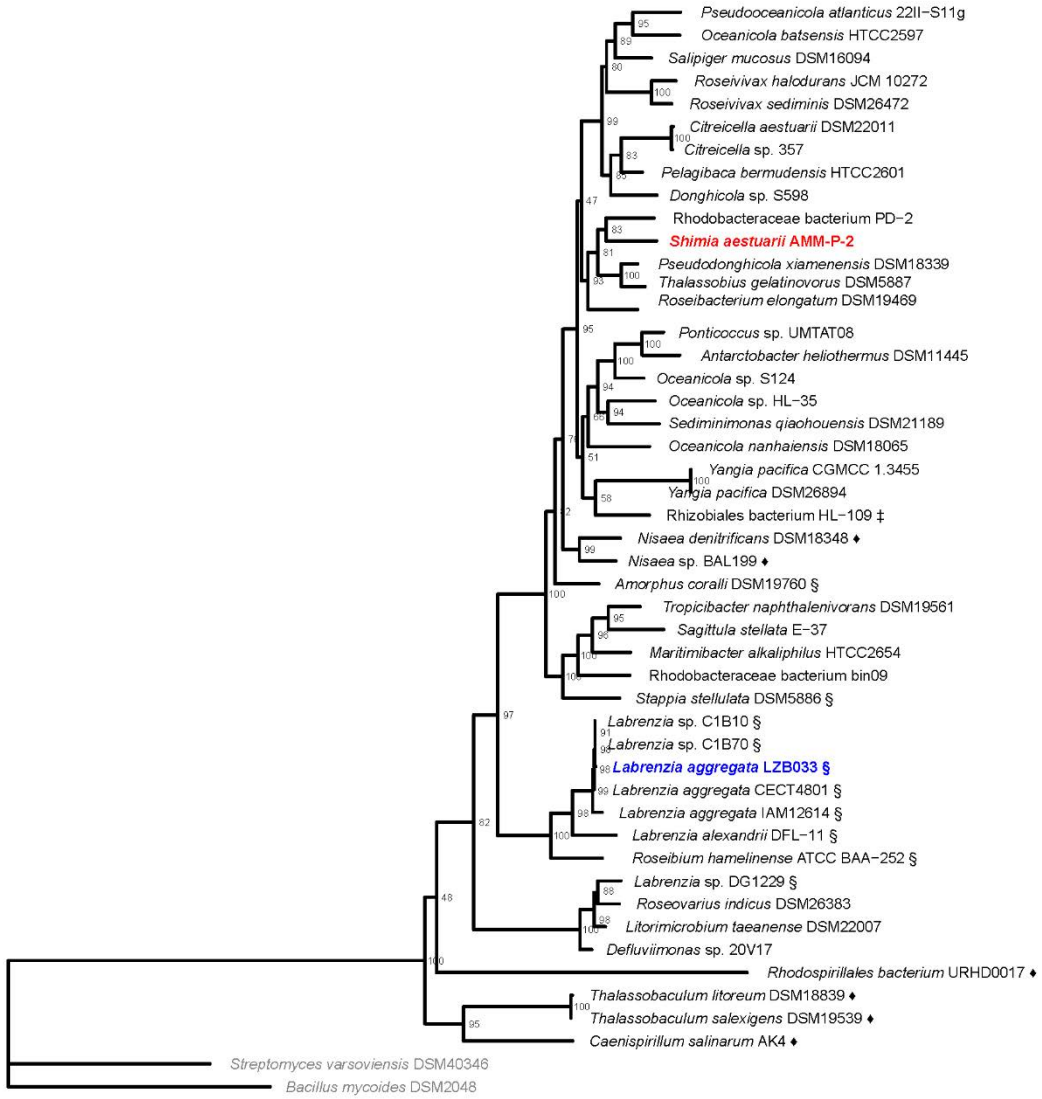

Figure 3.3. Maximum likelihood tree of known prokaryotic DsyB amino acid sequences constructed using the LG + R4 model based on the Bayesian Information Criterion. All DsyB sequences are from Alphaproteobacteria. The positions of the reference strain *Labrenzia aggregata* LZB033 and the *Shimia aestuarii* AMM-P-2 isolate are shown in blue and red, respectively. Sequences indicated in grey are non-DsyB proteins that were included in the analysis to act as an outgroup. Most of the known DsyB sequences are from members of the order Rhodobacterales, the few known from representatives of the Hyphomicrobiales (n=10, marked with §), Rhizobiales (n=1, marked with ‡), and Rhodospirillales (n=6, marked with ♦) are shown for comparison.

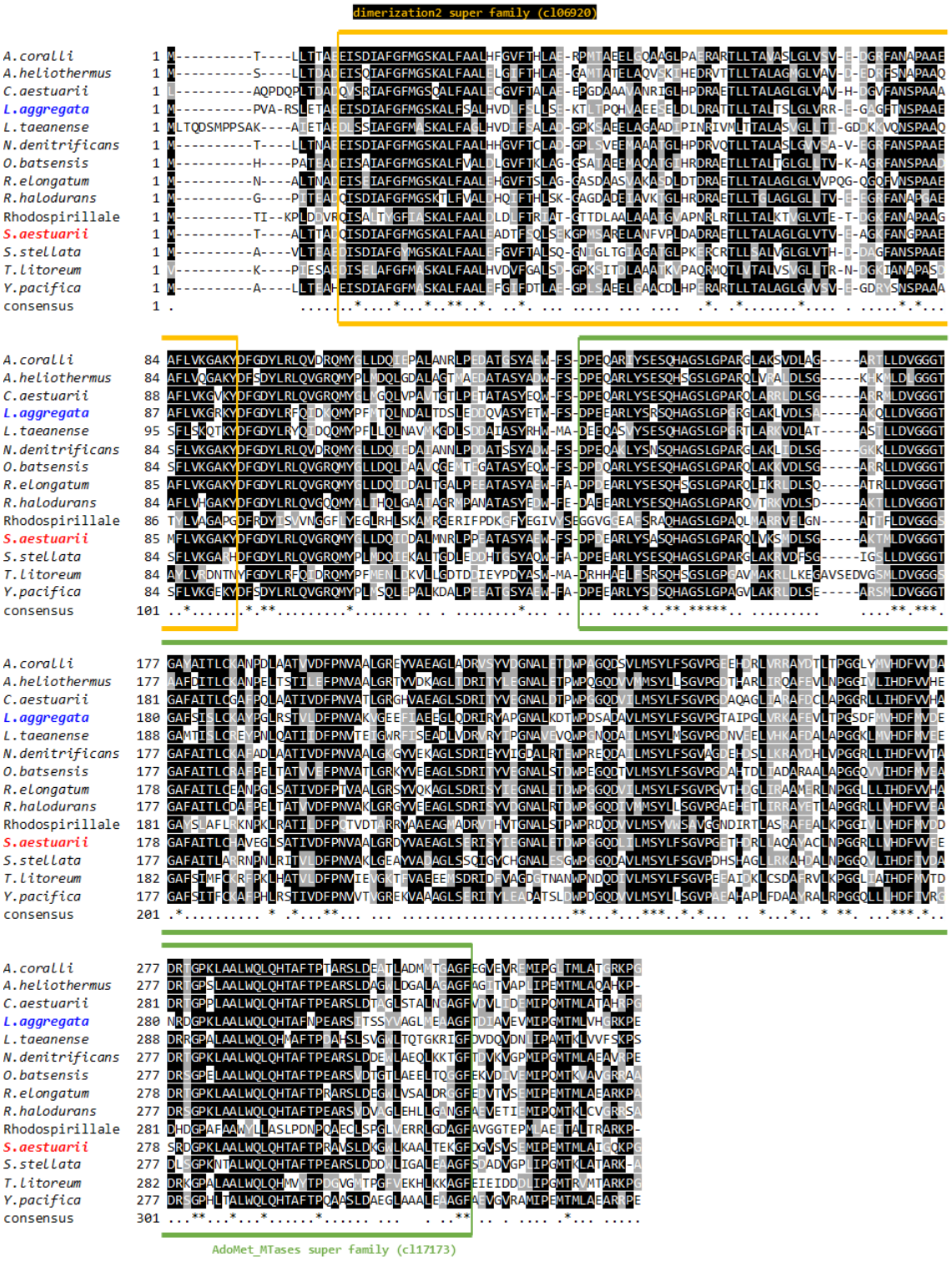

Figure 3.4. Multiple sequence alignment of DsyB homologues from different Alphaproteobacteria (n=14) representing the diversity of this protein family. Residues that are identical are shaded in black, while conserved substitutions are shaded in grey. Amino acid residues that are conserved across all 14 sequences are marked with asterisks below. The reference strain *Labrenzia aggregata* LZB033 and the *Shimia aestuarii* AMM-P-2 isolate are highlighted in blue and red, respectively. Conserved domains that were found within the protein are indicated with a yellow and green box, which represent the S-adenosylmethionine-dependent methyltransferases class I superfamily (cl17173) and dimerization2 superfamily (cl06920), respectively.

The predicted amino acid sequence of the *S. aestuarii* AMM-P-2 DsyB protein shares highly conserved regions with its close homologues. Proteins representing the diversity within the DsyB family (n=14) were selected on the basis of the phylogenetic tree (Figure 3.3) and the ClustalW+Lalign alignment (Notredame et al., 2000) used to visualise conserved regions (Figure 3.4). The *S. aestuarii* AMM-P-2 DsyB protein sequence contains two conserved domains corresponding to an S-adenosylmethionine-dependent methyltransferase (AdoMet-MTase) class I superfamily domain (pfam00891; E-value 4.02 e^{-16}) and a dimerization2 superfamily domain (pfam16864; E-value 4.13 e^{-7}), which frequently occurs in methyltransferases. This domain structure is common to all *dsyB* orthologues (Figure 3.4). Proteins containing AdoMet-MTase class I domains carry out a wide range of functions, and this is reflected in limited amino acid sequence conservation (as low as 10% in some cases). However, despite such low conservation at the sequence level, higher order domain structure, which is required for the binding and transfer of S-adenosyl-methionine, is highly conserved (Struck et al., 2012).

As in several other Rhodobacterales strains (*S. mucosus* DSM16094, *P. bermudensis* HTCC2601, *T. gelatinovorus* DSM5887, *D. xiamenensis* DSM18339, *A. heliothermus* DSM11445, *P. nanhaiensis* DSM18065, *Citreicella* sp. 357, *C. aestuarii* DSM22011, *S. qiaohouensis* DSM21189, *R. halodurans* JCM10272), the *S. aestuarii* AMM-P-2 *dsyB* gene is closely linked with *isc* [iron sulphur cluster] or *suf* [sulphur formation] gene clusters (Figure 3.5). The *suf*- gene clusters also shared synteny between the Rhodobacterales representatives used in the plot, but not with *L. aggregata*.

Whereas the organisation of genes 5' of *dsyB* is conserved in several Rhodobacterales (Curson et al., 2017), only limited conservation of gene organisation was observed in the region 3' of *dsyB* in this order. As shown in Figure 3.5, a cluster of genes consisting of *fabF_1*, *acpP_1* and *IpxD* located 3' of *dsyB* in the *Shimia* isolate were also located 3' of *dsyB* in *Pseudooceanicola nanhaiensis*, but no other clear cases of synteny on the 3'-side were observed. As noted in Curson et al. (2017), the arrangement of the genes surrounding *dsyB* in Rhodobacterales strains typically only differ in terms of the number of hypothetical proteins between the predicted SufC and SufB proteins (Figure 3.5).

In *L. aggregata*, genes neighbouring *dsyB* are more diverse in function. For example, *araC* (arabinose) is involved in carbon metabolism, stress responses, and pathogenesis (Gallegos et al., 1997), and *maoC*, an enoyl-CoA hydratase, encodes enzymes (Sugino et al., 1992; Fukui et al., 1998) required for acrylate detoxification (Figure 3.5). The *dsyB* gene in *L. aggregata* is also linked with *gnat*, a GCN5-related N-acetyltransferase which has been implicated in bacterial antibiotic resistance (Favrot et al., 2016), and *bluB* (cob(II)yrinic acid a,c-diamide reductase) which is a part of the biosynthetic pathway for vitamin B_{12} in bacteria (Pollich and Klug, 1995;

Rodionov et al., 2003; Campbell et al., 2006; Taga et al., 2007). Interestingly, a *mtap* (S-methyl-5'-thioadenosine phosphorylase) gene, whose product participates in the methionine salvage pathway (KEGG entry M00034), was located near *dsyB* in *Labrenzia*.

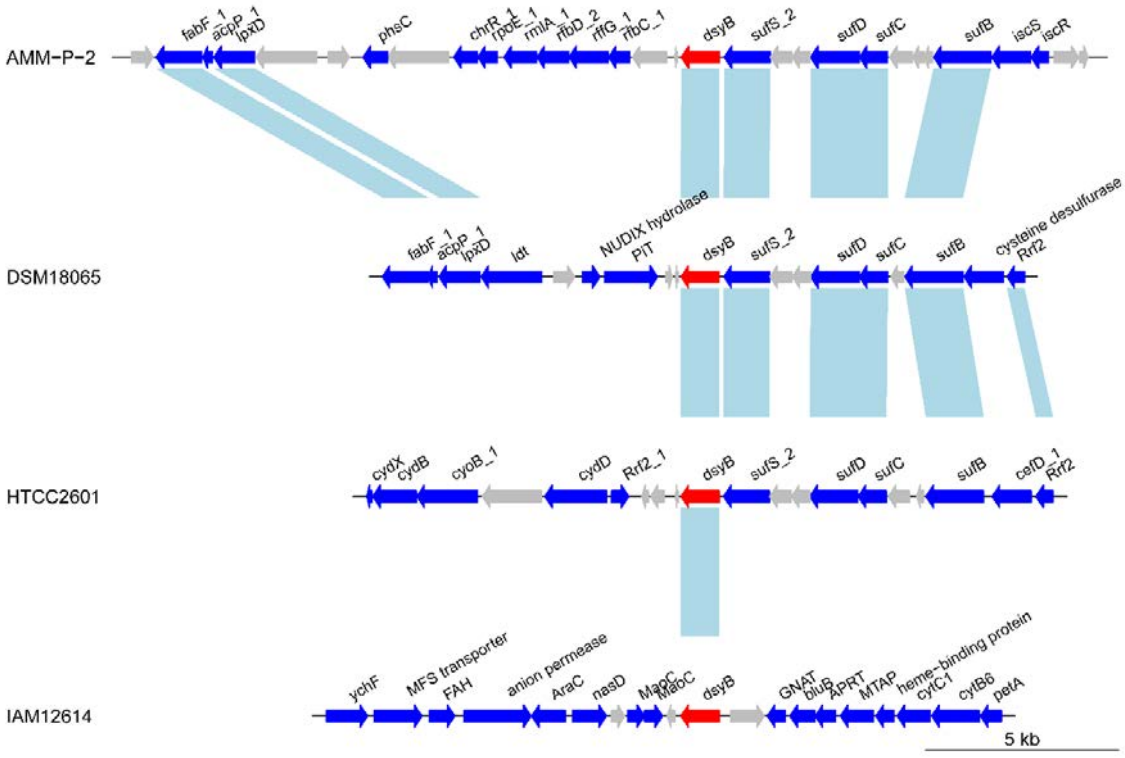

Figure 3.5. Microsynteny plot showing gene arrangement in four *dsyB*-containing bacteria. Bacteria are labelled according to taxonomic codes as follows: AMM-P-2, *Shimia aestuari*; DSM18065, *Pseudooceanicola nanhaiensis*; HTCC2601, *Pelagibaca bermudensis*; IAM12614, *Labrenzia aggregata*. Relationships between orthologous genes are shown in light blue bars. Genes with unknown function (hypothetical protein) are shown in grey arrows. The *dsyB* gene is shown in red arrows, while predicted genes are shown in dark blue arrows, and are denoted as follows: *fabF*, 3-oxoacyl-[acyl-carrier-protein] synthase II; *acpP*, acyl carrier protein; *lpxD*, UDP-3-O-acylglucosamine N-acyltransferase; *phsC*, thiosulphate reductase cytochrome B subunit; *chrR*, anti-sigma-E factor; *rpoE*, ECF RNA polymerase sigma factor; *rmlA*, glucose-1-phosphate thymidylyltransferase; *rfbD*, dTDP-4-dehydrorhamnose reductase; *rffG*, dTDP-glucose 4,6-dehydratase 2; *rfbC*, dTDP-4-dehydrorhamnose 3,5-epimerase; *dsyB*, 2-hydroxy-4-(methylsulphanyl)butanoate S-methyltransferase; *sufS*, cysteine desulphurase; *sufD*, Fe-S cluster assembly protein; *sufC*, Fe-S cluster assembly ATP-binding protein; *sufB*, Fe-S cluster assembly protein; *iscS*, cysteine desulphurase; *iscR*, HTH-type transcriptional regulator; *ldt*, L-2CD-transpeptidase family protein; *PiT*, inorganic phosphate transporter; *rrf2*, Rrf2 family transcriptional regulator; *cydX*, cytochrome bd-I oxidase subunit; *cydB*, cytochrome d ubiquinol oxidase subunit II; *cyoB*, cytochrome ubiquinol oxidase subunit I; cydD, thiol reductant ABC exporter subunit; *cefD*, aminotransferase class V-fold PLP-dependent enzyme; *ychF*, redox-regulated ATPase; FAH, fumarylacetoacetate hydrolase family protein; *araC*, AraC family transcriptional regulator; *nasD*, NAD(P)-dependent oxidoreductase; *maoC*, MaoC family dehydratase; *gnat*, GNAT family N-acetyltransferase; *bluB*, 5,6-dimethylbenzimidazole synthase; *aprt*, adenine phosphoribosyltransferase; *mtap*, S-methyl-5'-thioadenosine phosphorylase; *cytC*, cytochrome c1; *cytB*, cytochrome b/b6; *petA*, ubiquinol-cytochrome c reductase iron-sulphur subunit.

3.3.3 Sulphur metabolism genes

To determine whether *S. aestuarii* AMM-P-2 has the capacity to exploit inorganic sulphate from seawater as a sulphur source, or instead relies on reduced sulphur compounds produced exogenously, its genome was surveyed for other genes associated with sulphur metabolism. The presence of enzymes involved in uptake and assimilation of inorganic sulphate to cysteine were examined by reciprocal BLAST analyses. Sulphate assimilation genes which have been previously recorded from prokaryotic organisms were obtained from the KEGG database and compared against the *S. aestuarii* AMM-P-2 genome. The orthology of identified putative proteins with high similarity (E-value $\geq 1\ e^{-50}$) to known sulphate assimilation amino acid sequences was confirmed by conducting BLASTP analyses against the NCBI NR (non-redundant) database, followed by BLASTP analyses of retrieved best match against the *S. aestuarii* AMM-P-2 predicted proteins.

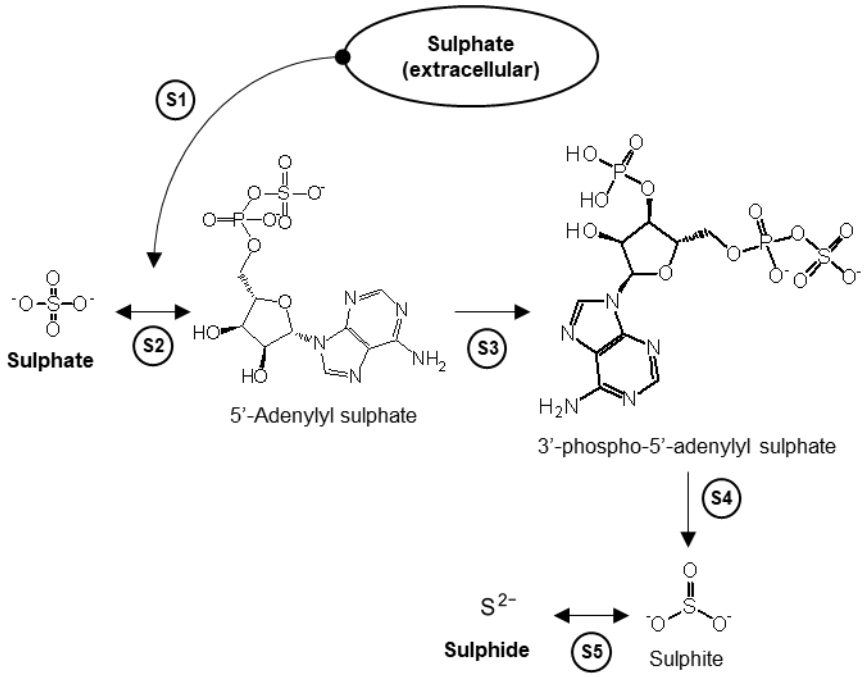

Figure 3.6. Assimilatory sulphate reduction pathway in *Shimia aestuarii* AMM-P-2, adapted from the KEGG database (M00176). Enzymes that mediate each step are listed in Table 3.2.

Table 3.2. Predicted proteins of *Shimia aestuarii* AMM-P-2 that encode enzymes involved in the assimilatory sulphate reduction pathway.

Catalyses step in pathway	KEGG identifier	Enzyme		*S. aestuarii* AMM-P-2 sequence	Reciprocal BLAST hit			
		Common name	EC number		Sequence identifier	Organism	E-value	% identity
S1	K02045	sulphate/thiosulphate transport system ATP-binding protein (*cysA*)	7.3.2.3	HEBAHGMP_00410	WP_058309570	*Shimia thalassica*	2.00E-173	92.91
				HEBAHGMP_02412	WP_127115693	*Thalassobius* sp. ZQ172	0.00E+00	97.05
	K02046	sulphate/thiosulphate transport system permease protein (*cysT*)	N/A	HEBAHGMP_02120	WP_028095055	*Pseudodonghicola xiamenensis*	1.00E-114	75.76
	K02047	sulphate/thiosulphate transport system permease protein (*cysW*)	N/A	HEBAHGMP_02120	WP_028095055	*Pseudodonghicola xiamenensis*	1.00E-114	75.76
	K03321	sulphate permease (*sulP* family)	N/A	HEBAHGMP_00688	WP_138014946	*Pelagicola litoralis*	0.00E+00	84.35
S2	K00957	sulphate adenylyltransferase subunit 2 (*cysND*)	2.7.7.4	HEBAHGMP_02373	NKW91153	Rhodobacteraceae bacterium R_SAG9	5.00E-172	89.06
	K00958	sulphate adenylyltransferase (*sat*)	2.7.7.4	HEBAHGMP_02840	WP_127115399	*Thalassobius* sp. ZQ172	0.00E+00	91.32
S2, S3	K00955	bifunctional enzyme (*cysNC*)	2.7.7.4; 2.7.1.25	HEBAHGMP_02840	WP_127115399	*Thalassobius* sp. ZQ172	0.00E+00	91.32
	K13811	3'-phosphoadenosine 5'-phosphosulphate synthase (*PAPSS*)	2.7.7.4; 2.7.1.25	HEBAHGMP_02840	WP_127115399	*Thalassobius* sp. ZQ172	0.00E+00	91.32
S3	K00860	adenylylsulphate kinase (*cysC*)	2.7.1.25	HEBAHGMP_02840	WP_127115399	*Thalassobius* sp. ZQ172	0.00E+00	91.32
S4	K00390	phosphoadenosine phosphosulphate reductase (*cysH*)	1.8.4.8	HEBAHGMP_00715	PIE11931	Rhodobacterales bacterium	4.00E-108	64.49
	K00392	sulphite reductase (ferredoxin) (*sir*)	1.8.7.1	HEBAHGMP_00716	TMV93179	*Thioclava* sp. BHET1	0.00E+00	80.58
S5	K00381	sulphite reductase (NADPH) hemoprotein beta-component (*cysI*)	1.8.1.2	HEBAHGMP_00716	TMV93179	*Thioclava* sp. BHET1	0.00E+00	80.58

This approach led to the identification of genes encoding clear homologues of each of the enzymes of the sulphate reduction pathway (Figure 3.6 and Table 3.2), confirming *S. aestuarii* AMM-P-2 has the genetic machinery required to catalyse the uptake and conversion of extracellular inorganic sulphate (via *cysA/T/W* and *sulP*; Table 3.2) to sulphide. As the concentration of sulphate in seawater is approximately 28 mM (Canfield, 2004), sulphur limitation is unlikely to present an issue for this bacterium, therefore it is not surprising they are metabolically equipped to assimilate exogeneous sulphur. However, as they exist within the coral holobiont, where a proportion of the available sulphate is in an organic form, it makes sense that this bacterium also has the capacity to recycle these compounds. The identification of genes whose products can mediate a range of similar transformations in the sulphate reduction pathway (e.g. *sat* and *cysND*, and *PAPSS* and *cysC*; Figure 3.7) provides *S. aestuarii* AMM-P-2 with alternative means of assimilating sulphur, should less energetically demanding sulphur sources become available.

Figure 3.7. Assimilatory sulphate reduction pathway adapted from the Kyoto Encyclopedia of Genes and Genomes (KEGG) database. Sulphate assimilatory genes that were found within the *Shimia aestuarii* AMM-P-2 genome are noted in bold.

Following sulphide production, *S. aestuarii* AMM-P-2 can produce cysteine (Figure 3.8, step C2; EC 2.5.1.47) and methionine, the latter being a precursor of DMSP (via aspartate; Figure 3.9). With respect to the cysteine biosynthesis pathway, *S. aestuarii* AMM-P-2 can produce cysteine through serine or homocysteine (mediated by *cysE/K* or *mccA/B* respectively; Figure 3.8). We also found *metK*, a S-adenosyl-methionine (SAM) synthase (Figure 3.8, step C3; EC 2.5.1.6) which encodes the first step in the reverse trans-sulphuration pathway (KEGG entry M00609), converting methionine to cysteine. While this indicates a potentially larger role for methionine as a sulphur source in *S. aestuarii* AMM-P-2, enzymes that mediate the subsequent steps in this pathway were not found.

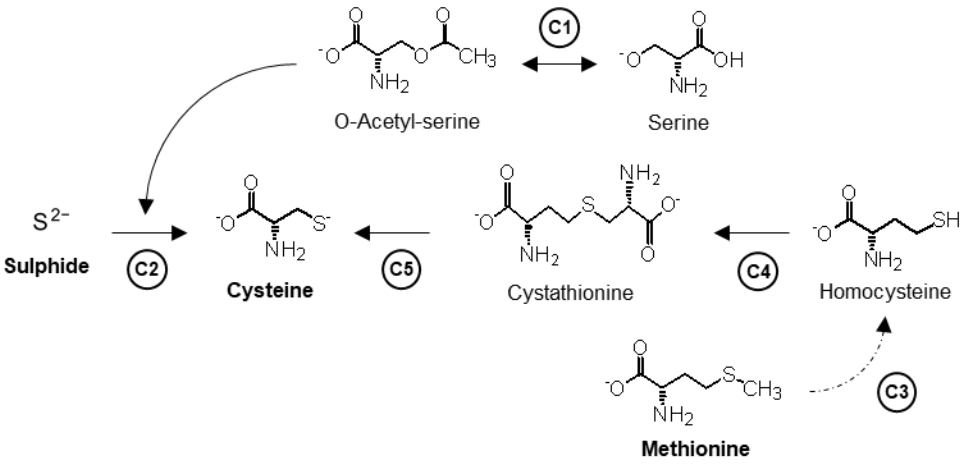

Figure 3.8. Cysteine biosynthesis pathways in *Shimia aestuarii* AMM-P-2, adapted from the KEGG database (M00021, M00338, and M00609). Incomplete pathways are denoted with a dash-dotted arrow indicating the presence of one or more genes involved in the pathway, but not all. Enzymes that mediate each step are listed in Table 3.3.

Table 3.3. Predicted proteins of *Shimia aestuarii* AMM-P-2 that encode enzymes involved in the cysteine biosynthesis pathway.

Catalyses step in pathway	KEGG identifier	Enzyme		*S. aestuarii* AMM-P-2 sequence	Reciprocal BLAST hit			
		Common name	EC number		Sequence identifier	Organism	E-value	% identity
C1	K00640	serine O-acetyltransferase (*cysE*)	2.3.1.30	HEBAHGMP_01916	WP_093094421	*Shimia aestuarii*	2.00E-177	89.43
C2	K01738	cysteine synthase (*cysK*)	2.5.1.47	HEBAHGMP_01557	WP_093094169	*Shimia aestuarii*	0.00E+00	87.21
C3	K00789	S-adenosylmethionine synthetase (*metK*)	2.5.1.6	HEBAHGMP_03728	WP_093089958	*Shimia aestuarii*	0.00E+00	86.01
C4	K17216	cystathionine beta-synthase (O-acetyl-L-serine) (*mccA*)	2.5.1.134	HEBAHGMP_01557	WP_093094169	*Shimia aestuarii*	0.00E+00	87.21
C5	K17217	cystathionine gamma-lyase / homocysteine desulphhydrase (*mccB*)	4.4.1.1	HEBAHGMP_00189	WP_093090600	*Shimia aestuarii*	0.00E+00	79.47
				HEBAHGMP_00185	WP_058309835	*Shimia thalassica*	0.00E+00	85.50
				HEBAHGMP_00999	WP_009814890	*Roseovarius nubinhibens*	0.00E+00	89.28

The *S. aestuarii* AMM-P-2 also has enzymes that encode a complete methionine biosynthesis pathway (KEGG entry M00017; Figure 3.9). Methionine and DMSP are compounds that are highly interrelated (del Valle et al., 2015), and the production and accumulation of DMSP can be influenced by methionine availability (Gröne and Kirst, 1992). The transformation of homocysteine to methionine (Figure 3.9, step M7; EC 2.1.1.13), which is the final step in this pathway, can be mediated by homologous enzymes *metH* (Banerjee et al., 1989) and *yitJ* (Grundy and Henkin, 1998). The *metH* gene utilises vitamin B_{12} as a co-factor in a reaction that is faster than other B_{12}-independent enzymes mediating the same reaction (Sekowska et al., 2000). Although *yitJ* is homologous to *metH*, we found two different matches within the predicted proteins of *S. aestuarii* AMM-P-2 which indicate the bacterium may contain both genes. The YitJ protein is a member of the S-box regulon (Grundy and Henkin, 1998) which plays a role in the regulation of genes involved in methionine biosynthesis, particularly during methionine starvation.

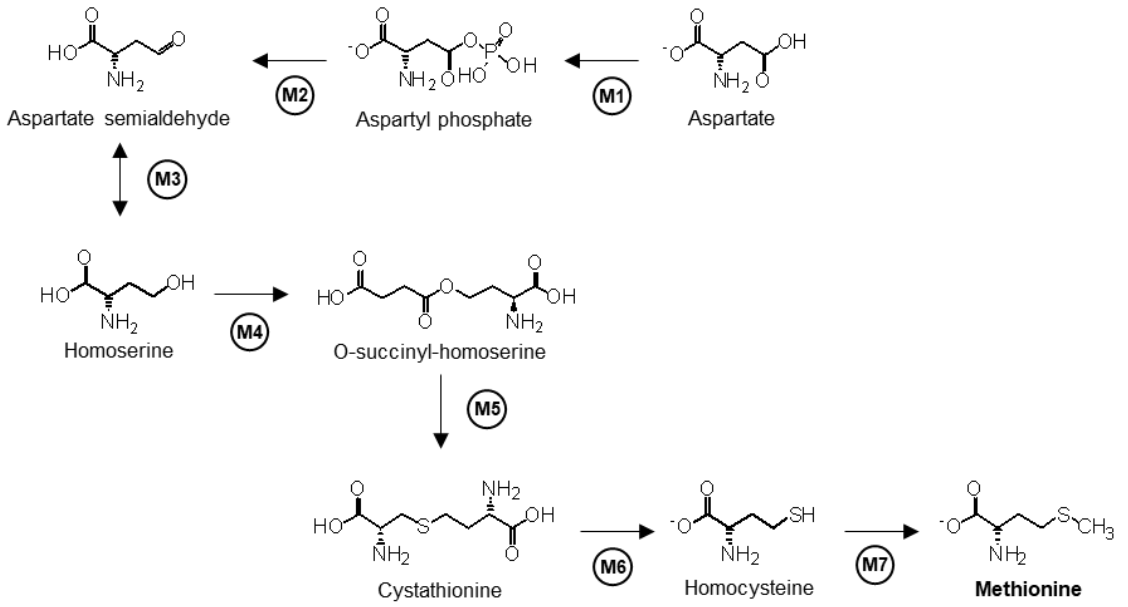

Figure 3.9. Methionine biosynthesis pathway in *Shimia aestuarii* AMM-P-2, adapted from the KEGG database (M00017). Enzymes that mediate each step are listed in Table 3.4.

Table 3.4. Predicted proteins of *Shimia aestuarii* AMM-P-2 that encode enzymes involved in the methionine biosynthesis pathway.

Catalyses step in pathway	KEGG identifier	Enzyme		*S. aestuarii* AMM-P-2 sequence	Reciprocal BLAST hit			
		Common name	EC number		Sequence identifier	Organism	E-value	% identity
M1	K00928	aspartate kinase (*lysC*)	2.7.2.4	HEBAHGMP_02930	WP_093028111	*Ruegeria marina*	0.00E+00	80.35
M2	K00133	aspartate-semialdehyde dehydrogenase (*asd*)	1.2.1.11	HEBAHGMP_00229	WP_093090633	*Shimia aestuarii*	0.00E+00	95.88
M3	K00003	homoserine dehydrogenase (*hom*)	1.1.1.3	HEBAHGMP_03385	WP_093095776	*Shimia aestuarii*	0.00E+00	84.81
M4	K00651	homoserine O-succinyltransferase/O-acetyltransferase (*metA*)	2.3.1.46	HEBAHGMP_02661	WP_093094066	*Shimia aestuarii*	0.00E+00	89.22
M5	K01739	cystathionine gamma-synthase (*metB*)	2.5.1.48	HEBAHGMP_00189	WP_093090600	*Shimia aestuarii*	0.00E+00	79.47
				HEBAHGMP_00185	WP_058309835	*Shimia thalassica*	0.00E+00	85.50
M6	K01760	cysteine-S-conjugate beta-lyase (*metC*)	4.4.1.13	HEBAHGMP_00185	WP_058309835	*Shimia thalassica*	0.00E+00	85.50
				HEBAHGMP_00189	WP_093090600	*Shimia aestuarii*	0.00E+00	79.47
	K14155	cysteine-S-conjugate beta-lyase (*patB*)	4.4.1.13	HEBAHGMP_02583	WP_157708104	*Roseovarius faecimaris*	0.00E+00	76.67
M7	K00548	5-methyltetrahydrofolate--homocysteine methyltransferase (*metH*)	2.1.1.13	HEBAHGMP_02613	WP_093094111	*Shimia aestuarii*	0.00E+00	89.20
				HEBAHGMP_01621	WP_058310851	*Shimia thalassica*	0.00E+00	91.50
	K24042	methionine synthase / methylenetetrahydrofolate reductase (NADPH) (*yitJ*)	2.1.1.13	HEBAHGMP_02613	WP_093094111	*Shimia aestuarii*	0.00E+00	89.20

Focussing on DMSP metabolism, the genome of *S. aestuarii* AMM-P-2 has genes encoding for the two known DMSP degrading pathways: demethylation (Figure 3.10, step D2;

EC 2.1.1.269) and lyase (Figure 3.10, step D6; EC 4.4.1.3). The bacterium has the entire *dmdA/B/C* suite of genes that converts DMSP to MeSH, as well as DMSP lyases *dddP* and *dddW* which produce equal amounts of DMS and acrylate. It is also able to metabolise acrylate to propionyl-CoA through *acuI* and *prpE* genes. Interestingly, we also obtained significant matches to *dddA* and *dddC* (E-values ≥ 1.39 e^{-93}) which catabolises 3-hydroxypropionyl-CoA (3HP) to acetyl-CoA (Table 3.5). However, we were unable to find convincing protein matches to *dddD* or *acuNK* which mediates the production of 3HP from DMSP. Finally, we were unable to identify any genes able to convert MeSH to methionine (EC: 1.8.3.4), which would have completed the entire cycle within the bacterium.

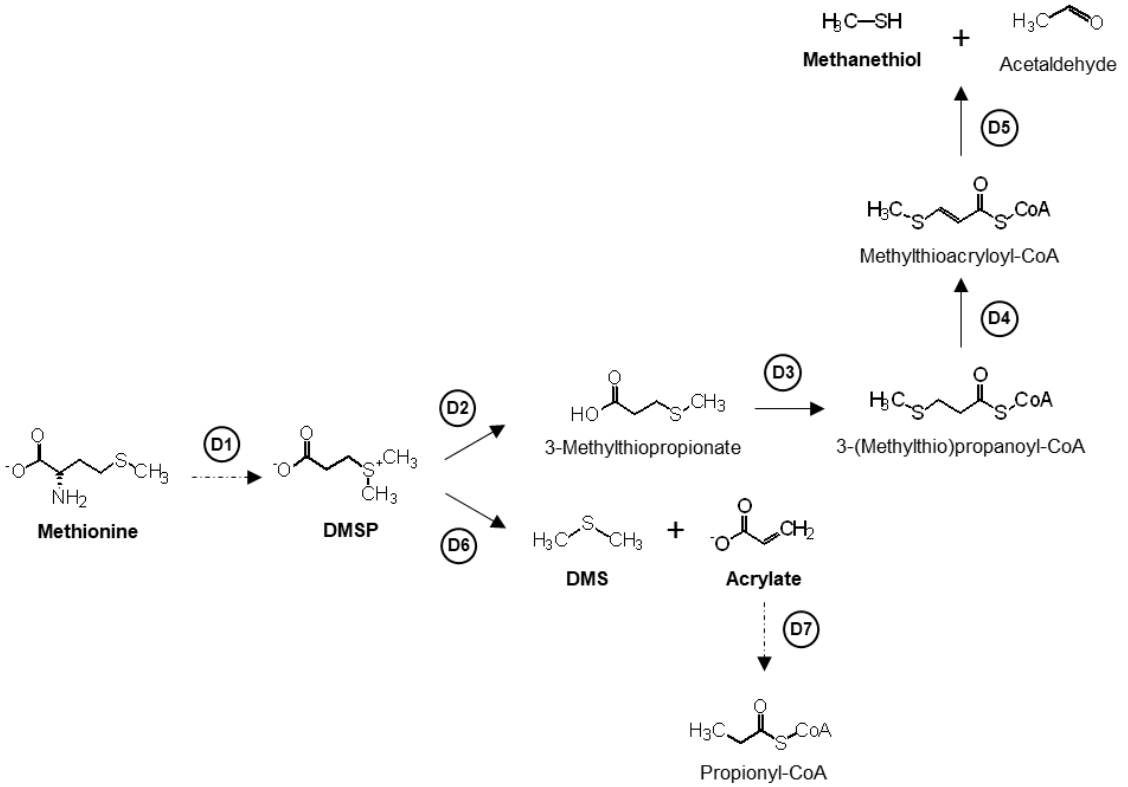

Figure 3.10. DMSP metabolism pathways in *Shimia aestuarii* AMM-P-2. Incomplete pathways are denoted with a dash-dotted arrow indicating the presence of one or more genes involved in the pathway, but not all. Enzymes that mediate each step are listed in Table 3.5.

Table 3.5. Predicted proteins of *Shimia aestuarii* AMM-P-2 that encode enzymes involved in DMSP metabolism.

Catalyses step in pathway	KEGG identifier	Enzyme		*S. aestuarii* AMM-P-2 sequence	Reciprocal BLAST hit			
		Common name	EC number		Sequence identifier	Organism	E-value	% identity
D1	N/A	2-hydroxy-4-(methylsulphanyl)butanoate S-methyltransferase (*dsyB*)	N/A	HEBAHGMP_01686	WP_132601883	*Rhodovulum adriaticum*	0.00E+00	77.22
D2	K17486	Dimethylsulphoniopropionate demethylase (*dmdA*)	2.1.1.269	HEBAHGMP_02450	NMM45499	Rhodospirillaceae bacterium KN72	0.00E+00	74.13
D3	N/A	3-(methylthio)propionyl-CoA ligase (*dmdB1*)	6.2.1.44	HEBAHGMP_01042	WP_058311441	*Shimia thalassica*	0.00E+00	78.41
	K20034	3-(methylthio)propionyl-CoA ligase (*dmdB2*)	6.2.1.44	HEBAHGMP_02920	WP_093094716	*Shimia aestuarii*	0.00E+00	82.22
				HEBAHGMP_03389	WP_132862155	*Shimia isoporae*	0.00E+00	80.48
D4	K20035	3-(methylthio)propionyl-CoA dehydrogenase (*dmdC1*)	1.3.8.-	HEBAHGMP_01405	WP_093094704	*Shimia aestuarii*	0.00E+00	81.09
				HEBAHGMP_01606	WP_009810607	*Roseobacter* sp. MED193	0.00E+00	76.03
	K20035	Acyl-CoA dehydrogenase family protein (*dmdC2*)	1.3.8.-	HEBAHGMP_03514	WP_058312065	*Shimia thalassica*	0.00E+00	87.19
				HEBAHGMP_01606	WP_009810607	*Roseobacter* sp. MED193	0.00E+00	76.03
	K20035	3-(methylthio)propionyl-CoA dehydrogenase (*dmdC3*)	1.3.8.-	HEBAHGMP_01035	WP_093095301	*Shimia aestuarii*	0.00E+00	92.05
				HEBAHGMP_01606	WP_009810607	*Roseobacter* sp. MED193	0.00E+00	76.03
D5	K20036	(methylthio)acryloyl-CoA hydratase (*dmdD*)	4.2.1.155	HEBAHGMP_01406	MAY87610	*Pseudooceanicola* sp.	0.00E+00	92.94
				HEBAHGMP_01611	OIQ40102	*Roseobacter* sp. MedPE-Swde	0.00E+00	89.41
	N/A	Acrylate utilization hydratase (*acuH*)	4.2.1.17	HEBAHGMP_02442	WP_127113488	*Thalassobius* sp. ZQ172	6.00E-173	91.09
D6	K16953	Dimethylsulphoniopropionate lyase (*dddP*)	4.4.1.3	HEBAHGMP_00789	AUR03903	*Phaeobacter inhibens*	0.00E+00	80.54
	K16953	Dimethylsulphoniopropionate lyase (*dddW*)	4.4.1.3	HEBAHGMP_01433	PHO04256	Rhodobacteraceae bacterium 4F10	1.00E-60	69.92
D7	K14469	Acryloyl-CoA reductase (*acuI*)	1.3.1.84	HEBAHGMP_01550	ASP23632	*Antarctobacter heliothermus*	0.00E+00	85.20
	K01908	Acrylate-CoA ligase (*prpE*)	6.2.1.17	HEBAHGMP_01052	WP_058311432	*Shimia thalassica*	0.00E+00	89.98
				HEBAHGMP_00838	WP_106606444	*Shimia abyssi*	0.00E+00	89.13
N/A	N/A	3-hydroxypropionate dehydrogenase (*dddA*)	N/A	HEBAHGMP_02567	WP_093091674	*Shimia aestuarii*	0.00E+00	87.40
				HEBAHGMP_02921	WP_093094639	*Shimia aestuarii*	0.00E+00	76.03
				HEBAHGMP_03579	WP_093455105	Rhodobacteraceae	0.00E+00	100.00
		Malonate-semialdehyde dehydrogenase (*dddC*)	N/A	HEBAHGMP_01889	WP_071675330	*Nioella nitratireducens*	0.00E+00	93.19

3.4 Discussion

3.4.1 Resolving the genomic basis of DMSP production in the AMT-P-4 culture

This study applied genomic methods to explore the capacity of an Alphaproteobacterium (*S. aestuarii*) and a Gammaproteobacterium (*V. hepatarius*), identified from coral tissues using 16S rRNA Sanger sequencing, to metabolise DMSP. A more thorough inspection of their

respective DNA exposed ambiguities in the sequenced 16S rRNA gene data of isolate AMT-P-4, initially identified as *V. hepatarius*, that could not be resolved due to the strict targeted approach of Sanger sequencing. As such, this method was unable to confirm the species homogeneity of the DNA (Montesino et al., 2007). The MinION method, used in conjunction with MiSeq which was applied to polish the data and remove minor systematic errors, proved critical in confirming this. Circular assemblies were obtained and enabled the unambiguous assignment of all genes to their organism of origin.

Both MiSeq and MinION sequencing are regularly used to generate *de novo* genome assemblies of various organisms including bacterial isolates (Quick et al., 2014; Allard et al., 2016). However, the higher quality short-reads obtained through MiSeq can lack contiguity (Goldstein et al., 2019) leading to fragmented contigs and ambiguous regions (Cahill et al., 2010; Kingsford et al., 2010; Koren et al., 2013; Neal-McKinney et al., 2021), as observed in Figure 3.2a for AMT-P-4. Meanwhile, longer reads obtained from MinION are often of lower quality (Laver et al., 2015; Jain et al., 2017) and are more prone to error (Ip et al., 2015), frequently requiring additional polishing steps (Goldstein et al., 2019). However, MinION can provide greater taxonomic resolution compared to MiSeq (Wommack et al., 2008; Nygaard et al., 2020). When both sequencing methods are used in conjunction (Pop, 2009; Henson et al., 2012) the outcomes can result in high-quality assemblies (Risse et al., 2015; Lu et al., 2016; Goldstein et al., 2019; Neal-McKinney et al., 2021) overcoming the limitations of short-read sequencing technologies and facilitating accurate annotation of genes, as can be seen in our efforts here, which resolved issues with the AMPT-P-4 culture.

Prior to the availability of genome sequence data presented here, the assumption was that the *dsyB* gene amplified from AMT-P-4 was encoded by *V. hepatarius,* resulting in the first report of a Gammaproteobacterium with a *dsyB* gene. However, the *dsyB* gene was eventually confirmed to belong to *S. aestuarii* and not *V. hepatarius*. This is in agreement with other studies that have confirmed DMSP production via the detection of DsyB proteins in prokaryotes belonging to the Alphaproteobacteria (Curson et al., 2017) or other ancient lineages including cyanobacteria, purple sulphur bacteria and purple non-sulphur bacteria (McParland and Levine, 2019). While genomic data are lacking for some non-Alphaproteobacteria prokaryotic groups at this time, it is important to recognise that the absence of sequence data supporting DMSP production by this particular group of bacteria does not mean they are necessarily incapable of producing this metabolite (Williams et al., 2019). In addition, the advent of more robust preliminary genetic screening able to establish the presence of the *dsyB* gene and neighbouring associated genes should expediate identification of bacteria with the genetic machinery to produce DMSP. Even though the combined MinION-MiSeq approach described here enables robust genetic screening

of mixed cultures and is capable of accurately identifying the origin of specific genes associated with the metabolism of DMSP, it remains necessary to conduct chemical analyses to establish whether the bacterium is actually able to produce intracellular DMSP (i.e., as reported in Chapter 2).

It is interesting that, to date, there is conservation of the *dsyB* gene within Alphaproteobacteria and that it has yet to be identified from any other bacteria class suggesting this Order plays a unique and important role in sulphur cycling. The gene *mmtN*, a separate but similarly robust reporter gene with the potential to synthesise DMSP (Williams et al., 2019), is common in Gammaproteobacteria. However, it is less abundant compared to *dsyB* (Williams et al., 2019; Sun et al., 2020). A Gammaproteobacterium belonging to the genus *Marinobacter* has also been found capable of producing DMSP, but lack *dsyB* and *mmtN* in its genome (Curson et al., 2017; Williams et al., 2019) indicating that unknown isoforms of the enzymes or other novel pathways (Dickschat et al., 2015) for the synthesis of DMSP exist. The possibility that more unknown bacteria capable of producing DMSP may exist must be taken into account when estimating DMSP budgets in the bacterial community and when bacteria are associated with other organisms such as corals.

3.4.2 DsyB protein in Shimia aestuarii *AMM-P-2*

Several *Shimia* species have been previously reported in coral microbial communities, notably, *S. isoporae* which was first isolated from the reef-building coral *Isopora palifera* (Chen et al., 2011), and *S. marina*, a potential coral pathogen which has been consistently identified within bacterial communities associated with *Porites* white patch syndrome (Séré et al., 2014). Until now little has been understood about sulphur metabolism by coral-associated *Shimia* spp., although there has been a report of a *Shimia* strain originating from marine sediment that is capable of aerobic and anaerobic sulphur cycling at the seafloor, which has the genetic machinery to produce DMS through the degradation of DMSP or the reduction of dimethylsulphoxide (Kanukollu et al., 2016). Here we report the presence of the DMSP biosynthesis gene, *dsyB*, in *Shimia* spp., thereby elevating the importance of this genus in the cycling of sulphur on coral reefs.

The proximity of *isc*/*suf* genes to *dsyB* in *S. aestuarii* suggests that DMSP may play a role in the bacterium's responses to environmental stressors faced by the coral holobiont. These groups of genes encode proteins involved in the Fe-S cluster assembly, which have a role in oxidative stress protection (Ayala-Castro et al., 2008). The IscS protein has been previously shown to interact with and transfer sulphur from cysteine to IscU scaffold proteins within the Fe-

S assembly. Meanwhile, the IscR protein is known to regulate *suf* transcription in response to oxidative stress (Yeo et al., 2006). Aside from *S. aestuarii* AMM-P-2, other well-characterised strains of bacteria capable of producing DMSP include *L. aggregata* LZB033 via *dsyB* (Curson et al., 2017) and *Novosphingobium* sp. BW1 via *mmtN* (Williams et al., 2019). DMSP production by *L. aggregata* LZB033 did not appear to be affected by varying conditions of salinity, temperature, oxidative stress, nitrogen supply, freezing, or combinations of these conditions (Curson et al., 2017), which is consistent with a notable lack of linkage in the functions of predicted proteins neighbouring DsyB (see Figure 3.6b). However, a more comprehensive study of the transcriptomics of *L. aggregata* is needed to confirm this. As the *dsyB* gene in *S. aestuarii* AMM-P-2 neighbours clusters of Fe-S genes (*sufX*) associated with stress responses (Figure 3.5a), it would also be pertinent to investigate how *dsyB* expression in *S. aestuarii* AMM-P-2 is potentially influenced by environmental stressors regularly experienced by the coral host. In addition, while the production of DMSP by *Novosphingobium* sp. BW1 has been shown to be significantly enhanced by the addition of methionine (Williams et al., 2019), the influence of environmental stressors is yet to be investigated.

3.4.3 Pathways to DMSP production in Shimia aestuarii *AMM-P-2*

Genome sequencing has revealed that *S. aestuarii* AMM-P-2 possesses a complete set of genes encoding for the DMSP biosynthesis pathway from inorganic sulphate, to DMSP, enabling it to produce DMSP *de novo*. *S. aestuarii* is capable of utilising sulfate from seawater, as well as select the least energetically-costly route to produce sulphur by-products as needed. Although the bacterium is capable of methionine synthesis through *metH* or *yitJ*, its growth on methionine-enriched media (as discussed in Chapter 2) indicates that it is also able to uptake exogenous sources of methylated sulphur compounds, boosting the pool of reduced sulphur intermediates available for the synthesis of DMSP.

The presence of *dsyB* in *S. aestuarii* AMM-P-2 confirms that it utilises the transamination pathway (see Figure 1.3 in Chapter 1) to produce DMSP (Curson et al., 2017). The intermediates for this pathway (4-methylthio-2-oxobutyrate, MTOB; 4-methylthio-2-hydroxybutyrate, MTHB; 4-dimethylsulphonio-2-hydroxybutyrate, DMSHB) are presumably present due to the committing step that *dsyB* mediates, which is the methylation of MTHB to DMSHB (Gage et al., 1997; Summers et al., 1998; Ito et al., 2011). Despite this knowledge, the genes that mediate the steps prior to methylation in the transamination pathway in bacteria are currently unconfirmed or unknown (Curson et al., 2017).

3.4.4 DMSP degradation pathways in Shimia aestuarii *AMM-P-2*

Aside from DMSP production, *S. aestuarii* AMM-P-2 also has a complete suite of genes capable of degrading DMSP into either MeSH (demethylation pathway) or equal amounts of DMS and acrylate (cleavage pathway). It has been previously hypothesised that concentration of environmental DMSP might be an important factor regulating the choice of degradation pathway used by bacteria (Kiene et al., 2000). This hypothesis was recently confirmed, revealing that when DMSP concentrations are low the demethylation pathway is favoured, whereas when concentrations are higher, most of the DMSP is converted to DMS through the cleavage pathway (Gao et al., 2020). Other factors have also been suggested to affect the regulatory juncture of DMSP degradation in bacteria including ultraviolet light stress (Slezak et al., 2007) and osmolyte requirements (Kiene et al., 2000; Reisch et al., 2008). Further physiological studies alongside measurements of gene regulation (Varaljay et al., 2015) are required to confirm the conditions that control the regulation of these competing pathways in *S. aestuarii* AMM-P-2.

It is noteworthy that *S. aestuarii* AMM-P-2 has the genetic machinery to degrade acrylate into less toxic compounds. Corals belonging to the genus *Acropora* are known to produce and accumulate within their tissues large quantities of intracellular acrylate from the degradation of DMSP (Tapiolas et al., 2010). It is therefore likely that coral-associated bacteria contribute to this large pool of acrylate. In addition, most of the known acrylate degrading genes have been identified in bacteria (Todd et al., 2010; Todd et al., 2012b). Interestingly *acuI* typically functions in conjunction with the demethylation gene, *dmdA* (Todd et al., 2012b), potentially affecting the partition of the DMSP catabolic flux between cleavage and demethylation routes.

3.4.5 Conclusions and future direction

This study showcases the importance of applying more robust, in-depth next-generation sequencing whenever possible to confirm the results of preliminary screening based on standard Sanger sequencing. When used together, MiSeq and MinION sequence data can generate high quality bacterial genomes while resolving ambiguities in preliminary screening data. Analyses of the genome of the coral-associated bacterium, *S. aestuarii* AMM-P-2, assembled using this strategy, permitted identification of genes involved in sulphate assimilation and DMSP metabolism, and suggest roles for this bacterium in sulphur cycling within the coral holobiont. A priority for future research must be the application of chemical and/or physical techniques to test hypothetical roles that have been proposed for *S. aestuarii* AMM-P-2 based on the genome data.

Chapter 4:
The effect of environmental stressors on DMSP biosynthesis in coral-associated bacteria

Abstract

Dimethylsulphoniopropionate (DMSP), a central compound in the marine sulphur cycle, is produced in large amounts by corals. Its production is impacted by environmental stressors experienced by coral reefs in the Anthropocene. The discovery that coral-associated bacteria can also produce DMSP has introduced an additional factor influencing DMSP dynamics within the coral holobiont. In Chapter 4, cultures of *S. aestuarii* AMM-P-2 were exposed to variation in both temperature and salinity, high UV radiation, and complete darkness, and DMSP concentrations monitored. Intracellular DMSP concentrations increased almost two-fold under both hypersaline conditions (40 PSU) and following UV exposure. Meanwhile, conditions that are stressful for the coral host but not necessarily for the bacteria, such as fluctuations beyond the average temperature range (22 and 32°C), did not induce significant changes in intracellular DMSP concentrations. DMSP production in response to variable salinity and UV suggests that under stress, *S. aestuarii* AMM-P-2 favoured the DMSP cleavage pathways, which in addition to acrylate, produce the antioxidant DMS. Overall, these results indicate that DMSP biosynthesis by *S. aestuarii AMM-P-2* is impacted by specific environmental conditions which are not necessarily tied to coral stress.

4.1 Introduction

In recent years, coral reefs have been severely impacted by climate change and other anthropogenic stressors, threatening their ecological integrity and function (Field, 2014). In addition to ocean acidification, which can compromise coral calcification (Hoegh-Guldberg et al., 2007; Erez et al., 2011; Mollica et al., 2018), increases in the frequency and intensity of exposure to thermal stress leads to mass bleaching events (Hoegh-Guldberg, 1999; Hughes et al., 2003; Hughes et al., 2018b; Hughes et al., 2018a; Hughes et al., 2019). These stressors have significant ecological impact on coral reef ecosystems: they reduce habitat complexity (Hughes et al., 2018b) and change community structure (Glynn, 1993; Hughes, 1994; Shulman and Robertson, 1996; Ostrander et al., 2000; Bellwood et al., 2006b). A well-documented stress response in corals is the increase or decrease of dimethylsulphoniopropionate (DMSP) concentrations measured in coral tissue. For example, heat stress can result in increases in DMSP levels in hard corals from the genus *Acropora* (Raina et al., 2013; Deschaseaux et al., 2014a; Jones et al., 2014; Gardner et

al., 2017). Variation in seawater salinity can also induce major changes (both increases or decreases) of intracellular DMSP concentrations (Gardner et al., 2016; Aguilar et al., 2017). Previous studies have shown that other stressors such as irradiance (Fischer and Jones, 2012; Cropp et al., 2018), or elevated exposure to copper (Yost et al., 2010) or zinc (Deschaseaux et al., 2018) can also affect DMSP levels in corals.

DMSP can be produced by multiple members of the coral holobiont: Symbiodiniaceae (Keller et al., 1989; Hill et al., 1995; Broadbent et al., 2002; Van Alstyne et al., 2009; Yost and Mitchelmore, 2009; Steinke et al., 2011), the coral host (Raina et al., 2013; Aguilar et al., 2017), and coral-associated bacteria (see Chapter 2). It has several functions, acting as an osmolyte (Kirst, 1996; Stefels, 2000; Yoch, 2002), an antioxidant (Sunda et al., 2002; Deschaseaux et al., 2014b; Gardner et al., 2016), a chemoattractant (Steinke et al., 2002; DeBose and Nevitt, 2007; Seymour et al., 2010) or a cryoprotectant (Karsten et al., 1996). Deciphering which members are responsible for the variation in DMSP concentrations observed during stress is challenging due to the intertwined nature of the holobiont. Testing the response to stress of holobiont members in isolation is one avenue to understand DMSP dynamics in corals and this approach has previously been applied to Symbiodiniaceae in culture (Gage et al., 1997; Van Alstyne et al., 2009) and aposymbiotic coral juveniles (Raina et al., 2013; Aguilar et al., 2017). To date, the stress response of DMSP-producing coral-associated bacteria has not been investigated.

Curson et al. (2017) has recently reported the discovery that marine bacteria are capable of producing DMSP. One of the genes responsible for this biosynthesis was identified as *dsyB*, which encodes the key methyltransferase enzyme of the methionine transamination route (see Chapter 1, Figure 1.3), a pathway also used by macroalgae and phytoplankton (Gage et al., 1997). DMSP production and *dsyB* transcription were upregulated in cultures of the alphaproteobacterium *Labrenzia aggregata* exposed to increased salinity, nitrogen limitation and low temperature (Curson et al., 2017). Homologues of DsyB proteins have since been found in many marine Alphaproteobacteria (Curson et al., 2017), including in five species of coral-associated bacteria recently isolated from *Acropora millepora* (see Chapter 2). Of these, *Shimia aestuarii* is the most prolific DMSP producer, however, the environmental conditions that regulate the biosynthesis of this molecule are currently unknown.

Here we used a combination of quantitative nuclear magnetic resonance (qNMR) and quantitative polymerase chain reaction (qPCR) to investigate the effect of multiple environmental stressors on the expression of *dsyB* and subsequent production of DMSP in the coral-associated bacterium *S. aestuarii* AMM-P-2. These stressors included high and low growth temperatures, constant darkness, UV exposure, and hyper-/hyposaline conditions, all of which are known to alter DMSP concentrations in the coral holobiont (Fischer and Jones, 2012; Raina et al., 2013;

Jones et al., 2014; Aguilar et al., 2017; Gardner et al., 2017). By using stressor levels that are relevant for coral reefs, this work aims to characterise the role that environmental factors play in DMSP production in coral-associated bacteria.

4.2 Methodology

4.2.1 Bacteria culture and growth

Isolate AMM-P-2 (Chapter 2) was revived from 20% v/v glycerol stock using 6 ml of modified minimal basal media (MBM) (Curson et al., 2017). Methionine (final concentration 0.5 mM) was added as a source of sulphur to the modified MBM and the culture incubated at 27°C and 180 RPM (Innova 44R, New Brunswick Scientific, New Jersey, United States). Once growth was visible to the naked eye (approximately 3-4 days), an aliquot of the starter culture was inoculated (1:10 dilution) into 60 ml of modified MBM. As previously, 0.5 mM methionine was added, and the culture maintained at 27°C and 180 RPM.

Two replicate cultures were prepared to monitor the bacterium's growth. Modified MBM (60 ml) containing 0.5 mM methionine maintained under the same conditions acted as the control. Every two hours for 48 hours, all three cultures were gently shaken to ensure homogeneous distribution within the media, and 100 µl aliquots transferred by pipette into sterile microcentrifuge tubes. The optical density of the three cultures (2 µl each) was measured at 600 nm (OD_{600}) on a NanoDrop 1000 spectrophotometer (Thermo Fisher Scientific, Massachusetts, United States) and a standard growth curve generated.

4.2.2 Bacteria stress experiment

Starter cultures of *S. aestuarii* AMM-P-2 were grown under different environmental conditions simulating those that induce stress in tropical corals: temperature, UV and salinity. Bacteria cultures were initially grown under standard conditions: 27°C at 180 RPM, ambient lighting, and 35 practical salinity units (PSU). To test the effect of temperature, the bacterial cultures were grown at 22°C (low temperature; T_{22}) and 32°C (high temperature; T_{32}). To test the effect of extreme UV, the bacteria were exposed to UV through a combination of Deluxlite Black Light Blue (18W) and Reptile One UVB 5.0 (18W) UVR fluorescent tubes or grown in complete darkness. Full spectrum radiation emitted by the UVR fluorescent tubes was measured using a Solarmeter Model 5.0 UVA + UVB meter (Solar Technology, Pennsylvania, United States), with an average UV emission in the incubator of 1.328 mW cm^{-2}. These measurements included the attenuation of the UVR through the glass flasks used for the cultures. To test the effect of extreme

salinity, the quantity of sea salts (Sigma-Aldrich, Missouri, United States) was adjusted using a 8410A Portasal salinometer (Guildline Instruments, Ontario, Canada) calibrated with IAPSO SS (International Association for Physical Sciences of the Ocean Standard Seawater; Ocean Scientific International, Hampshire, United Kingdom) to give a final salinity equivalent to 25 PSU (low) and 40 PSU (high) in the modified MBM. Three biological replicates were grown for each of the described conditions, including control conditions.

Cultures were sampled over four time points corresponding to the mid-exponential (24 hours), late exponential (28 hours), early stationary (32 hours), and late stationary (36 hours) growth stages of the bacterium, as established from the standard growth curve. At each time point, one culture per treatment was removed and aliquots taken for: protein estimation (1 ml; snap frozen and stored in -80°C until required), RNA extraction (10 ml) and quantitative nuclear magnetic resonance (qNMR) analysis (49 ml; centrifuged for 5 min at 3,000 *g*, pellet snap frozen and stored at -20°C until analysis).

4.2.3 Protein estimation

The frozen cells (1 ml aliquots taken from each culture at each time point) were defrosted gradually at room temperature, then vortexed quickly for 3 s to resuspend. Resuspended cells were lysed by sonication for 10 s on ice (to ensure samples did not overheat). Sonication was repeated three times with 30 s rest between each event, after which samples were centrifuged at a maximum speed (21,130 *g*) for 5 min and the supernatant collected. The protein content was estimated using the Bradford method (Bradford, 1976) and the protein extraction performed using the Quick Start Bradford Protein Assay Kit 1 (Bio-Rad, California, United States) following the manufacturer's protocol. Protein concentrations were then measured on a Cytation 3 Cell Imaging Multi-Mode Reader (Biotek, Vermont, United States).

4.2.4 Bacterial cell counts

To determine the conversion factor between optical density and bacterial cell number, OD_{600} and flow cytometry counts were carried out simultaneously on *S. aestuarii* grown under standard conditions in triplicate (27°C at 180 RPM, ambient lighting, 35 PSU, in modified MBM). After each OD_{600} measurement, 100 µl of cells were fixed for 15 min in 2% glutaraldehyde for subsequent flow cytometry analysis. Samples were then stained with SYBR Green (1:10,000 final dilution; ThermoFisher, Massachusetts, United States), incubated for 15 min in the dark and

analysed on a CytoFLEX S flow cytometer (Beckman Coulter, California, United States) with filtered MilliQ water as the sheath fluid. For each sample, forward scatter (FSC), side scatter (SSC), and green (SYBR) fluorescence were recorded. The samples were analysed at a flow rate of 25 µl min^{-1}. Microbial populations were characterized according to SSC and SYBR Green fluorescence (Marie et al., 1997) and cell abundances were calculated by running a standardized volume (50 µl) per sample.

4.2.5 RNA extraction and cDNA synthesis

Bacterial RNA was extracted from 10 ml of culture using RNeasy Plus Mini Kits (Qiagen, Hilden, Germany). The 10 ml aliquots were initially centrifuged for 5 min at 5,000 *g* and then processed following the manufacturer's protocol with some modifications (see below). Once processed, the supernatant was decanted, and the bacterial pellets stored at -80°C until required.

Bacterial pellets kept frozen in a liquid nitrogen bath were extracted as follows: 1 ml of Buffer RLT Plus was added into each microcentrifuge tube and pipetted up and down repeatedly until a homogeneous mix was achieved. The suspension was transferred into 2 ml Powerbead tubes (0.1 mm glass beads; Qiagen, Hilden, Germany) and the bacterial cells disrupted using a FastPrep-24 5G bead beating system (MP Biomedicals, California, United States) for 40 s at 6.0 m s^{-1}. The homogenised lysate was loaded onto a gDNA Eliminator spin column (Qiagen, Hilden, Germany) set in a 2 ml microcentrifuge collection tube and centrifuged for 30 s at 8,000 *g*. Equal volumes of 70% ethanol were added to the eluant and mixed well by gentle pipetting. The lysate was then transferred into a RNeasy spin column (Qiagen, Hilden, Germany) set in a 2 ml microcentrifuge collection tube and centrifuged for 30 s at 8,000 *g*. The ensuing eluant was discarded and 700 µl of Buffer RW1 added to the spin column which was again centrifuged for 30 s at 8,000 *g*. The eluant was again discarded and 500 µl of Buffer RPE added followed by centrifugation for 30 s at 8,000 *g*. Treatment of the retentate with Buffer RPE was repeated with a longer centrifugation step (2 min) after which the spin column was transferred to a clean 2 ml microcentrifuge collection tube. RNase-free water (50 µl) was added directly to the spin column membrane and centrifuged for 1 min at 8,000 *g*. The eluate containing the RNA was stored at -20°C and analysed within a week.

The extracted bacterial RNA was treated with TURBO DNase (Invitrogen, California, United States) following the manufacturer's protocol to eliminate traces of genomic DNA. Each sample was then analysed on a Qubit 3.0 Fluorometer using the protocol for Qubit RNA HS Assay Kit (Thermo Fisher Scientific, Massachusetts, United States), to determine the quantity and quality of the RNA. Reverse transcription of the DNA-free RNA samples was achieved using

SuperScript IV VILO Master Mix (Invitrogen, California, United States) according to the manufacturer's protocol. No reverse transcriptase (NRT) controls were performed on randomly selected samples to confirm samples were free of DNA or other contaminants.

4.2.6 Real-time quantitative polymerase chain reaction (RT-qPCR)

The SYBR qPCR assay system was applied to quantify the *dsyB* transcript and that of the housekeeping gene, *recA*, in the samples. Assays were prepared with an epMotion 5075l automated liquid handling system (Eppendorf, Hamburg, Germany) and performed on a Bio-Rad CFX384 Touch Real-Time PCR System (California, United States) with three technical replicates, a standard curve, and negative controls. A melting curve analysis was also carried out at the end of every run to confirm the presence of a single PCR product. The reaction mixture for each assay was: 2.5 µl iTaq Universal SYBR Green Supermix (Bio-Rad, California, United States), 0.2 µl of each 10 µM forward and 10 µM reverse primers, 1 µl of template DNA, and 1.1 µl of sterile water for a final reaction volume of 5 µl.

A set of RT–qPCR primers specific for *dsyB* and *recA*, as described in Curson et al. (2017), were used. The bacterial DMSP biosynthesis gene (*dsyB*) was amplified with dsyB_F (5'–CTTGACGCCACAGCATGTTG–3') and dsyB_R (5'– TCCGTCCTTTCACCAGAAAC–3') with the following cycling conditions: 95°C for 3 min followed by 40 cycles of 95°C for 15 s, 50°C for 15 s, and 72°C for 45 s. The housekeeping gene (*recA*) was amplified with recA_F (5'-CACTGGAAATTGCCGATACG-3') and recA_R (5'- CACCATGCACTTCGACTTG-3') with the following cycling conditions: 95°C for 3 min followed by 45 cycles of 95°C for 15 s, and 60°C for 1 min.

For quality control, the coefficient of variation (CV) was calculated for the technical triplicates (1.5 ± 1.3; average ± standard deviation), and where necessary, triplicates with a CV greater than 2% were removed from the analysis.

4.2.7 Quantitative nuclear magnetic resonance (qNMR)

Frozen bacteria pellets were lyophilised overnight in a Dynavac FD-12 freeze drier (Massachusetts, United States). The dried pellets were then resuspended in 1 ml of deuterated methanol (CD_3OD; Cambridge Isotope Laboratories, Massachusetts, United States), vortexed at maximum speed for 5 min, and sonicated for 5 min at room temperature. A further 1 ml of CD_3OD and 666 µl of deuterium oxide (D_2O; Cambridge Isotope Laboratories, Massachusetts, United

States) were added into the mixture (for a final CD_3OD to D_2O ratio of 3:1), which were then vortexed at maximum speed for 5 min and sonicated for 10 min at room temperature. A clean spatula was used to break up any remaining pellet chunks. The bacteria extracts were subsequently centrifuged at 3,000 *g* for 5 min. A 700 µl aliquot of each particulate-free extract was transferred into a 5 mm Norell 509-UP NMR tube (North Carolina, United States) and analysed immediately using qNMR via the ERETIC method (Electronic REference To access In vivo Concentrations) (Akoka and Trierweiler, 2002) to measure the concentration of DMSP, as described in Tapiolas et al. (2013).

^{1}H NMR spectra were acquired on a Bruker Avance 600 MHz NMR (Massachusetts, United States) with TXI cryoprobe operated by Topspin 2.1, non-spinning at 290 K (22°C) with a spectral width of 20 ppm, a 90° pulse to maximize sensitivity, a relaxation delay of 35 seconds, receiver gain of 57, two dummy scans, 16 acquisition scans, and 64,000 data points. The spectra were referenced against CD_3OD (δH 3.31 ppm), phase and baseline corrected, then integrated. DMSP concentrations were calculated via the methyl singlet (2.98-2.90 ppm; $6H^+$) while acrylate concentrations were calculated via two integrals, whereby the two downfield doublet of doublet signals were integrated together (6.17-5.97 ppm; $2H^+$). Intra-compound integrals were compared to ensure consistency of the expected proton values.

The ERETIC method was performed using stock solutions of 1 mM DMSP prepared in CD_3OD and D_2O (ratio of 3:1). A synthetic ERETIC signal was applied at -0.5 ppm and its integral used as a reference, against which DMSP and acrylate peak concentrations were determined. The integral of the ERETIC signal was equivalent to 1 mM DMSP, where the measured integrals were equal to the actual concentrations of DMSP and acrylate in the samples.

4.2.8 Data analyses

Statistics were performed using IBM SPSS Statistics version 27.0.1. qNMR signals associated with DMSP and acrylate were normalised to cell density and tested for significance using repeated measures ANOVA, with Greenhouse-Geisser correction applied. A simple main effects analysis was done to determine the difference between treatments at each time point for both DMSP and acrylate. Further, a Pearson product-moment correlation was run to determine the relationship between DMSP and acrylate concentrations in *S. aestuarii* AMM-P-2. Detailed statistical data are presented in Supplementary Data Tables 4.1 to 4.5.

4.3 Results

4.3.1 Bacteria standard growth curve

S. aestuarii AMM-P-2, grown in methionine-enriched MBM under standard conditions and monitored by measuring the optical density, exhibited four distinct phases of growth during a 48 hours incubation (lag, exponential, stationary, and decline). From the growth curve (Figure 4.1), the sampling time points for the exposure experiments were chosen: mid-exponential (24 hours after inoculation), late exponential (28 hours after inoculation), early stationary (32 hours after inoculation), and mid-stationary (36 hours after inoculation).

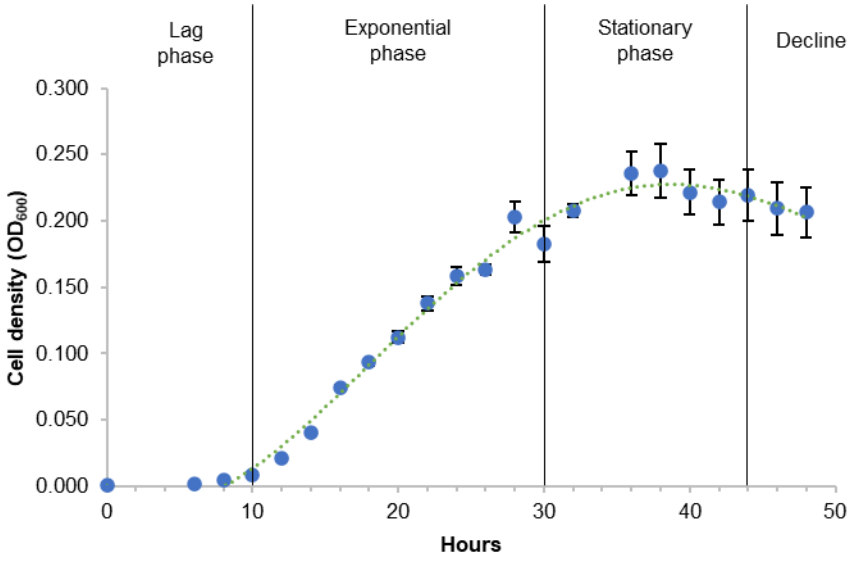

Figure 4.1. Growth curve of *Shimia aestuarii* AMM-P-2, grown in methionine-enriched modified minimal basal medium under standard conditions (27°C at 180 RPM, ambient lighting, and 35 PSU). phase. Error bars display standard error.

4.3.2 Protein estimation and bacterial cell counts

Total protein of *S. aestuarii* AMM-P-2 cultures grown under each experimental condition was measured at all four time points to allow normalisation of the chemistry produced by the bacterium. However, the protein concentrations (Figure 4.2) did not show an increase concomitant to cell density across time (Figure 4.3). Although previous studies into DMSP production by bacteria (Curson et al., 2017; Williams et al., 2019) have used total protein to normalise chemical data, the lack of correlation between protein concentration and bacterial density in *S. aestuarii* AMM-P-2 cultures precluded this. A lack of glycerol addition to the snap-

frozen culture aliquots was most likely responsible for the variable total protein measurements; samples stored at -80 °C without cryoprotectant can be compromised by the effects of freeze/thawing degrading bacterial cell integrity (Elliott et al., 2017). The supernatant was also observed to be slightly viscous, an indication that high molecular weight DNA may be present which could potentially interfere with the total protein measurements (Groves et al., 1968). Therefore, these data were assumed to be compromised and not used further.

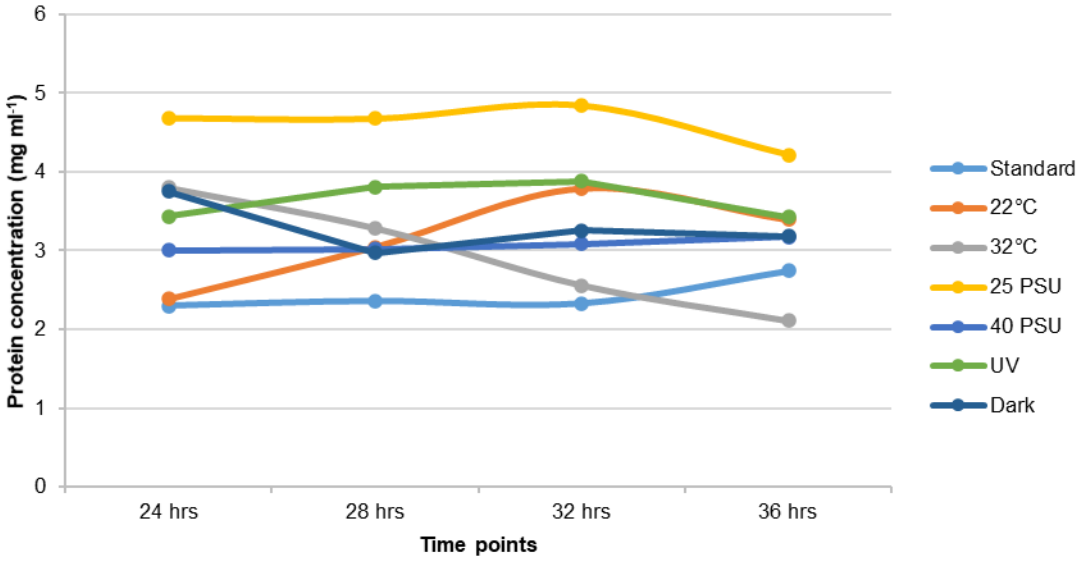

Figure 4.2. Protein concentration estimates for *Shimia aestuarii* AMM-P-2 cultures grown under varying experimental conditions of temperature (22 and 32°C), salinity (25 and 40 PSU), UV exposure and constant darkness.

Bacterial cell counts for *S. aestuarii* AMM-P-2 were obtained as an alternative method to normalise subsequent chemical data. For this purpose, culture cell numbers were quantified over a wide range of optical densities (at 600 nm; Figure 4.3). The equation obtained from the line of best fit was used to normalise production of DMSP and acrylate by the number of cells in subsequent experiments (Chiu et al., 2016).

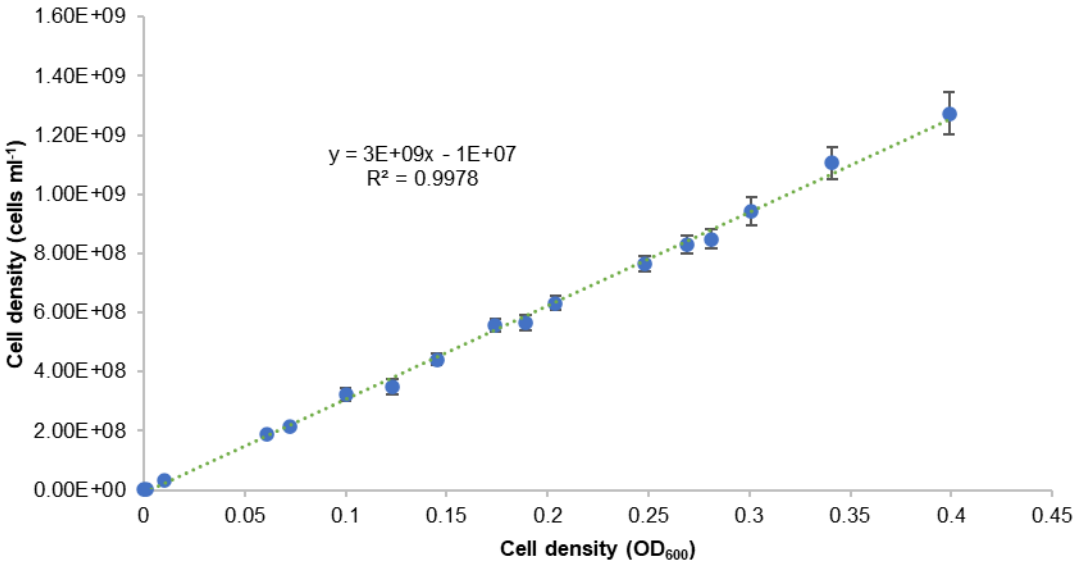

Figure 4.3. Calibration curve showing the relationship between optical density (OD_{600}) and cell density for *Shimia aestuarii* AMM-P-2. Error bars display standard error.

4.3.3 DMSP production under different stress conditions

Intracellular DMSP concentrations in *S. aestuarii* cells were not statistically different between the four time points, irrespective of the treatments (ANOVA, p = 0.078; see Supplementary Data Table 4.1). No significant interaction was identified between time and treatments (ANOVA, p = 0.204; see Supplementary Data Table 4.1). Under standard conditions, the average concentration of DMSP was 0.464 (±0.041) fmol cell^{-1}. The concentration of DMSP in cultures grown at 22°C was the only treatment that was not significantly different from the standard condition among the range of experimental conditions. Of the treatments, variations in salinity affected DMSP concentrations the most. Indeed, cultures grown in hyposaline conditions (25 PSU) had the lowest DMSP levels, with an average of 0.175 (±0.009) fmol cell^{-1}, 63% lower than standard conditions. In contrast, the highest DMSP measurements were recorded under hypersaline conditions (40 PSU), with an average of 0.836 (±0.032) fmol cell^{-1}, or 80% more intracellular DMSP compared to standard conditions. Changes in DMSP levels occurred at 24 and 32 hours under hyposaline conditions, and at all time points under hypersaline conditions. Intracellular DMSP concentrations were also altered when grown under high UV conditions and in complete darkness. Both UV and dark treatments resulted in major increases in intracellular DMSP levels with an overall increase of 65% and 43% compared to growth under standard conditions, or 0.767 and 0.665 fmol cell^{-1}, respectively. Impacts on DMSP concentrations were observed in the late exponential stage (28 hours) and with levels increasing as the experiment progressed. Darkness induced significant increases in DMSP concentrations in the stationary

phase (32 and 36 hours). Temperature variations resulted in lower DMSP concentrations compared to standard growth conditions. Of the two, only the higher temperature (32°C) was found to be significantly different between 28-32 hours. On average, the DMSP concentrations at 32°C were 42% less (0.271 fmol cell^{-1}) than what was produced at optimal, standard conditions.

The presence of DMS in *S. aestuarii* AMM-P-2 extracts was initially established by its distinctive smell. Although it cannot be measured quantitatively by qNMR due to its volatile nature, its production was corroborated by the detection of acrylate. qNMR analysis demonstrated acrylate was present in each sample and its concentration was approximately one order of magnitude lower than that of DMSP (Figure 4.4b). Together, these observations confirm the bacterium utilises the DMSP cleavage pathway. Unlike DMSP, however, acrylate concentrations differed significantly between time points (ANOVA, $p = 0.003$; see Supplementary Data Table 4.2), and the interaction between time and treatments was significant (ANOVA, $p = 0.047$; see Supplementary Data Table 4.2). Under standard growth conditions, the average acrylate level measured throughout the experiment was 0.125 (±0.008) fmol cell^{-1}, with an overall 38% drop in concentration between 24-36 hours, peaking at 0.128 (±0.017) fmol cell^{-1} at 32 hours.

The variations observed between treatments for DMSP concentrations were not as pronounced for acrylate. The 32°C treatment was the only condition that significantly affected acrylate concentrations across all four time points (with an average of 68% less acrylate compared to standard conditions). Cultures grown in the dark had significantly lower concentrations of acrylate than those grown under standard conditions, with an average of 0.075 fmol cell^{-1} (40% less). Salinity had the greatest impact on intracellular acrylate concentrations, with significant decreases (average 46% less than standard conditions) between 24-32 hours under hyposaline conditions, and significant increases (average 36% more than standard conditions) between 28-36 hours under hypersaline conditions.

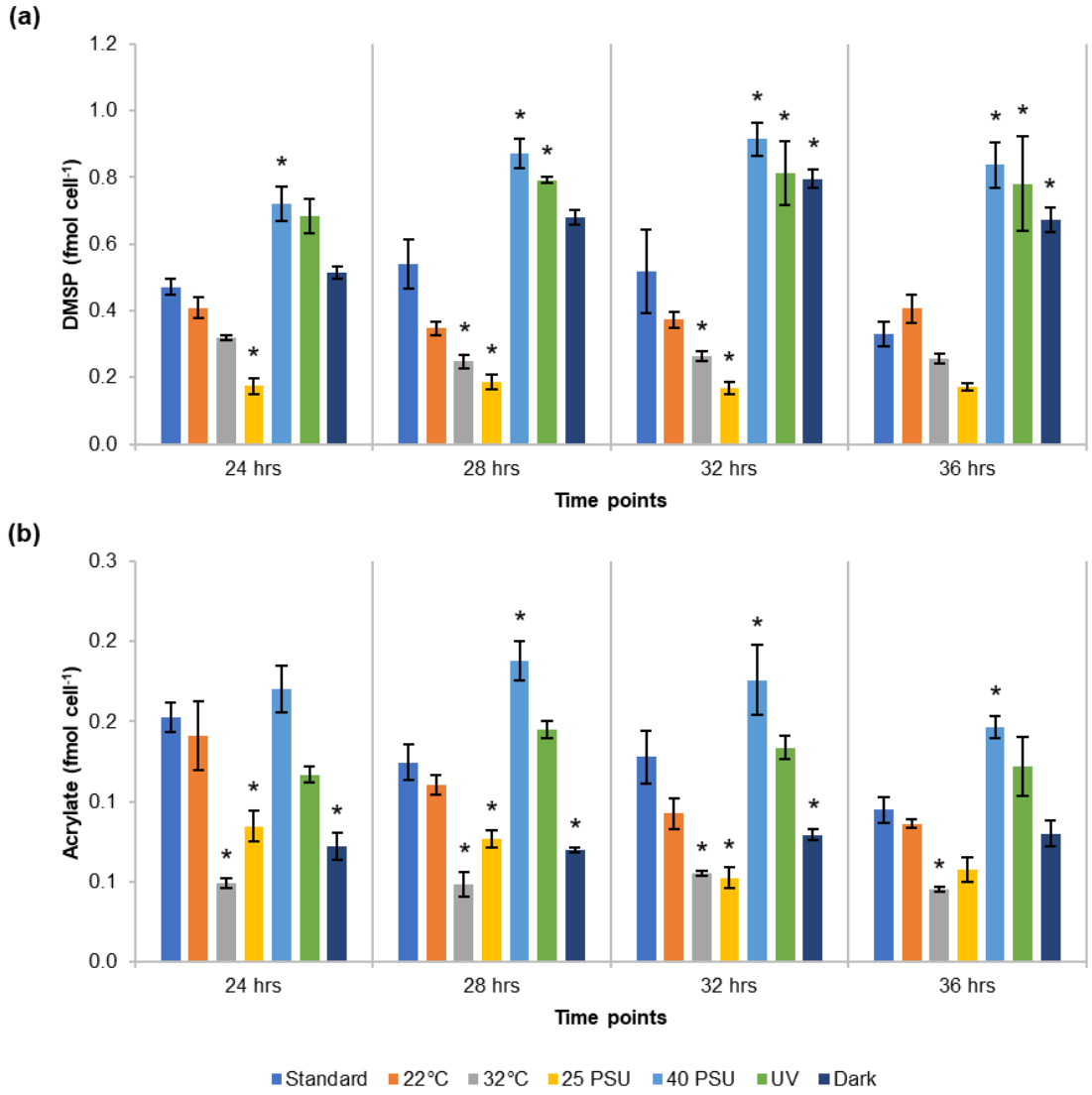

Figure 4.4. Changes in the concentration of (a) DMSP and (b) acrylate by *Shimia aestuarii* AMM-P-2 exposed to temperature (22 and 32°C), salinity (25 and 40 PSU), constant darkness, and UV exposure, measured at four growth time points. Standard conditions: cultures were grown at 27°C in modified MBM media adjusted to 35 PSU and supplemented with 0.5 mM methionine. Error bars indicate standard error ($n = 3$). Significance was determined using repeated measures ANOVA ($p \leq 0.05$), experimental conditions marked with an asterisk (*) are significantly different from the standard conditions.

A positive correlation was identified between the intracellular concentrations of DMSP and acrylate across the different conditions tested (Pearson Correlation, $r(28) = 0.708$, $p < .001$, Figure 4.5a; see Supplementary Data Table 4.5). Conditions were separated between two categories: (1) conditions that are stressors for bacteria (i.e., high UV, 25 and 40 PSU), and (2) those that are unlikely to elicit a stress in bacteria but are coral-related stress conditions (i.e., darkness, 22 and 32°C), and the responses reanalysed. No significant correlation was identified between DMSP and acrylate concentrations with respect to coral-related stress conditions

(R^2=0.054; Figure 4.5b), however, the increase in DMSP concentrations was closely mirrored by a concomitant increase in acrylate concentration in the bacterial-related stress treatments, resulting in a strong positive correlation (R^2=0.761; Figure 4.5c).

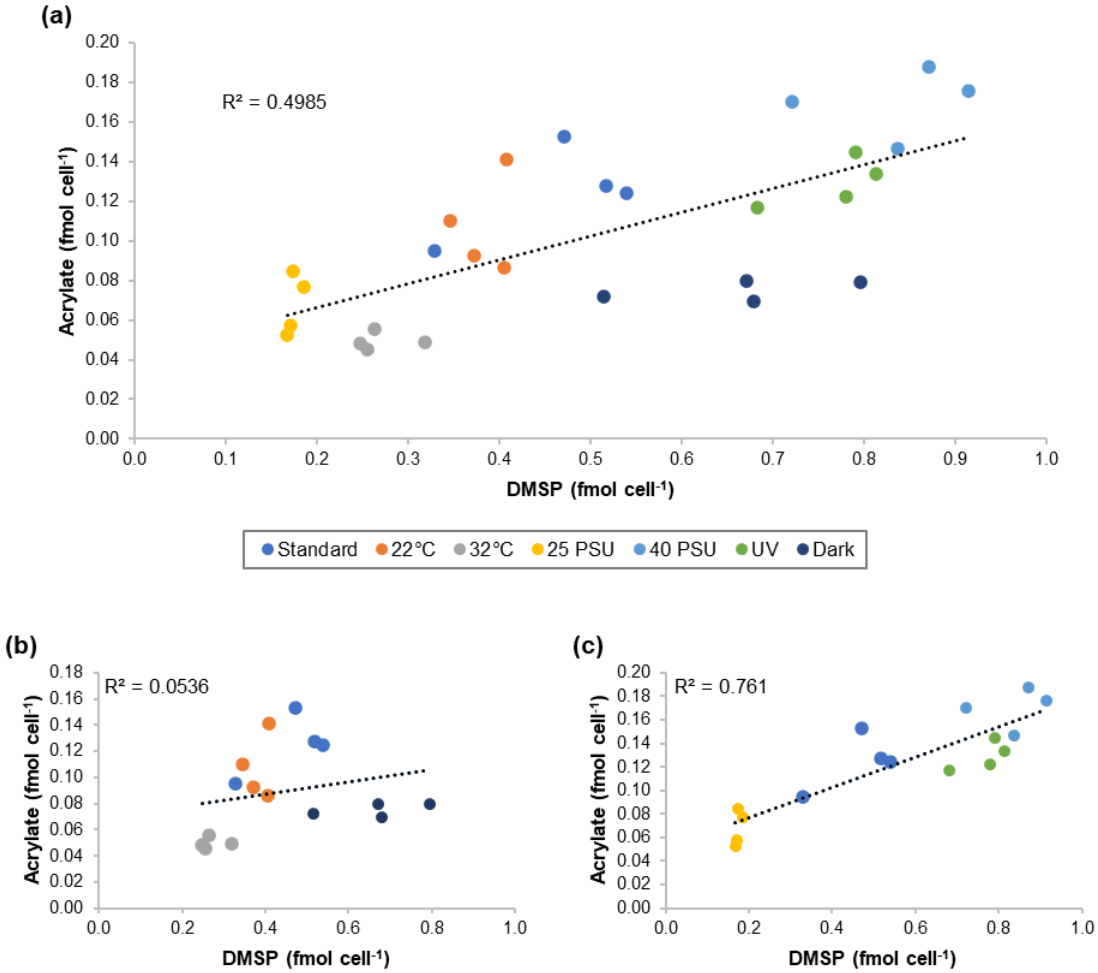

Figure 4.5. Correlation between the concentrations of DMSP and acrylate in *Shimia aestuarii* AMM-P-2 under (a) all experimental conditions (temperature [22 and 32°C]; salinity [25 and 40 PSU], constant darkness, and UV exposure), (b) coral-related stress conditions: temperature (22 and 32°C) and darkness, and (c) bacteria-related stress conditions: salinity (25 and 40 PSU) and high UV.

4.3.4 dsyB *gene regulation*

Having confirmed that the DMSP biosynthesis gene *dsyB* is present in the genome of the *S. aestuarii* AMM-P-2 and that the gene is functional through preliminary NMR measurements of its extract (reported in Chapters 2 and 3), the expression of *dsyB* was monitored across all experimental conditions employed in section 4.3.3 (Figure 4.6). The samples were run in

triplicates (see Supplementary Data Table 4.6), but some replicates failed during the qPCR runs. Compared to cultures grown in standard conditions, stress elicited a decreasing trend in *dsyB* expression across all conditions tested. In addition, these expression results were found to be highly variable and, within each treatment, the *dsyB* expression patterns did not correlate with the qNMR data (Figure 4.4a).

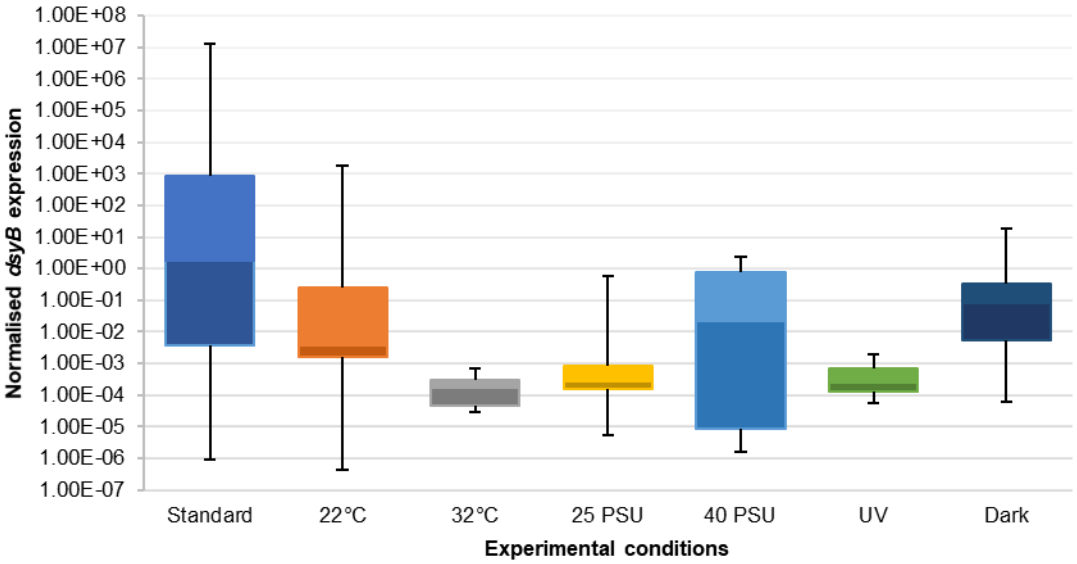

Figure 4.6. *dsyB* transcription in *Shimia aestuarii* AMM-P-2 under varying experimental conditions of temperature (22 and 32°C), salinity (25 and 40 PSU), constant darkness, and UV exposure.

4.4 Discussion

DMSP production by the coral animal and associated Symbiodiniaceae exhibit similar trends, with elevated intracellular concentrations occurring when the isolated partner is subjected to stressors commonly experienced by the holobiont on the reef (Jones and King, 2015). Our results show that, compared to control conditions, *S. aestuarii* AMM-P-2, a bacterial symbiont isolated from *Acropora millepora*, produced almost twice as much DMSP when exposed to hypersaline and high UV stress. In contrast, exposure to temperature stress (22 and 32°C), which induces changes in DMSP levels in the coral holobiont, had no effect. The detection of acrylate in *S. aestuarii* AMM-P-2 extracts confirmed the DMSP degrading genes identified in its the genome (see Chapter 3) are active. Overall, acrylate concentration was positively correlated with DMSP production. Changes in DMSP and acrylate concentrations over time mirrored the bacterium's growth curve, with concentrations of both metabolites falling as the culture aged. This decline in concentrations was more pronounced under hypo/hypersaline conditions and high

UV exposure, which are known to cause stress in a variety of bacteria (Stanley and Morita, 1968; Joux et al., 1999; Santos et al., 2013).

4.4.1 DMSP metabolism by Shimia aestuarii *AMM-P-2*

The DMSP concentrations in *S. aestuarii* cells were not significantly different between sampling time points within each of the seven culture treatments (i.e,. control, temperature [22ºC and 32ºC], salinity [25 and 40PSU], UV, and complete darkness). However, some treatments displayed larger changes in DMSP concentrations in relation to the control treatment. Salinity is a factor known to influence DMSP concentrations in corals (Gardner et al., 2016; Aguilar et al., 2017), while also affecting subsequent DMSP degradation in bacteria (Salgado et al., 2014; Liu et al., 2018). Results presented here corroborate past studies whereby hypersalinity induces higher DMSP synthesis in various organisms (Vairavamurthy et al., 1985; Kirst et al., 1991; Karsten et al., 1992; Trossat et al., 1998). The higher levels of intracellular DMSP under hypersaline conditions (~0.836 fmol $cell^{-1}$) compared to lower levels observed in hyposaline conditions (~0.175 fmol $cell^{-1}$) also supports the role of DMSP as an osmolyte in bacteria (Burg and Ferraris, 2008). This pattern was also observed in *L. aggregata* LZB033, currently the only other bacterial model for DMSP production (Curson et al., 2017).

Short term high UV exposure can generate hydroxyl radicals (•OH) and other reactive oxygen species (ROS), which can be detoxified by DMSP (Sunda et al., 2002; Darroch et al., 2015). The levels of UV radiation in this study were approximately double the values previously measured at the surface of Great Barrier Reef waters (~0.9 mW cm^{-2}) (Michael et al., 2012; Nordborg et al., 2018) or other coastal and oceanic locations (Tedetti and Sempéré, 2006; Barron et al., 2009). This high UV exposure, which acts as a proxy for oxidative stress, induced a nearly two-fold increase in DMSP concentration compared to control conditions, which suggests that this compound plays a role in protection against oxidative stress in *S. aestuarii* AMM-P-2.

The experimental growth conditions selected for this study were related to environmental stressors that the coral holobiont may experience on a reef (Fitt et al., 2001; Hughes et al., 2003; Hoegh-Guldberg et al., 2007), however, marine bacteria have a broad physiological capacity and these coral stress conditions are not likely stressful to the bacterial cells. For example, small temperature variations (e.g. ± 5°C) are likely not sufficient to induce a stress response in the bacteria as temperature alone is rarely a limiting factor for marine heterotrophic bacteria, particularly if grown *ex situ* (Pomeroy and Wiebe, 2001). This explains why DMSP concentrations were less affected by these conditions. Another condition not expected to be a stressor for heterotrophic bacteria is complete darkness. The increases in DMSP concentration recorded in cultures grown in absence of light supports the notion that light is not a limiting factor

for DMSP production, which has implications for DMSP dynamics of mesophotic coral ecosystems. Mesophotic corals generally support fewer algal cells per coral cell (Dustan, 1979; McCloskey et al., 1984; Ziegler et al., 2015), which limits the DMSP contribution of Symbiodiniaceae within the coral holobiont. Previously, DMSP production observed in Symbiodiniaceae (Borell et al., 2016) and corals (Laverick et al., 2019) in mesophotic zones were hypothesised as a possible defence against depth-related stress. A recent study revealed that deep-sea bacteria inhabiting the marine seafloor of the Mariana Trench produce substantial amounts of DMSP, the production of which increased with hydrostatic pressure (Zheng et al., 2020). As such, our results suggest coral-associated bacteria contribute more prominently to the holobiont DMSP pool in mesophotic corals, however, further targeted investigation is needed to confirm this.

Intracellular acrylate concentrations measured in *S. aestuarii* AMM-P-2 were almost one order of magnitude lower than those of DMSP and decreased significantly over time in all growth conditions. Acrylate and DMSP concentrations were strongly and positively correlated under conditions eliciting a stress for the bacteria (e.g., salinity, UV), but were decoupled under conditions that are stressful for the coral host but not necessarily for the bacteria (e.g., temperature, darkness). This suggests that under stress conditions, more DMSP is channelled towards the DMSP cleavage pathway, forming equal amounts of DMS and acrylate, rather than the demethylation pathway which forms MeSH and 3-mercaptopropionate (Howard et al., 2006; Todd et al., 2007; Curson et al., 2008; Gao et al., 2020). DMS can function as an antioxidant (Sunda et al., 2002; Deschaseaux et al., 2014b), and therefore may be the more useful compound (compared to MeSH), acting as a protective mechanism against oxidative stress and potential build-up of reactive oxygen species (ROS) which may accumulate due to intracellular stress.

4.4.2 dsyB regulation by Shimia aestuarii *AMM-P-2*

Unfortunately, we are unable to relate measured concentrations of DMSP in *S. aestuarii* cells with the level of expression of the *dsyB* gene. Indeed, levels of the *S. aestuarii dsyB* mRNA across the experimental conditions were highly variable within each treatment and were generally lower under all the treatments compared to the controls. Our results are not consistent with previous studies (Curson et al., 2017) and the large variability recorded within each treatment (several orders of magnitudes) stands in stark contrast with the low variance recorded with our qNMR measurements. Some of this variability may be due to the selection of the housekeeping gene used to normalise the expression of *dsyB*. We chose *recA* because it has previously been used to normalise *dsyB* expression (Curson et al., 2017), and the transcription of this gene appears to be constitutive in pure bacterial cultures as well as in the environment (Lloyd and Sharp, 1993;

Eisen, 1995; Cox, 2003; Giloteaux et al., 2013). However, given the involvement of recA proteins in DNA repair (Miller and Kokjohn, 1990), it may not be an appropriate standard for stress experiments, particularly in the case UV treatment, and other genes should be assessed for their suitability in this bacterium.

4.4.3 Conclusions and future direction

In summary, this study has shown that *de novo* production of DMSP by the coral-associated bacterium *S. aestuarii* AMM-P-2 is dynamic and regulated by specific environmental conditions. Variations in salinity, constant darkness, and UV exposure elicited the greatest effect on DMSP concentrations, confirming its role in bacterial stress response. The confirmed production of the antioxidant acrylate by the bacterium also establishes a link between the catabolism of DMSP and the bacterial stress response. These results indicate that the role bacteria play in the metabolism of DMSP and acrylate in the coral holobiont is complex, as stressors may elicit distinct effects on different members of the holobiont. Future studies should elucidate the regulatory dynamics of *dsyB* and other DMSP and acrylate degradation genes across a broad range of environmental stressors. It is important to note that coral-associated bacteria are likely to demonstrate different physiologies under stress in laboratory cultures compared to their natural symbiotic state within the coral host (Ohbayashi et al., 2019). Together with culture-independent studies investigating the effects of these stressors on microbial communities *in situ* within the coral holobiont, these additional investigations will further our understanding of the role these compounds play in the coral stress response in a changing climate.

Chapter 5:
Identification of polyacrylate in the skeleton of *Acropora millepora*, and its potential role in coral calcification

Abstract

Acrylate is directly derived from DMSP catabolism and is produced in high concentrations by fast-growing, reef-building corals, including *Acropora millepora*, constituting a substantial carbon source in the coral holobiont. While possible functions of acrylate in corals have been hypothesized, the reason for its accumulation in these organisms is still unknown. In industrial applications, its polymerised form, polyacrylate, can produce a stable scaffold for the precipitation of calcium carbonate ($CaCO_3$), which is the major component of coral skeleton. In Chapter 5, the potential role of acrylate in coral skeleton formation was investigated. One-week old aposymbiotic *A. millepora* juvenile corals were supplemented with ^{13}C-labelled acrylate and the coral skeleton examined using nanoscale secondary ion mass spectrometry (NanoSIMS) and confocal Raman spectroscopy, for the presence of polyacrylate. Although the NanoSIMS results were inconclusive, polyacrylate was detected by Raman at the growing edge of the skeleton, suggesting a role in the biomineralization of $CaCO_3$ and growth of the skeleton. These results suggest the presence of an alternate biomineralization mechanism that can be adopted by acrylate-producing corals, potentially contributing to the fast accretion rate of these coral genera.

5.1 Introduction

A wide range of marine taxa have the cellular machinery to biomineralize calcium carbonate ($CaCO_3$) and utilise some of its polymorphs (e.g. aragonite, calcite, and vaterite) as specialised structures for growth (i.e. skeleton and spicules) or defence (i.e. shells and spines) (Cusack and Freer, 2008). This makes $CaCO_3$ one of the most abundant minerals formed by living organisms (Ni and Ratner, 2008), and biomineralisation an integral biogeochemical process in marine ecosystems. Scleractinian corals are among the most prolific marine mineralisers, producing exoskeletons of $CaCO_3$ that form the structural basis of coral reefs (Chave et al., 1972; Barnes and Devereux, 1984). This ecosystem provides a habitat for approximately 25% of marine organisms (Fisher et al., 2015) and supports numerous ecosystem services generating hundreds of billions of dollars annually (Costanza et al., 2014). Besides being one of the most diverse ecosystems on the planet (Moberg and Folke, 1999; Bellwood et al., 2006a), coral reefs also act as a natural barrier for coastlines by providing a vast defensive buffer against the physical stress

generated by extreme weather events such as tropical cyclones or tsunamis (Pendleton, 1995; Moberg and Folke, 1999; Hoegh-Guldberg et al., 2007; Ferrario et al., 2014).

Despite the importance of coral calcification for coral physiology, ecosystem structure and primary production, this process remains poorly understood. The coral skeleton was initially predicted to form as a result of a purely physical process through the precipitation of inorganic aragonite from seawater (Falini et al., 2013; Higuchi et al., 2014). However, oxygen and carbon isotopes, which are widely used as environmental indicators, are not incorporated into the coral skeleton at the expected ratios. Microscopic comparison of $CaCO_3$ crystals in corals with those in inorganic minerals revealed a strong resemblance, however, the highly intricate and complex structures observed in the coral skeleton led Bryan and Hill (1941) to propose the concept of an organic "gel" enveloping each sclerodermite (fan-like, fine aragonite crystals) and guiding further crystal growth. Subsequently, Barnes (1970) hypothesized that the space located between the coral polyp and the skeletal surface harboured a viscous micro-scale layer of supersaturated $CaCO_3$ buffered with organic molecules, with this limited space favouring the precipitation of aragonite crystals. Since then, the existence and composition of this skeletal organic matrix (SOM) has been heavily debated (Tambutté et al., 2011; Falini et al., 2015). Studies into the sensitivities of coral calcification rates to seawater saturation of aragonite (Ω_A, a measure of the concentrations of dissolved calcium [Ca^{2+}] and carbonate [CO_3^{2-}] ions available for $CaCO_3$ precipitation) (Gattuso et al., 1998; Langdon et al., 2003; Langdon and Atkinson, 2005; Chan and Connolly, 2013; Farfan et al., 2018) have supported the idea that coral calcification is a physicochemical process whereby aragonite crystal formation is dependent on Ω_A (Ries, 2011). This is referred to as 'biologically-induced mineralisation' and promotes the precipitation of minerals along the surface of the cells through inorganic processes (Lowenstam, 1981; Allemand et al., 2011). However, it has also been argued that the calcification process may be mediated by biomolecules within the SOM (Mann, 1983), some of which have now been linked to the nucleation of aragonite crystals. This has been referred to as 'biologically-controlled mineralisation' (DeCarlo et al., 2018). Several of these biomolecules have been identified, including glutamate ($C_5H_8NO_4^-$) and aspartate ($C_4H_6NO_4^-$) (Figure 5.1a and b, respectively) and acidic proteins thereof, all of which have been closely associated with the initiation and development of the coral skeleton (Falini et al., 1996; Michenfelder et al., 2003; Ajikumar et al., 2005; Goffredo et al., 2011; Weiner and Addadi, 2011; Kalmar et al., 2012; DeCarlo et al., 2018; Kellock et al., 2020). These acidic proteins can form strong interactions with Ca^{2+}, producing lattice structures (Ni and Ratner, 2008; Reggi et al., 2014; Sancho-Tomás et al., 2014) to which CO_3^{2-} is also delivered (Allemand et al., 2011; DeCarlo et al., 2018), thereby creating an environment inducive to the nucleation of $CaCO_3$ crystals (Brennan et al., 2004; Ramos-Silva et al., 2014; Smeets et al., 2015; Sevilgen et al., 2019). Other large molecular weight biomolecules

such as polysaccharides and lipids (Reggi et al., 2016; Naggi et al., 2018), many of which are produced in large amounts by reef-building corals, might also play a role in calcification.

Past studies into the role of large molecular weight organic molecules within the coral skeleton (Mitterer, 1978; Weiner, 1979) have confirmed that complex biochemical processes are occurring within the space between the skeleton-forming calicoblastic tissue layer and the growing surface of the $CaCO_3$ skeleton (Barnes, 1970; Cohen and McConnaughey, 2003; Venn et al., 2011; Tambutté et al., 2012). The concentration of macromolecules and ions within the SOM have been attributed to certain roles in crystal growth including the spontaneous induction of aragonite precipitation from seawater (Mass et al., 2013). Additionally, acidic proteins (polyaspartate and polyglutamate) within the SOM provide the foundation for the mineral lattice structure (Postolache and Matei, 2007; Cantaert et al., 2013) which acts as a three-dimensional blueprint and facilitates the formation of coordinate bonds between carboxylate oxygen atoms and Ca^{2+} in either a bidentate or syn/anti monodentate mode (Holm et al., 1996). The electrostatic displacement of protons from bicarbonate anions in this process allows the precipitation of inorganic carbonates on an organic scaffold (Greenfield et al., 1984).

Corals produce a plethora of small molecular weight compounds including dimethylsulphoniopropionate (DMSP) and its breakdown product acrylate (Figure 5.1c) (Cantoni and Anderson, 1956; Todd et al., 2010; Curson et al., 2011b), both of which were found in high levels in reef-building corals (Tapiolas et al., 2010). In corals, DMSP plays a significant role as an antioxidant (Deschaseaux et al., 2014b) and chemoattractant (Garren et al., 2014). In the marine environment, it is a key source of carbon and sulphur for marine food webs and the global sulphur cycle (Yoch, 2002). Compared to DMSP, less is known about the role of acrylate in marine ecosystems, although it has been established to function as a cellular antioxidant (Sunda et al., 2002) and an antimicrobial (Sieburth, 1961; White-Stevens et al., 1962; Todd et al., 2012b). Acrylate is readily protonated to acrylic acid, which is responsible for inducing cytotoxicity (Frederick et al., 2002; Todd et al., 2012b), therefore organisms require effective systems for both the utilization and detoxification of acrylate (Wang et al., 2017). Surprisingly, the concentration of acrylate in reef-building corals from the genus *Acropora* can reach up to 680 μmol g^{-1}, or 15% of the total carbon content of coral tissue (Tapiolas et al., 2010; Tapiolas et al., 2013), representing some of the highest levels reported in the environment (Tapiolas et al., 2010; Tapiolas et al., 2013; Curson et al., 2014). Although the intracellular acrylate concentration is influenced by temperature stress, supporting its role as an antioxidant (Raina et al., 2013; Westmoreland et al., 2017), the reason for its accumulation in fast-growing scleractinian corals is currently unknown.

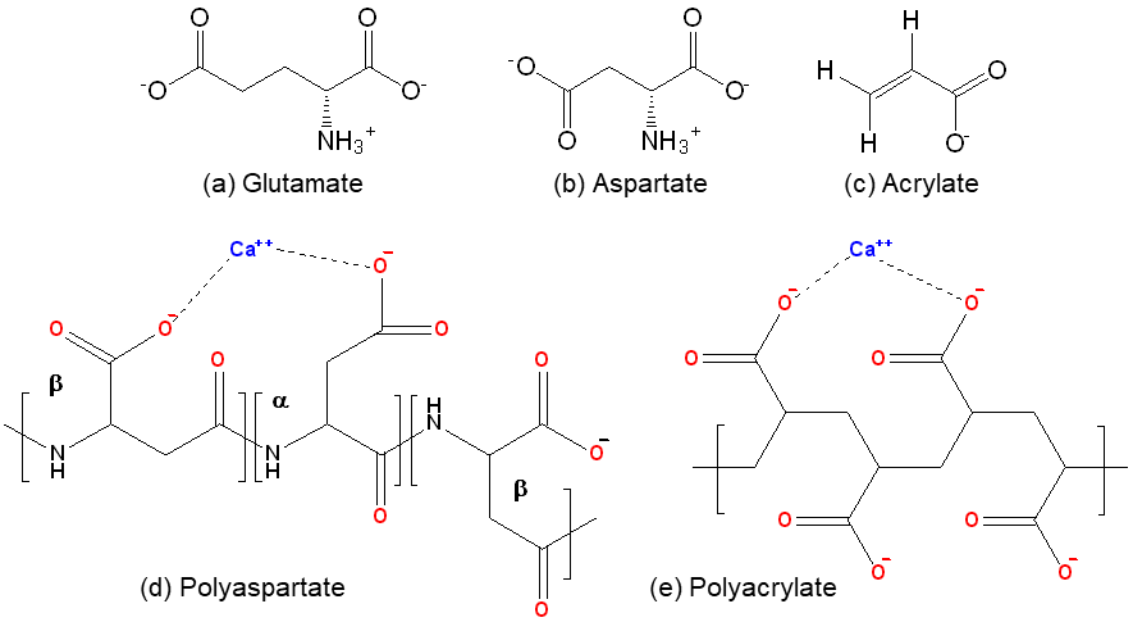

Figure 5.1. Chemical structures of the major constituents of biomineralisation within the calcifying liquid of the coral skeletal organic matrix, (a) glutamate and (b) aspartate, compared to (c) acrylate, and chelation of calcium ions [Ca^{2+}] by the polymerised products (d) polyaspartate and (e) polyacrylate.

Acrylate accumulation in marine organisms has been overlooked (Todd et al., 2012b; Curson et al., 2014) and was initially speculated to act as a food reserve or a structural material, due to its ability to autopolymerise (Sieburth, 1961). The polymerisation properties of acrylate have been exploited in the construction and building industries (Donnet et al., 2005). For example, in the presence of a polymerisation catalyst, it provides a stable scaffold for precipitation of $CaCO_3$, reminiscent of skeletal calcification (Postolache and Matei, 2007; Ozawa et al., 2008; Nudelman et al., 2013) (Figure 5.1d). Akin to the acidic protein polymers polyaspartate and polyglutamate (Postolache and Matei, 2007; Cantaert et al., 2013), polyacrylate can chelate Ca^{2+} through its carboxylate groups thus inducing nucleation of $CaCO_3$ (Figure 5.1d and e). However, the polymerisation of acrylate in natural systems, such as corals, has not been explored.

Given the reactivity of acrylate, which readily yields polyacrylate, and its accumulation in high concentrations in reef-building corals from the *Acropora* genus, both acrylate and polyacrylate were investigated for their potential role in coral skeletal development. Here we used a combination of stable isotope tracking, nanoscale secondary ion mass spectrometry (NanoSIMS) and Raman spectroscopy to elucidate the fate of acrylate in corals and investigate its presence in the newly formed SOM of aposymbiotic juveniles of the coral *Acropora millepora*.

5.2 Methodology

5.2.1 Coral spawning and larval settlement

Gravid colonies of *Acropora millepora* and *Platygyra daedalea* were collected from Davies Reef (18°49'03.7"S, 147°38'39.6"E) and Magnetic Island (19°10'16.6"S, 146°50'54.5"E) a week before the full moon in November 2016. The colonies were then acclimated in the National Sea Simulator (SeaSIM) at the Australian Institute of Marine Science (AIMS) prior to spawning. Released gametes were collected, randomly fertilised as per Pollock et al. (2017), and the viable larvae transferred into 500 l tanks supplied with 0.5 µm filtered seawater (FSW). Two weeks post fertilisation, aposymbiotic coral larvae were collected using 1 µm mesh nets, rinsed in 0.2 µm FSW, and placed in a 500 ml container. Active, swimming larvae were randomly selected using a sterile plastic pipette and rinsed three times in 0.2 µm FSW, before being added to pre-conditioned six-well plates (six plates per species, 30 larvae per well).

Plates were prepared by placing a 22×22 mm Thermanox coverslip (polyolefin polymer; Thermo Scientific, Massachusetts, United States) into each well. Fresh chips of the coralline crustose algae (CCA; ~2×2 mm) *Porolithon onkodes* (Maneveldt and Keats, 2014) were positioned in the centre of the well to ensure coral larvae settled on the coverslip and not on the wall of the well. Each well was then filled with 20 ml of 0.2 µm FSW. The six-well plates were incubated at 27°C in the dark to prevent the growth of potential photosynthetic organisms originating from the CCA. Twelve hours after larval settlement, CCA chips were carefully removed from each well, and the FSW decanted to eliminate any remaining unmetamorphosed larvae and unattached juvenile corals. Each well was then gently rinsed and refilled with 20 ml of 0.2 µm FSW. Settled juvenile corals were inspected daily and FSW exchanged every second day to remove any dead or detached recruits.

5.2.2 Supplementation with acrylate

One-week old coral juveniles (*A. millepora* and *P. daedalea*), successfully settled into the 6-well plates were divided into three treatment groups 1) 10 mM ^{12}C-acrylate (Sigma-Aldrich, Missouri, United States; two plates per species), 2) 10 mM ^{13}C-acrylate (0.13 g) (Cambridge Isotope Laboratories, Massachusetts, United States; two plates per species), and 3) 0.2 µm FSW (one plate per species to act as negative controls). The concentration of acrylate chosen was based on previous findings by Tapiolas et al. (2010) and Motti et al. (unpublished data) with 1 M stock solutions of ^{12}C-acrylate and ^{13}C-acrylate prepared in Milli-Q water. Each carbon of acrylate was labelled with 100% ^{13}C (i.e., 1-^{13}C, 2-^{13}C, 3-^{13}C-acrylate)-acrylate, ensuring detection of the

$^{13}C/^{12}C$ ratio above natural abundance (1.12%) in the SOM should the molecule be polymerised or metabolised.

At the start of the experiment (t=0; 1-week old coral juveniles) one plate per species of the ^{12}C- and ^{13}C-acrylate treatments were sacrificed by adding methanol (CH_3OH) and used as a control to assess for potential passive accumulation of acrylate in the skeleton. All plates were then supplemented with 20 ml of the designated treatment (^{12}C-acrylate, ^{13}C-acrylate; 10 mM final concentration of acrylate) or FSW (as control). Every 24 hours thereafter the wells were emptied, gently washed with FSW and fresh aliquots of the treatment added. The plates were placed on a rocking mixer for 5 min to ensure homogeneity before being transferred into incubators maintained at 27°C.

After 72 hours (representing three acrylate-enriched water exchanges), the wells were decanted, and the coral juveniles gently rinsed three times with FSW to remove any residual dissolved acrylate. Residual liquid was carefully absorbed using a sterile cotton bud. CH_3OH (250 µl) was added into each well, ensuring that the settled corals were fully immersed, and swirled gently for 1 min to remove tissues from the skeleton. A glass pipette was used to remove the methanolic coral tissue extract, and the remaining skeleton rinsed in Milli-Q water three times to ensure removal of any remnant CH_3OH. The coral skeletons were dried at 60°C followed by lyophilisation (Dynavac model FD12, Massachusetts, United States). Plates were then sealed with parafilm (Bemis, Wisconsin, United States) and stored for further analysis using nanoscale secondary ion mass spectrometry (NanoSIMS) and confocal Raman spectroscopy (CRM).

5.2.3 Scanning Electron Microscopy (SEM)

Intact and cross-sectioned skeletons of juvenile *A. millepora* and *P. daedalea* were visualised by SEM. To prepare flat cross-sections, each Thermanox coverslip was trimmed with scissors, leaving a 2 mm band around the coral skeleton. The trimmed coverslip was covered with a droplet of Milli-Q water, attached to a cryo-pin and frozen in place using vapour of liquid nitrogen. The mounted frozen skeleton was then placed in an EM UC6/FC6 Ultra cryo-microtome (Leica Microsystems, Wetzlar, Germany) and the surrounding temperature maintained at -120°C to ensure the sample remained frozen and fixed in position. Approximately 10 µm of skeleton was removed from the top of the coral skeleton using a diamond knife (DiATOME Histo 45°), resulting in flat cross-sections through the upper part of the skeletal septa. The cryo-pin was then removed from the Ultramicrotome instrument and dried at 60°C for 20 min.

Intact and cross-sectioned skeletal preparations attached to Thermanox strips were mounted on stubs using carbon tape. The samples were then coated with 10 nm of platinum and 10 nm of carbon. Images were acquired at 5 kV using a Zeiss 55 Field Emission Scanning Electron Microscope (Oberkochen, Germany).

5.2.4 Nanoscale secondary ion mass spectrometry (NanoSIMS)

Juvenile coral skeletons from the ^{13}C-acrylate treatment (n=1) and FSW control (n=1) were analysed using NanoSIMS. Dried juvenile coral skeletons were embedded in anhydrous Araldite 502 resin (Sigma-Aldrich, Missouri, United States) and once set, the Thermanox coverslips were carefully removed using forceps. The exposed basal surface of resin-encased skeletons was sandpapered and polished down to 1 µm using a RotoPol-35 (Struers, Ohio, United States). The polished surface was then carefully rinsed with demineralised water, air dried, and coated with 5 nm of gold using a 208HR High Resolution Sputter Coater (Ted Pella, California, United States).

A NanoSIMS-50 (Cameca, Gennevilliers, France; located at the Centre for Microscopy, Characterisation and Analysis (CMCA) at The University of Western Australia) was used to investigate ^{13}C enrichment in the skeleton of the coral juveniles. Four isotopic species were simultaneously detected (^{12}C, ^{13}C, ^{18}O, and ^{12}C^{14}N). Enrichment of ^{13}C in carbonates was investigated by performing a line scan using a 50 pA beam.

5.2.5 Confocal Raman microscopy (CRM)

Juvenile coral skeletons from the ^{12}C-acrylate treatment, and from the FSW and non-living (passive accumulation) controls were analysed by CRM (n=2 per treatment). Samples were prepared as for SEM (see above). Briefly, a 10 µm thin horizontal section was removed from the top of each skeleton by Ultramicrotome and dried at 60°C for 20 min.

CRM measurements were made with an Alpha 300RA+ Raman spectrometer (WITec, Ulm, Germany) using a 785 nm laser source with an Andor iDUS 401 CCD (Charge Coupled Device) detector maintained at -60°C, a 20× objective with a 0.5 numerical aperture, and a grating of 600 g/mm at 750 nm blaze. The first-order Raman peak of silicon at 520.2 cm^{-1} was used for calibration and to optimise the alignment and signal intensity of the instrument before each analysis. Raman spectra of sodium acrylate (monomer; Sigma-Aldrich, Missouri, United States), commercial grade polyacrylate (MW = 450,000), crushed adult coral skeleton (a source of

biogenic aragonite), and a mix of polyacrylate and crushed adult coral skeleton were obtained and used as experimental standards to generate a basis analysis mask to identify diagnostic regions from which fluorescence maps of target chemical compounds could be generated.

CRM measurements of the juvenile coral skeletons were conducted along the coral septum (first located by the instrument camera), with septum size dictating the scan area. A full image map of each skeleton was built by stitching together 10-25 scanned areas, with scanning integration time of 0.5s. The spectral analysis and imaging processing were performed using the Project FOUR software (build 4.0.12.9, WITec, Ulm, Germany).

5.3 Results

5.3.1 Coral settlement

A. millepora larvae were successfully settled in the presence of CCA chips at 27°C, with most settling at the edges of the well or directly on top of the CCA chips. However, on average, five juveniles settled per well directly on the Thermanox coverslip. Unlike *A. millepora*, *P. daedalea* larvae did not settle after 72 hours under the same conditions. However, they were successfully settled by increasing both the larval density per well (n=40 in 20 ml FSW) and the temperature (30°C). As for *A. millepora* larvae, the majority of *P. daedalea* larvae settled in the corners of the well or directly on the CCA chips. An average of three juveniles per well settled on each coverslip. Juvenile corals were observed growing and developing over the seven-day pre-exposure period.

Septa were clearly observed in the fast-growing *A. millepora* (Figure 5.2a) but were absent in *P. daedalea* (Figure 5.2b). Cross-sections of samples earmarked for SEM and Raman analyses were prepared according to standard protocols. However, as the crystalline structure of juvenile coral skeletons is extremely fragile, attempts to polish and cross-section proved futile, with skeletons simply crumbling when cut. To stabilise the skeleton, samples were embedded in resin, however, due to their porosity, the resin fully infiltrated the skeleton and interfered with subsequent analyses. This method was therefore modified, whereby the fragile skeleton was instead successfully stabilised by freezing in a drop of water, remaining intact during cross-section planing. Drying exposed an otherwise unchanged cross-sectioned of the skeleton.

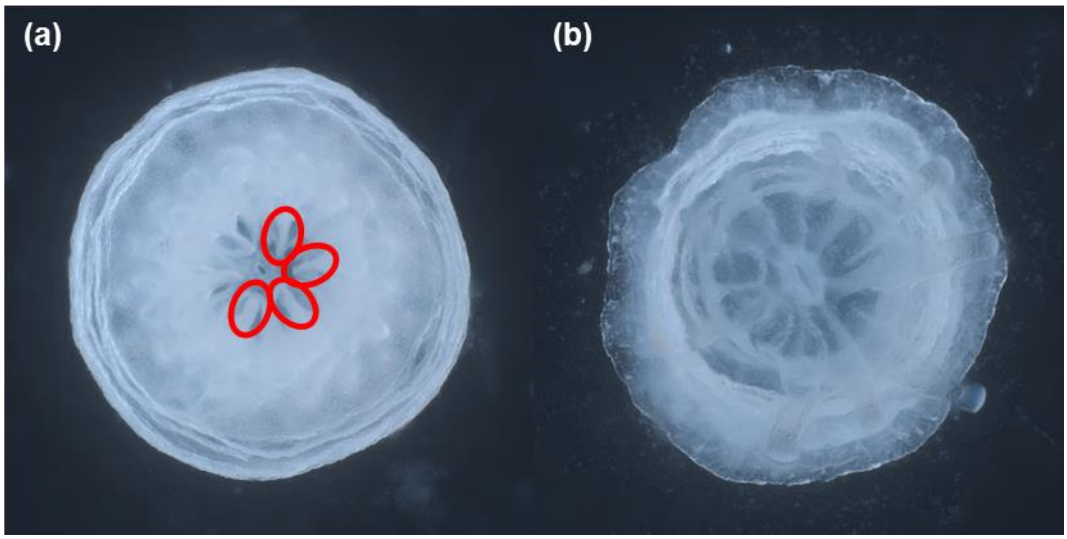

Figure 5.2. Microscope images of aposymbiotic (a) *Acropora millepora* and (b) *Platygyra daedalea* juvenile corals after 72-hours incubation in acrylate-enriched sea water. The septa of *A. millepora* can be observed (in red circles) while the septa of *P. daedalea* were not visible.

Microtomed flat sections of *A. millepora* (sacrificed using CH_3OH) revealed an intricate skeletal structure (Figure 5.3b). In contrast, the slower growing *P. daedalea* displayed thin walls with no septa evident one-week post-settlement (Figure 5.3c). Unfortunately, and in spite of repeated attempts to modify the preparation method, the fragile skeleton of *P. daedalea* shattered during microtoming (Figure 5.3d), preventing any further analysis. All subsequent results relate directly to *A. millepora* settled juveniles.

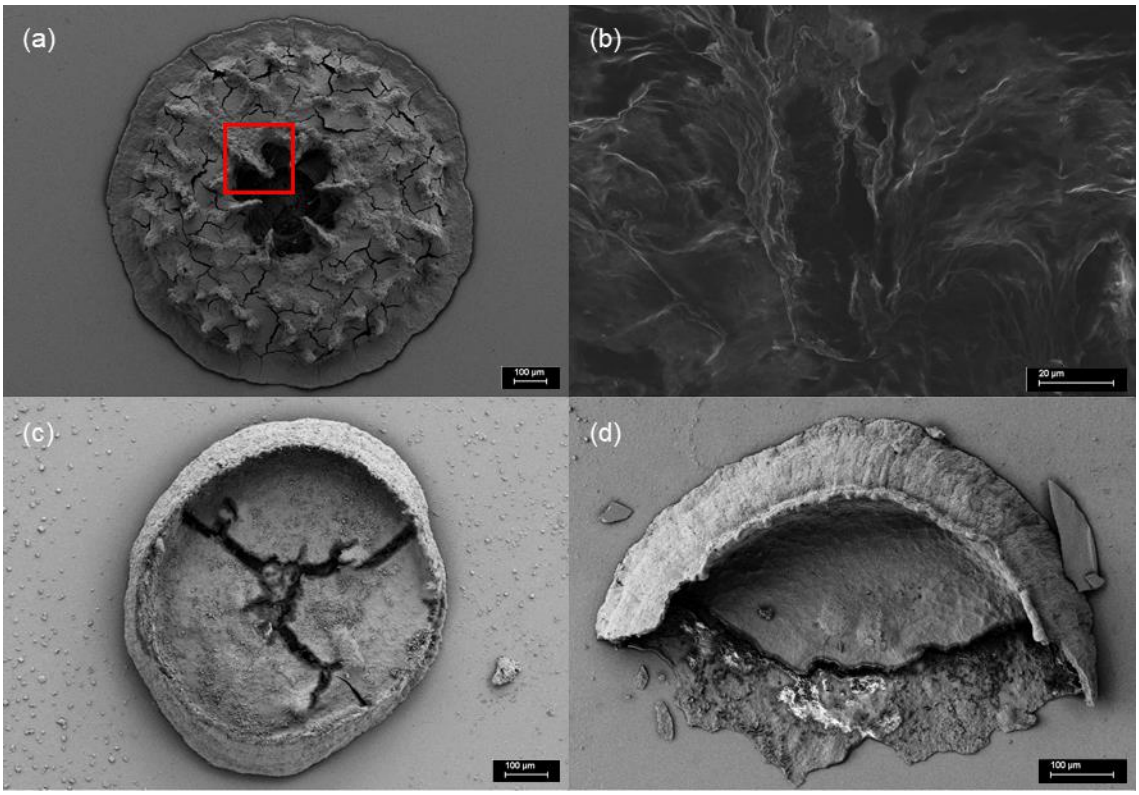

Figure 5.3. Scanning electron microscopy images of (a) 7-day old *Acropora millepora*, the region in the red box expanded to show (b) the exposed cross-section of an individual septum, (c) 7-day old *Platygyra daedalea*, and (d) collapse of the skeleton of *P. daedalea* caused by microtome planing.

5.3.2 NanoSIMS

To establish whether the carbon from acrylate is directly incorporated into aragonite, *A. millepora* juveniles co-incubated with ^{13}C-labelled acrylate were analysed. The $^{13}C/^{12}C$ ratio of the skeleton was statistically indistinguishable between the specimen incubated with ^{13}C-labelled acrylate and the control (independent sample t-test; $p > 0.05$; Figure 5.5). However, the $^{13}C/^{12}C$ ratio of both treatments was on average 25% lower than the natural abundance values detected from the mounting resin (Figure 5.4a-e). These results indicate that the isotopic composition of coral skeleton is not adequately captured by NanoSIMS, and unfortunately do not permit the assessment of the incorporation of ^{13}C acrylate in the newly formed aragonite of the juvenile corals.

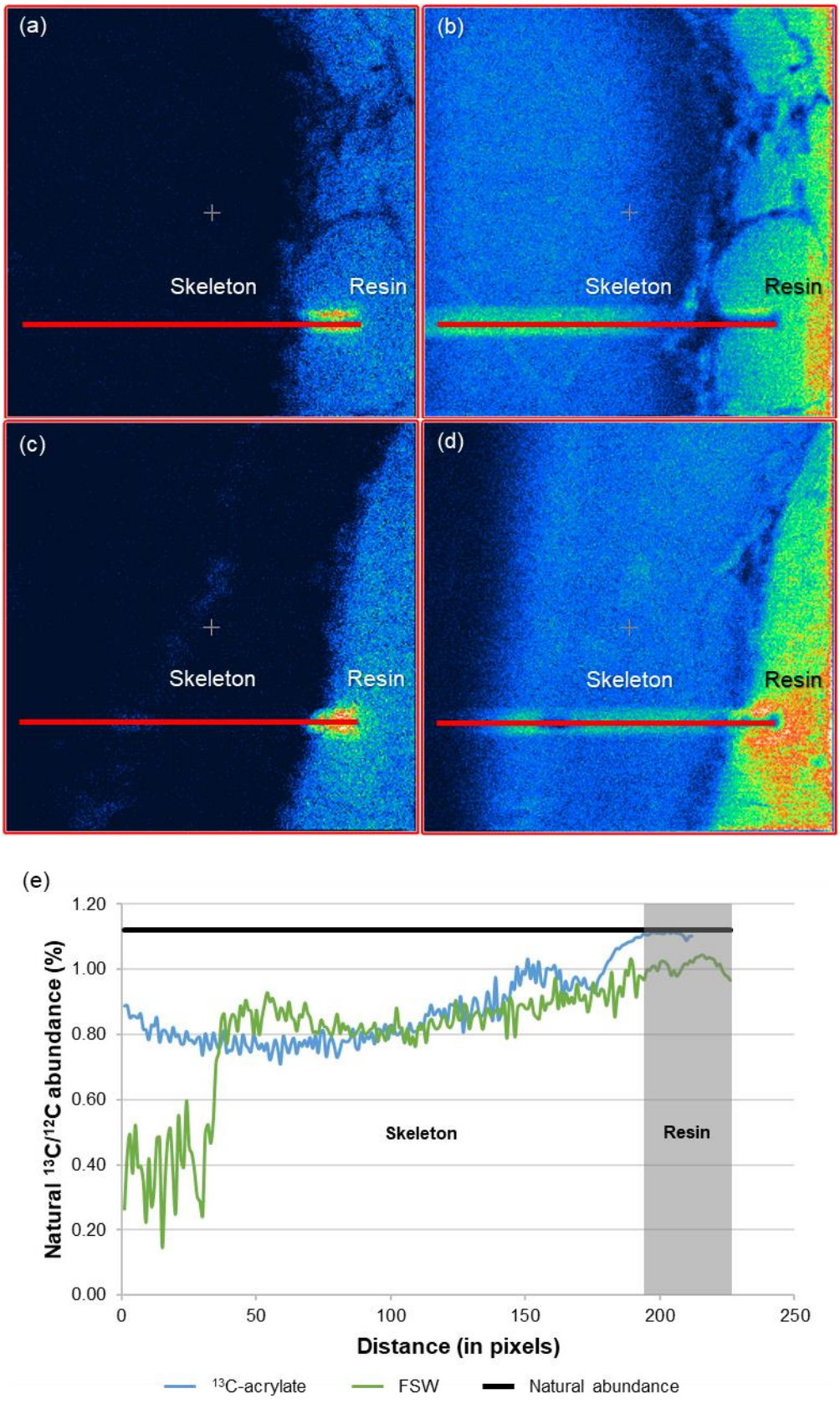

Figure 5.4. ^{13}C (a and c) and ^{18}O (b and d) NanoSIMS images revealing the skeletal structure of *Acropora millepora* incubated with ^{13}C-acrylate (a and b) and with filtered seawater (FSW; control; c and d) - the location of the line scans are shown by the red lines, and (e) the $^{13}C/^{12}C$ abundance obtained from the line scans compared with the natural $^{13}C/^{12}C$ abundance at 1.12% (black line).

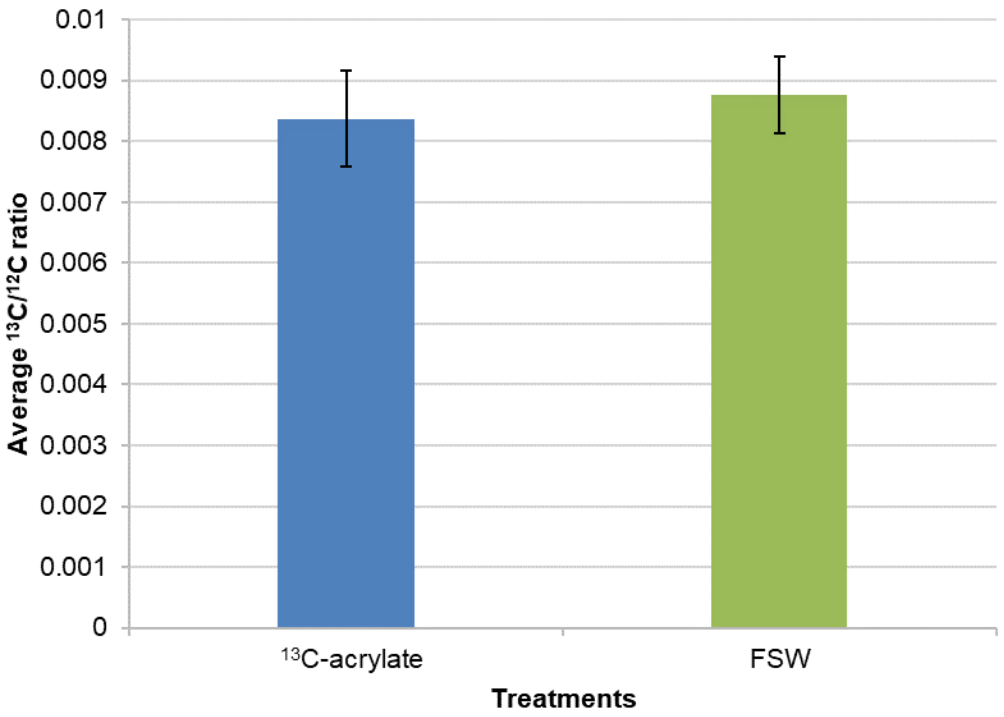

Figure 5.5. The average $^{13}C/^{12}C$ ratio in juvenile *Acropora millepora* skeleton obtained from NanoSIMS line scans.

5.3.3 Raman spectroscopy

To provide a baseline for our Raman mapping of coral skeleton samples, Raman spectra of polyacrylate, biogenic aragonite and acrylate standards were acquired (Figure 5.6). The acrylate standard (Figure 5.6a) displayed sharp peaks at 530, 862, 898, 967, 1,060, 1,283, 1,458, and 1,636 cm^{-1}. The spectrum of the polyacrylate standard (Figure 5.6b) exhibited several diagnostic signals at 502, 841, 1,100, and 1,325 cm^{-1}, including a sharp and narrow peak at 1,453 cm^{-1}. These are reminiscent of local conformations of the polyacrylate polymeric chain (Todică et al., 2015). The aragonite standard, obtained from a biogenic source (crushed adult *A. millepora* skeleton; Figure 5.6c), revealed a strong peak at 205 cm^{-1} which is unique to aragonite (Dandeu et al., 2006). No calcite signals (expected at 281 cm^{-1}) were observed, indicating that the mineral formed is purely aragonite, corroborating literature results (Clode et al., 2011; Ivankina et al., 2020). A mixture of polyacrylate and biogenic aragonite was also scanned to ascertain if there was any interference by the stronger aragonite peaks or whether they are coincidental with the diagnostic signals for polyacrylate. The indicative peak for aragonite remained resolved and visible in the spectrum (Figure 5.6d). Other peaks associated with polyacrylate were also observed in the mixture at 851, 888, 982, 1,062, 1,130, 1,295, 1,417, 1,439, and 1,462 cm^{-1}.

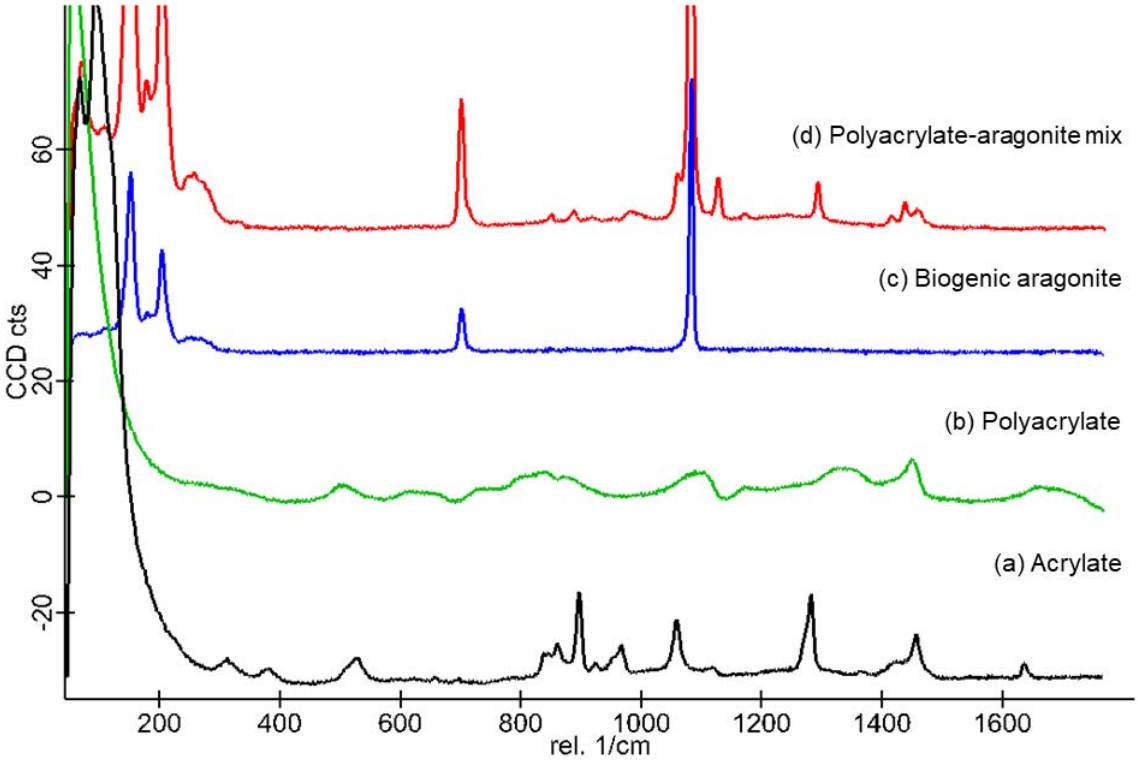

Figure 5.6. Raman spectra of (a) acrylate standard, (b) polyacrylate standard (MW = 450,000), (c) biogenic aragonite standard, and (d) mixture of biogenic aragonite and polyacrylate.

Raman mapping of the flat cross-sectioned regions of skeletons of 7-day old *A. millepora* juveniles identified the presence of polyacrylate. Diagnostic signals of the compounds of interest were targeted (see Figure 5.6), revealing the spatial distribution of aragonite (regions of spectra mapped: 56.62-351.85 cm^{-1}, 652.22-754.91 cm^{-1}, and 1,045.00-119.50 cm^{-1}), polyacrylate (regions of spectra mapped: 1,050.10-1,070.70 cm^{-1}, 1,119.50-1,140.00 cm^{-1}, 1,281.20-1,309.40 cm^{-1}, and 1,404.40-1,504.50 cm^{-1}) and acrylate (regions of spectra mapped: 56.62-351.85 and 652.22-1,504.50 cm^{-1}). In FSW control and ^{12}C-acrylate supplemented skeleton samples, aragonite was homogeneously distributed (Figure 5.7c and g), however, polyacrylate was localised within the newly deposited septal regions of the corallite (Figure 5.7d and h). The highest concentrations of polyacrylate, reflected as high CCD counts, were observed at the edges of the corallite where skeletal growth occurs (Barnes, 1970). In contrast, acrylate was not detected. The absence of this compound in the ^{12}C-acrylate supplemented skeleton also confirmed that rinsing and cleaning steps were effective at removing any residual dissolved acrylate from the samples.

A polyacrylate signal in the scanned heat maps was also observed across the skeleton of the non-living controls in the false colour maps in Figure 5.7j. The intensity of this signal differed from that of the FSW control (Figure 5.7b-d) and ^{12}C-acrylate supplemented treatments (Figure

5.7f-h), and appears to be accumulated along the gaps or cracks in the developing skeleton (Figure 5.7j and l), as visualised via SEM imaging (Figure 5.8).

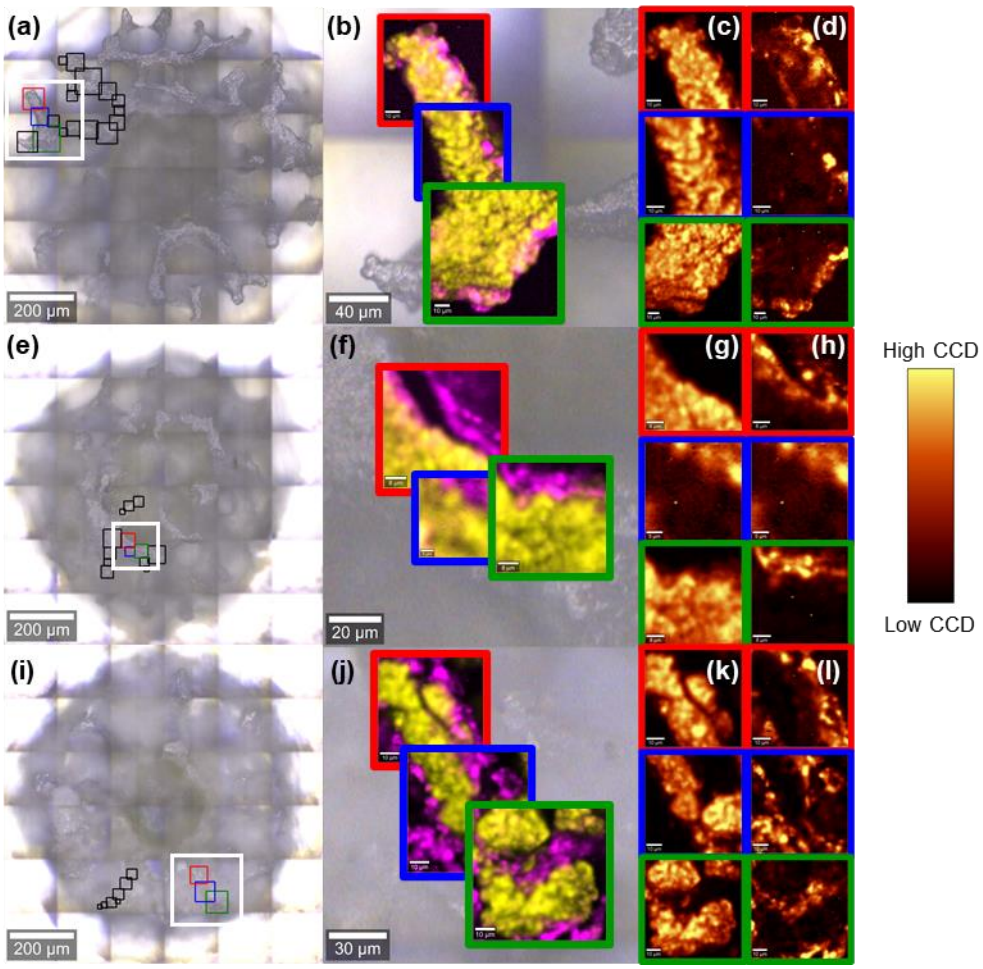

Figure 5.7. Confocal Raman microscopy of the skeleton of aposymbiotic *Acropora millepora* juveniles. (a) Control juveniles grown in filtered seawater, (e) juveniles supplemented with ^{12}C-acrylate, and (i) non-living controls, showing the regions along newly formed septa selected for analysis (black boxes), and (b, f and j) expanded view of a single septum (coloured boxes), with the false colour composite maps of aragonite (in yellow) and polyacrylate (in pink). Heat maps show the spatial distribution of (c, g and k) aragonite and (d, h and l) polyacrylate obtained from the scanned regions (scale bar = 10 µm).

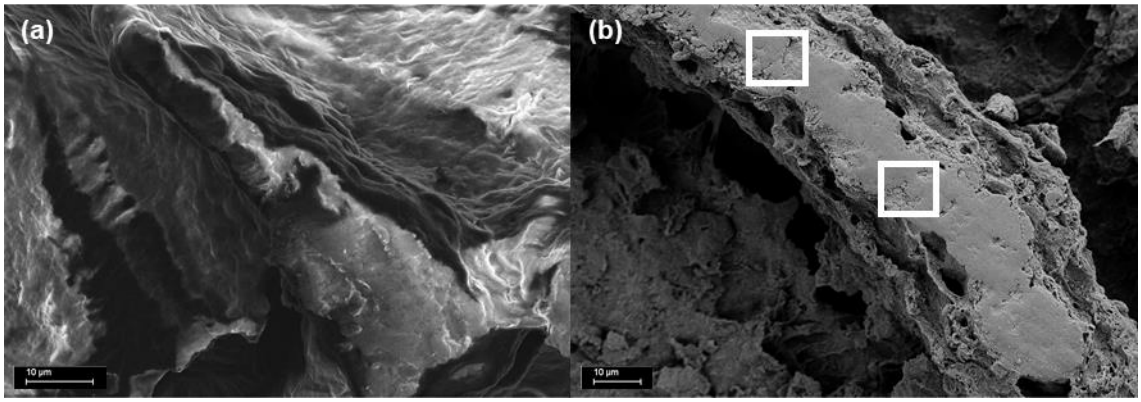

Figure 5.8. SEM imaging of a horizontal plane of *Acropora millepora* septa from (a) ^{12}C-acrylate supplemented juvenile and (b) non-living control, with white boxes indicating the gaps/cracks along the septum.

Comparison of the average distribution of both polyacrylate and aragonite across all treatments revealed a higher accumulation of both compounds in the skeleton of FSW controls (Figure 5.9). Aragonite levels in juveniles incubated with ^{12}C-acrylate were slightly lower than in FSW controls, although no difference was observed in their average polyacrylate:aragonite ratios (Figure 5.10). CRM revealed lower levels of aragonite in non-living specimens incubated in ^{12}C-acrylate, however, they exhibited a larger polyacrylate:aragonite ratio compared to the other two treatments.

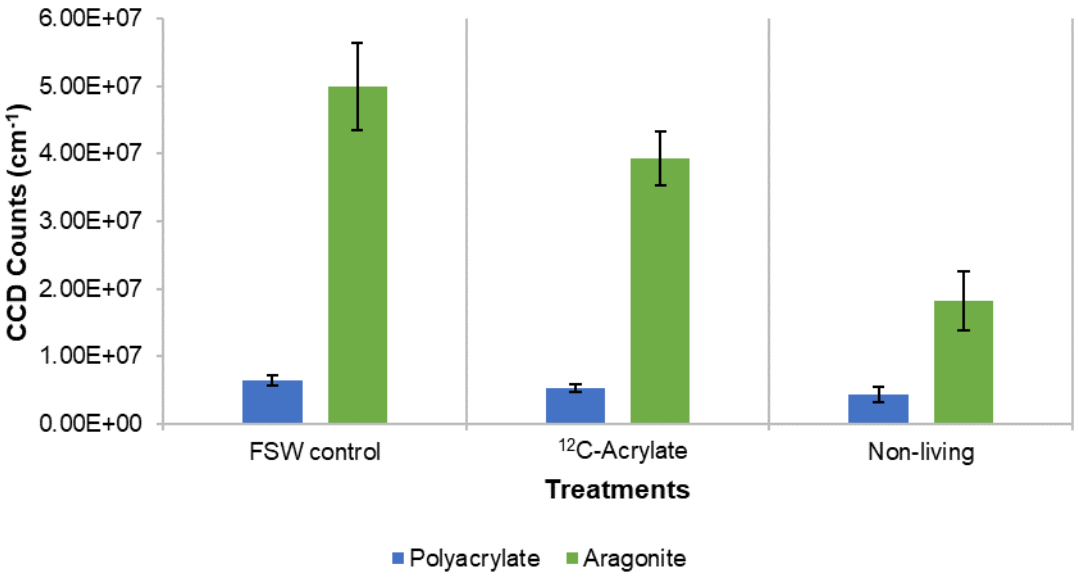

Figure 5.9. Average distribution of polyacrylate and aragonite in juvenile coral skeleton across all three treatments: incubation of live specimens in ^{12}C-acrylate, incubation of non-living specimens in ^{12}C-acrylate,

and incubation of live specimens in filtered seawater (FSW). CCD = charge coupled device; n = 2 per treatment.

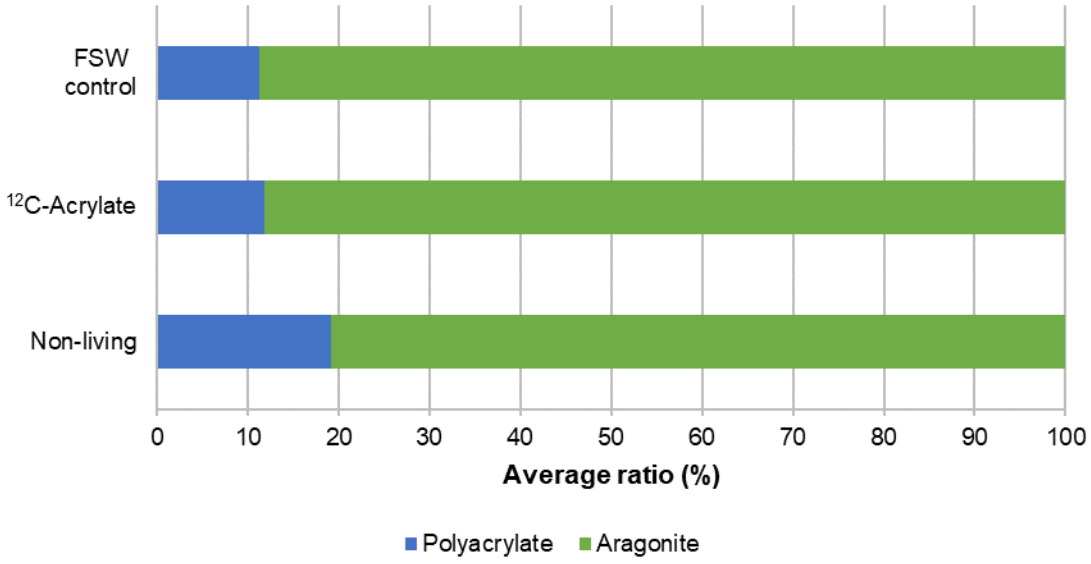

Figure 5.10. The average ratio of polyacrylate to aragonite found in skeletons of juvenile corals across three treatments: incubation of live specimens in ^{12}C-acrylate, incubation of non-living specimens in ^{12}C-acrylate, and incubation of live specimens in filtered seawater (FSW).

5.4 Discussion

Reef-building corals from the genus *Acropora* produce acrylate through the catabolism of DMSP (Raina et al., 2013; Alcolombri et al., 2015). The accumulation of this toxic compound in the tissue of this fast-growing coral genus (Tapiolas et al., 2010) suggests it serves a specific purpose for the biology of these organisms. The hypothesis that acrylate may be involved in skeletal formation and may therefore directly impact the growth capabilities of acroporid corals was tested. While the application of NanoSIMS proved inconclusive and was unable to establish whether acrylate acts as a direct source of carbon for $CaCO_3$ deposition during coral biomineralisation due to the inherent properties of $CaCO_3$, CRM revealed that polyacrylate is present at the growing edge of the newly formed juvenile *A. millepora* coral skeleton and likely supports the accretion of $CaCO_3$ and skeletal growth. These findings have provided further insight into the complex process of coral calcification and imply a role for acrylate.

5.4.1 Detection of ^{13}C in the coral skeleton using NanoSIMS

NanoSIMS has been used to monitor the incorporation of several elements including ^{43}Ca, ^{86}Sr and ^{87}Sr in coral skeleton (Brahmi et al., 2012; Gagnon et al., 2012), ^{13}C in coral tissue (Clode et al., 2007), and ^{15}N and ^{34}S in microalgae from the family Symbiodiniaceae (Pernice et al., 2012; Raina et al., 2017). Here NanoSIMS was used to assess the potential incorporation of ^{13}C into the newly deposited skeleton of coral juveniles incubated with ^{13}C-acrylate. Unexpectedly, surface scans of intact coral skeleton did not yield carbon counts reflecting the chemical composition of this $CaCO_3$ structure. Indeed, ^{12}C counts were much lower than expected and the ^{13}C signal was undetectable (which is abnormal given that ^{13}C represents 1.1% of all natural carbon on Earth (Midani et al., 2017); see Figure 5.3a and c). To increase the strength of the carbon signal recovered from the coral skeletons, a line scan analysis was applied, using a beam that was 25× more powerful (50 pA) than that typically used for routine NanoSIMS analysis. Although we were able to detect a ^{13}C signal using this approach, the $^{13}C/^{12}C$ ratio was still lower than the natural abundance values as the beam moved from the surface of the resin (which embedded the coral skeleton) into the $CaCO_3$ skeleton (see Figure 5.4c). No difference was detected between the $^{13}C/^{12}C$ ratios of corals incubated in ^{13}C-acrylate vs FSW. These unexpected low carbon values are likely due to the lack of conductivity of biomineralized carbonates (Sugiura et al., 2010), which is seemingly dampening the detection of natural abundance ^{12}C and ^{13}C signals associated with $CaCO_3$. As a result, these data are inconclusive with respect to the incorporation of ^{13}C into the coral skeleton, either as $Ca^{13}CO_3$ or any other ^{13}C-product and indicate that NanoSIMS is not a suitable technique for ^{13}C-related analysis of the coral skeleton.

5.4.2 Detection of polyacrylate in the Acropora millepora *coral skeleton using CRM*

CRM mapping has been used to establish the microstructural arrangement and SOM distribution within the coral skeleton. This technique has been used to study microscale fibres in blue coral (Zhang et al., 2011), characterise coral skeleton mineralogy (DeCarlo, 2018), and investigate the origin and role of the SOM (DeCarlo et al., 2018). Using this technique, we detected signals diagnostic of polyacrylate in the skeleton of aposymbiotic coral juveniles, including those not supplemented with an exogeneous acrylate. Polyacrylate contains carboxylate functionality that is exploited in industrial processes to control the precipitation of $CaCO_3$, a process reminiscent of coral acid-rich protein (CARPs)-controlled calcification. While the production of polyacrylate in acroporids requires further verification, its presence in the juvenile coral skeleton suggests it is possibly linked to the accelerated calcification process and skeletal formation. This not only correlates with the high production of acrylate in fast-growing corals

(Tapiolas et al., 2010; Tapiolas et al., 2013) but also with the recent discovery in *Acropora* species of several paralogs of the *Alma1* gene, which enables the production of acrylate from DMSP (Alcolombri et al., 2015; Shinzato et al., 2020).

The heat maps obtained via CRM (see Figure 5.7) show the distribution of polyacrylate is localised at the edges of the corallite, where the new skeleton is deposited (DeCarlo, 2018). Heat maps, generated from the acrylate standard spectrum, were unable to detect any trace of acrylate in the coral skeleton, including at the edges of the corallite, in any of the treatments. This confirmed that (i) rinsing corals with FSW prior to tissue extraction had removed any exogeneous acrylate, (ii) methanolic extraction of any endogenous acrylate within tissues was complete, and (iii) the presence of polyacrylate within the skeleton is unlikely to have resulted from passive polymerisation of surface acrylate. This lends support to the hypothesis that polyacrylate plays a role in the biomineralisation process, and that this process may be biologically-controlled. Furthermore, incubation with acrylate did not increase the polyacrylate:aragonite ratio suggesting that corals did not uptake significant amounts of exogenous acrylate, but that they instead utilised endogenously produced acrylate via the catabolism of DMSP (Shinzato et al., 2020).

Polyacrylate was also detected in the control corals, sacrificed prior to incubation with exogenous acrylate. Biologically-controlled polymerisation of acrylate is not possible in the absence of live tissue, however, the average ratio of polyacrylate:aragonite in these non-living samples was higher than in the FSW controls and ^{12}C-acrylate supplemented juveniles. Larger amounts of polyacrylate may have been deposited at the onset of the skeletal formation within the first seven days of growth to support the initial precipitation and accretion of $CaCO_3$, but then ceased upon sacrifice resulting in a higher polyacrylate:aragonite ratio. Alternatively, physical absorption of exogeneous acrylate onto the surface of the skeleton of non-living juveniles may have occurred, and in turn undergone passive polymerisation thereby increasing the polyacrylate:aragonite ratio. However, with higher levels of polyacrylate present on the surface of these controls, the environment would be conducive for passive $CaCO_3$ precipitation, therefore the polyacrylate:aragonite ratio would not be expected to increase unless $CaCO_3$ is precipitated in other forms. An additional study into the crystal structure of the detected polyacrylate in both live and non-living samples incubated with acrylate is needed to confirm if it is formed through biologically-controlled or biologically-induced mineralisation processes (Lowenstam and Weiner, 1989; Cuif and Dauphin, 2005; Veis, 2005).

While signals diagnostic for polyacrylate were detected at the surface of the skeleton in fast-growing *A. millepora*, supporting the role of acrylate in coral calcification, attempts to analyse juveniles of the slow-growing non-acrylate producing *P. daedalea*, were unsuccessful. The limited biomineralisation over the course of the experiment and the lack of structural

morphology (i.e., septa) for this species meant the skeleton was too fragile and could not withstand the sample preparation process without intractable damage. If polyacrylate is important in skeletal formation, the lack of acrylate production in *P. daedalea* might influence the initial thickness of its skeleton and might explain the results observed here. *P. daedalea* requires approximately four to eight months of growth to achieve similar skeletal morphology as a one-week old *A. millepora* (Babcock et al., 2003), at which point its skeleton may be able to survive the sample processing used in this study. Previous studies by Tapiolas et al (2010) demonstrated that acroporids contained high levels of acrylate, though other species have far lower concentrations. Hence, the generalisation of incorporation of polyacrylate into the skeletons of other corals genera (and species) should be avoided until further studies specifically investigating this process are undertaken. Recently Shinzato et al. (2020) reported the DMSP lyase gene, *Alma1* is highly duplicated in *Acropora* species, which further supports the hypothesis that Acroporids have evolved mechanisms for synthesising acrylate which may aid rapid skeleton growth.

The precipitation of $CaCO_3$ biominerals is affected by ocean acidification conditions (Anthony et al., 2011). Increasing atmospheric CO_2 (pCO_2) elevates dissolved CO_2 concentrations which in turn decreases the pH of seawater. The lower pH influences the availability of [CO_3^{2-}] ions in seawater by driving the equilibrium towards the formation of [HCO_3^-] ions. This can alter the net negative charge of biomolecules, such as CARPs, thereby inhibiting $CaCO_3$ precipitation (Elhadj et al., 2006) as well as decreasing the Ω_A resulting in skeleton dissolution (Marubini et al., 2008; Erez et al., 2011; Jokiel, 2011; Steiner et al., 2018). These chemical changes can negatively impact coral calcification leading to stunted reef formation (Anthony et al., 2011; Moya et al., 2012). The ability to biosynthesise alternative macromolecules such as polyacrylate that are potentially capable of sequestering low levels of CO_3^{2-} may enhance skeletal growth and provide an ecological advantage to specific coral species. This concept requires further investigation in the context of predicted increases in ocean acidification. Specifically, a comparative study is needed to establish the polyacrylate:aragonite ratio in fast-growing acroporid coral skeletons compared to other slower-growing coral genera.

5.4.3 Conclusions and future direction

The thin SOM (microns or less in size and less than 0.1% of the skeleton by mass) (Goffredo et al., 2011), where the site of calcification occurs, is challenging to investigate *in situ* given its location directly underneath the living polyp (Tambutté et al., 2011). Therefore, most studies have used indirect methods through proxies such as ^{14}C-aspartic acid (Allemand et al.,

2004), extraction of the SOM (Reggi et al., 2014) and skeleton-bound organic nitrogen (CS-$\delta^{15}N$) (Wang et al., 2015b) to characterise more precisely the location of the SOM within the skeleton and its chemical constituents (e.g. aspartate or glutamate). Indeed, the process of chemical extraction to remove the tissue from the skeleton usually results in the dissolution, at least in part, of the SOM (Falini et al., 2013). To overcome these limitations and shed further light on the role acrylate plays in coral calcification, this study applied two direct detection methods NanoSIMS and CRM. The high levels of acrylate in fast growing hard corals and the detection of signals diagnostic of polyacrylate at the growing edge of the *A. millepora* coral skeleton, along with the recent reporting of the *Alma1* gene being the most duplicated DMSP lyase gene in *Acropora* species (Shinzato et al., 2020), suggest that acrylate-producing corals have a significant ecological advantage over slower growing species, which may impact their response to rapidly shifting ocean chemistry.

To garner further supporting evidence for the hypothesis that acrylate is involved in coral calcification, this study should be replicated with alternate slow-growing coral species that lack the ability to accumulate acrylate and confirm the presence or otherwise of polyacrylate components within their skeleton (once developed). As this study only focussed on coral juveniles, future studies should investigate established adult corals to determine whether the accumulation of polyacrylate as a component of the organic scaffold is a process that occurs only in the early stages of coral skeletal development, or if polyacrylate remains as an important and relevant biomolecule in biomineralisation in adult colonies as well.

Acrylate is a key metabolite derived from DMSP catabolism and while the coral animal has the capacity to produce and accumulate acrylate, their endosymbiotic Symbiodiniaceae (Broadbent et al., 2002) and associated microbes (as revealed in Chapters 2 and 3) are also producers of DMSP and subsequently acrylate. While the juvenile corals used in this study are aposymbiotic, they are not axenic. Although it is highly likely that coral juveniles were harbouring DMSP-degrading bacteria (Raina et al., 2013), it is important to note that the highly duplicated presence of the *Alma1* gene in acroporid corals (Shinzato et al., 2020) indicates that the coral animal can produce acrylate independently from their microbial partners. Future investigations looking into whether the inclusion of Symbiodiniaceae and key microbial partners within the developing holobiont increases the concentration of polyacrylate within the coral skeleton will further aid our understanding of the roles each partner plays within the coral holobiont. These additional studies will further elucidate the role of acrylate in coral calcification, and its potential role to alleviate the effect of increasing ocean acidification.

While no enzyme is currently known to mediate the polymerisation of acrylate in any organism, our study indicates that a biologically-controlled mechanism is occurring in corals. The

localisation of accumulated acrylate in *Acropora* species is unknown, however, it is possible that corals concentrate this compound in specific compartments, possibly situated at or near the SOM-skeleton interface, which could induce its autopolymerisation. Identifying the process that mediates the production, transport, and deposition of polyacrylate into coral skeleton is critical to understand how these ecosystem engineers are able to create the intricate three-dimensional structures that support the most productive marine ecosystem on earth and harbour 25% of all marine species.

Chapter 6:
General discussion

This research has substantially contributed to the current understanding and knowledge of sulphur cycling via metabolism of dimethylsulphoniopropionate (DMSP) by coral-associated bacteria, while also laying the foundation to explore a novel coral biomineralisation mechanism driven by its catabolism product, acrylate. Here, a synthesis of the experimental work and results is presented and discussed in the context of the role of DMSP within the coral holobiont and highlights the importance and relevance of this metabolite in a changing environment. Future research directions are offered to further advance our understanding of DMSP metabolism within the coral holobiont, while emphasising the importance of microbe associations in underpinning coral health.

6.1 Coral-associated bacteria contribute to DMSP synthesis in the holobiont

Tropical coral reefs are rich sources of DMSP, with the coral holobiont responsible for the bulk of methylated sulphur released into the water column. Subsequent emissions of sulphur into the atmosphere via DMS is speculated to have a role influencing local climate regimes (Hill et al., 1995; Broadbent et al., 2002; Broadbent and Jones, 2004). Quantification of sulphur budgets within the coral holobiont has highlighted gaps in our knowledge of sources and sinks of DMSP and other derived sulphur organic compounds (Deschaseaux et al., 2014b). Due to our previously limited understanding of the genetic machinery responsible for DMSP biosynthesis (Stefels, 2000), potentially unknown or cryptic sources of DMSP within the coral holobiont may still exist. The discovery of *dsyB*, a key DMSP biosynthesis gene in marine bacteria mediating the committing step (4-methylthio-2-hydroxybutyrate to 4-dimethylsulphonio-2-hydroxybutyrate; see Figure 1.3 in Chapter 1) in the methylation pathway (Curson et al., 2017), has greatly improved our understanding of organic sulphur cycling in environmental systems. Due to the coral holobiont being a large contributor to the DMSP pool in tropical reef ecosystems, identifying and characterising the roles coral-associated bacteria play in its biosynthesis is an important step towards the quantification and further refinement of oceanic sulphur biogeochemical budgets and may potentially reveal additional roles for these organic sulphur compounds in corals.

Corals host highly diverse microbial communities (Blackall et al., 2015) shaped by the varying physiochemical microenvironments within the coral holobiont (Sweet et al., 2011; Pollock et al., 2018). Bacterial communities from coral mucus are usually highly diverse (Sweet

et al., 2011), while communities within coral tissues might be less so and have predominantly been identified in aggregates dominated by members of the Gammaproteobacteria (Ainsworth et al., 2006; Work and Aeby, 2014; van de Water et al., 2015; Wada et al., 2019), such as the ubiquitous *Endozoicomonas* (Neave et al., 2017). In addition, the coral skeleton is dominated by endolithic microbes such as filamentous cyanobacteria, anoxygenic phototrophic bacteria, and anaerobic green sulphur bacteria (Pernice et al., 2020). To date, few coral-associated bacteria have been cultivated, as such there is renewed effort to create publicly available isolate collections that are more representative of broader coral-associated bacterial taxa (Sweet et al., 2021). Among the coral-associated bacteria previously isolated, specific traits (such as DMSP biodegradation, or nitrogen fixation) have been targeted using specialised growth media and approaches (Raina et al., 2009; Lema et al., 2016).

In this study, two non-selective growth media, marine agar (MA) and minimal basal medium (MBM; see Chapter 2 for details), were used to culture a broad range of bacteria and to maximise the chances of isolating DMSP-producing bacteria. Mucus, tissue, and skeleton were selectively sampled from six coral species (*Acropora millepora, A. spathulata, A. tenuis, Montipora spumosa, Pocillopora acuta* and *Stylophora pistillata*) to obtain isolates from different communities across the microhabitats within these holobionts. Two hundred and forty bacterial isolates were obtained and the near complete 16S rRNA gene sequence of each strain used to construct a taxonomic profile (see figure 2.1 in Chapter 2). In total, 47 different genera were isolated, the majority derived from the mucus (i.e., mucus swabs 35% and coral mucus 33%). Gammaproteobacteria were the dominant class, followed by Alphaproteobacteria and Flavobacteria. In addition, many of the isolated bacteria, such as *Aquimarina*, *Endozoicomonas*, *Halomonas*, and *Pseudoalteromonas*, have been commonly identified as members of the coral microbiome through culture-independent studies (Sweet et al., 2011; Nguyen-Kim et al., 2014; Roder et al., 2015; Silva et al., 2019; Ziegler et al., 2019).

The first gene confirmed to mediate DMSP biosynthesis, *dsyB*, was characterised from an alphaproteobacterium (Curson et al., 2017), with homologues identified in members of the orders Rhodobacterales, Rhizobiales and Rhodospirillales. *dsyB* has since been identified in a number of marine metagenomes (Curson et al., 2017; Curson et al., 2018). An adapted polymerase chain reaction (PCR)-based assay (Williams et al., 2019) using degenerate primers designed to target *dsyB* revealed that 6% of the 240 isolates possessed the gene (n=14 see Chapter 2), the majority of these (n=11; 79%) were retrieved from coral tissues. The proportion of *dsyB*-positive coral-associated bacterial strains identified is higher than the predicted environmental abundance of the gene in marine metagenomes (0.35-0.50%) reported from the *Tara* Oceans, Global Ocean Sampling (GOS), and the ocean microbial reference gene catalogue (OM-RGC) metagenomic

datasets (Curson et al., 2017; Curson et al., 2018). All *dsyB*-positive isolates identified here were from the family Rhodobacteraceae, with the majority (71%; n=10 strains) related to the *Shimia* genus, the remainder belonging to *Roseivivax halotolerans, R. lentus*, and *Pseudooceanicola nitratireducens*. The *dsyB* gene has thus far only been identified within the Alphaproteobacteria, and the outcomes of this study are consistent with the gene being restricted to this taxonomic group. All isolates possessing the *dsyB* gene were recovered from *Acropora* spp., a fast-growing coral genus known for producing large amounts of DMSP (Raina et al., 2013; Tapiolas et al., 2013). Hence, the bacteria associated with this coral genus likely contribute to the DMSP budgets of the coral holobiont.

Due to the inherent limitation of growing bacteria *ex situ* in laboratory conditions (Rappé and Giovannoni, 2003; Kirchman, 2010), it is almost certain that many coral-associated bacteria capable of DMSP biosynthesis were unculturable under conditions employed here. Even if bacteria can be cultured, possessing the genetic repertoire to produce DMSP does not equate to its metabolic synthesis. For example, if key precursors such as methionine, which is assimilated through the transamination pathway (see Box B in Figure 6.1) (Curson et al 2017), are not available, then the bacterium may not be able to produce DMSP. Here, chemical analysis of intracellular extracts of the *dsyB*-positive bacterial cultures grown in methionine-enriched MBM confirmed the production of DMSP. However, as there are other pathways for DMSP production beyond the *dsyB*-mediated transamination pathway (Curson et al., 2017) (see Figure 1.3 in Chapter 1, and Box B in Figure 6.1), sulphur intermediates such as 2-oxo-4-methylthiobutanoate (MTOB) or S-methylmethionine (SMM), and media optimised to target a broad range of Alphaproteobacteria (Senechkin et al., 2010; Karimi et al., 2019; Kurm et al., 2019) should be used to maximise the likelihood of obtaining novel DMSP-producing bacterial strains.

Culture-independent studies using conserved gene-specific primers to target *dsyB* can be conducted to screen for this gene in coral-associated bacteria (i.e., mucus, tissue, and skeleton microhabitats) and establish the relative abundance of bacteria that are capable of DMSP biosynthesis within the coral microbiome. Using the *dsyB*-specific primers previously developed (Williams et al. (2019), these future studies should be able to identify a greater diversity of *dsyB*-harbouring bacteria from corals. Other culture-independent bioinformatic investigations focussing on the *dsyB* gene, including metagenomic or metatranscriptomic screening of the microbiomes derived from corals species with high or low DMSP concentrations should also be undertaken to obtain a clear understanding of the relative abundance and potential contribution of DMSP-producing bacteria in the coral holobiont. Recently another gene, *mmtN*, has been identified in marine bacteria as being responsible for DMSP biosynthesis, albeit via a methylation pathway (see Figure 1.3 in Chapter 1) (Williams et al., 2019). *mmtN* is less abundant than *dsyB*

in environmental samples, but has been identified in a greater number of bacteria classes including Alphaproteobacteria, Gammaproteobacteria, and Actinobacteria (Williams et al., 2019). There is currently a lack of information regarding its abundance and function in coral-associated bacteria communities, hence, including *mmtN* in future studies of the coral holobiont is also warranted. GeneFISH probes (Moraru et al., 2010) which can link gene presence directly with cell identity *in situ*, could also be designed to target *dsyB* and *mmtN* to identify the location of DMSP-producing bacteria in corals.

6.1.1 Shimia aestuarii *AMM-P-2: from sulphur assimilation to DMSP production*

The majority of *dsyB*-positive bacteria strains isolated in this study were related to *Shimia aestuarii* (64%; n=9), a marine bacterium affiliated with the *Roseobacter* group within the family Rhodobacteraceae that was originally recovered from tidal flat sediments (Yi and Chun, 2006). Little information is available on the ability of *Roseobacters* to synthesise DMSP *de novo*, but this is hardly surprising given that most progress in this area has occurred relatively recently, since 2017. As is the case for many marine bacteria (Kanukollu et al., 2016), this study shows *S. aestuarii* AMM-P-2 can assimilate exogeneous sulphate (see Chapter 3; Figure 6.1). Furthermore, as for *Shimia* strain SK013 and *S. haliotis* (Kanukollu et al., 2016), the *S. aestuarii* AMM-P-2 genome encodes the enzymatic machinery for assimilation of sulphide into cysteine and methionine, which are precursors of DMSP. Stable isotope incorporation in combination with mass spectrometry techniques have been used to investigate sulphate assimilation in higher plants (Stefels, 2000) and the coral-associated microalgae, Symbiodiniaceae (Raina et al., 2017). Such experiments not only enable *in vivo* confirmation of metabolic pathways inferred *in silico*, but also provide estimates of fluxes and sinks of sulphur metabolites. Applying similar stable isotope tracers to *S. aestuarii* AMM-P-2 during growth under different conditions should be carried out to follow the assimilation of sulphate and the production of other sulphur compounds by the cells. Likewise, conducting these same experiments on the coral holobiont or simplified model systems, although technically demanding, would also be highly informative in predicting the impacts of environmental variables on sulphur metabolism in corals, and relating these impacts to broader ecological impacts on the reef.

Experiments on the coral animal and its associated Symbiodiniaceae have confirmed that DMSP production *in vitro* is influenced by a range of environmental parameters that are considered stressful on the reef (Fischer and Jones, 2012; Raina et al., 2013; Deschaseaux et al., 2014a; Jones et al., 2014; Gardner et al., 2016; Aguilar et al., 2017; Gardner et al., 2017; Cropp et al., 2018). These conditions include variations in temperature and salinity, light limitation, and

UV-exposure, all of which when prolonged, can lead to coral bleaching (Hoegh-Guldberg, 1999; Hughes et al., 2003; Hughes et al., 2018b; Hughes et al., 2018a; Hughes et al., 2019) or weakened coral immunity, both permitting the onset of coral disease (Rozenblat and Rosenberg, 2004; Bourne et al., 2009; Rädecker et al., 2021). Similar parameters were used as a baseline to gather insights into the ecological function of DMSP in coral-associated bacteria (see Chapter 4). We found a decoupling between the coral host and *S. aestuarii* AMM-P-2 in their responses to stressful conditions, whereby the intracellular DMSP concentrations of the bacterial cells were not necessarily affected by environment stressors known to negatively impact the coral host. While corals typically have a narrow range of optimal thermal tolerance (Coles et al., 1976; Fitt et al., 2001; Schoepf et al., 2015; de Oliveira Soares et al., 2019), variation in *S. aestuarii* AMM-P-2 culture growth conditions of ±5°C from the optimal tropical reef temperature of ~27°C did not result in significant changes in its intracellular DMSP concentrations. Since bacterial communities in the coral surface mucus layer are likely to be exposed to greater variations in temperature throughout the day than the internal tissues, it is likely that they are less susceptible to the small (±5°C) variations employed here. Their high densities in the coral surface mucus layer (Garren and Azam, 2012) and thermal tolerance support their role as the first line of defence for corals (Shnit-Orland and Kushmaro, 2009; Bakshani et al., 2018).

Exposure to extreme salinity and oxidative (through UV-exposure) stressors induce changes in DMSP production in corals and Symbiodiniaceae (Sunda et al., 2002; Darroch et al., 2015; Gardner et al., 2016; Aguilar et al., 2017). In these instances DMSP is known to function as an osmolyte (Burg and Ferraris, 2008) in bacteria to confer short-term tolerance towards changes in salinity, and as an antioxidant (Sunda et al., 2002; Deschaseaux et al., 2014b; Gardner et al., 2016) detoxifying hydroxyl radicals and other reactive oxygen species produced under UV-induced oxidative stress. These same extreme conditions triggered significant responses in intracellular DMSP concentrations of *S. aestuarii* AMM-P-2 (see Chapter 4) and suggest that this bacterium likely contributes to the pool of DMSP in the mucus to mediate this stress. Interestingly, under prolonged darkness, significant increases in intracellular DMSP concentrations were measured (see Chapter 4), indicating that bacteria such as *S. aestuarii* may be beneficial to corals in low-light mesophotic or deep-sea environments. As eukaryotic homologues of *dsyB* (*DSYB*) have also been identified in both corals (including *Acropora* spp.) and microalgae such as Symbiodiniaceae (Curson et al., 2018), it would be interesting to simultaneously analyse transcriptomic responses of *dsyB* and *DSYB* to environmental variables and combine this with chemical determination of DMSP levels in the various compartments to better understand organic sulphur metabolism in corals from different environments.

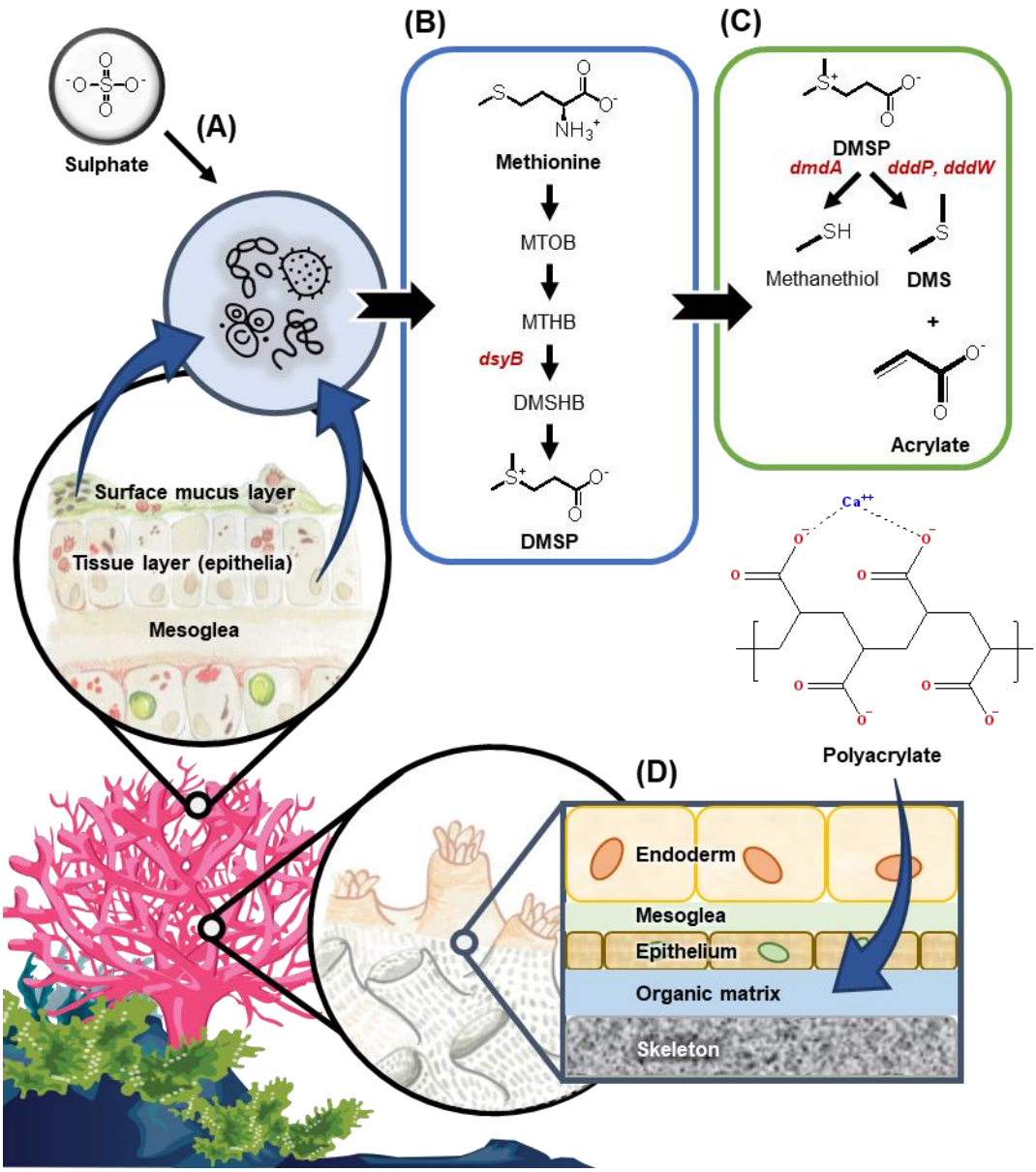

Figure 6.1. Overview highlighting the major findings of this thesis. Coral-associated bacteria isolated from coral tissue and mucus were discovered to be active DMSP-producers, capable of (A) assimilating sulphate, (B) biosynthesising DMSP through the *dsyB*-mediated transamination pathway, and (C) degrading DMSP via demethylation (*dmdA*) and cleavage (*dddP* and *dddW*) pathways. (D) One of the DMSP breakdown product, acrylate, which is present in high concentration in some coral species can form a polymer called polyacrylate, which has been detected within the skeleton of juvenile corals from the genus *Acropora* and might enhance biomineralisation within the coral skeletal organic matrix.

6.2 DMSP degradation – pathways and implications

Coral-associated bacteria are also known to play a role in DMSP degradation. DMSP is an important source of carbon and sulphur for coral-associated bacteria (Raina et al., 2009; Raina et al., 2010), and can be catabolised through two pathways, namely the demethylation pathway

yielding methanethiol (MeSH), and the cleavage pathway yielding equal amounts of dimethyl sulphide (DMS) and acrylate (see Figure 1.4 in Chapter 1 and Box C in Figure 6.1). A large fraction of the bacteria known to degrade DMSP and DMS are typically found in corals, and gene sequences matching *dddP* and *dmdA* were identified in metagenomes from the coral *Porites lutea* (Robbins et al., 2019).

The analyses of cellular extracts from *S. aestuarii* AMM-P-2 cells also revealed the production of acrylate (see Chapter 4). This implies that *S. aestuarii* AMM-P-2 was not only able to produce DMSP, but also degrade it via the cleavage pathway (see Box C in Figure 6.1). The ability to degrade DMSP appears to be widespread amongst *Shimia* spp. and *Roseobacters* more generally (Kanukollu et al., 2016). Investigations into the genome of *S. aestuarii* AMM-P-2 (see Chapter 3) revealed that the bacterium has the genetic machinery to degrade DMSP using both the demethylation (via *dmdA*) and cleavage pathways (using *dddP* and *dddW* genes), which is common among marine bacteria (Kiene and Linn, 2000). Two interconnected hypotheses proposed more than 20 years ago suggest that DMSP concentration is an important factor regulating the degradation pathway used (DMSP Availability Hypothesis (Kiene et al., 2000)), and that bacteria control the fate of sulphur fixed in DMSP by modifying the relative expression of the demethylation and cleavage pathways (Bacterial Switch hypothesis (Simó, 2001)). It was recently confirmed that external DMSP concentrations drive the relative expression of the two pathways in planktonic bacteria, with most of the DMSP channelled through the demethylation route when external DMSP concentrations are low, and that the production of DMS increases, through the cleavage pathway, when DMSP concentrations are higher (Gao et al., 2020). These results suggest that in environments with high DMSP concentrations, such as within the coral holobiont, a large fraction of the DMSP pool will be channelled towards the production of DMS. This is consistent with the high levels of DMS measured in reef building corals and surrounding environments (Jones et al., 1994; Jones and Trevena, 2005; Broadbent and Jones, 2006; Hill et al., 2010; Jones and Ristovski, 2010; Fischer and Jones, 2012; Swan et al., 2012). Indeed, DMS concentrations in mucus from acroporid corals are the highest ever measured in any environment (Broadbent and Jones, 2004).

Considering that the coral animal, Symbiodiniaceae, and coral-associated bacteria can metabolise DMSP, further studies investigating the impacts of extreme environmental conditions on their ability to produce and utilise DMSP as individuals and within the coral holobiont will provide insight into how corals will fare under future predicted climate change conditions.

6.2.1 Acrylate, a potential driver of coral biomineralisation

As for DMS, acrylate concentrations are also extremely high in some corals (Tapiolas et al., 2013) particularly acroporids (Tapiolas et al., 2010). It has been reported that acrylate represents up to 15% of the total carbon present in organic extracts from *A. millepora*, with similar levels detected in *A. spathulata* and *A. tenuis* (Tapiolas et al., 2010). Analysis of the genome of *S. aestuarii* AMM-P-2 (see Chapter 3) confirmed that this bacterium encodes DddP and DddW enzymes which mediate the DMSP cleavage pathway (see Box C in Figure 6.1) to yield acrylate. In addition, other members of the coral holobiont can contribute to the large pool of acrylate: paralogues of the *alma1* gene, which was first discovered in the alga *Emiliania huxleyi* and can cleave DMSP (Alcolombri et al., 2015), is also found in the coral animal *A. millepora*, and Symbiodiniaceae (Robbins et al., 2019). When using specific inhibitors targeting Alma1, but not the bacterial enzymes, DMSP lyase activity decreased by more than 90% in extracts from *Acropora millepora* (Alcolombri et al., 2017), indicating that the eukaryotic component of the coral holobiont (i.e., host and Symbiodiniaceae) plays a key role in DMS and acrylate production.

Tapiolas et al. (2013) noted that acrylate concentrations measured in *Acropora* spp. were consistently an order of magnitude higher than those of DMSP, suggesting either a slower catabolism of the metabolite or that the corals are purposefully sequestering it. Acidic proteins containing polyaspartate residues (see Figure 5.1 in Chapter 5) are present at high concentrations within the coral skeletal organic matrix (SOM) (Reggi et al., 2014) and have been linked to the initiation and development of the coral skeleton (Falini et al., 1996; Michenfelder et al., 2003; Ajikumar et al., 2005; Goffredo et al., 2011; Weiner and Addadi, 2011; Kalmar et al., 2012; DeCarlo et al., 2018; Kellock et al., 2020). In the presence of a catalyst, acrylate can polymerise to form polyacrylate (Sieburth, 1961), which in turn supports the formation of mineral lattice structures (Ni and Ratner, 2008; Reggi et al., 2014; Sancho-Tomás et al., 2014) by inducing the crystallisation of calcium carbonate (see Figure 1.7 in Chapter 1). This is reminiscent of the biomineralisation mechanism controlled by the coral SOM (see Figure 6.1) to produce the calcium carbonate skeleton (Postolache and Matei, 2007; Ozawa et al., 2008; Nudelman et al., 2013).

Given the similarities in the structures of polyaspartate and polyacrylate and their potential biomineralisation capabilities, we hypothesised a link between the high cellular concentrations of acrylate and coral skeletal development. The presence of polyacrylate within the skeleton of aposymbiotic juvenile *A. millepora* was confirmed through Raman spectroscopy (see Figure 5.6 in Chapter 5), supporting the hypothesis that acrylate can be a potential driver of coral biomineralisation. Comparative analyses should be undertaken in the future to test if intracellular acrylate levels in different coral species correlate with their growth rates.

The spectroscopic detection of polyacrylate within the coral skeleton warrants further investigation. Specifically, isolation and characterisation of polyacrylate from the coral skeleton is critical to support our finding. In addition, mapping the localisation of acrylate within the various compartments of the coral holobiont (including bacterial communities) will improve understanding of its metabolism and flux, and shed further light on its role in coral skeletal formation. Identifying the catalysts inducing the polymerisation of acrylate in corals would also be highly informative and help to establish whether this metabolite supports an alternative biomineralisation process facilitating enhanced production of calcium carbonate skeleton.

6.3 Concluding remarks

Tropical coral reefs are vital as a habitat for many marine organisms and can influence the community structure. However, reefs are under considerable and increasing pressure from global and local stressors. Coral resilience into the future is unknown and is currently the subject of intense research investigation. A better fundamental understanding of the functions that underpin coral fitness within the holobiont will support predictions of how coral reefs will respond to a rapidly changing climate.

This thesis has provided additional important insights and filled several gaps in our understanding of the coral holobiont by focussing specifically on the role of the organic sulphur compound DMSP and its break-down product acrylate. While the coral host and Symbiodiniaceae are known to produce DMSP, this is the first study to demonstrate that coral-associated bacteria (i.e., *S. aestuarii* AMM-P-2) can and do produce this metabolite, thereby contributing to the total pool of organic sulphur compounds within the holobiont. Genomic sequencing of a representative bacterium, *S. aestuarii* AMM-P-2, determined its physiological responses to parameters relevant to those experience by corals under environmental stress, further emphasising the importance of coral-associated bacteria within the coral holobiont. Coral calcification is a central process in reef-building, and this study revealed a novel link between the DMSP breakdown product acrylate and the mechanism of calcification of the coral skeleton in fast-growing coral species. While more rigorous studies are needed to test the hypothesis of acrylate involvement in coral skeletogenesis, findings reported here provide a basis to further explore this novel idea.

DMSP and its breakdown products are central to the health and function of the coral holobiont. Confirmation that bacterial members of the coral holobiont are involved in the metabolism of DMSP and acrylate is crucial to our understanding of the roles these bacteria play in coral health and resilience.

References

Aguilar, C., Raina, J.-B., Motti, C.A., Fôret, S., Hayward, D.C., Lapeyre, B. et al. (2017) Transcriptomic analysis of the response of *Acropora millepora* to hypo-osmotic stress provides insights into DMSP biosynthesis by corals. *BMC Genomics* **18**: 612.

Ainsworth, T.D., Fine, M., Blackall, L.L., and Hoegh-Guldberg, O. (2006) Fluorescence In Situ Hybridization and Spectral Imaging of Coral-Associated Bacterial Communities. *Applied and Environmental Microbiology* **72**: 3016-3020.

Ainsworth, T.D., Krause, L., Bridge, T., Torda, G., Raina, J.-B., Zakrzewski, M. et al. (2015) The coral core microbiome identifies rare bacterial taxa as ubiquitous endosymbionts. *The ISME Journal* **9**: 2261-2274.

Ajikumar, P.K., Low, B.J.M., and Valiyaveettil, S. (2005) Role of soluble polymers on the preparation of functional thin films of calcium carbonate. *Surface and Coatings Technology* **198**: 227-230.

Akoka, S., and Trierweiler, M. (2002) Improvement of the ERETIC method by digital synthesis of the signal and addition of a broadband antenna inside the NMR probe. *Instrumentation Science & Technology* **30**: 21-29.

Alcolombri, U., Elias, M., Vardi, A., and Tawfik, D.S. (2014) Ambiguous evidence for assigning DddQ as a dimethylsulfoniopropionate lyase and oceanic dimethylsulfide producer. *Proceedings of the National Academy of Sciences* **111**: E2078-E2079.

Alcolombri, U., Lei, L., Meltzer, D., Vardi, A., and Tawfik, D.S. (2017) Assigning the Algal Source of Dimethylsulfide Using a Selective Lyase Inhibitor. *ACS Chemical Biology* **12**: 41-46.

Alcolombri, U., Ben-Dor, S., Feldmesser, E., Levin, Y., Tawfik, D.S., and Vardi, A. (2015) Identification of the algal dimethyl sulfide–releasing enzyme: A missing link in the marine sulfur cycle. *Science* **348**: 1466-1469.

Allard, M.W., Strain, E., Melka, D., Bunning, K., Musser, S.M., Brown, E.W., and Timme, R. (2016) Practical Value of Food Pathogen Traceability through Building a Whole-Genome Sequencing Network and Database. *Journal of Clinical Microbiology* **54**: 1975-1983.

Allemand, D., Tambutté, É., Girard, J.P., and Jaubert, J. (1998) Organic matrix synthesis in the scleractinian coral *Stylophora pistillata*: role in biomineralization and potential target of the organotin tributyltin. *Journal of Experimental Biology* **201**: 2001.

Allemand, D., Tambutté, É., Zoccola, D., and Tambutté, S. (2011) Coral Calcification, Cells to Reefs. In *Coral Reefs: An Ecosystem in Transition*. Dubinsky, Z., and Stambler, N. (eds). Dordrecht: Springer Netherlands, pp. 119-150.

Allemand, D., Ferrier-Pagès, C., Furla, P., Houlbrèque, F., Puverel, S., Reynaud, S. et al. (2004) Biomineralisation in reef-building corals: from molecular mechanisms to environmental control. *Comptes Rendus Palevol* **3**: 453-467.

Altschul, S.F., Gish, W., Miller, W., Myers, E.W., and Lipman, D.J. (1990) Basic local alignment search tool. *Journal of Molecular Biology* **215**: 403-410.

Altschul, S.F., Madden, T.L., Schäffer, A.A., Zhang, J., Zhang, Z., Miller, W., and Lipman, D.J. (1997) Gapped BLAST and PSI-BLAST: a new generation of protein database search programs. *Nucleic Acids Research* **25**: 3389-3402.

Andreae, M.O., Barnard, W.R., and Ammons, J.M. (1983) The Biological Production of Dimethylsulfide in the Ocean and Its Role in the Global Atmospheric Sulfur Budget. *Ecological Bulletins*: 167-177.

Andreae, M.O., Ferek, R.J., Bermond, F., Byrd, K.P., Engstrom, R.T., Hardin, S. et al. (1985) Dimethyl sulfide in the marine atmosphere. *Journal of Geophysical Research: Atmospheres* **90**: 12891-12900.

Anthony, K.R.N., A. Kleypas, J., and Gattuso, J.-P. (2011) Coral reefs modify their seawater carbon chemistry – implications for impacts of ocean acidification. *Global Change Biology* **17**: 3655-3666.

Archer, S.D., Widdicombe, C.E., Tarran, G.A., Rees, A.P., and Burkill, P.H. (2001) Production and turnover of particulate dimethylsulphoniopropionate during a coccolithophore bloom in the northern North Sea. *Aquatic Microbial Ecology* **24**: 225-241.

Asher, E.C., Dacey, J.W.H., Mills, M.M., Arrigo, K.R., and Tortell, P.D. (2011) High concentrations and turnover rates of DMS, DMSP and DMSO in Antarctic sea ice. *Geophysical Research Letters* **38**: n/a-n/a.

Ausma, T., Kebert, M., Stefels, J., and De Kok, L.J. (2017) DMSP: Occurrence in Plants and Response to Salinity in *Zea mays*. In. Cham: Springer International Publishing, pp. 87-91.

Ayala-Castro, C., Saini, A., and Outten, F.W. (2008) Fe-S Cluster Assembly Pathways in Bacteria. *Microbiology and Molecular Biology Reviews* **72**: 110-125.

Babcock, R.C., Baird, A.H., Piromvaragorn, S., Thomson, D.P., and Willis, B.L. (2003) Identification of Scleractinian Coral Recruits from Indo-Pacific Reefs. *Zoological Studies* **42**: 211-226.

Bakshani, C.R., Morales-Garcia, A.L., Althaus, M., Wilcox, M.D., Pearson, J.P., Bythell, J.C., and Burgess, J.G. (2018) Evolutionary conservation of the antimicrobial function of mucus: a first defence against infection. *npj Biofilms and Microbiomes* **4**: 14.

Banerjee, R.V., Johnston, N.L., Sobeski, J.K., Datta, P., and Matthews, R.G. (1989) Cloning and Sequence Analysis of the *Escherichia coli metH* Gene Encoding Cobalamin-dependent Methionine Synthase and Isolation of a Tryptic Fragment Containing the Cobalamin-binding Domain. *Journal of Biological Chemistry* **264**: 13888-13895.

Bankevich, A., Nurk, S., Antipov, D., Gurevich, A.A., Dvorkin, M., Kulikov, A.S. et al. (2012) SPAdes: A New Genome Assembly Algorithm and Its Applications to Single-Cell Sequencing. *Journal of Computational Biology* **19**: 455-477.

Bar-On, Y.M., Phillips, R., and Milo, R. (2018) The biomass distribution on Earth. *Proceedings of the National Academy of Sciences* **115**: 6506-6511.

Barnes, D.J. (1970) Coral Skeletons: An Explanation of Their Growth and Structure. *Science* **170**: 1305.

Barnes, D.J., and Devereux, M.J. (1984) Productivity and calcification on a coral reef: A survey using pH and oxygen electrode techniques. *Journal of Experimental Marine Biology and Ecology* **79**: 213-231.

Barron, M.G., Vivian, D.N., Yee, S.H., and Santavy, D.L. (2009) Methods to estimate solar radiation dosimetry in coral reefs using remote sensed, modeled, and in situ data. *Environmental Monitoring and Assessment* **151**: 445-455.

Bates, T.S., Charlson, R.J., and Gammon, R.H. (1987) Evidence for the climatic role of marine biogenic sulphur. *Nature* **329**: 319-321.

Baumann, P., and Baumann, L. (1981) The marine Gram-negative eubacteria: genera Photobacterium, Beneckea, Alteromonas, Pseudomonas, and Alcaligenes. In *The Prokaryotes: A Handbook on Habitats, Isolation and Identification of Bacteria*. Starr, M.P., Stolp, H., Trüper, H.G., Balows, A., and Schlegel, H.G. (eds). Berlin: Springer-Verlag, pp. 1302-1331.

Bax, A., and Summers, M.F. (1986) Proton and carbon-13 assignments from sensitivity-enhanced detection of heteronuclear multiple-bond connectivity by 2D multiple quantum NMR. *Journal of the American Chemical Society* **108**: 2093-2094.

Behringer, G., Ochsenkühn, M.A., Fei, C., Fanning, J., Koester, J.A., and Amin, S.A. (2018) Bacterial Communities of Diatoms Display Strong Conservation Across Strains and Time. *Frontiers in Microbiology* **9**.

Bellwood, D.R., Wainwright, P.C., Fulton, C.J., and Hoey, A.S. (2006a) Functional versatility supports coral reef biodiversity. *Proceedings of the Royal Society B: Biological Sciences* **273**: 101-107.

Bellwood, D.R., Hoey, A.S., Ackerman, J.L., and Depczynski, M. (2006b) Coral bleaching, reef fish community phase shifts and the resilience of coral reefs. *Global Change Biology* **12**: 1587-1594.

Bigg, E.K., and Turvey, D.E. (1978) Sources of atmospheric particles over Australia. *Atmospheric Environment (1967)* **12**: 1643-1655.

Blackall, L.L., Wilson, B., and van Oppen, M.J.H. (2015) Coral—the world's most diverse symbiotic ecosystem. *Molecular Ecology* **24**: 5330-5347.

Bolger, A.M., Lohse, M., and Usadel, B. (2014) Trimmomatic: a flexible trimmer for Illumina sequence data. *Bioinformatics* **30**: 2114-2120.

Borell, E.M., Steinke, M., and Fine, M. (2013) Direct and indirect effects of high *p*CO2 on algal grazing by coral reef herbivores from the Gulf of Aqaba (Red Sea). *Coral Reefs* **32**: 937-947.

Borell, E.M., Steinke, M., Horwitz, R., and Fine, M. (2014) Increasing *p*CO2 correlates with low concentrations of intracellular dimethylsulfoniopropionate in the sea anemone *Anemonia viridis*. *Ecology and Evolution* **4**: 441-449.

Borell, E.M., Pettay, D.T., Steinke, M., Warner, M., and Fine, M. (2016) Symbiosis-specific changes in dimethylsulphoniopropionate concentrations in *Stylophora pistillata* along a depth gradient. *Coral Reefs* **35**: 1383-1392.

Bourne, D.G., and Munn, C.B. (2005) Diversity of bacteria associated with the coral *Pocillopora damicornis* from the Great Barrier Reef. *Environmental Microbiology* **7**: 1162-1174.

Bourne, D.G., and Webster, N.S. (2013) Coral Reef Bacterial Communities. In *The Prokaryotes: Prokaryotic Communities and Ecophysiology*. Rosenberg, E., DeLong, E.F., Lory, S., Stackebrandt, E., and Thompson, F. (eds). Berlin, Heidelberg: Springer Berlin Heidelberg, pp. 163-187.

Bourne, D.G., Garren, M., Work, T.M., Rosenberg, E., Smith, G.W., and Harvell, C.D. (2009) Microbial disease and the coral holobiont. *Trends in Microbiology* **17**: 554-562.

Bradford, M.M. (1976) A rapid and sensitive method for the quantitation of microgram quantities of protein utilizing the principle of protein-dye binding. *Analytical Biochemistry* **72**: 248-254.

Brahmi, C., Domart-Coulon, I., Rougée, L., Pyle, D.G., Stolarski, J., Mahoney, J.J. et al. (2012) Pulsed ^{86}Sr-labeling and NanoSIMS imaging to study coral biomineralization at ultra-structural length scales. *Coral Reefs* **31**: 741-752.

Brennan, S.T., Lowenstein, T.K., and Horita, J. (2004) Seawater chemistry and the advent of biocalcification. *Geology* **32**: 473-476.

Broadbent, A., and Jones, G. (2006) Seasonal and Diurnal Cycles of Dimethylsulfide, Dimethylsulfoniopropionate and Dimethylsulfoxide at One Tree Reef Lagoon. *Environmental Chemistry* **3**: 260-267.

Broadbent, A.D., and Jones, G.B. (2004) DMS and DMSP in mucus ropes, coral mucus, surface films and sediment pore waters from coral reefs in the Great Barrier Reef. *Marine and Freshwater Research* **55**: 849-855.

Broadbent, A.D., Jones, G.B., and Jones, R.J. (2002) DMSP in Corals and Benthic Algae from the Great Barrier Reef. *Estuarine, Coastal and Shelf Science* **55**: 547-555.

Bryan, W.H., and Hill, D. (1941) Spherulitic crystallization as a mechanism of skeletal growth in the hexacorals. *Proceedings of the Royal Society of Queensland* **52**: 78–91.

Bullock, H.A., Luo, H.W., and Whitman, W.B. (2017) Evolution of Dimethylsulfoniopropionate Metabolism in Marine Phytoplankton and Bacteria. *Frontiers in Microbiology* **8**: 17.

Burdett, H.L., Keddie, V., MacArthur, N., McDowall, L., McLeish, J., Spielvogel, E. et al. (2014) Dynamic photoinhibition exhibited by red coralline algae in the red sea. *BMC Plant Biology* **14**: 139.

Burg, M.B., and Ferraris, J.D. (2008) Intracellular Organic Osmolytes: Function and Regulation*. *Journal of Biological Chemistry* **283**: 7309-7313.

Bürgmann, H., Howard, E.C., Ye, W., Sun, F., Sun, S., Napierala, S., and Moran, M.A. (2007) Transcriptional response of *Silicibacter pomeroyi* DSS-3 to dimethylsulfoniopropionate (DMSP). *Environmental Microbiology* **9**: 2742-2755.

Cahill, M.J., Köser, C.U., Ross, N.E., and Archer, J.A.C. (2010) Read Length and Repeat Resolution: Exploring Prokaryote Genomes Using Next-Generation Sequencing Technologies. *PLOS ONE* **5**: e11518.

Campbell, G.R.O., Taga, M.E., Mistry, K., Lloret, J., Anderson, P.J., Roth, J.R., and Walker, G.C. (2006) *Sinorhizobium meliloti bluB* is necessary for production of 5,6-dimethylbenzimidazole, the lower ligand of B_{12}. *Proceedings of the National Academy of Sciences of the United States of America* **103**: 4634-4639.

Canfield, D.E. (2004) The evolution of the Earth surface sulfur reservoir. *American Journal of Science* **304**: 839-861.

Cantaert, B., Beniash, E., and Meldrum, F.C. (2013) The role of poly(aspartic acid) in the precipitation of calcium phosphate in confinement. *Journal of Materials Chemistry B* **1**: 6586-6595.

Cantoni, G.L., and Anderson, D.G. (1956) Enzymatic Cleavage of Dimethylpropriothetin by *Polysiphonia Lanosa*. *Journal of Biological Chemistry* **222**: 171-177.

Capella-Gutiérrez, S., Silla-Martínez, J.M., and Gabaldón, T. (2009) trimAl: a tool for automated alignment trimming in large-scale phylogenetic analyses. *Bioinformatics* **25**: 1972-1973.

Carrión, O., Curson, A.R.J., Kumaresan, D., Fu, Y., Lang, A.S., Mercadé, E., and Todd, J.D. (2015) A novel pathway producing dimethylsulphide in bacteria is widespread in soil environments. *Nature Communications* **6**.

Challenger, F., and Simpson, M.I. (1948) 320. Studies on biological methylation. Part XII. A precursor of the dimethyl sulphide evolved by *Polysiphonia fastigiata*. dimethyl-2-carboxyethylsulphonium hydroxide and its salts. *Journal of the Chemical Society (Resumed)*: 1591-1597.

Chambers, S.T., Kunin, C.M., Miller, D., and Hamada, A. (1987) Dimethylthetin can substitute for glycine betaine as an osmoprotectant molecule for *Escherichia coli*. *Journal of Bacteriology* **169**: 4845-4847.

Chan, N.C.S., and Connolly, S.R. (2013) Sensitivity of coral calcification to ocean acidification: a meta-analysis. *Global Change Biology* **19**: 282-290.

Chaumeil, P.-A., Mussig, A.J., Hugenholtz, P., and Parks, D.H. (2019) GTDB-Tk: a toolkit to classify genomes with the Genome Taxonomy Database. *Bioinformatics* **36**: 1925-1927.

Chave, K.E., Smith, S.V., and Roy, K.J. (1972) Carbonate production by coral reefs. *Marine Geology* **12**: 123-140.

Chen, M.-H., Sheu, S.-Y., Chen, C.A., Wang, J.-T., and Chen, W.-M. (2011) *Shimia isoporae* sp. nov., isolated from the reef-building coral *Isopora palifera*. *International Journal of Systematic and Evolutionary Microbiology* **61**: 823-827.

Chen, M.-H., Sheu, S.-Y., Chen, C.A., Wang, J.-T., and Chen, W.-M. (2012) *Roseivivax isoporae* sp. nov., isolated from a reef-building coral, and emended description of the genus *Roseivivax*. *International Journal of Systematic and Evolutionary Microbiology* **62**: 1259-1264.

Chin, M., and Jacob, D.J. (1996) Anthropogenic and natural contributions to tropospheric sulfate: A global model analysis. *Journal of Geophysical Research: Atmospheres* **101**: 18691-18699.

Chiu, C.-Y., Lin, G., Cheng, M.-L., Chiang, M.-H., Tsai, M.-H., Lai, S.-H. et al. (2016) Metabolomic Profiling of Infectious Parapneumonic Effusions Reveals Biomarkers for Guiding Management of Children with *Streptococcus pneumoniae* Pneumonia. *Scientific Reports* **6**: 24930.

Chiu, J.M.Y., Li, S., Li, A., Po, B., Zhang, R., Shin, P.K.S., and Qiu, J.-W. (2012) Bacteria associated with skeletal tissue growth anomalies in the coral *Platygyra carnosus*. *FEMS Microbiology Ecology* **79**: 380-391.

Choi, D.H., and Cho, B.C. (2006) *Shimia marina* gen. nov., sp. nov., a novel bacterium of the *Roseobacter* clade isolated from biofilm in a coastal fish farm. *International Journal of Systematic and Evolutionary Microbiology* **56**: 1869-1873.

Choi, D.H., Park, K.-T., An, S.M., Lee, K., Cho, J.-C., Lee, J.-H. et al. (2015) Pyrosequencing Revealed SAR116 Clade as Dominant *dddP*-Containing Bacteria in Oligotrophic NW Pacific Ocean. *PLOS ONE* **10**: e0116271.

Clode, P.L., Stern, R.A., and Marshall, A.T. (2007) Subcellular imaging of isotopically labeled carbon compounds in a biological sample by ion microprobe (NanoSIMS). *Microscopy Research and Technique* **70**: 220-229.

Clode, P.L., Lema, K., Saunders, M., and Weiner, S. (2011) Skeletal mineralogy of newly settling *Acropora millepora* (Scleractinia) coral recruits. *Coral Reefs* **30**: 1-8.

Cohen, A.L., and McConnaughey, T.A. (2003) Geochemical Perspectives on Coral Mineralization. *Reviews in Mineralogy and Geochemistry* **54**: 151-187.

Coles, S.L., Jokiel, P.L., and Lewis, C.R. (1976) Thermal tolerance in tropical versus subtropical Pacific reef corals. *Pacific Science* **30**: 159-166.

Consortium, T.U. (2018) UniProt: a worldwide hub of protein knowledge. *Nucleic Acids Research* **47**: D506-D515.

Costanza, R., de Groot, R., Sutton, P., van der Ploeg, S., Anderson, S.J., Kubiszewski, I. et al. (2014) Changes in the global value of ecosystem services. *Global Environmental Change* **26**: 152-158.

Cox, M.M. (2003) The Bacterial RecA Protein as a Motor Protein. *Annual Review of Microbiology* **57**: 551-577.

Croft, M.T., Lawrence, A.D., Raux-Deery, E., Warren, M.J., and Smith, A.G. (2005) Algae acquire vitamin B12 through a symbiotic relationship with bacteria. *Nature* **438**: 90-93.

Cropp, R., Gabric, A., van Tran, D., Jones, G., Swan, H., and Butler, H. (2018) Coral reef aerosol emissions in response to irradiance stress in the Great Barrier Reef, Australia. *Ambio*.

Cuhel, R.L., Taylor, C.D., and Jannasch, H.W. (1982) Assimilatory Sulfur Metabolism in Marine Microorganisms: Considerations for the Application of Sulfate Incorporation into Protein as a Measurement of Natural Population Protein Synthesis. *Applied and Environmental Microbiology* **43**: 160-168.

Cuif, J.P., and Dauphin, Y. (2005) The Environment Recording Unit in coral skeletons – a synthesis of structural and chemical evidences for a biochemically driven, stepping-growth process in fibres. *Biogeosciences* **2**: 61-73.

Curson, A.R.J., Sullivan, M.J., Todd, J.D., and Johnston, A.W.B. (2011a) DddY, a periplasmic dimethylsulfoniopropionate lyase found in taxonomically diverse species of Proteobacteria. *The ISME Journal* **5**: 1191-1200.

Curson, A.R.J., Todd, J.D., Sullivan, M.J., and Johnston, A.W.B. (2011b) Catabolism of dimethylsulphoniopropionate: microorganisms, enzymes and genes. *Nature Reviews Microbiology* **9**: 849-859.

Curson, A.R.J., Rogers, R., Todd, J.D., Brearley, C.A., and Johnston, A.W.B. (2008) Molecular genetic analysis of a dimethylsulfoniopropionate lyase that liberates the climate-changing gas dimethylsulfide in several marine α-proteobacteria and Rhodobacter sphaeroides. *Environmental Microbiology* **10**: 757-767.

Curson, A.R.J., Burns, O.J., Voget, S., Daniel, R., Todd, J.D., McInnis, K. et al. (2014) Screening of Metagenomic and Genomic Libraries Reveals Three Classes of Bacterial Enzymes That Overcome the Toxicity of Acrylate. *PLOS ONE* **9**: e97660.

Curson, A.R.J., Liu, J., Bermejo Martínez, A., Green, R.T., Chan, Y., Carrión, O. et al. (2017) Dimethylsulfoniopropionate biosynthesis in marine bacteria and identification of the key gene in this process. *Nature Microbiology* **2**: 17009.

Curson, A.R.J., Williams, B.T., Pinchbeck, B.J., Sims, L.P., Martínez, A.B., Rivera, P.P.L. et al. (2018) DSYB catalyses the key step of dimethylsulfoniopropionate biosynthesis in many phytoplankton. *Nature Microbiology* **3**: 430-439.

Cusack, M., and Freer, A. (2008) Biomineralization: Elemental and Organic Influence in Carbonate Systems. *Chemical Reviews* **108**: 4433-4454.

Dandeu, A., Humbert, B., Carteret, C., Muhr, H., Plasari, E., and Bossoutrot, J.M. (2006) Raman Spectroscopy – A Powerful Tool for the Quantitative Determination of the Composition of Polymorph Mixtures: Application to CaCO3 Polymorph Mixtures. *Chemical Engineering & Technology* **29**: 221-225.

Dang, H., Li, T., Chen, M., and Huang, G. (2008) Cross-Ocean Distribution of Rhodobacterales Bacteria as Primary Surface Colonizers in Temperate Coastal Marine Waters. *Applied and Environmental Microbiology* **74**: 52-60.

Daniels, C.A., Zeifman, A., Heym, K., Ritchie, K.B., Watson, C.A., Berzins, I., and Breitbart, M. (2011) Spatial heterogeneity of bacterial communities in the mucus of *Montastraea annularis*. *Marine Ecology Progress Series* **426**: 29-40.

Darroch, L.J., Lavoie, M., Levasseur, M., Laurion, I., Sunda, W.G., Michaud, S. et al. (2015) Effect of short-term light- and UV-stress on DMSP, DMS, and DMSP lyase activity in Emiliania huxleyiÃÂ *Aquatic Microbial Ecology* **74**: 173-185.

de Oliveira Soares, M., Teixeira, C.E.P., Ferreira, S.M.C., Gurgel, A.L.A.R., Paiva, B.P., Menezes, M.O.B. et al. (2019) Thermal stress and tropical reefs: mass coral bleaching in a stable temperature environment? *Marine Biodiversity*.

de Souza, M.P., Chen, Y.P., and Yoch, D.C. (1996) Dimethylsulfoniopropionate lyase from the marine macroalga Ulva curvata: purification and characterization of the enzyme. *Planta* **199**: 433-438.

DeBose, J.L., and Nevitt, G.A. (2007) Investigating the association between pelagic fish and dimethylsulfoniopropionate in a natural coral reef system. *Marine and Freshwater Research* **58**: 720-724.

DeCarlo, T.M. (2018) Characterizing coral skeleton mineralogy with Raman spectroscopy. *Nature Communications* **9**: 5325.

DeCarlo, T.M., Ren, H., and Farfan, G.A. (2018) The Origin and Role of Organic Matrix in Coral Calcification: Insights From Comparing Coral Skeleton and Abiogenic Aragonite. *Frontiers in Marine Science* **5**.

del Valle, D.A., Martínez-García, S., Sañudo-Wilhelmy, S.A., Kiene, R.P., and Karl, D.M. (2015) Methionine and dimethylsulfoniopropionate as sources of sulfur to the microbial community of the North Pacific Subtropical Gyre. *Aquatic Microbial Ecology* **75**: 103-116.

Deschaseaux, E., Jones, G., and Swan, H. (2016) Dimethylated sulfur compounds in coral-reef ecosystems. *Environmental Chemistry* **13**: 239-251.

Deschaseaux, E., Hardefeldt, J., Jones, G., and Reichelt-Brushett, A. (2018) High zinc exposure leads to reduced dimethylsulfoniopropionate (DMSP) levels in both the host and endosymbionts of the reef-building coral *Acropora aspera*. *Marine Pollution Bulletin* **126**: 93-100.

Deschaseaux, E.S.M., Beltran, V.H., Jones, G.B., Deseo, M.A., Swan, H.B., Harrison, P.L., and Eyre, B.D. (2014a) Comparative response of DMS and DMSP concentrations in *Symbiodinium* clades C1 and D1 under thermal stress. *Journal of Experimental Marine Biology and Ecology* **459**: 181-189.

Deschaseaux, E.S.M., Jones, G.B., Deseo, M.A., Shepherd, K.M., Kiene, R.P., Swan, H.B. et al. (2014b) Effects of environmental factors on dimethylated sulfur compounds and their potential role in the antioxidant system of the coral holobiont. *Limnology and Oceanography* **59**: 758-768.

Di Tommaso, P., Moretti, S., Xenarios, I., Orobitg, M., Montanyola, A., Chang, J.-M. et al. (2011) T-Coffee: a web server for the multiple sequence alignment of protein and RNA sequences using structural information and homology extension. *Nucleic Acids Research* **39**: W13-W17.

Dickschat, J.S., Rabe, P., and Citron, C.A. (2015) The chemical biology of dimethylsulfoniopropionate. *Organic & Biomolecular Chemistry* **13**: 1954-1968.

Donnet, M., Bowen, P., Jongen, N., Lemaître, J., and Hofmann, H. (2005) Use of Seeds to Control Precipitation of Calcium Carbonate and Determination of Seed Nature. *Langmuir* **21**: 100-108.

Douglas, A.E. (2003) Coral bleaching—how and why? *Marine Pollution Bulletin* **46**: 385-392.

Ducklow, H.W., and Mitchell, R. (1979) Bacterial populations and adaptations in the mucus layers on living corals1. *Limnology and Oceanography* **24**: 715-725.

Dustan, P. (1979) Distribution of Zooxanthellae and Photosynthetic Chloroplast Pigments of the Reef-Building Coral Montastrea Annularis Ellis and Solander in Relation to Depth on a West Indian Coral Reef. *Bulletin of Marine Science* **29**: 79-95.

Eisen, J.A. (1995) The RecA protein as a model molecule for molecular systematic studies of bacteria: Comparison of trees of RecAs and 16S rRNAs from the same species. *Journal of Molecular Evolution* **41**: 1105-1123.

Elhadj, S., De Yoreo, J.J., Hoyer, J.R., and Dove, P.M. (2006) Role of molecular charge and hydrophilicity in regulating the kinetics of crystal growth. *Proceedings of the National Academy of Sciences* **103**: 19237-19242.

Elliott, G.D., Wang, S., and Fuller, B.J. (2017) Cryoprotectants: A review of the actions and applications of cryoprotective solutes that modulate cell recovery from ultra-low temperatures. *Cryobiology* **76**: 74-91.

Erez, J., Reynaud, S., Silverman, J., Schneider, K., and Allemand, D. (2011) Coral Calcification Under Ocean Acidification and Global Change. In *Coral Reefs: An Ecosystem in Transition*. Dubinsky, Z., and Stambler, N. (eds). Dordrecht: Springer Netherlands, pp. 151-176.

Falini, G., Fermani, S., and Goffredo, S. (2015) Coral biomineralization: A focus on intra-skeletal organic matrix and calcification. *Seminars in Cell & Developmental Biology* **46**: 17-26.

Falini, G., Albeck, S., Weiner, S., and Addadi, L. (1996) Control of Aragonite or Calcite Polymorphism by Mollusk Shell Macromolecules. *Science* **271**: 67.

Falini, G., Reggi, M., Fermani, S., Sparla, F., Goffredo, S., Dubinsky, Z. et al. (2013) Control of aragonite deposition in colonial corals by intra-skeletal macromolecules. *Journal of Structural Biology* **183**: 226-238.

Falkowski, P.G., Fenchel, T., and Delong, E.F. (2008) The Microbial Engines That Drive Earth's Biogeochemical Cycles. *Science* **320**: 1034.

Farfan, G.A., Cordes, E.E., Waller, R.G., DeCarlo, T.M., and Hansel, C.M. (2018) Mineralogy of Deep-Sea Coral Aragonites as a Function of Aragonite Saturation State. *Frontiers in Marine Science* **5**.

Favrot, L., Blanchard, J.S., and Vergnolle, O. (2016) Bacterial GCN5-Related N-Acetyltransferases: From Resistance to Regulation. *Biochemistry* **55**: 989-1002.

Feely, R.A., Doney, S.C., and Cooley, S.R. (2009) Ocean Acidification

Present Conditions and Future Changes in a High-CO_2 World. *Oceanography* **22**: 36-47.

Ferrario, F., Beck, M.W., Storlazzi, C.D., Micheli, F., Shepard, C.C., and Airoldi, L. (2014) The effectiveness of coral reefs for coastal hazard risk reduction and adaptation. *Nature Communications* **5**: 3794.

Field, C.B. (2014) *Climate change 2014–Impacts, adaptation and vulnerability: Regional aspects*: Cambridge University Press.

Fischer, E., and Jones, G. (2012) Atmospheric dimethysulphide production from corals in the Great Barrier Reef and links to solar radiation, climate and coral bleaching. *Biogeochemistry* **110**: 31-46.

Fisher, R., O'Leary, Rebecca A., Low-Choy, S., Mengersen, K., Knowlton, N., Brainard, Russell E., and Caley, M.J. (2015) Species Richness on Coral Reefs and the Pursuit of Convergent Global Estimates. *Current Biology* **25**: 500-505.

Fitt, W.K., Brown, B.E., Warner, M.E., and Dunne, R.P. (2001) Coral bleaching: interpretation of thermal tolerance limits and thermal thresholds in tropical corals. *Coral Reefs* **20**: 51-65.

Frade, P.R., Schwaninger, V., Glasl, B., Sintes, E., Hill, R.W., Simó, R., and Herndl, G.J. (2016) Dimethylsulfoniopropionate in corals and its interrelations with bacterial assemblages in coral surface mucus. *Environmental Chemistry* **13**: 252-265.

Frederick, C.B., Lomax, L.G., Black, K.A., Finch, L., Scribner, H.E., Kimbell, J.S. et al. (2002) Use of a Hybrid Computational Fluid Dynamics and Physiologically Based Inhalation Model for Interspecies Dosimetry Comparisons of Ester Vapors. *Toxicology and Applied Pharmacology* **183**: 23-40.

Frias-Lopez, J., Zerkle, A.L., Bonheyo, G.T., and Fouke, B.W. (2002) Partitioning of Bacterial Communities between Seawater and Healthy, Black Band Diseased, and Dead Coral Surfaces. *Applied and Environmental Microbiology* **68**: 2214-2228.

Fukui, T., Shiomi, N., and Doi, Y. (1998) Expression and Characterization of (*R*)-Specific Enoyl Coenzyme A Hydratase Involved in Polyhydroxyalkanoate Biosynthesis by *Aeromonas caviae*. *Journal of Bacteriology* **180**: 667-673.

Fuse, H., Takimura, O., Kamimura, K., Murakami, K., Yamaoka, Y., and Murooka, Y. (1995) Transformation of Dimethyl Sulfide and Related Compounds by Cultures and Cell Extracts of Marine Phytoplankton. *Bioscience, Biotechnology, and Biochemistry* **59**: 1773-1775.

Gage, D.A., Rhodes, D., Nolte, K.D., Hicks, W.A., Leustek, T., Cooper, A.J.L., and Hanson, A.D. (1997) A new route for synthesis of dimethylsulphoniopropionate in marine algae. *Nature* **387**: 891-894.

Gagnon, A.C., Adkins, J.F., and Erez, J. (2012) Seawater transport during coral biomineralization. *Earth and Planetary Science Letters* **329-330**: 150-161.

Gallegos, M.T., Schleif, R., Bairoch, A., Hofmann, K., and Ramos, J.L. (1997) Arac/XylS family of transcriptional regulators. *Microbiology and Molecular Biology Reviews* **61**: 393-410.

Gao, C., Fernandez, V.I., Lee, K.S., Fenizia, S., Pohnert, G., Seymour, J.R. et al. (2020) Single-cell bacterial transcription measurements reveal the importance of dimethylsulfoniopropionate (DMSP) hotspots in ocean sulfur cycling. *Nature Communications* **11**: 1942.

Gardner, S.G., Raina, J.-B., Ralph, P.J., and Petrou, K. (2017) Reactive oxygen species (ROS) and dimethylated sulphur compounds in coral explants under acute thermal stress. *Journal of Experimental Biology* **220**: 1787–1791.

Gardner, S.G., Nielsen, D.A., Laczka, O., Shimmon, R., Beltran, V.H., Ralph, P.J., and Petrou, K. (2016) Dimethylsulfoniopropionate, superoxide dismutase and glutathione as stress response indicators in three corals under short-term hyposalinity stress. *Proceedings of the Royal Society B: Biological Sciences* **283**: 20152418.

Garren, M., and Azam, F. (2010) New Method for Counting Bacteria Associated with Coral Mucus. *Applied and Environmental Microbiology* **76**: 6128-6133.

Garren, M., and Azam, F. (2012) Corals shed bacteria as a potential mechanism of resilience to organic matter enrichment. *The ISME Journal* **6**: 1159-1165.

Garren, M., Son, K., Raina, J.-B., Rusconi, R., Menolascina, F., Shapiro, O.H. et al. (2014) A bacterial pathogen uses dimethylsulfoniopropionate as a cue to target heat-stressed corals. *The ISME Journal* **8**: 999-1007.

Gattuso, J.P., Frankignoulle, M., Bourge, I., Romaine, S., and Buddemeier, R.W. (1998) Effect of calcium carbonate saturation of seawater on coral calcification. *Global and Planetary Change* **18**: 37-46.

Gilmore, D.F., Godchaux, W., and Leadbetter, E.R. (1989) Regulation of sulfate assimilation in Cytophaga johnsonae. *Archives of Microbiology* **152**: 387-392.

Giloteaux, L., Holmes, D.E., Williams, K.H., Wrighton, K.C., Wilkins, M.J., Montgomery, A.P. et al. (2013) Characterization and transcription of arsenic respiration and resistance genes during in situ uranium bioremediation. *The ISME Journal* **7**: 370-383.

Giovanelli, J. (1987) Sulfur amino acids of plants: An overview. In *Methods in Enzymology*: Academic Press, pp. 419-426.

Giovanelli, J., and Harvey Mudd, S. (1967) Synthesis of homocysteine and cysteine by enzyme extracts of spinach. *Biochemical and Biophysical Research Communications* **27**: 150-156.

Glynn, P.W. (1993) Coral reef bleaching: ecological perspectives. *Coral Reefs* **12**: 1-17.

Goffredo, S., Vergni, P., Reggi, M., Caroselli, E., Sparla, F., Levy, O. et al. (2011) The skeletal organic matrix from Mediterranean coral *Balanophyllia europaea* influences calcium carbonate precipitation. *PLOS ONE* **6**: e22338-e22338.

Goldstein, S., Beka, L., Graf, J., and Klassen, J.L. (2019) Evaluation of strategies for the assembly of diverse bacterial genomes using MinION long-read sequencing. *BMC Genomics* **20**: 23.

González, J.M., Kiene, R.P., and Moran, M.A. (1999) Transformation of Sulfur Compounds by an Abundant Lineage of Marine Bacteria in the α-Subclass of the Class *Proteobacteria*. *Applied and Environmental Microbiology* **65**: 3810-3819.

González, J.M., Whitman, W.B., Hodson, R.E., and Moran, M.A. (1996) Identifying numerically abundant culturable bacteria from complex communities: an example from a lignin enrichment culture. *Applied and Environmental Microbiology* **62**: 4433-4440.

Greene, R.C. (1962) Biosynthesis of Dimethyl-β-propiothetin. *Journal of Biological Chemistry* **237**: 2251-2254.

Greenfield, E.M., Wilson, D.C., and Crenshaw, M.A. (1984) Ionotropic Nucleation of Calcium Carbonate by Molluscan Matrix1. *American Zoologist* **24**: 925-932.

Gröne, T., and Kirst, G.O. (1992) The effect of nitrogen deficiency, methionine and inhibitors of methionine metabolism on the DMSP contents of Tetraselmis subcordiformis (Stein). *Marine Biology* **112**: 497-503.

Gross, R., Simon, J., and Kröger, A. (2001) Periplasmic methacrylate reductase activity in Wolinella succinogenes. *Archives of Microbiology* **176**: 310-313.

Groves, W.E., Davis, F.C., and Sells, B.H. (1968) Spectrophotometric determination of microgram quantities of protein without nucleic acid interference. *Analytical Biochemistry* **22**: 195-210.

Grundy, F.J., and Henkin, T.M. (1998) The S box regulon: a new global transcription termination control system for methionine and cysteine biosynthesis genes in Gram-positive bacteria. *Molecular Microbiology* **30**: 737-749.

Haas, P. (1935) The liberation of methyl sulphide by seaweed. *Biochemical Journal* **29**: 1297-1299.

Hanson, A.D., Rivoal, J., Paquet, L., and Gage, D.A. (1994) Biosynthesis of 3-Dimethylsulfoniopropionate in Wollastonia biflora (L.) DC. (Evidence That S-Methylmethionine Is an Intermediate). *Plant Physiology* **105**: 103-110.

Harrison, P., and Booth, D. (2007) Coral Reefs: naturally dynamic and increasingly disturbed ecosystems. *Marine Ecology*.

Harrison, P.L. (2011) Sexual Reproduction of Scleractinian Corals. In *Coral Reefs: An Ecosystem in Transition*. Dubinsky, Z., and Stambler, N. (eds). Dordrecht: Springer Netherlands, pp. 59-85.

Henson, J., Tischler, G., and Ning, Z. (2012) Next-generation sequencing and large genome assemblies. *Pharmacogenomics* **13**: 901-915.

Hernandez-Agreda, A., Gates, R.D., and Ainsworth, T.D. (2017) Defining the Core Microbiome in Corals' Microbial Soup. *Trends in Microbiology* **25**: 125-140.

Hernandez-Agreda, A., Leggat, W., Bongaerts, P., Herrera, C., and Ainsworth, T.D. (2018) Rethinking the Coral Microbiome: Simplicity Exists within a Diverse Microbial Biosphere. *mBio* **9**: e00812-00818.

Herrmann, G., Selmer, T., Jessen, H.J., Gokarn, R.R., Selifonova, O., Gort, S.J., and Buckel, W. (2005) Two beta-alanyl-CoA:ammonia lyases in Clostridium propionicum. *FEBS Journal* **272**: 813-821.

Higuchi, T., Fujimura, H., Yuyama, I., Harii, S., Agostini, S., and Oomori, T. (2014) Biotic Control of Skeletal Growth by Scleractinian Corals in Aragonite–Calcite Seas. *PLOS ONE* **9**: e91021.

Hill, R.W., Dacey, J.W.H., and Krupp, D.A. (1995) Dimethylsulfoniopropionate in Reef Corals. *Bulletin of Marine Science* **57**: 489-494.

Hill, R.W., Li, C., Jones, A.D., Gunn, J.P., and Frade, P.R. (2010) Abundant betaines in reef-building corals and ecological indicators of a photoprotective role. *Coral Reefs* **29**: 869-880.

Hoegh-Guldberg, O. (1999) Climate change, coral bleaching and the future of the world's coral reefs. *Marine and Freshwater Research* **50**: 839-866.

Hoegh-Guldberg, O., Mumby, P.J., Hooten, A.J., Steneck, R.S., Greenfield, P., Gomez, E. et al. (2007) Coral Reefs Under Rapid Climate Change and Ocean Acidification. *Science* **318**: 1737-1742.

Holm, R.H., Kennepohl, P., and Solomon, E.I. (1996) Structural and Functional Aspects of Metal Sites in Biology. *Chemical Reviews* **96**: 2239-2314.

Hopkins, F.E., Bell, T.G., Yang, M., Suggett, D.J., and Steinke, M. (2016) Air exposure of coral is a significant source of dimethylsulfide (DMS) to the atmosphere. *Scientific Reports* **6**: 36031.

Howard, E.C., Sun, S., Biers, E.J., and Moran, M.A. (2008) Abundant and diverse bacteria involved in DMSP degradation in marine surface waters. *Environmental Microbiology* **10**: 2397-2410.

Howard, E.C., Henriksen, J.R., Buchan, A., Reisch, C.R., Bürgmann, H., Welsh, R. et al. (2006) Bacterial Taxa That Limit Sulfur Flux from the Ocean. *Science* **314**: 649-652.

Hughes, T.P. (1994) Catastrophes, Phase Shifts, and Large-Scale Degradation of a Caribbean Coral Reef. *Science* **265**: 1547-1551.

Hughes, T.P., Kerry, J.T., and Simpson, T. (2018a) Large-scale bleaching of corals on the Great Barrier Reef. *Ecology* **99**: 501-501.

Hughes, T.P., Kerry, J.T., Baird, A.H., Connolly, S.R., Dietzel, A., Eakin, C.M. et al. (2018b) Global warming transforms coral reef assemblages. *Nature* **556**: 492-496.

Hughes, T.P., Baird, A.H., Bellwood, D.R., Card, M., Connolly, S.R., Folke, C. et al. (2003) Climate Change, Human Impacts, and the Resilience of Coral Reefs. *Science* **301**: 929.

Hughes, T.P., Kerry, J.T., Baird, A.H., Connolly, S.R., Chase, T.J., Dietzel, A. et al. (2019) Global warming impairs stock–recruitment dynamics of corals. *Nature* **568**: 387-390.

Hunt, M., Silva, N.D., Otto, T.D., Parkhill, J., Keane, J.A., and Harris, S.R. (2015) Circlator: automated circularization of genome assemblies using long sequencing reads. *Genome Biology* **16**: 294.

Ip, C., Loose, M., Tyson, J., de Cesare, M., Brown, B., Jain, M. et al. (2015) MinION Analysis and Reference Consortium: Phase 1 data release and analysis [version 1; peer review: 2 approved]. *F1000Research* **4**.

Ito, T., Asano, Y., Tanaka, Y., and Takabe, T. (2011) Regulation of biosynthesis of dimethylsulfoniopropionate and its uptake in sterile mutant of *Ulva pertusa* (Chlorophyta)[1] *Journal of Phycology* **47**: 517-523.

Ivankina, T.I., Kichanov, S.E., Duliu, O.G., Abdo, S.Y., and Sherif, M.M. (2020) The structure of scleractinian coral skeleton analyzed by neutron diffraction and neutron computed tomography. *Scientific Reports* **10**: 12869.

Jain, M., Tyson, J., Loose, M., Ip, C., Eccles, D., O'Grady, J. et al. (2017) MinION Analysis and Reference Consortium: Phase 2 data release and analysis of R9.0 chemistry [version 1; peer review: 1 approved, 2 approved with reservations]. *F1000Research* **6**.

James, F., Paquet, L., Sparace, S.A., Gage, D.A., and Hanson, A.D. (1995) Evidence Implicating Dimethylsulfoniopropionaldehyde as an Intermediate in Dimethylsulfoniopropionate Biosynthesis. *Plant Physiology* **108**: 1439-1448.

Johnston, A., Todd, J., and Curson, A. (2012) Microbial Origins and Consequences of Dimethyl Sulfide. In *Microbe Magazine*, pp. 181-185.

Johnston, A.W.B. (2015) Who can cleave DMSP? *Science* **348**: 1430-1431.

Johnston, A.W.B., Todd, J.D., Sun, L., Nikolaidou-Katsaridou, M.N., Curson, A.R.J., and Rogers, R. (2008) Molecular diversity of bacterial production of the climate-changing gas, dimethyl sulphide, a molecule that impinges on local and global symbioses. *Journal of Experimental Botany* **59**: 1059-1067.

Jokiel, P.L. (2011) Ocean Acidification and Control of Reef Coral Calcification by Boundary Layer Limitation of Proton Flux. *Bulletin of Marine Science* **87**: 639-657.

Jones-Mortimer, M.C. (1968) Positive control of sulphate reduction in Escherichia coli. Isolation, characterization and mapping of cysteineless mutants of E. coli K 12. *Biochemical Journal* **110**: 589-595.

Jones, G., and Ristovski, Z. (2010) Reef emissions affect climate. *Australasian Science* **31**: 26.

Jones, G., Curran, M., and Broadbent, A. (1994) Dimethylsulfide in the South Pacific. In *Recent Advances in Marine Science and Technology'94, 6th Pacific Congress on Marine Science and Technology*, pp. 183-190.

Jones, G., Curran, M., Broadbent, A., King, S., Fischer, E., and Jones, R. (2007) Factors affecting the cycling of dimethylsulfide and dimethylsulfoniopropionate in coral reef waters of the Great Barrier Reef. *Environmental Chemistry* **4**: 310-322.

Jones, G.B., and Trevena, A.J. (2005) The influence of coral reefs on atmospheric dimethylsulphide over the Great Barrier Reef, Coral Sea, Gulf of Papua and Solomon and Bismarck Seas. *Marine and Freshwater Research* **56**: 85-93.

Jones, G.B., and King, S. (2015) Dimethylsulphoniopropionate (DMSP) as an Indicator of Bleaching Tolerance in Scleractinian Corals. *Journal of Marine Science and Engineering* **3**: 444-465.

Jones, G.B., Fischer, E., Deschaseaux, E.S.M., and Harrison, P.L. (2014) The effect of coral bleaching on the cellular concentration of dimethylsulphoniopropionate in reef corals. *Journal of Experimental Marine Biology and Ecology* **460**: 19-31.

Joux, F., Jeffrey, W.H., Lebaron, P., and Mitchell, D.L. (1999) Marine Bacterial Isolates Display Diverse Responses to UV-B Radiation. *Applied and Environmental Microbiology* **65**: 3820-3827.

Kalmar, L., Homola, D., Varga, G., and Tompa, P. (2012) Structural disorder in proteins brings order to crystal growth in biomineralization. *Bone* **51**: 528-534.

Kamenos, N.A., Strong, S.C., Shenoy, D.M., Wilson, S.T., Hatton, A.D., and Moore, P.G. (2008) Red coralline algae as a source of marine biogenic dimethylsulphoniopropionate. *Marine Ecology Progress Series* **372**: 61-66.

Kanehisa, M., Goto, S., Kawashima, S., Okuno, Y., and Hattori, M. (2004) The KEGG resource for deciphering the genome. *Nucleic Acids Research* **32**: D277-D280.

Kanukollu, S., Voget, S., Pohlner, M., Vandieken, V., Petersen, J., Kyrpides, N.C. et al. (2016) Genome sequence of *Shimia* str. SK013, a representative of the *Roseobacter* group isolated from marine sediment. *Standards in Genomic Sciences* **11**: 25.

Karimi, E., Keller-Costa, T., Slaby, B.M., Cox, C.J., da Rocha, U.N., Hentschel, U., and Costa, R. (2019) Genomic blueprints of sponge-prokaryote symbiosis are shared by low abundant and cultivatable Alphaproteobacteria. *Scientific Reports* **9**: 1999.

Karsten, U., Kirst, G.O., and Wiencke, C. (1992) Dimethylsulphoniopropionate (DMSP) accumulation in green macioalgae from polar to temperate regions: interactive effects of light versus salinity and light versus temperature. *Polar Biology* **12**: 603-607.

Karsten, U., Kück, K., Vogt, C., and Kirst, G.O. (1996) Dimethylsulfoniopropionate Production in Phototrophic Organisms and its Physiological Functions as a Cryoprotectant. In *Biological and Environmental Chemistry of DMSP and Related Sulfonium Compounds*. Kiene, R.P., Visscher, P.T., Keller, M.D., and Kirst, G.O. (eds). Boston, MA: Springer US, pp. 143-153.

Katoh, K., and Standley, D.M. (2013) MAFFT Multiple Sequence Alignment Software Version 7: Improvements in Performance and Usability. *Molecular Biology and Evolution* **30**: 772-780.

Katoh, K., Misawa, K., Kuma, K.i., and Miyata, T. (2002) MAFFT: a novel method for rapid multiple sequence alignment based on fast Fourier transform. *Nucleic Acids Research* **30**: 3059-3066.

Keller, M.D., Bellows, W.K., and Guillard, R.R.L. (1989) Dimethyl Sulfide Production in Marine Phytoplankton. In *Biogenic Sulfur in the Environment*: American Chemical Society, pp. 167-182.

Kellock, C., Cole, C., Penkman, K., Evans, D., Kröger, R., Hintz, C. et al. (2020) The role of aspartic acid in reducing coral calcification under ocean acidification conditions. *Scientific Reports* **10**: 12797.

Kerrison, P., Suggett, D.J., Hepburn, L.J., and Steinke, M. (2012) Effect of elevated pCO2 on the production of dimethylsulphoniopropionate (DMSP) and dimethylsulphide (DMS) in two species of Ulva (Chlorophyceae). *Biogeochemistry* **110**: 5-16.

Kettle, A.J., and Andreae, M.O. (2000) Flux of dimethylsulfide from the oceans: A comparison of updated data sets and flux models. *Journal of Geophysical Research: Atmospheres* **105**: 26793-26808.

Kettle, A.J., Andreae, M.O., Amouroux, D., Andreae, T.W., Bates, T.S., Berresheim, H. et al. (1999) A global database of sea surface dimethylsulfide (DMS) measurements and a procedure to predict sea surface DMS as a function of latitude, longitude, and month. *Global Biogeochemical Cycles* **13**: 399-444.

Kettles, N.L., Kopriva, S., and Malin, G. (2014) Insights into the Regulation of DMSP Synthesis in the Diatom <italic>Thalassiosira pseudonana</italic> through APR Activity, Proteomics and Gene Expression Analyses on Cells Acclimating to Changes in Salinity, Light and Nitrogen. *PLOS ONE* **9**: e94795.

Kiene, R.P. (1996) Turnover of Dissolved DMSP in Estuarine and Shelf Waters of the Northern Gulf of Mexico. In *Biological and Environmental Chemistry of DMSP and Related Sulfonium Compounds*. Kiene, R.P., Visscher, P.T., Keller, M.D., and Kirst, G.O. (eds). Boston, MA: Springer US, pp. 337-349.

Kiene, R.P., and Linn, L.J. (2000) The fate of dissolved dimethylsulfoniopropionate (DMSP) in seawater: tracer studies using 35S-DMSP. *Geochimica et Cosmochimica Acta* **64**: 2797-2810.

Kiene, R.P., Linn, L.J., and Bruton, J.A. (2000) New and important roles for DMSP in marine microbial communities. *Journal of Sea Research* **43**: 209-224.

Kiene, R.P., Linn, L.J., González, J., Moran, M.A., and Bruton, J.A. (1999) Dimethylsulfoniopropionate and Methanethiol Are Important Precursors of Methionine and Protein-Sulfur in Marine Bacterioplankton. *Applied and Environmental Microbiology* **65**: 4549-4558.

Kingsford, C., Schatz, M.C., and Pop, M. (2010) Assembly complexity of prokaryotic genomes using short reads. *BMC Bioinformatics* **11**: 21.

Kirchman, D.L. (2010) *Microbial ecology of the oceans*: John Wiley & Sons.

Kirst, G.O. (1996) Osmotic Adjustment in Phytoplankton and MacroAlgae. In *Biological and Environmental Chemistry of DMSP and Related Sulfonium Compounds*. Kiene, R.P., Visscher, P.T., Keller, M.D., and Kirst, G.O. (eds). Boston, MA: Springer US, pp. 121-129.

Kirst, G.O., Thiel, C., Wolff, H., Nothnagel, J., Wanzek, M., and Ulmke, R. (1991) Dimethylsulfoniopropionate (DMSP) in icealgae and its possible biological role. *Marine Chemistry* **35**: 381-388.

Kocsis, M.G., and Hanson, A.D. (2000) Biochemical Evidence for Two Novel Enzymes in the Biosynthesis of 3-Dimethylsulfoniopropionate in *Spartina alterniflora*. *Plant Physiology* **123**: 1153-1162.

Kocsis, M.G., Nolte, K.D., Rhodes, D., Shen, T.-L., Gage, D.A., and Hanson, A.D. (1998) Dimethylsulfoniopropionate Biosynthesis in *Spartina alterniflora*[1]. *Plant Physiology* **117**: 273-281.

Kooperman, N., Ben-Dov, E., Kramarsky-Winter, E., Barak, Z., and Kushmaro, A. (2007) Coral mucus-associated bacterial communities from natural and aquarium environments. *FEMS Microbiology Letters* **276**: 106-113.

Koren, O., and Rosenberg, E. (2006) Bacteria Associated with Mucus and Tissues of the Coral Oculina patagonica in Summer and Winter. *Applied and Environmental Microbiology* **72**: 5254-5259.

Koren, S., Walenz, B.P., Berlin, K., Miller, J.R., Bergman, N.H., and Phillippy, A.M. (2017) Canu: scalable and accurate long-read assembly via adaptive k-mer weighting and repeat separation. *Genome Research* **27**: 722-736.

Koren, S., Harhay, G.P., Smith, T.P.L., Bono, J.L., Harhay, D.M., McVey, S.D. et al. (2013) Reducing assembly complexity of microbial genomes with single-molecule sequencing. *Genome Biology* **14**: R101.

Kredich, N.M. (1971) Regulation of l-Cysteine Biosynthesis in *Salmonella typhimurium* : I. Effects of Growth on Varying Sulfur Sources and O-Acetyl-I-Serine on Gene Expression. *Journal of Biological Chemistry* **246**: 3474-3484.

Kurm, V., van der Putten, W.H., and Hol, W.H.G. (2019) Cultivation-success of rare soil bacteria is not influenced by incubation time and growth medium. *PLOS ONE* **14**: e0210073.

LaJeunesse, T.C., Parkinson, J.E., Gabrielson, P.W., Jeong, H.J., Reimer, J.D., Voolstra, C.R., and Santos, S.R. (2018) Systematic Revision of Symbiodiniaceae Highlights the Antiquity and Diversity of Coral Endosymbionts. *Current Biology*.

Lana, A., Bell, T.G., Simó, R., Vallina, S.M., Ballabrera-Poy, J., Kettle, A.J. et al. (2011) An updated climatology of surface dimethlysulfide concentrations and emission fluxes in the global ocean. *Global Biogeochemical Cycles* **25**: GB1004.

Lane, D. (1991) 16S/23S rRNA sequencing. In *Nucleic Acid Techniques in Bacterial Systematics*. Stackebrandt, E., and Goodfellow, M. (eds). New York, NY, USA: John Wiley & Sons, pp. 115–175.

Langdon, C., and Atkinson, M.J. (2005) Effect of elevated pCO_2 on photosynthesis and calcification of corals and interactions with seasonal change in temperature/irradiance and nutrient enrichment. *Journal of Geophysical Research: Oceans* **110**.

Langdon, C., Broecker, W.S., Hammond, D.E., Glenn, E., Fitzsimmons, K., Nelson, S.G. et al. (2003) Effect of elevated CO_2 on the community metabolism of an experimental coral reef. *Global Biogeochemical Cycles* **17**.

Lauro, F.M., McDougald, D., Thomas, T., Williams, T.J., Egan, S., Rice, S. et al. (2009) The genomic basis of trophic strategy in marine bacteria. *Proceedings of the National Academy of Sciences* **106**: 15527-15533.

Laver, T., Harrison, J., O'Neill, P.A., Moore, K., Farbos, A., Paszkiewicz, K., and Studholme, D.J. (2015) Assessing the performance of the Oxford Nanopore Technologies MinION. *Biomolecular Detection and Quantification* **3**: 1-8.

Laverick, J.H., Green, T.K., Burdett, H.L., Newton, J., and Rogers, A.D. (2019) Depth alone is an inappropriate proxy for physiological change in the mesophotic coral *Agaricia lamarcki*. *Journal of the Marine Biological Association of the United Kingdom* **99**: 1535-1546.

Lema, K.A., Willis, B.L., and Bourne, D.G. (2014) Amplicon pyrosequencing reveals spatial and temporal consistency in diazotroph assemblages of the *Acropora millepora* microbiome. *Environmental Microbiology* **16**: 3345-3359.

Lema, K.A., Clode, P.L., Kilburn, M.R., Thornton, R., Willis, B.L., and Bourne, D.G. (2016) Imaging the uptake of nitrogen-fixing bacteria into larvae of the coral *Acropora millepora*. *The ISME Journal* **10**: 1804-1808.

Lenk, S., Moraru, C., Hahnke, S., Arnds, J., Richter, M., Kube, M. et al. (2012) *Roseobacter* clade bacteria are abundant in coastal sediments and encode a novel combination of sulfur oxidation genes. *The ISME Journal* **6**: 2178-2187.

Levine, N.M., Varaljay, V.A., Toole, D.A., Dacey, J.W.H., Doney, S.C., and Moran, M.A. (2012) Environmental, biochemical and genetic drivers of DMSP degradation and DMS production in the Sargasso Sea. *Environmental Microbiology* **14**: 1210-1223.

Li, C.-Y., Wei, T.-D., Zhang, S.-H., Chen, X.-L., Gao, X., Wang, P. et al. (2014) Molecular insight into bacterial cleavage of oceanic dimethylsulfoniopropionate into dimethyl sulfide. *Proceedings of the National Academy of Sciences* **111**: 1026-1031.

Li, H. (2018) Minimap2: pairwise alignment for nucleotide sequences. *Bioinformatics* **34**: 3094-3100.

Li, J., Kuang, W., Long, L., and Zhang, S. (2017) Production of quorum-sensing signals by bacteria in the coral mucus layer. *Coral Reefs* **36**: 1235-1241.

Liu, J., Liu, J., Zhang, S.-H., Liang, J., Lin, H., Song, D. et al. (2018) Novel Insights Into Bacterial Dimethylsulfoniopropionate Catabolism in the East China Sea. *Frontiers in Microbiology* **9**.

Lloyd, A.T., and Sharp, P.M. (1993) Evolution of the recA gene and the molecular phylogeny of bacteria. *Journal of Molecular Evolution* **37**: 399-407.

Lovelock, J.E., Maggs, R.J., and Rasmussen, R.A. (1972) Atmospheric Dimethyl Sulphide and the Natural Sulphur Cycle. *Nature* **237**: 452-453.

Lowenstam, H.A. (1981) Minerals formed by organisms. *Science* **211**: 1126.

Lowenstam, H.A., and Weiner, S. (1989) *On Biomineralization*: Oxford University Press.

Lu, H., Giordano, F., and Ning, Z. (2016) Oxford Nanopore MinION Sequencing and Genome Assembly. *Genomics, Proteomics & Bioinformatics* **14**: 265-279.

Lu, S., Wang, J., Chitsaz, F., Derbyshire, M.K., Geer, R.C., Gonzales, N.R. et al. (2019) CDD/SPARCLE: the conserved domain database in 2020. *Nucleic Acids Research* **48**: D265-D268.

Luo, H., and Moran, M.A. (2014) Evolutionary Ecology of the Marine *Roseobacter* Clade. *Microbiology and Molecular Biology Reviews* **78**: 573-587.

Lyon, B.R., Lee, P.A., Bennett, J.M., DiTullio, G.R., and Janech, M.G. (2011) Proteomic Analysis of a Sea-Ice Diatom: Salinity Acclimation Provides New Insight into the Dimethylsulfoniopropionate Production Pathway. *Plant Physiology* **157**: 1926-1941.

Malin, G., and Erst, G.O. (1997) Algal Production of Dimethyl Sulfide and its Atmospheric Role. *Journal of Phycology* **33**: 889-896.

Malin, G., Turner, S.M., and Liss, P.S. (1992) Sulfur: The Plankton/Climate Connection. *Journal of Phycology* **28**: 590-597.

Malmstrom, R.R., Kiene, R.P., and Kirchman, D.L. (2004) Identification and enumeration of bacteria assimilating dimethylsulfoniopropionate (DMSP) in the North Atlantic and Gulf of Mexico. *Limnology and Oceanography* **49**: 597-606.

Maneveldt, G.W., and Keats, D.W. (2014) Taxonomic review based on new data of the reef-building alga Porolithon onkodes (Corallinaceae, Corallinales, Rhodophyta) along with other taxa found to be conspecific. *Phytotaxa* **190**: 216-249.

Mann, S. (1983) Mineralization in biological systems. In *Inorganic Elements in Biochemistry*. Connett, P.H., Folłmann, H., Lammers, M., Mann, S., Odom, J.D., and Wetterhahn, K.E. (eds). Berlin, Heidelberg: Springer Berlin Heidelberg, pp. 125-174.

Marchler-Bauer, A., and Bryant, S.H. (2004) CD-Search: protein domain annotations on the fly. *Nucleic Acids Research* **32**: W327-W331.

Marchler-Bauer, A., Derbyshire, M.K., Gonzales, N.R., Lu, S., Chitsaz, F., Geer, L.Y. et al. (2014) CDD: NCBI's conserved domain database. *Nucleic Acids Research* **43**: D222-D226.

Marchler-Bauer, A., Lu, S., Anderson, J.B., Chitsaz, F., Derbyshire, M.K., DeWeese-Scott, C. et al. (2010) CDD: a Conserved Domain Database for the functional annotation of proteins. *Nucleic Acids Research* **39**: D225-D229.

Marhaver, K.L., Edwards, R.A., and Rohwer, F. (2008) Viral communities associated with healthy and bleaching corals. *Environmental Microbiology* **10**: 2277-2286.

Marie, D., Partensky, F., Jacquet, S., and Vaulot, D. (1997) Enumeration and Cell Cycle Analysis of Natural Populations of Marine Picoplankton by Flow Cytometry Using the Nucleic Acid Stain SYBR Green I. *Applied and Environmental Microbiology* **63**: 186-193.

Marubini, F., Ferrier-Pagès, C., Furla, P., and Allemand, D. (2008) Coral calcification responds to seawater acidification: a working hypothesis towards a physiological mechanism. *Coral Reefs* **27**: 491-499.

Mass, T., Drake, Jeana L., Haramaty, L., Kim, J.D., Zelzion, E., Bhattacharya, D., and Falkowski, Paul G. (2013) Cloning and Characterization of Four Novel Coral Acid-Rich Proteins that Precipitate Carbonates In Vitro. *Current Biology* **23**: 1126-1131.

Matrai, P.A., and Keller, M.D. (1994) Total organic sulfur and dimethylsulfoniopropionate in marine phytoplankton: intracellular variations. *Marine Biology* **119**: 61-68.

McCloskey, L.R., Muscatine, L., and Smith, D.C. (1984) Production and respiration in the Red Sea coral *Stylophora pistillata* as a function of depth. *Proceedings of the Royal Society of London Series B Biological Sciences* **222**: 215-230.

McGillis, W.R., Dacey, J.W.H., Frew, N.M., Bock, E.J., and Nelson, R.K. (2000) Water-air flux of dimethylsulfide. *Journal of Geophysical Research: Oceans* **105**: 1187-1193.

McParland, E.L., and Levine, N.M. (2019) The role of differential DMSP production and community composition in predicting variability of global surface DMSP concentrations. *Limnology and Oceanography* **64**: 757-773.

McParland, E.L., Lee, M.D., Webb, E., Alexander, H., and Levine, N.M. (2021) DMSP synthesis genes distinguish two types of DMSP producer phenotypes. *Environmental Microbiology* **23**.

Meskhidze, N., and Nenes, A. (2006) Phytoplankton and Cloudiness in the Southern Ocean. *Science* **314**: 1419-1423.

Michael, K.J., Veal, C.J., and Nunez, M. (2012) Attenuation coefficients of ultraviolet and photosynthetically active wavelengths in the waters of Heron Reef, Great Barrier Reef, Australia. *Marine and Freshwater Research* **63**: 142-149.

Michenfelder, M., Fu, G., Lawrence, C., Weaver, J.C., Wustman, B.A., Taranto, L. et al. (2003) Characterization of two molluscan crystal-modulating biomineralization proteins and identification of putative mineral binding domains. *Biopolymers* **70**: 522-533.

Midani, F.S., Wynn, M.L., and Schnell, S. (2017) The importance of accurately correcting for the natural abundance of stable isotopes. *Analytical Biochemistry* **520**: 27-43.

Mikoulinskaia, O., Akimenko, V., Galouchko, A., Thauer, R.K., and Hedderich, R. (1999) Cytochrome c-dependent methacrylate reductase from Geobacter sulfurreducens AM-1. *European Journal of Biochemistry* **263**: 346-352.

Miller, R.V., and Kokjohn, T.A. (1990) General Microbiology of *recA*: Environmental and Evolutionary Significance. *Annual Review of Microbiology* **44**: 365-394.

Miller, T.R., and Belas, R. (2004) Dimethylsulfoniopropionate Metabolism by *Pfiesteria*-Associated *Roseobacter* spp. *Applied and Environmental Microbiology* **70**: 3383-3391.

Minh, B.Q., Nguyen, M.A.T., and von Haeseler, A. (2013) Ultrafast Approximation for Phylogenetic Bootstrap. *Molecular Biology and Evolution* **30**: 1188-1195.

Mitterer, R.M. (1978) Amino Acid Composition and Metal Binding Capability of the Skeletal Protein of Corals. *Bulletin of Marine Science* **28**: 173-180.

Moberg, F., and Folke, C. (1999) Ecological goods and services of coral reef ecosystems. *Ecological Economics* **29**: 215-233.

Mollica, N.R., Guo, W., Cohen, A.L., Huang, K.-F., Foster, G.L., Donald, H.K., and Solow, A.R. (2018) Ocean acidification affects coral growth by reducing skeletal density. *Proceedings of the National Academy of Sciences* **115**: 1754-1759.

Montesino, M., Salas, A., Crespillo, M., Albarrán, C., Alonso, A., Álvarez-Iglesias, V. et al. (2007) Analysis of body fluid mixtures by mtDNA sequencing: An inter-laboratory study of the GEP-ISFG working group. *Forensic Science International* **168**: 42-56.

Moran, M.A., Reisch, C.R., Kiene, R.P., and Whitman, W.B. (2012) Genomic Insights into Bacterial DMSP Transformations. *Annual Review of Marine Science* **4**: 523-542.

Moran, M.A., Buchan, A., Gonzalez, J.M., Heidelberg, J.F., Whitman, W.B., Kiene, R.P. et al. (2004) Genome sequence of Silicibacter pomeroyi reveals adaptations to the marine environment. *Nature* **432**: 910-913.

Moraru, C., Lam, P., Fuchs, B.M., Kuypers, M.M.M., and Amann, R. (2010) GeneFISH – an in situ technique for linking gene presence and cell identity in environmental microorganisms. *Environmental Microbiology* **12**: 3057-3073.

Mouchka, M.E., Hewson, I., and Harvell, C.D. (2010) Coral-Associated Bacterial Assemblages: Current Knowledge and the Potential for Climate-Driven Impacts. *Integrative and Comparative Biology* **50**: 662-674.

Moya, A., Huisman, L., Ball, E.E., Hayward, D.C., Grasso, L.C., Chua, C.M. et al. (2012) Whole Transcriptome Analysis of the Coral *Acropora millepora* Reveals Complex Responses to CO_2-driven Acidification during the Initiation of Calcification. *Molecular Ecology* **21**: 2440-2454.

Muscatine, L., and Porter, J.W. (1977) Reef Corals: Mutualistic Symbioses Adapted to Nutrient-Poor Environments. *BioScience* **27**: 454-460.

Naggi, A., Torri, G., Iacomini, M., Colombo Castelli, G., Reggi, M., Fermani, S. et al. (2018) Structure and Function of Stony Coral Intraskeletal Polysaccharides. *ACS Omega* **3**: 2895-2901.

Neal-McKinney, J.M., Liu, K.C., Lock, C.M., Wu, W.-H., and Hu, J. (2021) Comparison of MiSeq, MinION, and hybrid genome sequencing for analysis of Campylobacter jejuni. *Scientific Reports* **11**: 5676.

Neave, M.J., Rachmawati, R., Xun, L., Michell, C.T., Bourne, D.G., Apprill, A., and Voolstra, C.R. (2017) Differential specificity between closely related corals and abundant Endozoicomonas endosymbionts across global scales. *The ISME Journal* **11**: 186-200.

Needleman, S.B., and Wunsch, C.D. (1970) A general method applicable to the search for similarities in the amino acid sequence of two proteins. *Journal of Molecular Biology* **48**.

Nguyen-Kim, H., Bouvier, T., Bouvier, C., Doan-Nhu, H., Nguyen-Ngoc, L., Rochelle-Newall, E. et al. (2014) High occurrence of viruses in the mucus layer of scleractinian corals. *Environmental Microbiology Reports* **6**: 675-682.

Nguyen, L.-T., Schmidt, H.A., von Haeseler, A., and Minh, B.Q. (2014) IQ-TREE: A Fast and Effective Stochastic Algorithm for Estimating Maximum-Likelihood Phylogenies. *Molecular Biology and Evolution* **32**: 268-274.

Ni, M., and Ratner, B.D. (2008) Differentiating calcium carbonate polymorphs by surface analysis techniques—an XPS and TOF-SIMS study. *Surface and Interface Analysis* **40**: 1356-1361.

Noordkamp, D.J.B., Gieskes, W.W.C., Gottschal, J.C., Forney, L.J., and van Rijssel, M. (2000) Acrylate in *Phaeocystis* colonies does not affect the surrounding bacteria. *Journal of Sea Research* **43**: 287-296.

Nordborg, F.M., Flores, F., Brinkman, D.L., Agustí, S., and Negri, A.P. (2018) Phototoxic effects of two common marine fuels on the settlement success of the coral *Acropora tenuis*. *Scientific Reports* **8**: 8635.

Notredame, C., Higgins, D.G., and Heringa, J. (2000) T-coffee: a novel method for fast and accurate multiple sequence alignment. *Journal of Molecular Biology* **302**: 205-217.

Nudelman, F., Lausch, A.J., Sommerdijk, N.A.J.M., and Sone, E.D. (2013) In vitro models of collagen biomineralization. *Journal of Structural Biology* **183**: 258-269.

Nygaard, A.B., Tunsjø, H.S., Meisal, R., and Charnock, C. (2020) A preliminary study on the potential of Nanopore MinION and Illumina MiSeq 16S rRNA gene sequencing to characterize building-dust microbiomes. *Scientific Reports* **10**: 3209.

Ochman, H., Lawrence, J.G., and Groisman, E.A. (2000) Lateral gene transfer and the nature of bacterial innovation. *Nature* **405**: 299-304.

Oduro, H., Kamyshny, A., Guo, W., and Farquhar, J. (2011) Multiple sulfur isotope analysis of volatile organic sulfur compounds and their sulfonium precursors in coastal marine environments. *Marine Chemistry* **124**: 78-89.

Ohbayashi, T., Futahashi, R., Terashima, M., Barrière, Q., Lamouche, F., Takeshita, K. et al. (2019) Comparative cytology, physiology and transcriptomics of *Burkholderia insecticola* in symbiosis with the bean bug *Riptortus pedestris* and in culture. *The ISME Journal* **13**: 1469-1483.

Okada, K., Iida, T., Kita-Tsukamoto, K., and Honda, T. (2005) Vibrios Commonly Possess Two Chromosomes. *Journal of Bacteriology* **187**: 752-757.

Orr, J.C., Fabry, V.J., Aumont, O., Bopp, L., Doney, S.C., Feely, R.A. et al. (2005) Anthropogenic ocean acidification over the twenty-first century and its impact on calcifying organisms. *Nature* **437**: 681-686.

Osman, E.O., Suggett, D.J., Voolstra, C.R., Pettay, D.T., Clark, D.R., Pogoreutz, C. et al. (2020) Coral microbiome composition along the northern Red Sea suggests high plasticity of bacterial and specificity of endosymbiotic dinoflagellate communities. *Microbiome* **8**: 8.

Ostrander, G.K., Armstrong, K.M., Knobbe, E.T., Gerace, D., and Scully, E.P. (2000) Rapid transition in the structure of a coral reef community: The effects of coral bleaching and physical disturbance. *Proceedings of the National Academy of Sciences* **97**: 5297-5302.

Ozawa, H., Hoshi, K., and Amizuka, N. (2008) Current Concepts of Bone Biomineralization. *Journal of Oral Biosciences* **50**: 1-14.

Pendleton, L.H. (1995) Valuing coral reef protection. *Ocean & Coastal Management* **26**: 119-131.

Pernice, M., Raina, J.-B., Rädecker, N., Cárdenas, A., Pogoreutz, C., and Voolstra, C.R. (2020) Down to the bone: the role of overlooked endolithic microbiomes in reef coral health. *The ISME Journal* **14**: 325-334.

Pernice, M., Meibom, A., Van Den Heuvel, A., Kopp, C., Domart-Coulon, I., Hoegh-Guldberg, O., and Dove, S. (2012) A single-cell view of ammonium assimilation in coral–dinoflagellate symbiosis. *The ISME Journal* **6**: 1314-1324.

Pollich, M., and Klug, G. (1995) Identification and sequence analysis of genes involved in late steps in cobalamin (vitamin B12) synthesis in Rhodobacter capsulatus. *Journal of Bacteriology* **177**: 4481-4487.

Pollock, F.J., McMinds, R., Smith, S., Bourne, D.G., Willis, B.L., Medina, M. et al. (2018) Coral-associated bacteria demonstrate phylosymbiosis and cophylogeny. *Nature Communications* **9**: 4921.

Pollock, F.J., Katz, S.M., van de Water, J.A.J.M., Davies, S.W., Hein, M., Torda, G. et al. (2017) Coral larvae for restoration and research: a large-scale method for rearing Acropora millepora larvae, inducing settlement, and establishing symbiosis. *PeerJ* **5**: e3732.

Pomeroy, L.R., and Wiebe, W.J. (2001) Temperature and substrates as interactive limiting factors for marine heterotrophic bacteria. *Aquatic Microbial Ecology* **23**: 187-204.

Pop, M. (2009) Genome assembly reborn: recent computational challenges. *Briefings in Bioinformatics* **10**: 354-366.

Postolache, C., and Matei, L. (2007) Synthesis of [α-T]polyacrylic acid. *Journal of Labelled Compounds and Radiopharmaceuticals* **50**: 444-445.

Pratte, Z.A., Richardson, L.L., and Mills, D.K. (2015) Microbiota shifts in the surface mucopolysaccharide layer of corals transferred from natural to aquaria settings. *Journal of Invertebrate Pathology* **125**: 42-44.

Puverel, S., Houlbrèque, F., Tambutté, E., Zoccola, D., Payan, P., Caminiti, N. et al. (2007) Evidence of low molecular weight components in the organic matrix of the reef building coral, *Stylophora pistillata*. *Comparative Biochemistry and Physiology Part A: Molecular & Integrative Physiology* **147**: 850-856.

Quick, J., Quinlan, A.R., and Loman, N.J. (2014) A reference bacterial genome dataset generated on the MinION™ portable single-molecule nanopore sequencer. *GigaScience* **3**.

R Core Team (2020) R: A language and environment for statistical computing. In. Vienna, Austria: R Foundation for Statistical Computing.

Rädecker, N., Pogoreutz, C., Gegner, H.M., Cárdenas, A., Roth, F., Bougoure, J. et al. (2021) Heat stress destabilizes symbiotic nutrient cycling in corals. *Proceedings of the National Academy of Sciences* **118**: e2022653118.

Rahman, M.A., and Oomori, T. (2008) Aspartic Acid-rich Proteins in Insoluble Organic Matrix Play a Key Role in the Growth of Calcitic Sclerites in Alcyonarian Coral. *Chinese Journal of Biotechnology* **24**: 2127-2128.

Raina, J.-B., Tapiolas, D., Willis, B.L., and Bourne, D.G. (2009) Coral-Associated Bacteria and Their Role in the Biogeochemical Cycling of Sulfur. *Applied and Environmental Microbiology* **75**: 3492-3501.

Raina, J.-B., Dinsdale, E.A., Willis, B.L., and Bourne, D.G. (2010) Do the organic sulfur compounds DMSP and DMS drive coral microbial associations? *Trends in Microbiology* **18**: 101-108.

Raina, J.-B., Tapiolas, D., Motti, C.A., Foret, S., Seemann, T., Tebben, J. et al. (2016) Isolation of an antimicrobial compound produced by bacteria associated with reef-building corals. *PeerJ* **4**: e2275.

Raina, J.-B., Tapiolas, D.M., Foret, S., Lutz, A., Abrego, D., Ceh, J. et al. (2013) DMSP biosynthesis by an animal and its role in coral thermal stress response. *Nature* **502**: 677-680.

Raina, J.B., Clode, P.L., Cheong, S., Bougoure, J., Kilburn, M.R., Reeder, A. et al. (2017) Subcellular tracking reveals the location of dimethylsulfoniopropionate in microalgae and visualises its uptake by marine bacteria. *Elife* **6**: 17.

Ramos-Silva, P., Kaandorp, J., Herbst, F., Plasseraud, L., Alcaraz, G., Stern, C. et al. (2014) The skeleton of the staghorn coral *Acropora millepora*: molecular and structural characterization. *PLOS ONE* **9**: e97454-e97454.

Rappé, M.S., and Giovannoni, S.J. (2003) The Uncultured Microbial Majority. *Annual Review of Microbiology* **57**: 369-394.

Ravanel, S., Gakière, B., Job, D., and Douce, R. (1998) The specific features of methionine biosynthesis and metabolism in plants. *Proceedings of the National Academy of Sciences* **95**: 7805-7812.

Reggi, M., Fermani, S., Samorì, C., Gizzi, F., Prada, F., Dubinsky, Z. et al. (2016) Influence of intra-skeletal coral lipids on calcium carbonate precipitation. *CrystEngComm* **18**: 8829-8833.

Reggi, M., Fermani, S., Landi, V., Sparla, F., Caroselli, E., Gizzi, F. et al. (2014) Biomineralization in Mediterranean Corals: The Role of the Intraskeletal Organic Matrix. *Crystal Growth & Design* **14**: 4310-4320.

Reisch, C.R., Moran, M.A., and Whitman, W.B. (2008) Dimethylsulfoniopropionate-Dependent Demethylase (DmdA) from Pelagibacter ubique and Silicibacter pomeroyi. *Journal of Bacteriology* **190**: 8018-8024.

Reisch, C.R., Moran, M.A., and Whitman, W.B. (2011a) Bacterial Catabolism of Dimethylsulfoniopropionate. *Frontiers in Microbiology* **2**.

Reisch, C.R., Stoudemayer, M.J., Varaljay, V.A., Amster, I.J., Moran, M.A., and Whitman, W.B. (2011b) Novel pathway for assimilation of dimethylsulphoniopropionate widespread in marine bacteria. *Nature* **473**: 208-211.

Reisch, C.R., Crabb, W.M., Gifford, S.M., Teng, Q., Stoudemayer, M.J., Moran, M.A., and Whitman, W.B. (2013) Metabolism of dimethylsulphoniopropionate by Ruegeria pomeroyi DSS-3. *Molecular Microbiology* **89**: 774-791.

Reshef, L., Koren, O., Loya, Y., Zilber-Rosenberg, I., and Rosenberg, E. (2006) The Coral Probiotic Hypothesis. *Environmental Microbiology* **8**: 2068-2073.

Rhodes, D., Gage, D.A., Cooper, A., and Hanson, A.D. (1997) S-Methylmethionine Conversion to Dimethylsulfoniopropionate: Evidence for an Unusual Transamination Reaction. *Plant Physiology* **115**: 1541-1548.

Ries, J.B. (2011) A physicochemical framework for interpreting the biological calcification response to CO2-induced ocean acidification. *Geochimica et Cosmochimica Acta* **75**: 4053-4064.

Risse, J., Thomson, M., Patrick, S., Blakely, G., Koutsovoulos, G., Blaxter, M., and Watson, M. (2015) A single chromosome assembly of Bacteroides fragilis strain BE1 from Illumina and MinION nanopore sequencing data. *GigaScience* **4**.

Ritchie, K.B. (2006) Regulation of microbial populations by coral surface mucus and mucus-associated bacteria. *Marine Ecology Progress Series* **322**: 1-14.

Ritchie, K.B., and Smith, G.W. (2004) Microbial Communities of Coral Surface Mucopolysaccharide Layers. In *Coral Health and Disease*. Rosenberg, E., and Loya, Y. (eds). Berlin, Heidelberg: Springer Berlin Heidelberg, pp. 259-264.

Robbins, S.J., Singleton, C.M., Chan, C.X., Messer, L.F., Geers, A.U., Ying, H. et al. (2019) A genomic view of the reef-building coral *Porites lutea* and its microbial symbionts. *Nature Microbiology* **4**: 2090-2100.

Roder, C., Bayer, T., Aranda, M., Kruse, M., and Voolstra, C.R. (2015) Microbiome structure of the fungid coral *Ctenactis echinata* aligns with environmental differences. *Molecular Ecology* **24**: 3501-3511.

Rodionov, D.A., Vitreschak, A.G., Mironov, A.A., and Gelfand, M.S. (2003) Comparative Genomics of the Vitamin B_{12} Metabolism and Regulation in Prokaryotes. *Journal of Biological Chemistry* **278**: 41148-41159.

Rohwer, F., Seguritan, V., Azam, F., and Knowlton, N. (2002) Diversity and distribution of coral-associated bacteria. *Marine Ecology Progress Series* **243**: 1-10.

Rosenberg, E., Koren, O., Reshef, L., Efrony, R., and Zilber-Rosenberg, I. (2007) The role of microorganisms in coral health, disease and evolution. *Nature Reviews Microbiology* **5**: 355-362.

Rozenblat, Y.B.-H., and Rosenberg, E. (2004) Temperature-Regulated Bleaching and Tissue Lysis of *Pocillopora damicornis* by the Novel Pathogen *Vibrio coralliilyticus*. In *Coral Health and Disease*. Rosenberg, E., and Loya, Y. (eds). Berlin, Heidelberg: Springer Berlin Heidelberg, pp. 301-324.

RStudio Team (2015) RStudio: Integrated Development for R. In. Boston, MA: RStudio, Inc.

Rusch, D.B., Halpern, A.L., Sutton, G., Heidelberg, K.B., Williamson, S., Yooseph, S. et al. (2007) The Sorcerer II Global Ocean Sampling Expedition: Northwest Atlantic through Eastern Tropical Pacific. *PLOS Biology* **5**: e77.

Salgado, P., Kiene, R., Wiebe, W., and Magalhães, C. (2014) Salinity as a regulator of DMSP degradation in Ruegeria pomeroyi DSS-3. *Journal of Microbiology* **52**: 948-954.

Sancho-Tomás, M., Fermani, S., Goffredo, S., Dubinsky, Z., García-Ruiz, J.M., Gómez-Morales, J., and Falini, G. (2014) Exploring coral biomineralization in gelling environments by means of a counter diffusion system. *CrystEngComm* **16**: 1257-1267.

Santos, A.L., Oliveira, V., Baptista, I., Henriques, I., Gomes, N.C.M., Almeida, A. et al. (2013) Wavelength dependence of biological damage induced by UV radiation on bacteria. *Archives of Microbiology* **195**: 63-74.

Schoepf, V., Stat, M., Falter, J.L., and McCulloch, M.T. (2015) Limits to the thermal tolerance of corals adapted to a highly fluctuating, naturally extreme temperature environment. *Scientific Reports* **5**: 17639.

Schöttner, S., Hoffmann, F., Wild, C., Rapp, H.T., Boetius, A., and Ramette, A. (2009) Inter- and intra-habitat bacterial diversity associated with cold-water corals. *The ISME Journal* **3**: 756-759.

Schwarz, G. (1978) Estimating the dimension of a model. *Annals of Statistics* **6**: 461-464.

Seemann, T. (2014) Prokka: rapid prokaryotic genome annotation. *Bioinformatics* **30**: 2068-2069.

Sekowska, A., Kung, H.-F., and Danchin, A. (2000) Sulfur metabolism in *Escherichia coli* and related bacteria: facts and fiction. *Journal of Molecular Microbiology and Biotechnology* **2**: 145-177.

Senechkin, I.V., Speksnijder, A.G.C.L., Semenov, A.M., van Bruggen, A.H.C., and van Overbeek, L.S. (2010) Isolation and Partial Characterization of Bacterial Strains on Low Organic Carbon Medium from Soils Fertilized with Different Organic Amendments. *Microbial Ecology* **60**: 829-839.

Séré, M., Wilkinson, D.A., Schleyer, M.H., Chabanet, P., Quod, J.-P., and Tortosa, P. (2016) Characterisation of an atypical manifestation of black band disease on *Porites lutea* in the Western Indian Ocean. *PeerJ* **4**: e2073.

Séré, M.G., Tortosa, P., Chabanet, P., Turquet, J., Quod, J.-P., and Schleyer, M.H. (2014) Bacterial Communities Associated with *Porites* White Patch Syndrome (PWPS) on Three Western Indian Ocean (WIO) Coral Reefs. *PLOS ONE* **8**: e83746.

Sevilgen, D.S., Venn, A.A., Hu, M.Y., Tambutté, E., de Beer, D., Planas-Bielsa, V., and Tambutté, S. (2019) Full in vivo characterization of carbonate chemistry at the site of calcification in corals. *Science Advances* **5**: eaau7447.

Seymour, J.R., Simó, R., Ahmed, T., and Stocker, R. (2010) Chemoattraction to Dimethylsulfoniopropionate Throughout the Marine Microbial Food Web. *Science* **329**: 342-345.

Sharp, K.H., Sneed, J.M., Ritchie, K.B., McDaniel, L., and Paul, V.J. (2015) Induction of Larval Settlement in the Reef Coral *Porites astreoides* by a Cultivated Marine *Roseobacter* Strain. *The Biological Bulletin* **228**: 98-107.

Shinzato, C., Khalturin, K., Inoue, J., Zayasu, Y., Kanda, M., Kawamitsu, M. et al. (2020) Eighteen coral genomes reveal the evolutionary origin of *Acropora* strategies to accommodate environmental changes. *Molecular Biology and Evolution* **38**: 16-30.

Shnit-Orland, M., and Kushmaro, A. (2009) Coral mucus-associated bacteria: a possible first line of defense. *FEMS Microbiology Ecology* **67**: 371-380.

Shon, Z.-H., Davis, D., Chen, G., Grodzinsky, G., Bandy, A., Thornton, D. et al. (2001) Evaluation of the DMS flux and its conversion to SO_2 over the southern ocean. *Atmospheric Environment* **35**: 159-172.

Shulman, M.J., and Robertson, D.R. (1996) Changes in the coral reefs of San Blas, Caribbean Panama: 1983 to 1990. *Coral Reefs* **15**: 231-236.

Sieburth, J.M. (1959) Gastrointestinal Microflora of Antarctic Birds. *Journal of Bacteriology* **77**: 521-531.

Sieburth, J.M. (1960) Acrylic Acid, an "Antibiotic" Principle in Phaeocystis Blooms in Antarctic Waters. *Science* **132**: 676-677.

Sieburth, J.M. (1961) Antibiotic Properties of Acrylic Acid, a Factor in the Gastrointestinal Antibiosis of Polar Marine Animals. *Journal of Bacteriology* **82**: 72-79.

Sievert, S.M., Kiene, R.P., and Schulz-Vogt, H.N. (2007) The Sulfur Cycle. *Oceanography* **20**: 117-123.

Silva, S.G., Blom, J., Keller-Costa, T., and Costa, R. (2019) Comparative genomics reveals complex natural product biosynthesis capacities and carbon metabolism across host-associated and free-living *Aquimarina* (*Bacteroidetes, Flavobacteriaceae*) species. *Environmental Microbiology* **21**: 4002-4019.

Simó, R. (2001) Production of atmospheric sulfur by oceanic plankton: biogeochemical, ecological and evolutionary links. *Trends in Ecology & Evolution* **16**: 287-294.

Simó, R., Archer, S.D., Pedrós-Alió, C., Gilpin, L., and Stelfox-Widdicombe, C.E. (2002) Coupled dynamics of dimethylsulfoniopropionate and dimethylsulfide cycling and the microbial food web in surface waters of the North Atlantic. *Limnology and Oceanography* **47**: 53-61.

Slezak, D., Kiene, R.P., Toole, D.A., Simó, R., and Kieber, D.J. (2007) Effects of solar radiation on the fate of dissolved DMSP and conversion to DMS in seawater. *Aquatic Sciences* **69**: 377-393.

Smeets, P.J.M., Cho, K.R., Kempen, R.G.E., Sommerdijk, N.A.J.M., and De Yoreo, J.J. (2015) Calcium carbonate nucleation driven by ion binding in a biomimetic matrix revealed by in situ electron microscopy. *Nature Materials* **14**: 394-399.

Spiese, C.E., Kieber, D.J., Nomura, C.T., and Kiene, R.P. (2009) Reduction of dimethylsulfoxide to dimethylsulfide by marine phytoplankton. *Limnology and Oceanography* **54**: 560-570.

Stanley, S.O., and Morita, R.Y. (1968) Salinity Effect on the Maximal Growth Temperature of Some Bacteria Isolated from Marine Environments. *Journal of Bacteriology* **95**: 169-173.

Stefels, J. (2000) Physiological aspects of the production and conversion of DMSP in marine algae and higher plants. *Journal of Sea Research* **43**: 183-197.

Stefels, J., Steinke, M., Turner, S., Malin, G., and Belviso, S. (2007) Environmental constraints on the production and removal of the climatically active gas dimethylsulphide (DMS) and implications for ecosystem modelling. *Biogeochemistry* **83**: 245-275.

Steiner, Z., Turchyn, A.V., Harpaz, E., and Silverman, J. (2018) Water chemistry reveals a significant decline in coral calcification rates in the southern Red Sea. *Nature Communications* **9**: 3615.

Steinke, M., Wolfe, G.V., and Kirst, G.O. (1998) Partial characterisation of dimethylsulfoniopropionate (DMSP) lyase isozymes in 6 strains of Emiliania huxleyi. *Marine Ecology Progress Series* **175**: 215-225.

Steinke, M., Malin, G., and Liss, P.S. (2002) Trophic Interactions in the Sea: an Ecological Role for Climate Relevant Volatiles?[1]. *Journal of Phycology* **38**: 630-638.

Steinke, M., Brading, P., Kerrison, P., Warner, M.E., and Suggett, D.J. (2011) Concentration of Dimethylsulfoniopropionate and Dimethyl Sulfide are Strain-specific in Symbiotic Dinoflagellates (*Symbiodinium* sp., Dinophyceae)[1]. *Journal of Phycology* **47**: 775-783.

Stewart, E.J. (2012) Growing Unculturable Bacteria. *Journal of Bacteriology* **194**: 4151-4160.

Struck, A.-W., Thompson, M.L., Wong, L.S., and Micklefield, J. (2012) S-Adenosyl-Methionine-Dependent Methyltransferases: Highly Versatile Enzymes in Biocatalysis, Biosynthesis and Other Biotechnological Applications. *ChemBioChem* **13**: 2642-2655.

Sugino, H., Sasaki, M., Azakami, H., Yamashita, M., and Murooka, Y. (1992) A monoamine-regulated Klebsiella aerogenes operon containing the monoamine oxidase structural gene (maoA) and the maoC gene. *Journal of Bacteriology* **174**: 2485-2492.

Sugiura, N., Ichimura, K., Fujiya, W., and Takahata, N. (2010) Mn/Cr relative sensitivity factors for synthetic calcium carbonate measured with a NanoSIMS ion microprobe. *Geochemical Journal* **44**: e11-e16.

Summers, P.S., Nolte, K.D., Cooper, A.J.L., Borgeas, H., Leustek, T., Rhodes, D., and Hanson, A.D. (1998) Identification and Stereospecificity of the First Three Enzymes of 3-Dimethylsulfoniopropionate Biosynthesis in a Chlorophyte Alga. *Plant Physiology* **116**: 369-378.

Sun, H., Zhang, Y., Tan, S., Zheng, Y., Zhou, S., Ma, Q.-Y. et al. (2020) DMSP-Producing Bacteria Are More Abundant in the Surface Microlayer than Subsurface Seawater of the East China Sea. *Microbial Ecology*.

Sun, J., Todd, J.D., Thrash, J.C., Qian, Y., Qian, M.C., Temperton, B. et al. (2016) The abundant marine bacterium Pelagibacter simultaneously catabolizes dimethylsulfoniopropionate to the gases dimethyl sulfide and methanethiol. *Nature Microbiology*: 16065.

Sunagawa, S., Woodley, C.M., and Medina, M. (2010) Threatened corals provide underexplored microbial habitats. *PLOS ONE* **5**: e9554-e9554.

Sunagawa, S., Coelho, L.P., Chaffron, S., Kultima, J.R., Labadie, K., Salazar, G. et al. (2015) Structure and function of the global ocean microbiome. *Science* **348**.

Sunda, W., Kieber, D.J., Kiene, R.P., and Huntsman, S. (2002) An antioxidant function for DMSP and DMS in marine algae. *Nature* **418**: 317-320.

Swan, H.B., Jones, G.B., and Deschaseaux, E. (2012) Dimethylsulfide, Climate and Coral Reef Ecosystems. *Proceedings of the 12th International Coral Reef Symposium*.

Swanson, C.L.W., and Jacobson, H.G.M. (1955) Effect of Aqueous Solutions of Soil Conditioner Chemicals on Corn Seedlings Grown in Nutrient Solutions. *Soil Science* **79**: 133-146.

Sweet, M.J., Croquer, A., and Bythell, J.C. (2011) Bacterial assemblages differ between compartments within the coral holobiont. *Coral Reefs* **30**: 39-52.

Taga, M.E., Larsen, N.A., Howard-Jones, A.R., Walsh, C.T., and Walker, G.C. (2007) BluB cannibalizes flavin to form the lower ligand of vitamin B_{12}. *Nature* **446**: 449-453.

Tambutté, E., Tambutté, S., Segonds, N., Zoccola, D., Venn, A., Erez, J., and Allemand, D. (2012) Calcein labelling and electrophysiology: insights on coral tissue permeability and calcification. *Proceedings of the Royal Society B: Biological Sciences* **279**: 19-27.

Tambutté, S., Holcomb, M., Ferrier-Pagès, C., Reynaud, S., Tambutté, É., Zoccola, D., and Allemand, D. (2011) Coral biomineralization: From the gene to the environment. *Journal of Experimental Marine Biology and Ecology* **408**: 58-78.

Tan, D., Crabb, W.M., Whitman, W.B., and Tong, L. (2013) Crystal Structure of DmdD, a Crotonase Superfamily Enzyme That Catalyzes the Hydration and Hydrolysis of Methylthioacryloyl-CoA. *PLOS ONE* **8**: e63870.

Tapiolas, D.M., Motti, C.A., Holloway, P., and Boyle, S.G. (2010) High levels of acrylate in the Great Barrier Reef coral *Acropora millepora*. *Coral Reefs* **29**: 621-625.

Tapiolas, D.M., Raina, J.-B., Lutz, A., Willis, B.L., and Motti, C.A. (2013) Direct measurement of dimethylsulfoniopropionate (DMSP) in reef-building corals using quantitative nuclear magnetic resonance (qNMR) spectroscopy. *Journal of Experimental Marine Biology and Ecology* **443**: 85-89.

Taylor, B.F., and Gilchrist, D.C. (1991) New Routes for Aerobic Biodegradation of Dimethylsulfoniopropionate. *Applied and Environmental Microbiology* **57**: 3581-3584.

Taylor, J.J., and Sigmund, W.M. (2010) Adsorption of sodium polyacrylate in high solids loading calcium carbonate slurries. *Journal of Colloid and Interface Science* **341**: 298-302.

Tedetti, M., and Sempéré, R. (2006) Penetration of Ultraviolet Radiation in the Marine Environment. A Review. *Photochemistry and Photobiology* **82**: 389-397.

Todd, J.D., Kirkwood, M., Newton-Payne, S., and Johnston, A.W.B. (2012a) DddW, a third DMSP lyase in a model Roseobacter marine bacterium, *Ruegeria pomeroyi* DSS-3. *The ISME Journal* **6**: 223-226.

Todd, J.D., Curson, A.R.J., Dupont, C.L., Nicholson, P., and Johnston, A.W.B. (2009) The *dddP* gene, encoding a novel enzyme that converts dimethylsulfoniopropionate into dimethyl sulfide, is widespread in ocean metagenomes and marine bacteria and also occurs in some Ascomycete fungi. *Environmental Microbiology* **11**: 1376-1385.

Todd, J.D., Curson, A.R.J., Sullivan, M.J., Kirkwood, M., and Johnston, A.W.B. (2012b) The *Ruegeria pomeroyi acuI* Gene Has a Role in DMSP Catabolism and Resembles *yhdH* of *E. coli* and Other Bacteria in Conferring Resistance to Acrylate. *PLOS ONE* **7**: e35947.

Todd, J.D., Curson, A.R.J., Kirkwood, M., Sullivan, M.J., Green, R.T., and Johnston, A.W.B. (2011) DddQ, a novel, cupin-containing, dimethylsulfoniopropionate lyase in marine roseobacters and in uncultured marine bacteria. *Environmental Microbiology* **13**: 427-438.

Todd, J.D., Curson, A.R.J., Nikolaidou-Katsaraidou, N., Brearley, C.A., Watmough, N.J., Chan, Y. et al. (2010) Molecular dissection of bacterial acrylate catabolism – unexpected links with dimethylsulfoniopropionate catabolism and dimethyl sulfide production. *Environmental Microbiology* **12**: 327-343.

Todd, J.D., Rogers, R., Li, Y.G., Wexler, M., Bond, P.L., Sun, L. et al. (2007) Structural and Regulatory Genes Required to Make the Gas Dimethyl Sulfide in Bacteria. *Science* **315**: 666-669.

Todică , M., Răzvan, Ş., Pop, C.V.L., and Olar, L.E. (2015) IR and Raman Investigation of Some Poly(acrylic) Acid Gels in Aqueous and Neutralized State. *Acta Physica Polonica A* **128**: 128-135.

Tong, W., Xu, Y., Xian, M., Niu, W., Guo, J., Liu, H., and Zhao, G. (2016) Biosynthetic pathway for acrylic acid from glycerol in recombinant *Escherichia coli*. *Applied Microbiology and Biotechnology* **100**: 4901-4907.

Tout, J., Jeffries, T.C., Petrou, K., Tyson, G.W., Webster, N.S., Garren, M. et al. (2015) Chemotaxis by natural populations of coral reef bacteria. *The ISME Journal* **9**: 1764-1777.

Trench, R.K. (1979) The Cell Biology of Plant-Animal Symbiosis. *Annual Review of Plant Physiology* **30**: 485-531.

Trench, R.K. (1993) Microalgal-invertebrate symbioses-a review. *Endocytobiosis and Cell Research* **9**: 135-175.

Tripp, H.J., Kitner, J.B., Schwalbach, M.S., Dacey, J.W.H., Wilhelm, L.J., and Giovannoni, S.J. (2008) SAR11 marine bacteria require exogenous reduced sulphur for growth. *Nature* **452**: 741-744.

Trossat, C., Rathinasabapathi, B., Weretilnyk, E.A., Shen, T.-L., Huang, Z.-H., Gage, D.A., and Hanson, A.D. (1998) Salinity Promotes Accumulation of 3-Dimethylsulfoniopropionate and Its Precursor *S*-Methylmethionine in Chloroplasts. *Plant Physiology* **116**: 165-171.

Turner, S.M., Malin, G., Liss, P.S., Harbour, D.S., and Holligan, P.M. (1988) The seasonal variation of dimethyl sulfide and dimethylsulfoniopropionate concentrations in nearshore waters. *Limnology and Oceanography* **33**: 364-375.

Uchida, A., Ooguri, T., Ishida, T., Kitaguchi, H., and Ishida, Y. (1996) Biosynthesis of Dimethylsulfoniopropionate in *Crypthecodinium cohnii* (Dinophyceae). In *Biological and Environmental Chemistry of DMSP and Related Sulfonium Compounds*. Kiene, R.P., Visscher, P.T., Keller, M.D., and Kirst, G.O. (eds). Boston, MA: Springer US, pp. 97-107.

Vairavamurthy, A., Andreae, M.O., and Iverson, R.L. (1985) Biosynthesis of dimethylsulfide and dimethylpropiothetin by *Hymenomonas carterae* in relation to sulfur source and salinity variations. *Limnology and Oceanography* **30**: 59-70.

Vallino, J.J., Hopkinson, C.S., and Hobbie, J.E. (1996) Modeling bacterial utilization of dissolved organic matter: Optimization replaces Monod growth kinetics. *Limnology and Oceanography* **41**: 1591-1609.

Van Alstyne, K.L., and Puglisi, M.P. (2007) DMSP in marine macroalgae and macroinvertebrates: Distribution, function, and ecological impacts. *Aquatic Sciences* **69**: 394-402.

Van Alstyne, K.L., Schupp, P., and Slattery, M. (2006) The distribution of dimethylsulfoniopropionate in tropical Pacific coral reef invertebrates. *Coral Reefs* **25**: 321-327.

Van Alstyne, K.L., Dominique, V.J., and Muller-Parker, G. (2009) Is dimethylsulfoniopropionate (DMSP) produced by the symbionts or the host in an anemone–zooxanthella symbiosis? *Coral Reefs* **28**: 167-176.

van de Water, J.A.J.M., Ainsworth, T.D., Leggat, W., Bourne, D.G., Willis, B.L., and van Oppen, M.J.H. (2015) The coral immune response facilitates protection against microbes during tissue regeneration. *Molecular Ecology* **24**: 3390-3404.

van Duyl, F.C., Gieskes, W.W.C., Kop, A.J., and Lewis, W.E. (1998) Biological control of short-term variations in the concentration of DMSP and DMS during a *Phaeocystis* spring bloom. *Journal of Sea Research* **40**: 221-231.

van Oppen, M.J.H., and Blackall, L.L. (2019) Coral microbiome dynamics, functions and design in a changing world. *Nature Reviews Microbiology*.

Varaljay, V.A., Gifford, S.M., Wilson, S.T., Sharma, S., Karl, D.M., and Moran, M.A. (2012) Bacterial Dimethylsulfoniopropionate Degradation Genes in the Oligotrophic North Pacific Subtropical Gyre. *Applied and Environmental Microbiology* **78**: 2775-2782.

Varaljay, V.A., Robidart, J., Preston, C.M., Gifford, S.M., Durham, B.P., Burns, A.S. et al. (2015) Single-taxon field measurements of bacterial gene regulation controlling DMSP fate. *The ISME Journal* **9**: 1677-1686.

Veis, A. (2005) A Window on Biomineralization. *Science* **307**: 1419-1420.

Venn, A., Tambutté, E., Holcomb, M., Allemand, D., and Tambutté, S. (2011) Live Tissue Imaging Shows Reef Corals Elevate pH under Their Calcifying Tissue Relative to Seawater. *PLOS ONE* **6**: e20013.

Venter, J.C., Remington, K., Heidelberg, J.F., Halpern, A.L., Rusch, D., Eisen, J.A. et al. (2004) Environmental Genome Shotgun Sequencing of the Sargasso Sea. *Science* **304**: 66-74.

von Glasow, R., and Crutzen, P.J. (2004) Model study of multiphase DMS oxidation with a focus on halogens. *Atmospheric Chemistry and Physics* **4**: 589-608.

Wada, N., Ishimochi, M., Matsui, T., Pollock, F.J., Tang, S.-L., Ainsworth, T.D. et al. (2019) Characterization of coral-associated microbial aggregates (CAMAs) within tissues of the coral *Acropora hyacinthus*. *Scientific Reports* **9**: 14662.

Wagner-Döbler, I., and Biebl, H. (2006) Environmental Biology of the Marine *Roseobacter* Lineage. *Annual Review of Microbiology* **60**: 255-280.

Walker, B.J., Abeel, T., Shea, T., Priest, M., Abouelliel, A., Sakthikumar, S. et al. (2014) Pilon: An Integrated Tool for Comprehensive Microbial Variant Detection and Genome Assembly Improvement. *PLOS ONE* **9**: e112963.

Wang, P., Cao, H.-Y., Chen, X.-L., Li, C.-Y., Li, P.-Y., Zhang, X.-Y. et al. (2017) Mechanistic insight into acrylate metabolism and detoxification in marine dimethylsulfoniopropionate-catabolizing bacteria. *Molecular Microbiology* **105**: 674-688.

Wang, P., Chen, X.-L., Li, C.-Y., Gao, X., Zhu, D.-y., Xie, B.-B. et al. (2015a) Structural and molecular basis for the novel catalytic mechanism and evolution of DddP, an abundant peptidase-like bacterial Dimethylsulfoniopropionate lyase: a new enzyme from an old fold. *Molecular Microbiology* **98**: 289-301.

Wang, X.T., Sigman, D.M., Cohen, A.L., Sinclair, D.J., Sherrell, R.M., Weigand, M.A. et al. (2015b) Isotopic composition of skeleton-bound organic nitrogen in reef-building symbiotic corals: A new method and proxy evaluation at Bermuda. *Geochimica et Cosmochimica Acta* **148**: 179-190.

Wegley, L., Yu, Y., Breitbart, M., Casas, V., Kline, D.I., and Rohwer, F. (2004) Coral-associated Archaea. *Marine Ecology Progress Series* **273**: 89-96.

Weiner, S. (1979) Aspartic acid-rich proteins: Major components of the soluble organic matrix of mollusk shells. *Calcified Tissue International* **29**: 163-167.

Weiner, S., and Addadi, L. (2011) Crystallization Pathways in Biomineralization. *Annual Review of Materials Research* **41**: 21-40.

Westmoreland, L.S.H., Niemuth, J.N., Gracz, H.S., and Stoskopf, M.K. (2017) Altered acrylic acid concentrations in hard and soft corals exposed to deteriorating water conditions. *FACETS* **2**: 531.

White-Stevens, R.H., Pensack, J.M., Stokstad, E.L.R., and Sieburth, J.M. (1962) The Effect of Acrylic Acid Salts on Growth of Chicks. *Poultry Science* **41**: 1909-1915.

Wick, R.R., Schultz, M.B., Zobel, J., and Holt, K.E. (2015) Bandage: interactive visualization of de novo genome assemblies. *Bioinformatics* **31**: 3350-3352.

Wild, C., Woyt, H., and Huettel, M. (2005) Influence of coral mucus on nutrient fluxes in carbonate sands. *Marine Ecology Progress Series* **287**: 87-98.

Williams, B.T., Cowles, K., Bermejo Martínez, A., Curson, A.R.J., Zheng, Y., Liu, J. et al. (2019) Bacteria are important dimethylsulfoniopropionate producers in coastal sediments. *Nature Microbiology* **4**: 1815-1825.

Willker, W., Leibfritz, D., Kerssebaum, R., and Bermel, W. (1993) Gradient selection in inverse heteronuclear correlation spectroscopy. *Magnetic Resonance in Chemistry* **31**: 287-292.

Wilson, B., Aeby, G.S., Work, T.M., and Bourne, D.G. (2012) Bacterial communities associated with healthy and *Acropora* white syndrome-affected corals from American Samoa. *FEMS Microbiology Ecology* **80**: 509-520.

Wilson, K. (2001) Preparation of Genomic DNA from Bacteria. *Current Protocols in Molecular Biology* **56**: 2.4.1-2.4.5.

Wirtz, M., and Droux, M. (2005) Synthesis of the sulfur amino acids: cysteine and methionine. *Photosynthesis Research* **86**: 345-362.

Wommack, K.E., Bhavsar, J., and Ravel, J. (2008) Metagenomics: Read Length Matters. *Applied and Environmental Microbiology* **74**: 1453-1463.

Worden, A.Z., Follows, M.J., Giovannoni, S.J., Wilken, S., Zimmerman, A.E., and Keeling, P.J. (2015) Rethinking the marine carbon cycle: Factoring in the multifarious lifestyles of microbes. *Science* **347**: 1257594.

Work, T.M., and Aeby, G.S. (2014) Microbial aggregates within tissues infect a diversity of corals throughout the Indo-Pacific. *Marine Ecology Progress Series* **500**: 1-9.

Yellowlees, D., Rees, T.A.V., and Leggat, W. (2008) Metabolic interactions between algal symbionts and invertebrate hosts. *Plant, Cell & Environment* **31**: 679-694.

Yeo, W.-S., Lee, J.-H., Lee, K.-C., and Roe, J.-H. (2006) IscR acts as an activator in response to oxidative stress for the suf operon encoding Fe-S assembly proteins. *Molecular Microbiology* **61**: 206-218.

Yi, H., and Chun, J. (2006) *Thalassobius aestuarii* sp. nov., isolated from tidal flat sediment. *Journal of Microbiology* **44**: 171-176.

Yoch, D.C. (2002) Dimethylsulfoniopropionate: Its Sources, Role in the Marine Food Web, and Biological Degradation to Dimethylsulfide. *Applied and Environmental Microbiology* **68**: 5804-5815.

Yost, D.M., and Mitchelmore, C.L. (2009) Dimethylsulfoniopropionate (DMSP) lyase activity in different strains of the symbiotic alga *Symbiodinium microadriaticum*. *Marine Ecology Progress Series* **386**: 61-70.

Yost, D.M., Jones, R.J., and Mitchelmore, C.L. (2010) Alterations in dimethylsulfoniopropionate (DMSP) levels in the coral *Montastraea franksi* in response to copper exposure. *Aquatic Toxicology* **98**: 367-373.

Yu, G. (2020) Using ggtree to Visualize Data on Tree-Like Structures. *Current Protocols in Bioinformatics* **69**: e96.

Yu, G., Lam, T.T.-Y., Zhu, H., and Guan, Y. (2018) Two Methods for Mapping and Visualizing Associated Data on Phylogeny Using Ggtree. *Molecular Biology and Evolution* **35**: 3041-3043.

Yu, G., Smith, D.K., Zhu, H., Guan, Y., and Lam, T.T.-Y. (2017) ggtree: an r package for visualization and annotation of phylogenetic trees with their covariates and other associated data. *Methods in Ecology and Evolution* **8**: 28-36.

Zeyer, J., Eicher, P., Wakeham, S.G., and Schwarzenbach, R.P. (1987) Oxidation of Dimethyl Sulfide to Dimethyl Sulfoxide by Phototrophic Purple Bacteria. *Applied and Environmental Microbiology* **53**: 2026-2032.

Zhang, F., Cai, W., Zhu, J., Sun, Z., and Zhang, J. (2011) In Situ Raman Spectral Mapping Study on the Microscale Fibers in Blue Coral (*Heliopora coerulea*) Skeletons. *Analytical Chemistry* **83**: 7870-7875.

Zhang, L., Kuniyoshi, I., Hirai, M., and Shoda, M. (1991) Oxidation of dimethyl sulfide by *Pseudomonas acidovorans* DMR-11 isolated from peat biofilter. *Biotechnology Letters* **13**: 223-228.

Zhang, Y., Yang, Q., Ling, J., Van Nostrand, J.D., Shi, Z., Zhou, J., and Dong, J. (2016) The Shifts of Diazotrophic Communities in Spring and Summer Associated with Coral *Galaxea astreata*, *Pavona decussata*, and *Porites lutea*. *Frontiers in Microbiology* **7**: 1870.

Zheng, Y., Wang, J., Zhou, S., Zhang, Y., Liu, J., Xue, C.-X. et al. (2020) Bacteria are important dimethylsulfoniopropionate producers in marine aphotic and high-pressure environments. *Nature Communications* **11**: 4658.

Ziegler, M., Roder, C.M., Büchel, C., and Voolstra, C.R. (2015) Mesophotic coral depth acclimatization is a function of host-specific symbiont physiology. *Frontiers in Marine Science* **2**.

Ziegler, M., Grupstra, C.G.B., Barreto, M.M., Eaton, M., BaOmar, J., Zubier, K. et al. (2019) Coral bacterial community structure responds to environmental change in a host-specific manner. *Nature Communications* **10**: 3092.

Zubkov, M.V., Fuchs, B.M., Archer, S.D., Kiene, R.P., Amann, R., and Burkill, P.H. (2001) Linking the composition of bacterioplankton to rapid turnover of dissolved dimethylsulphoniopropionate in an algal bloom in the North Sea. *Environmental Microbiology* **3**: 304-311.

Supplementary data

S1: Supplementary data for Chapter 2

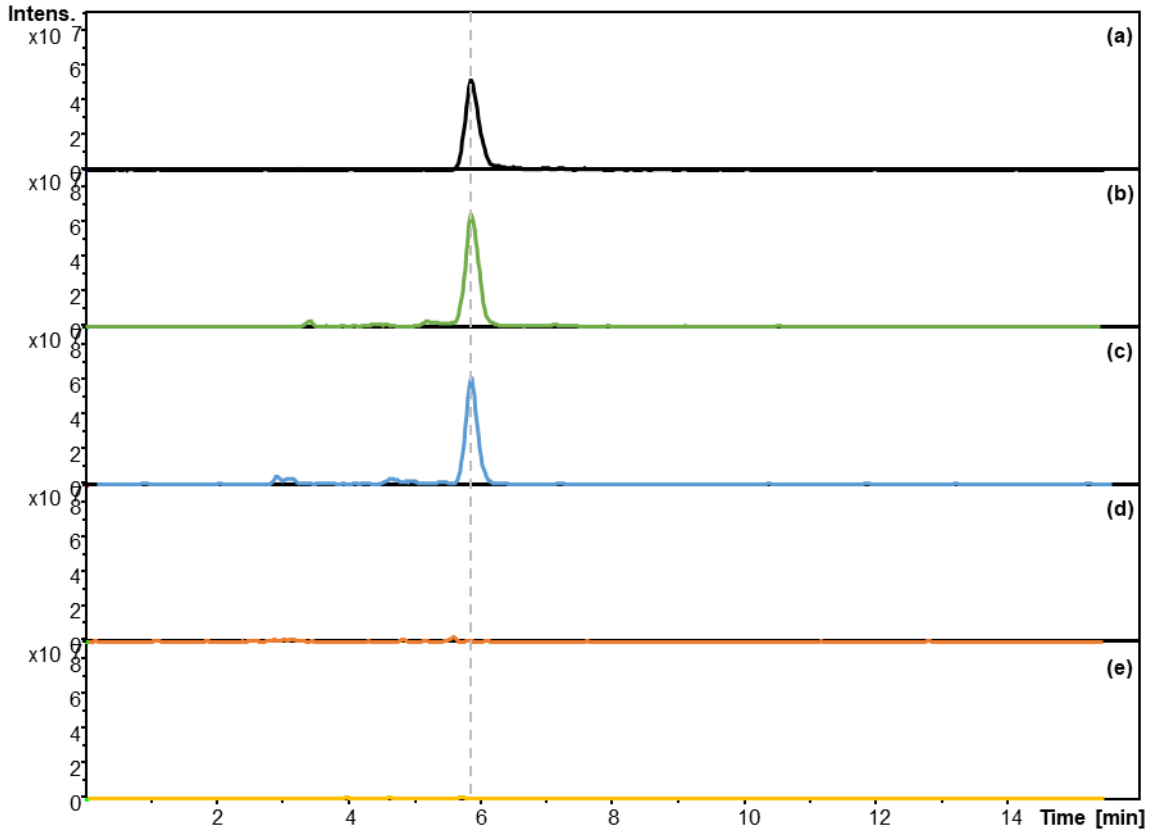

Supplementary Data Figure 2.1. An example of LC-MS extracted ion chromatograms (EIC) at 135 *m/z* of (a) a DMSP standard ($C_5H_{10}O_2S$; MW=134.197) compared to bacterial extracts of *Shimia* sp. AMM-P-2 cultured in (b) modified minimal basal media (MBM) spiked with DMSP, (c) modified MBM, (d) yeast tryptone sea salts (YTSS) media, and (e) marine broth, demonstrating that DMSP was only produced by the bacterium when cultured in modified MBM. DMSP was not detected in extracts of the bacterium grown in YTSS media or marine broth.

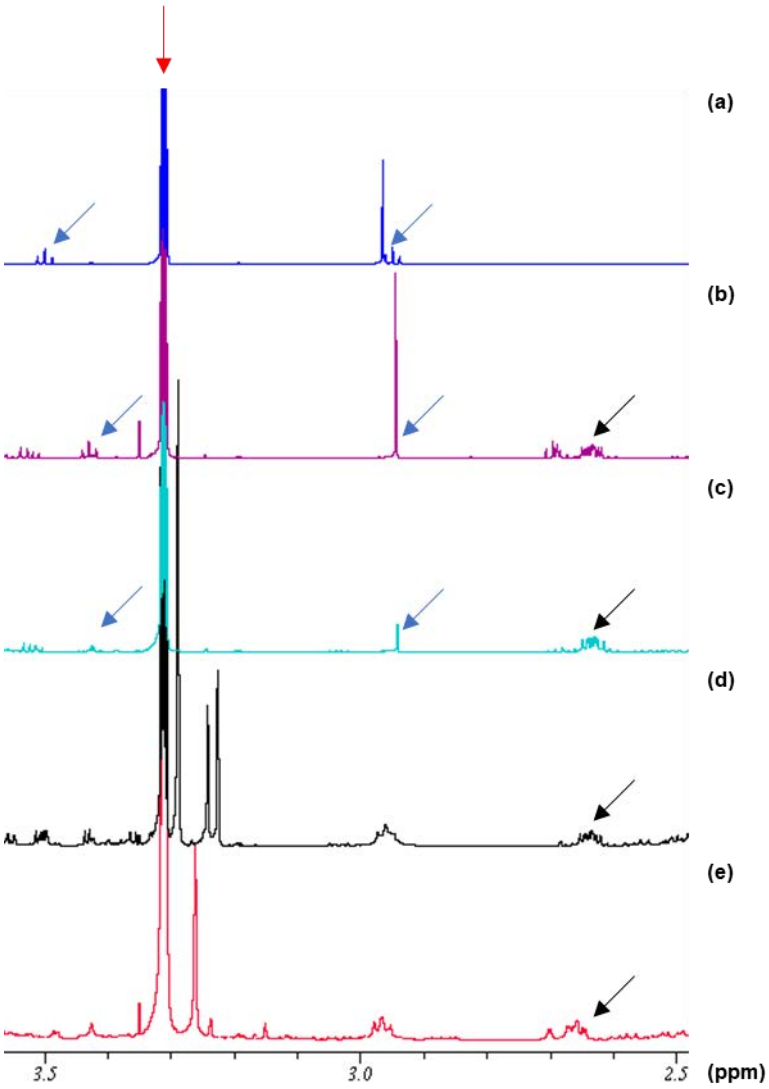

Supplementary Data Figure 2.2. An example of ^{1}H NMR spectra of: (a) 4mM DMSP standard in deuterated methanol (CD_3OD) compared to bacterial extracts of *Shimia* sp. AMM-P-2 cultured in (b) modified minimal basal media (MBM) spiked with DMSP, (c) modified MBM, (d) yeast tryptone sea salts (YTSS) media, and (e) marine broth, demonstrating that DMSP was only produced by the bacterium when cultured in modified MBM. The spectra of bacterial extracts were referenced to the CD_3OD signal (red arrow) and normalised to the signal at 2.65 ppm (black arrows), with blue arrows showing the position of DMSP signals (singlet at δ_H ~2.95 ppm and triplet at δ_H ~3.45 ppm). DMSP spiking was done to confirm the shift in DMSP signals in the bacterial extract. DMSP was not detected in extracts of the bacterium grown in YTSS media or marine broth.

S2: Supplementary data for Chapter 3

Supplementary Data Table 3.1. Nucleotide and amino acid sequences of *Shimia aestuarii* AMM-P-2 *dsyB* gene.

Nucleotide sequence	ATGACCGCCCTGACCACCGCCGACCAGATTTCCGATATCGCCTTCGGGTTCATGGGATCC AAGGCGCTTTTCGCGGCGCTTGAGGCGGATACCTTTTCGCAGCTCTCCGAGAAGGGACCG ATGAGCGCACGGGAACTGGCCAATTTCGTCCCCCTCGATGCCGACCGCGCCGAGACGCTT CTGACGGCACTGGCGGGGCTTGGCCTTGTGACGGTGGAGGCGGGTAAGTTCGCCAATGGT CCGGCGGCGGAAATGTTCCTTGTGAAGGGCGCGAAATACGATTTTGGCGACTACCTGCGC CTACAGGTGGGGCGCCAGATGTATGGCCTTCTCGACCAGATTGATGATGCGCTGATGAAC CGTCTGCCGCCCGAGGCGACGGCCTCTTATGCGGAATGGTTCTCGGACCCAGACGAGGCG CGGCTCTACTCGGCCTCGCAACATGCGGGCTCTCTCGGTCCGGCGCGTCAACTTGTGAAG TCGATGGACCTTTCTGGCGCCAAGACGATGCTCGACGTGGGCGGCGGCACCGGGGCCTTT GCCATCACGCTTTGTCACGCGGTCGAAGGGCTTTCCGCGACCATCGTCGATTTTCCCAAC GTGGCCGCGCTTGGCCGGGATTATGTCGCCGAGGCAGGCCTCTCCGAGCGGATTTCCTAC ATTGAGGGCAACGCGCTCGAGACCGACTGGCCGGGCGGGCAAGACCTGATCCTGATGTCT TATCTCTTCTCCGGCGTGCCCGGTGAAACCCATGATCGCCTCTTGGCGCAGGCCTATGCC TGTCTCAACCCCGGCGGGCGGCTCCTCGTGCATGATTTCGTCGTCGAGGAAAGCCGCGAC GGCCCCAAGCTCGCCGCCCTCTGGCAACTCCAGCACACCGCCTTTACCCCACGCGCCGTC TCGCTTGATAAGGGCTGGCTCAAGGCGGCTCTGACCGAGAAAGGGTTTGATGGGGTAAGT GTCTCGGAAATGATCCCCGAGATGACCATGCTCGCCATCGGCCAGAAGCCCGGCTGA
Amino acid sequence	MTALTTADQISDIAFGFMGSKALFAALEADTFSQLSEKGPMSARELANFVPLDADRAETL LTALAGLGLVTVEAGKFANGPAAEMFLVKGAKYDFGDYLRLQVGRQMYGLLDQIDDALMN RLPPEATASYAEWFSDPDEARLYSASQHAGSLGPARQLVKSMDLSGAKTMLDVGGGTGAF AITLCHAVEGLSATIVDFPNVAALGRDYVAEAGLSERISYIEGNALETDWPGGQDLILMS YLFSGVPGETHDRLLAQAYACLNPGGRLLVHDFVVEESRDGPKLAALWQLQHTAFTPRAV SLDKGWLKAALTEKGFDGVSVSEMIPEMTMLAIGQKPG

S3: Supplementary data for Chapter 4

Supplementary Data Table 4.1. Sums of squares, mean squares, and significance levels of repeated measures ANOVA for intracellular DMSP concentrations.

Mauchly's Test of Sphericity[a]

Within Subjects Effect	Mauchly's W	Approx. Chi-Square	df	Sig.	Epsilon[b]		
					Greenhouse-Geisser	Huynh-Feldt	Lower-bound
Time	0.418	11.108	5	0.050	0.660	1.000	0.333

Tests the null hypothesis that the error covariance matrix of the orthonormalized transformed dependent variables is proportional to an identity matrix.
a. Design: Intercept + Treatment
Within Subjects Design: Time
b. May be used to adjust the degrees of freedom for the averaged tests of significance. Corrected tests are displayed in the Tests of Within-Subjects Effects table.

Tests of Within-Subjects Effects

Source		Sum of Squares	df	Mean Square	F	Sig.	Partial Eta Squared
Time	Sphericity Assumed	0.075	3	0.025	2.803	0.051	0.167
	Greenhouse-Geisser	0.075	1.981	0.038	2.803	0.078	0.167
Time * Treatment	Sphericity Assumed	0.233	18	0.013	1.448	0.160	0.383
	Greenhouse-Geisser	0.233	11.888	0.020	1.448	0.204	0.383
Error (Time)	Sphericity Assumed	0.376	42	0.009			
	Greenhouse-Geisser	0.376	27.739	0.014			

Multiple Comparisons

Tukey HSD

Treatment		Mean Difference	Std. Error	Sig.	95% Confidence Interval	
					Lower Bound	Upper Bound
Standard	22°C	0.08108	0.030912	0.191	-0.02447	0.18663
	32°C	.19308*	0.030912	0.000	0.08753	0.29863
	25 PSU	.28925*	0.030912	0.000	0.18370	0.39480
	40 PSU	-.37142*	0.030912	0.000	-0.47697	-0.26587
	UV	-.30258*	0.030912	0.000	-0.40813	-0.19703
	Dark	-.20067*	0.030912	0.000	-0.30622	-0.09512

Based on observed means.
The error term is Mean Square (Error) = .001.
*. The mean difference is significant at the .05 level.

Supplementary Data Table 4.2. Sums of squares, mean squares, and significance levels of repeated measures ANOVA for intracellular acrylate concentrations.

Mauchly's Test of Sphericity[a]

Within Subjects Effect	Mauchly's W	Approx. Chi-Square	df	Sig.	Epsilon[b]		
					Greenhouse-Geisser	Huynh-Feldt	Lower-bound
Time	0.361	12.972	5	0.024	0.715	1.000	0.333

Tests the null hypothesis that the error covariance matrix of the orthonormalized transformed dependent variables is proportional to an identity matrix.

a. Design: Intercept + Treatment
Within Subjects Design: Time

b. May be used to adjust the degrees of freedom for the averaged tests of significance. Corrected tests are displayed in the Tests of Within-Subjects Effects table.

Tests of Within-Subjects Effects

Source		Sum of Squares	df	Mean Square	F	Sig.	Partial Eta Squared
Time	Sphericity Assumed	0.006	3	0.002	6.639	0.001	0.322
	Greenhouse-Geisser	0.006	2.144	0.003	6.639	0.003	0.322
Time * Treatment	Sphericity Assumed	0.011	18	0.001	2.097	0.024	0.473
	Greenhouse-Geisser	0.011	12.864	0.001	2.097	0.047	0.473
Error (Time)	Sphericity Assumed	0.012	42	0.000			
	Greenhouse-Geisser	0.012	30.017	0.000			

Multiple Comparisons

Tukey HSD

Treatment		Mean Difference	Std. Error	Sig.	95% Confidence Interval	
					Lower Bound	Upper Bound
Standard	22°C	0.01725	0.007873	0.358	-0.00963	0.04413
	32°C	.07533*	0.007873	0.000	0.04845	0.10222
	25 PSU	.05708*	0.007873	0.000	0.03020	0.08397
	40 PSU	-.04508*	0.007873	0.001	-0.07197	-0.01820
	UV	-0.00442	0.007873	0.997	-0.03130	0.02247
	Dark	.04950*	0.007873	0.000	0.02262	0.07638

Based on observed means.
The error term is Mean Square (Error) = 9.30E-005.

*. The mean difference is significant at the .05 level.

Supplementary Data Table 4.3. Simple main effects analysis of intracellular DMSP concentrations

Pairwise Comparisons

Dependent Variable:

Time			Mean Difference (I-J)	Std. Error	Sig.[b]	95% Confidence Interval for Difference[b]	
						Lower Bound	Upper Bound
T1	Standard	22°C	0.063	0.074	0.394	-0.084	0.211
		32°C	.153*	0.074	0.042	0.005	0.301
		25PSU	.297*	0.074	0.000	0.149	0.445
		40PSU	-.250*	0.074	0.001	-0.397	-0.102
		UV	-.211*	0.074	0.006	-0.359	-0.064
		Dark	-0.043	0.074	0.562	-0.191	0.105
T2	Standard	22°C	.193*	0.074	0.011	0.045	0.340
		32°C	.292*	0.074	0.000	0.144	0.440
		25PSU	.354*	0.074	0.000	0.206	0.501
		40PSU	-.331*	0.074	0.000	-0.479	-0.184
		UV	-.252*	0.074	0.001	-0.399	-0.104
		Dark	-0.140	0.074	0.063	-0.287	0.008
T3	Standard	22°C	0.145	0.074	0.054	-0.003	0.293
		32°C	.254*	0.074	0.001	0.106	0.402
		25PSU	.350*	0.074	0.000	0.202	0.497
		40PSU	-.397*	0.074	0.000	-0.545	-0.250
		UV	-.296*	0.074	0.000	-0.444	-0.148
		Dark	-.278*	0.074	0.000	-0.426	-0.131
T4	Standard	22°C	-0.077	0.074	0.303	-0.224	0.071
		32°C	0.073	0.074	0.325	-0.075	0.221
		25PSU	.157*	0.074	0.037	0.010	0.305
		40PSU	-.507*	0.074	0.000	-0.655	-0.360
		UV	-.451*	0.074	0.000	-0.598	-0.303
		Dark	-.341*	0.074	0.000	-0.489	-0.194

Based on estimated marginal means

*. The mean difference is significant at the .05 level.

b. Adjustment for multiple comparisons: Least Significant Difference (equivalent to no adjustments).

Supplementary Data Table 4.4. Simple main effects analysis of intracellular acrylate concentrations

Pairwise Comparisons

Dependent Variable:

Time			Mean Difference (I-J)	Std. Error	Sig.[b]	95% Confidence Interval for Difference[b]	
						Lower Bound	Upper Bound
T1	Standard	22°C	0.012	0.014	0.424	-0.017	0.041
		32°C	.104*	0.014	0.000	0.075	0.133
		25PSU	.068*	0.014	0.000	0.039	0.097
		40PSU	-0.017	0.014	0.246	-0.046	0.012
		UV	.036*	0.014	0.016	0.007	0.065
		Dark	.081*	0.014	0.000	0.052	0.110
T2	Standard	22°C	0.014	0.014	0.350	-0.015	0.043
		32°C	.076*	0.014	0.000	0.047	0.105
		25PSU	.048*	0.014	0.002	0.019	0.077
		40PSU	-.063*	0.014	0.000	-0.092	-0.034
		UV	-0.020	0.014	0.166	-0.049	0.009
		Dark	.054*	0.014	0.000	0.025	0.083
T3	Standard	22°C	.035*	0.014	0.019	0.006	0.064
		32°C	.072*	0.014	0.000	0.043	0.101
		25PSU	.075*	0.014	0.000	0.046	0.104
		40PSU	-.048*	0.014	0.002	-0.077	-0.019
		UV	-0.006	0.014	0.680	-0.035	0.023
		Dark	.048*	0.014	0.002	0.019	0.077
T4	Standard	22°C	0.009	0.014	0.552	-0.020	0.038
		32°C	.049*	0.014	0.001	0.020	0.078
		25PSU	.037*	0.014	0.013	0.008	0.066
		40PSU	-.052*	0.014	0.001	-0.081	-0.023
		UV	-0.027	0.014	0.064	-0.056	0.002
		Dark	0.015	0.014	0.316	-0.014	0.044

Based on estimated marginal means

*. The mean difference is significant at the .05 level.

b. Adjustment for multiple comparisons: Least Significant Difference (equivalent to no adjustments).

Supplementary Data Table 4.5. Correlation analysis of intracellular DMSP and acrylate concentrations

Correlations

		DMSP	Acrylate
DMSP	Pearson Correlation	1	.708**
	Sig. (2-tailed)		0.000
	Sum of Squares and Cross-products	1.636	0.199
	Covariance	0.061	0.007
	N	28	28
Acrylate	Pearson Correlation	.708**	1
	Sig. (2-tailed)	0.000	
	Sum of Squares and Cross-products	0.199	0.048
	Covariance	0.007	0.002
	N	28	28

**. Correlation is significant at the 0.01 level (2-tailed).

Supplementary Data Table 4.6. Raw *dsyB* transcription in *Shimia aestuarii* AMM-P-2 at four time points (24, 28, 32, and 36 hours after inoculation) under varying experimental conditions of temperature (22 and 32°C), salinity (25 and 40 PSU), constant darkness, and UV exposure. N/A denotes instances of failed qPCR runs.

Treatment	Time	R1	R2	R3	Average	Std. dev.
Standard	T1	3.85E-03	9.18E-07	5.89E-04	1.48E-03	2.07E-03
	T2	8.83E+02	1.73E+00	4.61E+02	4.49E+02	4.41E+02
	T3	7.75E-03	N/A	N/A	7.75E-03	N/A
	T4	N/A	6.56E+04	1.36E+07	6846387.85	9.59E+06
22°C	T1	6.06E-02	4.17E-06	2.08E-03	2.09E-02	3.44E-02
	T2	N/A	N/A	4.49E-07	4.49E-07	N/A
	T3	3.32E-03	4.49E-03	1.89E+03	6.28E+02	1.09E+03
	T4	N/A	7.89E-01	N/A	7.89E-01	N/A
32°C	T1	6.92E-04	1.70E-04	N/A	4.31E-04	3.69E-04
	T2	N/A	N/A	N/A	N/A	N/A
	T3	N/A	4.65E-05	2.96E-04	1.71E-04	1.76E-04
	T4	N/A	N/A	2.95E-05	2.95E-05	N/A
25 PSU	T1	6.95E-04	1.47E-03	1.29E-04	7.64E-04	6.71E-04
	T2	2.84E-04	5.56E-01	1.76E-04	1.85E-01	3.21E-01
	T3	2.43E-04	9.08E-04	6.81E-04	6.11E-04	3.38E-04
	T4	5.22E-06	N/A	3.92E-05	2.22E-05	2.41E-05
40 PSU	T1	1.04E-05	7.50E-01	3.15E-06	2.50E-01	4.33E-01
	T2	1.89E+00	1.54E-03	1.63E-06	6.30E-01	1.09E+00
	T3	2.27E+00	N/A	2.16E-02	1.15E+00	1.59E+00
	T4	6.78E-06	3.06E-01	8.04E-01	3.70E-01	4.06E-01
UV	T1	5.80E-05	5.48E-04	9.29E-05	2.33E-04	2.73E-04
	T2	N/A	1.89E-03	3.19E-04	1.11E-03	1.11E-03
	T3	N/A	1.24E-04	7.46E-04	4.35E-04	4.40E-04
	T4	1.23E-03	1.66E-04	1.52E-04	5.16E-04	6.18E-04
Dark	T1	N/A	3.77E-03	N/A	3.77E-03	N/A
	T2	6.35E-05	2.15E-02	2.92E-01	1.05E-01	1.63E-01
	T3	1.02E-02	2.13E+00	3.32E-01	8.25E-01	1.14E+00
	T4	1.48E-01	1.86E+01	2.75E-04	6.26E+00	1.07E+01

Appendix A

JOURNAL OF NATURAL PRODUCTS

pubs.acs.org/jnp Article

Identification and Characterization of a Peptide from the Stony Coral *Heliofungia actiniformis*

Casey A. Schmidt, David T. Wilson, Ira Cooke, Jeremy Potriquet, Katie Tungatt, Visai Muruganandah, Chloë Boote, Felicity Kuek, John J. Miles, Andreas Kupz, Stephanie Ryan, Alex Loukas, Paramjit S. Bansal, Rozita Takjoo, David J. Miller, Steve Peigneur, Jan Tytgat, and Norelle L. Daly*

Cite This: *J. Nat. Prod.* 2020, 83, 3454−3463 Read Online

ACCESS | Metrics & More | Article Recommendations | Supporting Information

ABSTRACT: Marine organisms produce a diverse range of toxins and bioactive peptides to support predation, competition, and defense. The peptide repertoires of stony corals (order Scleractinia) remain relatively understudied despite the presence of tentacles used for predation and defense that are likely to contain a range of bioactive compounds. Here, we show that a tentacle extract from the mushroom coral, *Heliofungia actiniformis*, contains numerous peptides with a range of molecular weights analogous to venom profiles from species such as cone snails. Using NMR spectroscopy and mass spectrometry we characterized a 12-residue peptide (Hact-1) with a new sequence (GCHYTPFGLICF) and well-defined β-hairpin structure stabilized by a single disulfide bond. The sequence is encoded within the genome of the coral and expressed in the polyp body tissue. The structure present is common among toxins and venom peptides, but Hact-1 does not show activity against select examples of Gram-positive and Gram-negative bacteria or a range of ion channels, common properties of such peptides. Instead, it appears to have a limited effect on human peripheral blood mononuclear cells, but the ecological function of the peptide remains unknown. The discovery of this peptide from *H. actiniformis* is likely to be the first of many from this and related species.

Content has been removed due to copyright restrictions

Received: September 9, 2020
Published: November 9, 2020

https://dx.doi.org/10.1021/acs.jnatprod.0c00981
J. Nat. Prod. 2020, 83, 3454−3463

Content has been removed
due to copyright restrictions

Content has been removed
due to copyright restrictions

Content has been removed
due to copyright restrictions

Content has been removed
due to copyright restrictions

Content has been removed
due to copyright restrictions

Content has been removed
due to copyright restrictions

Content has been removed
due to copyright restrictions

Content has been removed
due to copyright restrictions

Content has been removed
due to copyright restrictions

Appendix B

AMERICAN SOCIETY FOR MICROBIOLOGY | mSystems®

RESEARCH ARTICLE

Insights into the Cultured Bacterial Fraction of Corals

Michael Sweet,[a] Helena Villela,[b] Tina Keller-Costa,[c,d] Rodrigo Costa,[c,d,e] Stefano Romano,[f] David G. Bourne,[g,h] Anny Cárdenas,[i] Megan J. Huggett,[j,k] Allison H. Kerwin,[l] Felicity Kuek,[h,m] Mónica Medina,[n] Julie L. Meyer,[o] Moritz Müller,[p] F. Joseph Pollock,[n,q] Michael S. Rappé,[r] Mathieu Sere,[a] Koty H. Sharp,[s] Christian R. Voolstra,[i] Nathan Zaccardi,[s] Maren Ziegler,[t] Raquel Peixoto[b,u]

[a]Aquatic Research Facility, Environmental Sustainability Research Centre, University of Derby, Derby, United Kingdom
[b]Federal University of Rio de Janeiro, Rio de Janeiro, Brazil
[c]Institute for Bioengineering and Biosciences (iBB), University of Lisbon, Lisbon, Portugal
[d]Instituto Superior Técnico (IST), University of Lisbon, Lisbon, Portugal
[e]Department of Energy, Joint Genome Institute and Lawrence Berkeley National Laboratory, Berkeley, California, USA
[f]Gut Microbes and Health, Quadram Institute Bioscience, Norwich, United Kingdom
[g]College of Science and Engineering, James Cook University, Townsville, Australia
[h]Australian Institute of Marine Science, Townsville, Australia
[i]Department of Biology, University of Konstanz, Konstanz, Germany
[j]School of Environmental and Life Sciences, The University of Newcastle, Ourimbah, NSW, Australia
[k]Centre for Marine Ecosystems Research, Edith Cowan University, Joondalup, WA, Australia
[l]Department of Biology, McDaniel College, Westminster, Maryland, USA
[m]College of Public Health, Medical and Veterinary Sciences, James Cook University, Townsville, Australia
[n]Department of Biology, Pennsylvania State University, University Park, Pennsylvania, USA
[o]Soil and Water Sciences Department, Genetics Institute, University of Florida, Gainesville, Florida, USA
[p]Faculty of Engineering, Computing and Science, Swinburne University of Technology Sarawak Campus, Kuching, Sarawak, Malaysia
[q]Hawaii and Palmyra Programs, The Nature Conservancy, Honolulu, Hawaii, USA
[r]Hawaii Institute of Marine Biology, University of Hawaii, Kaneohe, Hawaii, USA
[s]Department of Biology and Marine Biology, Roger Williams University, Bristol, Rhode Island, USA
[t]Department of Animal Ecology and Systematics, Justus Liebig University Giessen, Giessen, Germany
[u]Red Sea Research Center (RSRC), Division of Biological and Environmental Science and Engineering (BESE), King Abdullah University of Science and Technology (KAUST), Thuwal, Saudi Arabia

Michael Sweet, Helena Villela, Tina Keller-Costa, Rodrigo Costa, Stefano Romano, and Raquel Peixoto contributed equally. Author order was determined by mutual agreement.

ABSTRACT Bacteria associated with coral hosts are diverse and abundant, with recent studies suggesting involvement of these symbionts in host resilience to anthropogenic stress. Despite their putative importance, the work dedicated to culturing coral-associated bacteria has received little attention. Combining published and unpublished data, here we report a comprehensive overview of the diversity and function of culturable bacteria isolated from corals originating from tropical, temperate, and cold-water habitats. A total of 3,055 isolates from 52 studies were considered by our metasurvey. Of these, 1,045 had full-length 16S rRNA gene sequences, spanning 138 formally described and 12 putatively novel bacterial genera across the *Proteobacteria*, *Firmicutes*, *Bacteroidetes*, and *Actinobacteria* phyla. We performed comparative genomic analysis using the available genomes of 74 strains and identified potential signatures of beneficial bacterium-coral symbioses among the strains. Our analysis revealed >400 biosynthetic gene clusters that underlie the biosynthesis of antioxidant, antimicrobial, cytotoxic, and other secondary metabolites. Moreover, we uncovered genomic features—not previously described for coral-bacterium symbioses—potentially involved in host colonization and host-symbiont recognition, antiviral defense mechanisms, and/or integrated metabolic interactions, which we suggest as novel targets for the screening of coral probiotics. Our results highlight the importance of bacterial cultures to elucidate coral holobiont functioning and guide the selection of probiotic candidates to

Citation Sweet M, Villela H, Keller-Costa T, Costa R, Romano S, Bourne DG, Cárdenas A, Huggett MJ, Kerwin AH, Kuek F, Medina M, Meyer JL, Müller M, Pollock FJ, Rappé MS, Sere M, Sharp KH, Voolstra CR, Zaccardi N, Ziegler M, Peixoto R. 2021. Insights into the cultured bacterial fraction of corals. mSystems 6:e01249-20. https://doi.org/10.1128/mSystems.01249-20.

Editor Nick Bouskill, Lawrence Berkeley National Laboratory

Ad Hoc Peer Reviewers Lauren Speare, University of North Carolina at Chapel Hill; Amanda Shore, Farmingdale State College

Address correspondence to Michael Sweet, m.sweet@derby.ac.uk, or Raquel Peixoto, raquel.peixoto@kaust.edu.sa.

Received 1 December 2020
Accepted 13 May 2021
Published 22 June 2021

promote coral resilience and improve holistic and customized reef restoration and rehabilitation efforts.

IMPORTANCE Our paper is the first study to synthesize currently available but decentralized data of cultured microbes associated with corals. We were able to collate 3,055 isolates across a number of published studies and unpublished collections from various laboratories and researchers around the world. This equated to 1,045 individual isolates which had full-length 16S rRNA gene sequences, after filtering of the original 3,055. We also explored which of these had genomes available. Originally, only 36 were available, and as part of this study, we added a further 38—equating to 74 in total. From this, we investigated potential genetic signatures that may facilitate a host-associated lifestyle. Further, such a resource is an important step in the selection of probiotic candidates, which are being investigated for promoting coral resilience and potentially applied as a novel strategy in reef restoration and rehabilitation efforts. In the spirit of open access, we have ensured this collection is available to the wider research community through the web site http://isolates.reefgenomics.org/ with the hope many scientists across the globe will ask for access to these cultures for future studies.

KEYWORDS symbiosis, holobiont, metaorganism, cultured microorganisms, coral, probiotics, beneficial microbes, genomes, symbiosis

In recent years, the concept of the metaorganism or holobiont, which defines the associations formed by a host organism and its microbiome (1–3), has become a cornerstone of biology (4). Scleractinian corals are an excellent example of host-microbe associations, as they build reefs through close symbiotic interactions between the host modular animal, its endosymbiotic dinoflagellates (*Symbiodiniaceae*), and an array of other microbial partners, including bacteria, archaea, and fungi (3, 4). The bacterial taxa associated with corals can vary between coral species and geographical origin, though often there are patterns in the community structure that link microbial and coral taxa (5, 6). Many original discoveries on the importance of coral-associated bacteria and their interactions with the coral host were made using culture-based methods (7, 8). However, the majority of recent studies exploring the importance of coral-associated microbes have focused on the use of cultivation-independent approaches, based on 16S rRNA gene amplicon sequencing (9) and, more recently, shotgun metagenomics (10, 11). Such methods are central in identifying what bacteria are associated with corals and how their metabolic and functional potential contribute to holobiont health and response to environmental conditions (9, 12–14). However, the bacterial metabolic pathways that interact with the host and respond to environmental changes are often best understood using culture-based approaches (15). This is particularly relevant because metagenomic information gives insights into potential functional traits and other cellular traits only, and often environmental changes have pleiotropic effects on holobiont physiology that are impossible to grasp using metagenomics alone (16–19).

Inherently, culture-based approaches retrieve only a small fraction of the total bacterial diversity within any given environment, a phenomenon known as the "great plate anomaly" (20–22). Often however, it is not a case of being "unculturable" but of not yet knowing the (range of) conditions needed to culture specific microorganisms (23). Cultivating host-associated microorganisms can be challenging, as their nutrient requirements and cross-feeding networks are often unknown (24). In addition, many "environmental" microorganisms grow very slowly (in contrast to clinical isolates), and are not adapted to or capable of growing on commonly used nutrient-rich media, and are outcompeted by copiotrophic bacteria (25, 26). To counter this, at least to some degree, recent studies have implemented novel and alternative culture-based methods to retrieve a higher proportion of the bacterial diversity present in any given sample (24, 27, 28), and these approaches have also been applied to corals (29–31).

Organismal, growth form, and tissue complexity create unique microenvironments

that are thought to contribute to the high bacterial diversity often seen in corals (32–34). The diverse coral bacteriome plays an integral role in the balance between health and disease of the coral holobiont (35, 36) and represents a valuable source of biotechnological products (37, 38). Disalvo (39) was perhaps the first to isolate bacteria from coral in 1969, recovering strains from the skeletal regions of *Porites lobata*, followed by Ducklow and Mitchell (40) who reported on bacteria isolated from mucus of *Porites astreoides* and two octocoral species 10 years later. Microbe-mediated diseases have also been well documented as driving declines in reef health, especially throughout the Caribbean for example (41). This has fostered a great interest in understanding coral disease causative agents, stimulating cultivation efforts of coral-associated bacteria (42–44). For example, Kushmaro et al. (45) isolated a bacterium that caused bleaching of the coral *Oculina patagonica*, and many subsequent studies have implicated vibrios in coral disease causation (46–48)—although it should be noted that coral bleaching is not typically considered a disease and is ascribed to dysbiosis of the coral host and associated *Symbiodiniaceae* (49). Regardless, many of these studies focused on targeted isolation and conducted reinfection studies to satisfy Koch's postulates, with varying success (reviewed in reference 50).

Counter to the notion of pathogenicity of certain bacteria, growing evidence underlines the key role secondary metabolites produced by (beneficial) bacteria have on host health (35, 51–54). For instance, Ritchie (55) was among the first to demonstrate that mucus-associated bacteria from healthy colonies inhibit the growth of potential pathogens. Subsequent studies revealed high antimicrobial activity among culturable coral-associated bacteria, with up to 25% of the isolates producing antimicrobial compounds (56). Kuek et al. (57) showed a strong link between observed antibiotic activity in well diffusion assays and existence of polyketide synthase (PKS) and/or nonribosomal peptide synthetase (NRPS) genes in the bacterial isolates. More recently, Raina et al. (17) found that the antimicrobial compound tropodithietic acid (TDA) was produced by the coral-associated bacterium *Pseudovibrio* sp. and subsequent studies found that *Pseudovibrio* species harbor several biosynthetic gene clusters for the synthesis of bioactive compounds (58, 59).

Bacterial isolates from corals represent an invaluable resource for assessing the virulence of potential pathogens, and for applying classical clinical approaches to elucidate disease etiology (60). Beneficial traits that bacteria may provide to coral holobiont functioning can also be elucidated using pure bacterial cultures (10, 18). Bacteria isolated from corals can also be used as probiotics to facilitate host health (61, 62), and such approaches have been proposed to promote coral resilience in the face of environmental stress. For example, Rosado et al. (53) showed that application of so-called "beneficial microorganisms for corals" (or BMCs) increases the resilience of the coral to temperature stress and pathogen challenge. However, despite the demonstrated importance of BMCs (63), a centralized and curated collection of isolates obtained from corals and their associated genetic information does not currently exist. Moreover, many culture-based studies often focus on relatively few bacteria (targeted for pathogenic agents for example), meaning a large-scale comparison of which bacterial isolates can be cultured and their genetic information is currently missing. Here, we sought to centralize and curate the current cultured fraction of coral bacteria by combining published data with unpublished collections from around the world (Fig. 1). Without doubt, some studies and culture collections will have been missed in this first compilation; however, our aim was to start building a resource that can be built upon. To highlight the importance of such a collection, we explore the relationships between the isolated bacteria, the host origin, and the media utilized for growth. Further, a total of 74 genomes of cultured coral bacteria, 36 of which are available in public databases and 38 of which are presented in this study for the first time, were investigated to infer potential genetic signatures that may facilitate a host-associated lifestyle. Finally, alternative ways and improvements for the isolation of bacterial groups not yet recovered from corals (including the specific targeting of obligate symbionts) are discussed. This

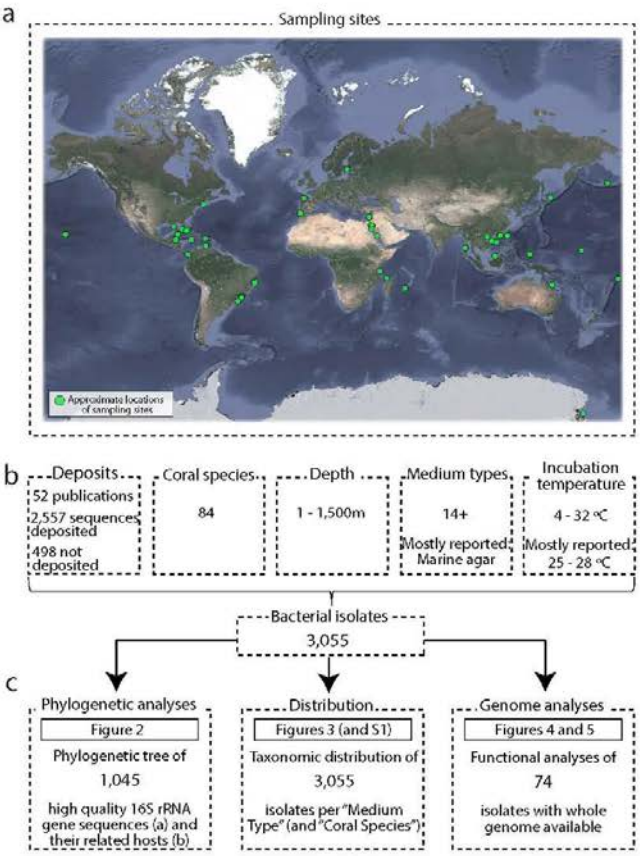

FIG 1 Overview of the data detailed in this article. (a) Sampling sites of the coral species used as isolation sources. Map data © 2020 Google. (b) Data summary recovered from the publications and accession numbers available in data banks. (c) Overview of the analyses performed in the current article using the available isolates.

study provides the most comprehensive synthesis of the cultured bacterial fraction of the coral holobiont thus far.

RESULTS

Phylogenetic analysis of culturable coral-associated bacteria. To define the relationships and a taxonomic overview of the groups of coral-associated bacteria isolated from around the world, published and unpublished data sets were interrogated, identifying 3,055 cultured coral-associated bacteria, for which 1,045 high-quality full-length 16S rRNA gene sequences are available (Fig. 2a). Altogether, these data indicate that bacteria from at least 138 genera can be cultured from corals using a variety of different media (12 defined commercial media and various bespoke custom media). While most isolates belong to the phylum *Proteobacteria* (72% of those cultured), strains from *Firmicutes* (14%), *Actinobacteria* (10%), and *Bacteroidetes* (5%) were also recovered. The genera *Ruegeria*, *Photobacterium*, *Pseudomonas*, *Pseudoalteromonas*, *Vibrio*, *Pseudovibrio*, and *Alteromonas* were commonly isolated across studies (see Tables S1, S3, and S4 in the supplemental material). Of 43 genera identified as putative beneficial microbes (proposed in current literature; see examples and references in Table S4),

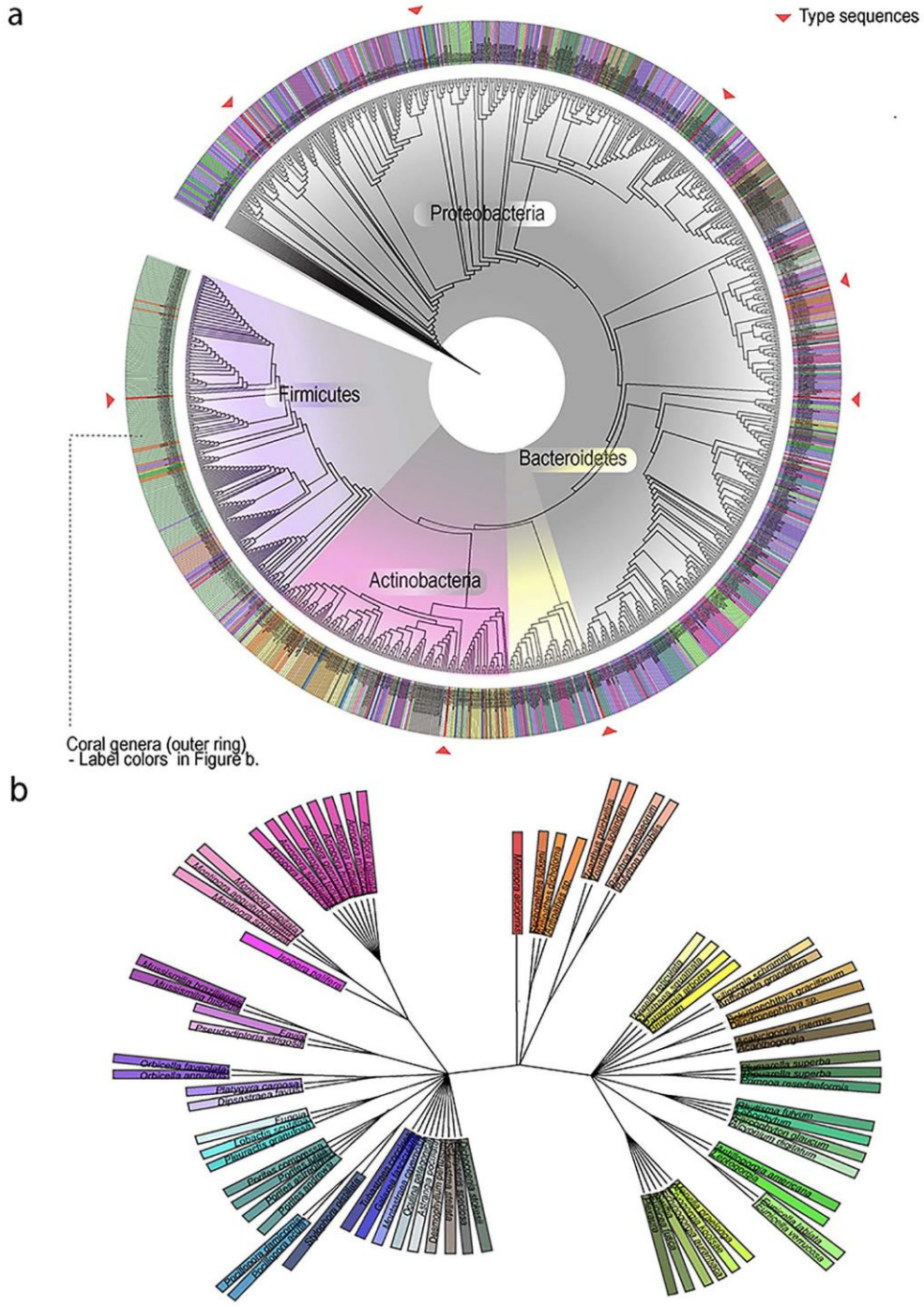

FIG 2 Phylogenetic trees of bacterial strains and coral species. (a) 16S rRNA gene-based phylogenetic inference of 1,045 coral-associated bacterial isolates, plus eight type strains (marked with red arrowheads) representing the species *Vibrio alginolyticus*, *Vibrio bivalvicida*,

(Continued on next page)

58% (i.e., 25 isolates) have been shown to be culturable and are represented in this collection (Table S4). Most of the isolates that have been cultured from diseased corals belong to the family *Vibrionaceae* (*Proteobacteria*). However, it should be noted that many of the studies reporting *Vibrionaceae* focused on a targeted approach to isolate these bacteria. Among the isolates from the phylum *Proteobacteria*, 25.5% were associated with diseased coral colonies, as were 7.4% of the isolates belonging to the phylum *Bacteroidetes*. *Firmicutes* and *Actinobacteria* had the lowest cultivation success from diseased corals, with 5.0% and 0.7%, respectively. Although the majority of the isolates were matched with other representatives in GenBank, 12 were highly divergent with low similarity to known isolates, suggesting that they may be novel genera.

Taxonomic composition of bacterial isolates by culture medium. The taxonomic patterns of the cultured bacterial strains at the phylum, order, and genus levels varied according to the type of medium used to isolate them (Fig. 3). Marine agar (MA) (including its diluted versions) was the most commonly utilized medium across studies and supported the growth of 715 distinct isolates collectively. Bacterial isolates belonging to the families *Vibrionaceae*, *Alteromonadaceae*, *Pseudoalteromonadaceae*, *Rhodobacteraceae*, *Flavobacteriaceae*, and *Micrococcaceae* could all be isolated from MA from a diverse set of coral species. The next most productive nonselective medium was glycerol artificial seawater agar (GASWA), which supported the growth of 572 distinct isolates, while a variety of "custom" media from different laboratories supported the growth of 523 isolates. Interestingly, the latter collection of media, i.e., the custom variants (along with blood agar specifically), favored the retrieval of *Firmicutes* (46.8% of isolates) and *Proteobacteria* representatives (35.2%) at the expense of *Actinobacteria* species (17.6%). In contrast, media commonly deployed to sample a wider bacterial diversity, such as marine agar, favored the growth of several *Proteobacteria* species, usually affiliated with diverse clades within the *Alphaproteobacteria* and *Gammaproteobacteria* classes (Fig. 2 and 3). Curiously, use of thiosulfate-citrate-bile salts-sucrose medium (TCBS) supported the growth of manifold bacterial lineages across the four phyla documented in this study, including *Micrococcus* and *Photobacterium* for example, despite its presumed selectivity for *Vibrio* species.

Bacteria belonging to the phylum *Proteobacteria* (the dominant isolates captured in this study, 72%) could be retrieved from nearly all cultivation media and conditions examined, according to the design and scope of the study (Fig. 2). Members of other abundant phyla, i.e., *Firmicutes*, *Actinobacteria*, and *Bacteroidetes*, also appeared to be cultured on most media (Fig. 3a). Orange serum agar seemed to be selective for *Actinobacteria* (Table S1). The media MA, R2A, and minimal basal agar shared a very similar pattern at the order level, all yielding similar proportions of members from the orders *Vibrionales*, *Rhodobacterales*, *Pseudomonadales*, *Flavobacteriales*, and *Actinomycetales* (Fig. 3). Likewise, LB, blood agar, and the "custom" media shared similar patterns, which included the orders *Vibrionales*, *Pseudomonadales*, *Bacillales*, *Alteromonadales*, and *Actinomycetales* (Fig. 3b). At the genus level, no immediate patterns seemed to be shared among the media (Fig. 3c). The highest number of unique isolates identified to genus level was obtained from MA, which had 115 unique isolates, followed by 55 isolates from custom media, 48 from minimal basal media, and 47 from GASWA (Table S1). However, when dividing the number of different genera by the total number of isolates in each medium, the normalized ratios show that nutrient agar (0.64), followed by dimethylsulfoniopropionate (DMSP)-enriched media (0.54) and R2A (0.4), supported the growth of higher bacterial diversity. Conversely, lowest bacterial diversities were found on TCBS (0.04), Nfb (0.04), and GASWA (0.08). The normalized ratios for each medium (considering all the isolates analyzed here) can be found in Table S1.

FIG 2 Legend (Continued)
Pseudoalteromonas aestuariivivens, *Pseudomonas guariconensis*, *Massilia namucuonensis*, *Vibrionimonas magnilacihabitans*, *Mycetocola tolaasinivorans*, and *Bacillus subtilis*. The colors on the outer ring refer to the coral genus from which the bacteria were isolated, and the background colors in the center refer to the bacteria phyla. (b) Phylogenetic tree of the species of corals used in this study produced via (https://www.ncbi.nlm.nih.gov/Taxonomy/CommonTree/wwwcmt.cgi). The label colors used to identify the genera are linked to the outer ring of Fig. 2A.

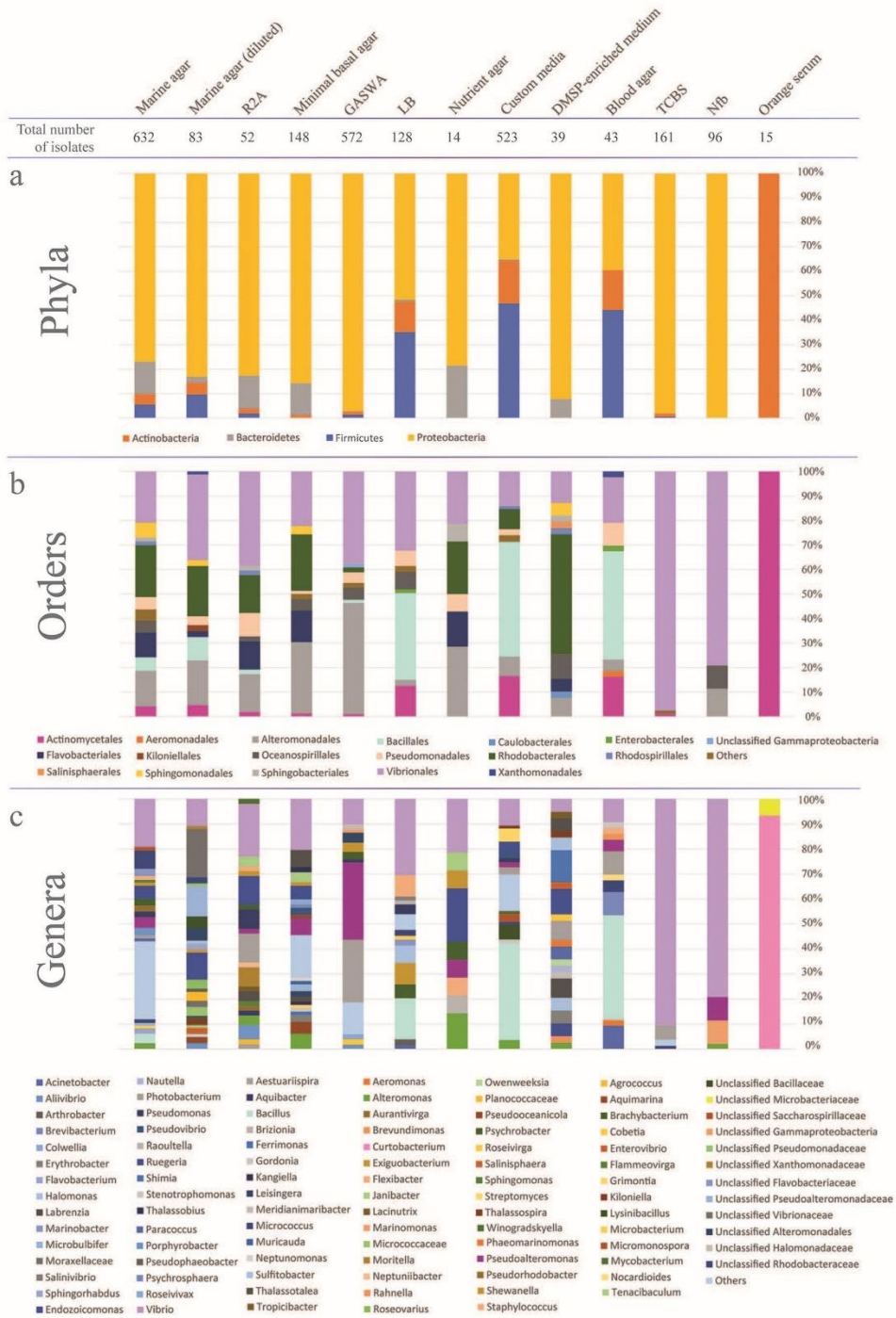

FIG 3 Phylum (a), order (b), and genus (C) level profiles of coral-associated bacteria isolated from each type of culture medium. Taxa (i.e., orders and genera) representing less than 1% of the total percentage of isolates were pulled together and classified as "Others."

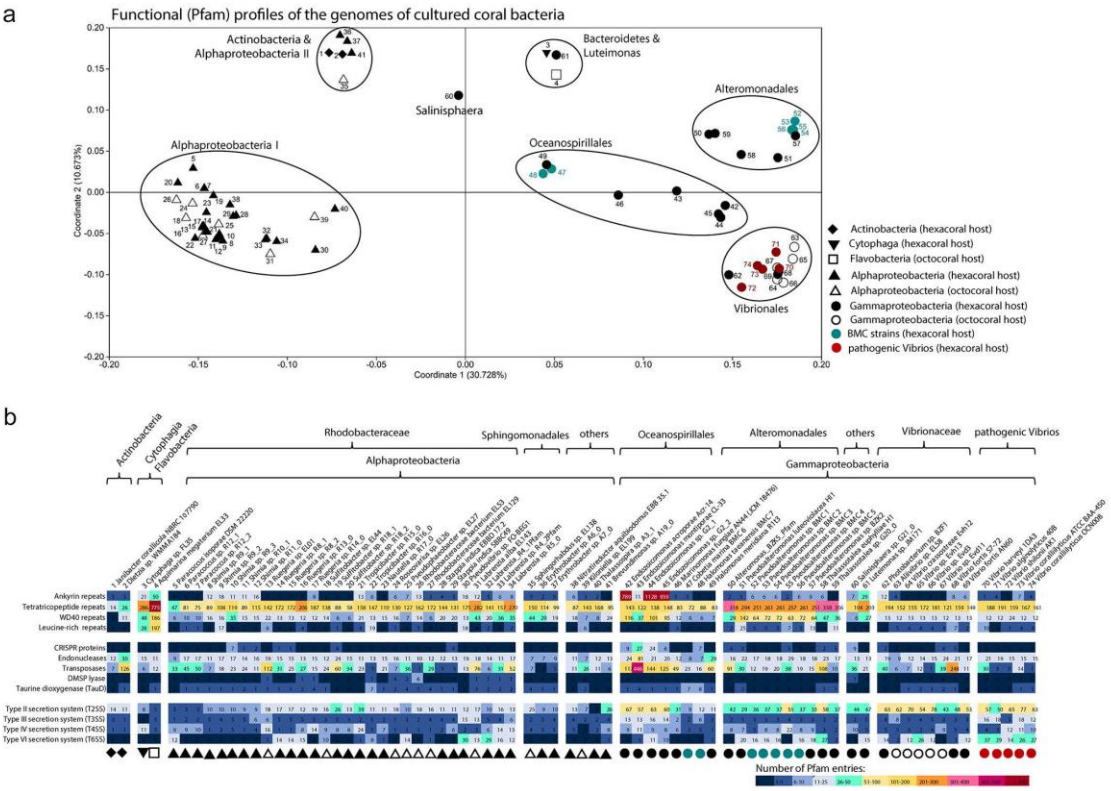

FIG 4 Functional analysis of 74 genomes of cultured coral bacteria according to their protein family (Pfam) profiles. Principal coordinate analysis (PCoA) was performed on the Pfam profiles using the Bray-Curtis similarity matrix calculated from Hellinger-transformed abundance data (a). The ordination is shown in eigenvalue-scale. Symbol shapes indicate the taxonomic class of each genome and the host origin (filled symbols for scleractinian corals; open symbols for octocorals). In addition, BMC bacteria are highlighted in cyan blue, while typical coral pathogens are highlighted in dark red. Isolate numbers (as in panel b) are given next to each symbol. The number of CDSs assigned to Pfam entries related to eukaryote-like proteins "ELPs" (i.e., ankyrin-, tetratricopeptide-, WD40- and leucine-rich repeats) and other features involved in host-microbe interactions are highlighted in the table below (b). The color code from dark blue to dark red reflects an increase in the number of CDSs related to each function. ELPs, CRISPR proteins, endonucleases, transposases, and secretion systems were each represented by more than one Pfam entry across the data set. The CDS counts of these functionally belonging Pfams were summed. The number of Pfams that contributed to each function were as follows: ankyrin repeats, 5 Pfam entries; tetratricopeptide repeats, 21 Pfam entries; WD40 repeats, 6 Pfam entries; leucine-rich repeats, 8 Pfam entries; CRISPR proteins, 21 Pfam entries; endonucleases, 42 Pfam entries; transposases, 37 Pfam entries; T2SS, 17 Pfam entries; T3SS, 19 Pfam entries; T4SS, 15 Pfam entries; T6SS, 18 Pfam entries (see Table S5 in the supplemental material for Pfam identifiers [IDs] and names). In the case of taurine and dimethylsulfoniopropionate (DMSP) catabolism, only one Pfam entry (PF02668.16 and PF16867.5) was found, respectively.

Functional genomics of coral bacterial isolates. A total of 74 cultured coral-associated bacteria had full or draft genomes available; 36 genomes were accessible as of February 2020, with a further 38 genomes now available from this study (Table S2). The genome sizes ranged from 2.71 Mb in *Erythrobacter* sp. strain A06_0 (associated with the scleractinian coral *Acropora humilis*) with only 2,669 coding sequences (CDSs), to 7.28 Mb in *Labrenzia alba* (synonym *Roseibium album*) EL143 (associated with the octocoral *Eunicella labiata*) with 7,593 CDSs (Table S2). The mean and median genome size was 4.77 Mb and 4.71 Mb, respectively. The average GC content of these genomes was 53%, with the lowest GC content (32.9%) found in *Aquimarina megaterium* strain EL33 (isolated from *E. labiata*), and the highest GC content (71.4%) found in *Janibacter corallicola* strain NBRC 107790 (from *Acropora gemmifera*).

Multivariate analysis, based on protein family (Pfam) profiles (Fig. 4a), unsurprisingly showed that the genomes grouped mostly according to their (class level) taxonomic affiliations (permutational multivariate analysis of variance [PERMANOVA], $F = 11.55$, $P =$

0.0001). Exceptions were the two *Actinobacteria* and two *Bacteroidetes* genomes, which clustered with four *Alphaproteobacteria* genomes of the order *Sphingomonadales* and *Caulobacterales* and the *Luteimonas* sp. strain JM171 (*Gammaproteobacteria*) genome, respectively. However, this is likely a reflection of the very low number of genomes available from coral-associated *Actinobacteria* and *Bacteroidetes*, rather than a significant functional overlap between the two phyla. Interestingly, a PERMANOVA analysis performed on the Pfam profiles of the *Vibrionales* genomes revealed that the five *Vibrio* genomes from known pathogens were significantly different from all nonpathogenic *Vibrionaceae* strains ($P = 0.0006$, df = 1, $F = 1.829$) (Table S5).

Functions that potentially have a role in host-microbe interactions, such as proteins containing eukaryote-like domains involved in host-symbiont recognition (11, 64, 65), secretion systems potentially important for host colonization, and biosynthetic gene clusters encoding secondary metabolites were investigated across the isolates (Fig. 4b). Eukaryote-like repeat proteins (ELPs), such as ankyrin repeats, WD40 repeats, tetratricopeptide repeats, and leucine-rich repeats, are widely existing protein motifs which mediate protein-protein interactions. They can be found in all domains of life but are most common in eukaryotes (66–69). The *Endozoicomonas* strains G2_1, G2_2, and Acr-14 had the highest number of ankyrin repeats (>789), and high numbers of WD40 repeats (between 37 and 116). In contrast, ankyrin repeats were absent or only present in low numbers in all *Vibrio* strains. *Alteromonadales* strains (including the *Pseudoalteromonas* BMCs), had high numbers of tetratricopeptide (>250) and 29 to 142 WD40 repeats. The strain with the overall highest number of eukaryote-like repeat protein-related entries (1,367 repeats) was *Endozoicomonas* sp. strain G2_01 from *Acropora cytherea*, closely followed by the octocoral associate *Aquimarina megaterium* EL33 (class *Flavobacteria*) (1,208 repeats). *Endozoicomonas montiporae* strain CL-33 displayed the highest number of domains related to antiviral defense mechanisms, such as CRISPR proteins and endonucleases, which are known to be enriched in the microbiomes of marine sponges (65, 70) and healthy octocorals (11). Further, 49 out of the 74 genomes assessed harbored the TauD (PF02668) gene. TauD is involved in the degradation of host-derived taurine (an amino-sulfonic acid widely distributed in animal tissue) into sulfide which is then assimilated into microbial biomass (71–73). An elevated number of TauD-encoding CDSs was found in the two BMC strains *Cobetia marina* BMC6 and *Halomonas tateanensis* BMC7, both isolated from *Pocillopora damicornis*. Further, several isolates ($N = 11$) of the *Rhodobacteraceae* family (*Alphaproteobacteria*) contained CDSs involved in dimethylsulfoniopropionate (DMSP) degradation, potentially contributing to sulfur cycling in corals.

Among secretion systems, type II (T2SS), III (T3SS), IV (T4SS), and VI (T6SS), known to be involved in host colonization (74), horizontal gene transfer (75), or interbacterial antagonism and/or virulence (76), dominated the genomes of coral-associated bacteria. We found a high number of entries related to T2SS in the *Gammaproteobacteria* associates, particularly in the *Endozoicomonas* and *Vibrio* genomes (see reference 77 for roles of the T2SS in symbiosis and pathogenicity). The *Vibrionales* genomes were further characterized by an elevated number of T6SS-related Pfam domains, whereby the five pathogenic *Vibrio* strains encoded a significantly higher number of T6SS domains (mean of 27 T6SS domains in CDSs) than the six nonpathogenic *Vibrio* strains (mean of 10 T6SS domains in CDSs; Mann-Whitney U-test, $P = 0.0126$).

We also assessed the secondary metabolite coding potential in the 74 genomes. AntiSMASH v.5.0 detected a total of 416 biosynthetic gene clusters (BGCs) across all genomes, whereby the number of BGCs varied substantially between strains, from no BGCs in *Endozoicomonas montiporae* CL-33 to 12 BGCs in *Pseudoalteromonas luteoviolacea* HI1 (Fig. 5). Bacteriocin clusters ($N = 75$), found in 81% of the strains, were the most frequently detected BGCs, followed by homoserine lactone ($N = 62$; in 43% of strains), nonribosomal peptide synthetase (NRPS; $N = 59$; in 51% of strains), beta-lactone ($N = 46$; in 53% of strains), terpene ($N = 34$; in 38% of strains), ectoine ($N = 28$; in 35% of strains), and siderophore ($N = 25$; in 28% of strains) clusters. The relatively large

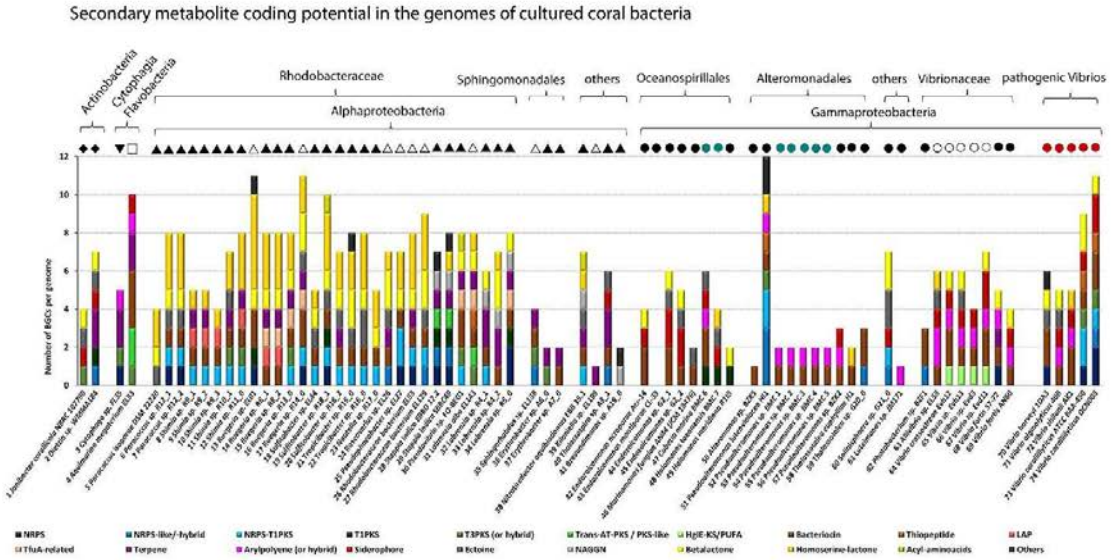

FIG 5 Distribution of biosynthetic gene clusters (BGCs) across 74 genomes of cultured coral bacteria. BGC counts per compound class were obtained using antiSMASH v.5.0 with default settings (and all extra features on). NAGGN, *N*-acetylglutaminylglutamine amide; LAP, linear azol(in)e-containing peptide; hglE-KS, heterocyst glycolipid synthase-like PKS; PUFA, polyunsaturated fatty acids; NRPS, nonribosomal peptide synthetase cluster; PKS, polyketide synthase cluster; TfuA-related, TfuA-related ribosomal peptides. The category "Others" comprises rare BGCs that had each less than three entries across the data set (among those were furan, ladderane-hybrid, phosphonate, polybrominated diphenyl ethers, lassopeptide, lanthipeptide, and butyrolactone BGCs). Symbol shapes above bars indicate the taxonomic class and the host origin of each genome (same as in Fig. 4).

group of coral-associated *Rhodobacteraceae* genomes analyzed in this study presented a consistently rich BGC profile, characterized by the presence of bacteriocin, homoserine lactone, and NRPS-T1PKS clusters, while siderophore clusters were typically absent in this group. Siderophores were typically found in the *Vibrio* genomes of this study as well as in three of the four *Endozoicomonas* genomes. Characteristic for all *Pseudoalteromonas* genomes, including the BMC strains, was the presence of aryl polyene clusters, a compound class functionally related to antioxidative carotenoids (78). The absence of known BGC in the genome of *E. montiporae* CL-33 is an unusual outcome, as for example the closely related strains in the *Oceanospirillales* order usually display >4 BGCs (Fig. 5). The *E. montiporae* CL33 genome is complete (100% completeness, 0.9% contamination, 95.5% quality; 1 contig); hence, low assembly quality—which sometimes compromises the identification of large BGCs—does not explain the lack of BGCs in this genome.

DISCUSSION

Here, we show that a taxonomically diverse array of bacteria can be isolated using a variety of medium and culture conditions. A total of 138 of these isolates (recruited from 52 studies) have been formally described, and at least 12 are putatively novel bacterial genera. It is promising that such extensive phylogenetic diversity can be captured from a limited number of culture media employed in the examined studies. Additional diversity is therefore likely to be captured through the implementation of alternative cultivation procedures that may improve our capacity to cultivate the "as-yet-uncultured" (28). Testimony to this is the observation that most of the strains assigned to the phylum *Firmicutes* in our meta-analysis were obtained almost exclusively from the various "custom media" utilized by different laboratories and blood agar alone, illustrating how diversification in cultivation design can widen the phylogenetic spectrum of the organisms isolated. In this regard, we anticipate that broader phylogenetic diversity will be gained within the culturable fraction if gradients in aerophilic conditions, temperature, and other physicochemical parameters are attempted along with innovative, less invasive

techniques to extract microbial cells from the host matrix. The richness of bacterial phyla uncovered in this study corresponds to the phyla more often reported to dominate bacterial communities in corals by cultivation-independent studies (12), namely, *Proteobacteria*, *Bacteroidetes*, *Actinobacteria*, and *Firmicutes*, yet how diversity at lower taxonomic ranks within each phylum is captured remains to be determined. Another exciting challenge ahead is the unveiling of host-microbe and microbe-microbe molecular interdependence networks (e.g., cross-kingdom signaling and cross-feeding cascades) (79, 80). Such knowledge would likely enable laboratory captivation of so-far "unculturable" coral-specific or enriched lineages. Increasing the diversity of these coral-associated culturable bacteria will likely help in the identification of genomic features that could underpin the interaction with the host and its microbiome representing the foundation for experimental validation.

Although one of the initial aims of this study was to ascertain the percentage of culturable bacteria from a given coral species, it was deemed too speculative to report the findings due to variation in culture effort across the various studies. Indeed, this highlights the paucity of studies dedicated to determine exactly this, and there is a need for such mechanistic projects deploying multiple culture media and conditions to comprehensively sample bacterial associates from a single or a few host species. Collectively, studies aimed at capturing the culturable microbiome will extend our understanding of coral bacterial communities and their putative function in the coral holobiont. A catalog of cultures (as presented here and one which will hopefully be expanded) provides a means to increase our understanding of host-symbiote relationships. The ability to describe, understand, and culture specific symbionts from any given organism (like corals) also opens up the potential to utilize them as probiotics to restore degraded habitats (53, 61). For example, specific traits found in certain coral-associated bacteria, such as the presence of the genes *nifH* (nitrogenase), *nirK* (nitrite reductase), or *dmdA* (DMSP demethylase) involved in nitrogen and sulfur cycling, or those known to control pathogens, the enzymatic mitigation of reactive oxygen species (ROS) or other toxic compounds, may have roles in increasing coral health when the host is experiencing stress (53, 63, 81, 82). Identifying these traits via molecular analyses and laboratory tests using cultured bacteria with defined coral hosts will allow for the more rapid administration of native bacteria with the potential to help rehabilitate damaged corals. In addition, such a resource increases the possibility of identifying novel compounds of biotechnological interest (83). This seems particularly relevant in the case of coral-microbe symbioses, which are known to rank as one of the most prolific sources of bioactive molecules in the oceans (38).

A search in public databases (National Center for Biotechnology Information [NCBI]) found that, despite the 1,045 cultured coral-associated bacterial sequences with full-length 16S rRNA gene sequences, only 36 had genomes available as of February 2020. Clearly, a systematic effort to disclose the genomic features of coral-associated bacteria is needed in order to better understand the holobiont ecology and identify potentially beneficial microbes. As part of this study, we were able to add a further 38 to this tally (see Table S2 in the supplemental material). Even with this addition, the number of publicly available coral-associated bacterial genomes remains scant, and it is recognized that to more fully understand the roles of the cultivable fraction of coral bacteria, a thorough characterization of the species kept in culture, including genome sequencing, needs to be fostered alongside experimental biology and manipulative approaches. Moreover, a large collection of coral-associated genomes could also help to identify specific traits that are needed to thrive in the various niches within the hosts or point to those bacteria which offer a specific benefit to their host.

All of the available genomes were screened for an array of functions potentially important in establishing and maintaining interactions between bacterial symbionts and their marine invertebrate hosts. Overall, the *Endozoicomonas* and *Pseudoalteromonas* strains displayed high numbers of eukaryote-like protein-encoding genes important for host-symbiont recognition in well-studied systems such as marine sponges (65, 84, 85). The strain with the second highest number of eukaryote-like repeat protein-related

entries (1,208 CDSs, after *Endozoicomonas* sp. G2_1 with 1,367 CDSs) was the octocoral associate *Aquimarina* sp. strain EL33 (class *Flavobacteria*). In the current culture collection, 15 additional *Aquimarina* isolates are reported, from the scleractinian corals *Porites lutea*, *Pocillopora acuta*, *Stylophora pistillata*, *Acropora millepora*, *Acropora tenuis*, and the octocoral *E. labiata*. Retrieving the genomes from these candidates will allow us to explore these emerging patterns in greater detail. For example, a recent comparative genomics survey of host-associated and free-living *Aquimarina* species revealed complex secondary metabolite biosynthesis and polycarbohydrate degradation capacities (86), but further investigation into their mechanisms of interactions with corals is warranted.

Only eight *Endozoicomonas* isolates (five of them type species) have so far been cultured from corals (according to our collated information). These are from the octocorals *Eunicea fusca* and *Plexaura* sp. and the scleractinian corals *Montipora aequituberculata*, *Acropora cytherea*, *Acropora hemprichii*, and *Acropora* sp. To date, only four of these (two from this study) have had their genomes sequenced (all from scleractinian corals) (18, 87). This is surprising given that numerous studies found that this genus is highly abundant in the healthy coral holobiont and seems to decrease in abundance upon deteriorating environmental conditions (e.g., reviewed in references 35, 88, and 89). Future cultivation efforts should therefore be directed toward the *Endozoicomonadaceae* family in order to increase the representation of their taxonomic and functional diversity in culture collections (29). In this regard, this study finds evidence that supplementing culture media with DMSP is an approach worth investing in future attempts to cultivate coral-associated *Endozoicomonas*, possible in combination with growth at lower temperatures (29). The metabolic data obtained from the comparative analysis of these four strains can be used, for example, to drive the selection of specific nutrients and conditions required to culture this particular genus of coral symbionts. Furthermore, there are 55 cultured *Pseudoalteromonas* strains in our collection which should also be explored regarding their symbiotic properties and their functional gene content (only 6 genomes currently available). Similar to *Endozoicomonas*, *Pseudoalteromonas* species are also frequent members of coral-associated microbiomes (35). A number of *Pseudoalteromonas* have been shown to display high antimicrobial activity, and many of these bacteria are isolated from coral mucus, lending support to the protective role the surface mucous layer has for the host and its importance in the coral holobiont's defense—against bacterial coral pathogens in particular (90). Indeed, five of the six *Pseudoalteromonas* (where genomes are available) were shown to be effective BMCs when corals were challenged with the coral pathogen *Vibrio coralliilyticus* (53).

Having genomes available from the potential pathogens also allows for greater insight into coral biology, especially when interested in ascertaining pathogenicity-related traits (91, 92). For example, from the 11 *Vibrio* species for which genomic data were available, we were able to show functional separation (based on Pfam profiles) of known pathogenic and nonpathogenic strains. This was further accompanied by a significantly higher abundance of CDSs encoding for the type VI secretion system, important for virulence in the pathogenic strains (76). Prevalence of siderophore-encoding genes was also noted in the *Vibrionaceae* strains, suggesting that these bacteria likely gain competitive advantages through efficient and extensive iron acquisition, which is a trait often seen in opportunistic and pathogenic bacteria (93, 94). Hypothetically, the selection of beneficial microbes that are also good siderophore producers could add to the biological control of these pathogens. Indeed, two proposed BMC strains *Cobetia marina* BMC6 and *Halomonas taenensis* BMC7 harbor such siderophore clusters on their genomes and so did three of the four *Endozoicomonas* strains. However, the five *Pseudoalteromonas* BMC strains and the *Endozoicomonas montiporae* CL-33 had low numbers of BGCs, possibly indicating a reduced investment into secondary metabolism. Indeed, the low number of BGCs in these *Pseudoalteromonas* strains is in contrast to the established prevalence of biologically active compounds in many marine host-associated *Pseudoalteromonas* strains (95). In part, this may reflect a limitation of the

software utilized to detect genes for all secondary metabolites, as genes for common metabolites (such as for the production of the antibiotic marinocin and those that produce tetrabromopyrrole coral larval settlement cues by *Pseudoalteromonas* [96, 97]) were not picked up. These bioinformatic limitations emphasize the importance of having bacterial cultures for the elucidation of the chemical ecology underpinning coral holobiont functioning.

Broader functional traits can also be ascertained from looking at the complete picture of isolates with annotated genomes. For example, 66% (49 out of 74) harbored the TauD gene, which is involved in taurine utilization (98). Two proposed BMCs, the *Cobetia marina* BMC7 and *Halomonas taeanensis* BMC7, revealed the highest copy number of TauD CDSs (seven and eight, respectively), while others range between one and five TauD copies. Taurine is an organo-sulfur compound widely present in animal tissues, and recent research has shown that obligate symbionts of sponges have enriched copies of taurine catabolism genes and taurine transporters in comparison with free-living bacteria (65, 72, 73). The widespread capability of the isolates studied here to potentially utilize host-derived taurine could guide the formulation of novel, taurine-containing cultivation media in the attempt to captivate coral symbionts, particularly from the important, yet underrepresented order *Oceanospirillales* (TauD was consistently present in all *Oceanospirillales* genomes [$N = 8$] analyzed here). The ubiquitous occurrence of bacteriocin clusters among the genomes is another example of broad-scale trends which we have identified in our genome meta-analysis. These may confer the specific culturable symbionts with particular competitive capacities toward closely related taxa in highly dense microbiomes (99, 100), as is commonly identified across corals and sponges. Moreover, the widespread presence of NRPS and beta-lactone clusters hints toward broad-spectrum antimicrobial and cytotoxic capabilities in multiple associates. It also corroborates the hypothesis that these marine metaorganisms are promising sources of novel bioactive compounds, representing targets for bioprospection (38). Many strains also possess homoserine lactone-encoding BGCs indicative of sophisticated, cell-density-dependent chemical communication mechanisms. Antioxidant activities are likely conferred by the presence of aryl polyene BGCs in the genomes (78, 101). These pigment type compounds, functionally related to carotenoids, characterized most of the proposed BMC strains. Furthermore, several coral-associated bacteria of different taxonomic origins are seemingly well equipped to handle osmotic stress as revealed by the occurrence of ectoine- and *N*-acetylglutaminylglutamine amide (NAGGN)-encoding genes. Therefore, there is a need to continue the effort in culturing coral-associated bacteria to explore new biosynthetic potentials, both for bioprospecting purposes and for better understanding the chemical ecology of the metaorganism.

Identifying likely candidates for symbiosis is one challenge, but once the candidates are confirmed and characterized, the need to understand how the animal host establishes symbiosis and retains the relationship will also be critical. However, this is a two-way street. Current research in sponges has revealed that bacteria expressing the ankyrin genes avoid phagocytosis by sponge amoebocytes, thus becoming residents of the sponge microbiome by evading the host's immune system (64, 70). Further, as ankyrin repeats are enriched in the microbial metagenomes of healthy corals (10, 11), it is expected that commensal coral-associated bacteria also use this aspect of ankyrin genes to establish symbiosis. The evolutionary forces shaping the symbiosis are even trickier here, as bacteriophages encode for ankyrin biosynthesis in their genomes and might transfer this information across different community members (70). As identified above with siderophore-encoding genes, similar patterns of symbiosis establishment and energy utilization may be adopted by both commensal and pathogenic bacteria.

To conclude, here we have highlighted that diverse coral-associated bacteria are already cultured, although these are often scattered across collections and rarely collated into one easily accessible location. Further, only a few of these have had their genomes sequenced. Despite the lack of genomes, we were able to identify a number of genetic features commonly encoded by these coral bacterial associates. These

features include broad-spectrum antimicrobial, antioxidant, and cytotoxic compound production capabilities, high abundance of ankyrin repeat entries, tetratricopeptide, and WD40 repeats, and taurine degradation genes. That said, this can only be quantitatively assessed through comparison of metagenome profiles from corals versus other environments, such as sediments and seawater in a comprehensive fashion (several samples with replication, etc.). Such metagenome-based analyses should be complemented by (large-scale) marker gene surveys and/or visualization techniques to determine the nature and holobiont site of bacterial association, in particular since any metaorganism (configuration) is specific to a time and place and not static given the temporal ("fluidic") nature of host-microbe interactions (102). Even though the statistical power, with only part of the representative genomes available from cultures (as in this study), is limited, we exemplify here the importance of the cultured bacterial fraction of corals in hypothesis testing and applied microbiology.

We end by highlighting the importance and need for a global initiative to create an online catalog of genomic and physiological features of cultured coral-associated bacteria. Combining the use of these genomic insights with innovative culturing techniques (37), aimed at improving the collection of coral-associated bacterial isolates, will see this field of coral biology move forward. Such an initiative should likely start with those microbes which have their complete genomes sequenced. This study pioneers the organization of such a global collection, as part of the efforts from the Beneficial Microbes for Marine Organisms network (BMMO), through a public invitation to researchers working in this field. As a result, we have here provided a list of cultured bacteria from corals that are currently available in public databases, plus isolates that were kept in collections from all the laboratories that responded to our invitation (Table S1 and available now, open access via http://isolates.reefgenomics.org). Now other researchers can access this virtual collection and/or contact specific laboratories for collaborations or solicitations of specific microbial strains.

MATERIALS AND METHODS

Literature search and data curation. Google Scholar and the National Center for Biotechnology Information (NCBI) were searched for publicly available 16S rRNA gene sequences of cultured coral-associated bacteria (as of 2018). Search terms, including coral, bacteria, 16S, and culture, were utilized as well as combinations of these. The results were supplemented with data from culture collections from laboratories around the world through a public invitation to researchers working in this field. In total, we were able to obtain bacterial isolates originating from 84 coral species (representing tropical, temperate, and cold-water habitats) from all major oceans (Fig. 1; see also Table S1 in the supplemental material). Due to the number and varied nature of the different contributing sources of these isolates, parts of the associated metadata for certain cultures are missing or incomplete.

Phylogenetic analysis and tree generation. In total, we were able to collate 3,055 individual isolates which had (at least) part of the 16S rRNA gene sequenced (see Table S1 for details). We selected only high-quality sequences by removing those shorter than 500 bp, or longer than 1,600 bp and containing more than one ambiguity. Further, we utilized the mothur (v.1.42.0) commands screen.seqs and filter.seqs to remove poorly aligned sequences and positions without sequence information, respectively (103). This resulted in 1,045 isolates with near full-length 16S rRNA gene sequences, which were used in downstream phylogenetic analyses. To this end, sequences were aligned using the SILVA 138.1 database as a reference (104), and the clear-cut command was used within mothur to generate a phylogenetic tree using the relaxed neighbor-joining method (RNJ) (105, 106). To generate the distance matric, the default of percent identities (so-called p-distances) was retained.

A phylogenetic tree of coral species was also generated using the Taxonomy Common Tree tool of NCBI (107). Species names were added manually to create a tree file. Tree features were optimized using iTOL v4 (108).

Taxonomic composition of bacterial isolates by medium. Bacterial strains listed in Table S1 were sorted by isolation medium and subsequently grouped at phylum, order, and genus levels according to the current SILVA (138.1) taxonomy (104). Stacked column graphs, showing relative abundances of the cultivated taxa were created thereafter. At the genus level, all groups representing less than 1% of the total pool in each medium were included in a group labeled "others."

Genome analysis. The integrated Microbial Genomes and Microbiomes database (IMG; https://img.jgi.doe.gov/) (109) from the Department of Energy's Joint Genome Institute (DOE-JGI), and the assembly database from NCBI (https://www.ncbi.nlm.nih.gov/assembly) were searched for publicly available genomes from cultured coral bacteria in February 2020. Thirty-six bacterial genome assemblies (21 from scleractinian coral and 15 from octocoral associates) were downloaded from NCBI and included in this analysis. The annotation of genomic features such as genome size, GC content, and number of coding

sequences (CDSs) was performed for all 74 genomes with the RAST server (110) (see Table S2). Protein families (Pfams) were predicted with the online server WebMGA (default settings) (111) using amino acid sequence files obtained from RAST. The resulting individual Pfam annotation files were then joined using a customized R script and the resulting count tables were Hellinger transformed for multivariate analyses (see Table S5). Dissimilarity between genomes based on the Pfam profiles were then calculated using the Bray-Curtis index. Ordination of the genomes based on their functional profiles was carried out using principal coordinate analysis (PCoA) and plotted in eigenvalue scale (i.e., scaling of each axis using the square root of the eigenvalue) with PAST software v3.25 (112). PERMANOVAs (permutational multivariate analyses of variance) were performed with 999 permutations to test for overall differences in functional profiles between bacterial genomes from different taxonomic classes. Five groups (classes) were used: *Alphaproteobacteria*, *Gammaproteobacteria*, *Actinobacteria*, *Cytophagia*, and *Flavobacteriia*. A separate PERMANOVA analysis of Bray-Curtis dissimilarities calculated for the 11 available *Vibrio* genomes was then performed in order to highlight differences between strains identified as potentially pathogenic ($N = 5$, group 1) and those apparently nonpathogenic ($N = 6$, group 2) (identification of pathogenicity from available literature—see references). Finally, AntiSMASH version 5.0 (113) was used with default parameters (and extra features "All on") to identify biosynthetic gene clusters (BGCs) in all genomes.

Data availability. The newly described genomes associated with this project (38 in total; also see Table S2) can be found in the following BioProjects on NCBI: accession no. PRJNA698462, PRJNA638634, and PRJNA343499.

SUPPLEMENTAL MATERIAL

Supplemental material is available online only.

FIG S1, JPG file, 0.6 MB.

TABLE S1, XLSX file, 0.8 MB.

TABLE S2, XLSX file, 0.03 MB.

TABLE S3, XLSX file, 0.02 MB.

TABLE S4, XLSX file, 0.01 MB.

TABLE S5, XLSX file, 2.1 MB.

ACKNOWLEDGMENTS

Part of this research was carried out in association with the ongoing R&D project registered as ANP 21005-4, "PROBIO-DEEP - Survey of potential impacts caused by oil and gas exploration on deep-sea marine holobionts and selection of potential bioindicators and bioremediation processes for these ecosystems" (UFRJ/Shell Brasil/ANP), sponsored by Shell Brasil under the ANP R&D levy as "Compromisso de Investimentos com Pesquisa e Desenvolvimento." This research project won the Great Barrier Reef Foundation's Out of the Blue Box Reef Innovation Challenge People's Choice Award supported by The Tiffany & Co. Foundation. The Institute of Bioengineering and Biosciences acknowledges funding provided by the Portuguese Foundation for Science and Technology (FCT) and the European Regional Development Fund (ERDF) through grant UIDB/04565/2020. Part of this work was supported by the research grant FA_05_2017_032 conceded to R.C. and T.K.-C. by the Portuguese Ministry of the Sea (Direção Geral de Política do Mar) under the program "Fundo Azul." T.K.-C. is the recipient of a Research Scientist contract with FCT (CEECIND/00788/2017). N.Z. and K.H.S. were supported in part by the INBRE-NIGMS by NIH grant P20GM103430.

M.S. designed the initial study and led the collection, analysis, and write-up of the paper. H.V. conducted the majority of the analysis on the 16S data, and T.K.-C. and R.C. conducted the majority of the analysis of the genome data. S.R. assisted with the meta-analysis component of the project, and R.P. co-funded the project with M.S. All authors assisted with data collection, analysis, and writing/editing.

We declare there are no known conflicts of interest associated with this study.

REFERENCES

1. Doolittle F, Inkpen AS. 2018. Processes and patterns of interaction as units of selection: an introduction to ITSNTS thinking. Proc Natl Acad Sci U S A 115:4006–4014. https://doi.org/10.1073/pnas.1722232115.
2. van Oppen MJH, Medina M. 2020. Coral evolutionary responses to microbial symbioses. Philos Trans R Soc Lond B Biol Sci 375:20190591. https://doi.org/10.1098/rstb.2019.0591.
3. Bang C, Dagan T, Deines P, Dubilier N, Duschl WJ, Fraune S, Hentschel U, Hirt H, Hülter N, Lachnit T, Picazo D, Pita L, Pogoreutz C, Rädecker N, Saad MM, Schmitz RA, Schulenburg H, Voolstra CR, Weiland-Bräuer N, Ziegler M, Bosch TCG. 2018. Metaorganisms in extreme environments: do microbes play a role in organismal adaptation? Zoology (Jena) 127:1–19. https://doi.org/10.1016/j.zool.2018.02.004.

4. Bosch TCG, McFall-Ngai MJ. 2011. Metaorganisms as the new frontier. Zoology (Jena) 114:185–190. https://doi.org/10.1016/j.zool.2011.04.001.
5. Rohwer F, Seguritan V, Azam F, Knowlton N. 2002. Diversity and distribution of coral-associated bacteria. Mar Ecol Prog Ser 243:1–10. https://doi.org/10.3354/meps243001.
6. Littman RA, Willis BL, Pfeffer C, Bourne DG. 2009. Diversities of coral-associated bacteria differ with location, but not species, for three acroporid corals on the Great Barrier Reef. FEMS Microbiol Ecol 68:152–163. https://doi.org/10.1111/j.1574-6941.2009.00666.x.
7. Shashar N, Cohen Y, Loya Y, Sar N. 1994. Nitrogen fixation (acetylene reduction) in stony corals: evidence for coral-bacteria interactions. Mar Ecol Prog Ser 111:259–264. https://doi.org/10.3354/meps111259.
8. Ritchie KB, Smith GW. 1995. Preferential carbon utilization by surface bacterial communities from water mass, normal, and white-band diseased Acropora. Mol Mar Biol Biotechnol 4:345–352.
9. Hernandez-Agreda A, Leggat W, Ainsworth TD. 2019. A place for taxonomic profiling in the study of the coral prokaryotic microbiome. FEMS Microbiol Lett 366:fnz063. https://doi.org/10.1093/femsle/fnz063.
10. Robbins SJ, Singleton CM, Chan CX, Messer LF, Geers AU, Ying H, Baker A, Bell SC, Morrow KM, Ragan MA, Miller DJ, Forêt S, ReFuGe2020 Consortium, Voolstra CR, Tyson GW, Bourne DG. 2019. A genomic view of the reef-building coral Porites lutea and its microbial symbionts. Nat Microbiol 4:2090–2100. https://doi.org/10.1038/s41564-019-0532-4.
11. Keller-Costa T, Lago-Lestón A, Saraiva JP, Toscan R, Silva SG, Gonçalves J, Cox CJ, Kyrpides N, Nunes da Rocha U, Costa R. 2021. Metagenomic insights into the taxonomy, function, and dysbiosis of prokaryotic communities in octocorals. Microbiome 9:72. https://doi.org/10.1186/s40168-021-01031-y.
12. Huggett MJ, Apprill A. 2019. Coral microbiome database: integration of sequences reveals high diversity and relatedness of coral-associated microbes. Environ Microbiol Rep 11:372–385. https://doi.org/10.1111/1758-2229.12686.
13. Ziegler M, Seneca FO, Yum LK, Palumbi SR, Voolstra CR. 2017. Bacterial community dynamics are linked to patterns of coral heat tolerance. Nat Commun 8:14213. https://doi.org/10.1038/ncomms14213.
14. Neave MJ, Rachmawati R, Xun L, Michell CT, Bourne DG, Apprill A, Voolstra CR. 2017. Differential specificity between closely related corals and abundant Endozoicomonas endosymbionts across global scales. ISME J 11:186–200. https://doi.org/10.1038/ismej.2016.95.
15. Shibl AA, Isaac A, Ochsenkühn MA, Cárdenas A, Fei C, Behringer G, Arnoux M, Drou N, Santos MP, Gunsalus KC, Voolstra CR, Amin SA. 2020. Diatom modulation of select bacteria through use of two unique secondary metabolites. Proc Natl Acad Sci U S A 117:27445–27455. https://doi.org/10.1073/pnas.2012088117.
16. Romano S, Schulz-Vogt HN, González JM, Bondarev V. 2015. Phosphate limitation induces drastic physiological changes, virulence-related gene expression, and secondary metabolite production in Pseudovibrio sp. strain FO-BEG1. Appl Environ Microbiol 81:3518–3528. https://doi.org/10.1128/AEM.04167-14.
17. Raina JB, Tapiolas D, Motti CA, Foret S, Seemann T, Tebben J, Willis BL, Bourne DG. 2016. Isolation of an antimicrobial compound produced by bacteria associated with reef-building corals. PeerJ 4:e2275. https://doi.org/10.7717/peerj.2275.
18. Neave MJ, Michell CT, Apprill A, Voolstra CR. 2017. Endozoicomonas genomes reveal functional adaptation and plasticity in bacterial strains symbiotically associated with diverse marine hosts. Sci Rep 7:40579. https://doi.org/10.1038/srep40579.
19. Karimi E, Keller-Costa T, Slaby BM, Cox CJ, da Rocha UN, Hentschel U, Costa R. 2019. Genomic blueprints of sponge-prokaryote symbiosis are shared by low abundant and cultivatable Alphaproteobacteria. Sci Rep 9:1999. https://doi.org/10.1038/s41598-019-38737-x.
20. Staley JT, Konopka A. 1985. Measurement of in situ activities of nonphotosynthetic microorganisms in aquatic and terrestrial habitats. Annu Rev Microbiol 39:321–346. https://doi.org/10.1146/annurev.mi.39.100185.001541.
21. Amann RI, Ludwig W, Schleifer KH. 1995. Phylogenetic identification and in situ detection of individual microbial cells without cultivation. Microbiol Rev 59:143–169. https://doi.org/10.1128/mr.59.1.143-169.1995.
22. Hugenholtz P, Goebel BM, Pace NR. 1998. Impact of culture-independent studies on the emerging phylogenetic view of bacterial diversity. J Bacteriol 180:4765–4774. https://doi.org/10.1128/JB.180.18.4765-4774.1998.
23. Wang F, Li M, Huang L, Zhang X-H. 2021. Cultivation of uncultured marine microorganisms. Mar Life Sci Technol 3:117–120. https://doi.org/10.1007/s42995-021-00093-z.
24. Stewart EJ. 2012. Growing unculturable bacteria. J Bacteriol 194:4151–4160. https://doi.org/10.1128/JB.00345-12.
25. Suzuki MT, Rappé MS, Haimberger ZW, Winfield H, Adair N, Ströbel J, Giovannoni SJ. 1997. Bacterial diversity among small-subunit rRNA gene clones and cellular isolates from the same seawater sample. Appl Environ Microbiol 63:983–989. https://doi.org/10.1128/AEM.63.3.983-989.1997.
26. Lagier JC, Edouard S, Pagnier I, Mediannikov O, Drancourt M, Raoult D. 2015. Current and past strategies for bacterial culture in clinical microbiology. Clin Microbiol Rev 28:208–236. https://doi.org/10.1128/CMR.00110-14.
27. Pham VHT, Kim J. 2012. Cultivation of unculturable soil bacteria. Trends Biotechnol 30:475–484. https://doi.org/10.1016/j.tibtech.2012.05.007.
28. Lewis WH, Tahon G, Geesink P, Sousa DZ, Ettema TJG. 2021. Innovations to culturing the uncultured microbial majority. Nat Rev Microbiol 19:225–240. https://doi.org/10.1038/s41579-020-00458-8.
29. Pogoreutz C, Voolstra CR. 2018. Isolation, culturing, and cryopreservation of Endozoicomonas (Gammaproteobacteria: Oceanospirillales: Endozoicomonadaceae) from reef-building corals. protocols.io. https://doi.org/10.17504/protocols.io.t2aeqae.
30. Raina JB, Tapiolas D, Willis BL, Bourne DG. 2009. Coral-associated bacteria and their role in the biogeochemical cycling of sulfur. Appl Environ Microbiol 75:3492–3501. https://doi.org/10.1128/AEM.02567-08.
31. Keller-Costa T, Eriksson D, Gonçalves JMS, Gomes NCM, Lago-Lestón A, Costa R. 2017. The gorgonian coral Eunicella labiata hosts a distinct prokaryotic consortium amenable to cultivation. FEMS Microbiol Ecol 93:143. https://doi.org/10.1093/femsec/fix143.
32. Sweet MJ, Croquer A, Bythell JC. 2011. Bacterial assemblages differ between compartments within the coral holobiont. Coral Reefs 30:39–52. https://doi.org/10.1007/s00338-010-0695-1.
33. Pollock FJ, McMinds R, Smith S, Bourne DG, Willis BL, Medina M, Thurber RV, Zaneveld JR. 2018. Coral-associated bacteria demonstrate phylosymbiosis and cophylogeny. Nat Commun 9:4921. https://doi.org/10.1038/s41467-018-07275-x.
34. Pernice M, Raina JB, Rädecker N, Cárdenas A, Pogoreutz C, Voolstra CR. 2020. Down to the bone: the role of overlooked endolithic microbiomes in reef coral health. ISME J 14:325–334. https://doi.org/10.1038/s41396-019-0548-z.
35. Sweet MJ, Bulling MT. 2017. On the importance of the microbiome and pathobiome in coral health and disease. Front Mar Sci 4:9.
36. Pogoreutz C, Voolstra CR, Rädecker N, Weis V, Cardenas A, Raina J-B. 2021. The coral holobiont highlights the dependence of cnidarian animal hosts on their associated microbes, p 91–118. *In* Bosch TCG, Hadfield MG (ed), Cellular dialogues in the holobiont. CRC Press, Boca Raton, FL.
37. Modolon F, Barno AR, Villela HDM, Peixoto RS. 2020. Ecological and biotechnological importance of secondary metabolites produced by coral-associated bacteria. J Appl Microbiol 129:1441–1457. https://doi.org/10.1111/jam.14766.
38. Raimundo I, Silva SG, Costa R, Keller-Costa T. 2018. Bioactive secondary metabolites from octocoral-associated microbes—new chances for blue growth. Mar Drugs 16:485. https://doi.org/10.3390/md16120485.
39. Disalvo LH. 1969. Isolation of bacteria from the corallum of Porites lobata (Vaughn) and its possible significance. Integr Comp Biol 9:735–740. https://doi.org/10.1093/icb/9.3.735.
40. Ducklow HW, Mitchell R. 1979. Bacterial populations and adaptations in the mucus layers on living corals. Limnol Oceanogr 24:715–725. https://doi.org/10.4319/lo.1979.24.4.0715.
41. Aronson RB, Precht WF. 2001. White band diseases and the changing face of Caribbean coral reefs. Hydrobiologia 460:25–38. https://doi.org/10.1023/A:1013103928980.
42. Peters EC, Oprandy JJ, Yevich PP. 1983. Possible causal agent of "white band disease" in caribbean acroporid corals. J Invertebr Pathol 41:394–396. https://doi.org/10.1016/0022-2011(83)90260-4.
43. Chet I, Mitchell R. 1976. Ecological aspects of microbial chemotactic behavior. Annu Rev Microbiol 30:221–239. https://doi.org/10.1146/annurev.mi.30.100176.001253.
44. Antonius A. 1981. Coral reef pathology: a review, p 3–14. *In* Proceedings of the 4th International Coral Reef Symposium. University of the Philippines, Manila, Philippines.
45. Kushmaro A, Rosenberg E, Fine M, Loya Y. 1997. Bleaching of the coral Oculina patagonica by Vibrio AK-1. Mar Ecol Prog Ser 147:159–165. https://doi.org/10.3354/meps147159.
46. Rozenblat YB-H, Rosenberg E. 2004. Temperature-regulated bleaching and tissue lysis of Pocillopora damicornis by the novel pathogen Vibrio

coralliilyticus, p 301–324. In Coral health and disease. Springer, Berlin, Germany.
47. Vidal-Dupiol J, Ladrière O, Meistertzheim AL, Fouré L, Adjeroud M, Mitta G. 2011. Physiological responses of the scleractinian coral Pocillopora damicornis to bacterial stress from Vibrio coralliilyticus. J Exp Biol 214:1533–1545. https://doi.org/10.1242/jeb.053165.
48. Ushijima B, Videau P, Burger AH, Shore-Maggio A, Runyon CM, Sudek M, Aeby GS, Callahan SM. 2014. Vibrio coralliilyticus strain OCN008 is an etiological agent of acute Montipora white syndrome. Appl Environ Microbiol 80:2102–2109. https://doi.org/10.1128/AEM.03463-13.
49. Rädecker N, Pogoreutz C, Gegner HM, Cárdenas A, Roth F, Bougoure J, Guagliardo P, Wild C, Pernice M, Raina JB, Meibom A, Voolstra CR. 2021. Heat stress destabilizes symbiotic nutrient cycling in corals. Proc Natl Acad Sci U S A 118:e2022653118. https://doi.org/10.1073/pnas.2022653118.
50. Bourne DG, Garren M, Work TM, Rosenberg E, Smith GW, Harvell CD. 2009. Microbial disease and the coral holobiont. Trends Microbiol 17:554–562. https://doi.org/10.1016/j.tim.2009.09.004.
51. Reshef L, Koren O, Loya Y, Zilber-Rosenberg I, Rosenberg E. 2006. The coral probiotic hypothesis. Environ Microbiol 8:2068–2073. https://doi.org/10.1111/j.1462-2920.2006.01148.x.
52. Rosenberg E, Koren O, Reshef L, Efrony R, Zilber-Rosenberg I. 2007. The role of microorganisms in coral health, disease and evolution. Nat Rev Microbiol 5:355–362. https://doi.org/10.1038/nrmicro1635.
53. Rosado PM, Leite DCA, Duarte GAS, Chaloub RM, Jospin G, Nunes da Rocha U, Saraiva JP, Dini-Andreote F, Eisen JA, Bourne DG, Peixoto RS. 2019. Marine probiotics: increasing coral resistance to bleaching through microbiome manipulation. ISME J 13:921–936. https://doi.org/10.1038/s41396-018-0323-6.
54. Voolstra CR, Ziegler M. 2020. Adapting with microbial help: microbiome flexibility facilitates rapid responses to environmental change. BioEssays 42:2000004. https://doi.org/10.1002/bies.202000004.
55. Ritchie KB. 2006. Regulation of microbial populations by coral surface mucus and mucus-associated bacteria. Mar Ecol Prog Ser 322:1–14. https://doi.org/10.3354/meps322001.
56. Shnit-Orland M, Kushmaro A. 2009. Coral mucus-associated bacteria: a possible first line of defense. FEMS Microbiol Ecol 67:371–380. https://doi.org/10.1111/j.1574-6941.2008.00644.x.
57. Kuek FWI, Lim LF, Ngu LH, Mujahid A, Lim PT, Leaw CP, Müller M. 2015. The potential roles of bacterial communities in coral defence: a case study at Talang-talang reef. Ocean Sci J 50:269–282. https://doi.org/10.1007/s12601-015-0024-2.
58. Romano S. 2018. Ecology and biotechnological potential of bacteria belonging to the genus Pseudovibrio. Appl Environ Microbiol 84:e02516-17. https://doi.org/10.1128/AEM.02516-17.
59. Hinger I, Ansorge R, Mussmann M, Romano S. 2020. Phylogenomic analyses of members of the widespread marine heterotrophic genus Pseudovibrio suggest distinct evolutionary trajectories and a novel genus, Polycladidibacter gen. nov. Appl Environ Microbiol 86:e02395-19. https://doi.org/10.1128/AEM.02395-19.
60. Work T, Meteyer C. 2014. To understand coral disease, look at coral cells. Ecohealth 11:610–618. https://doi.org/10.1007/s10393-014-0931-1.
61. Peixoto RS, Sweet M, Bourne DG. 2019. Customized medicine for corals. Front Mar Sci 6:686. https://doi.org/10.3389/fmars.2019.00686.
62. Peixoto RS, Rosado PM, Leite D. C d A, Rosado AS, Bourne DG. 2017. Beneficial Microorganisms for Corals (BMC): proposed mechanisms for coral health and resilience. Front Microbiol 8:341. https://doi.org/10.3389/fmicb.2017.00341.
63. Peixoto R, Sweet M, Villela HDM, Cardoso PM, Thomas T, Voolstra CR, Hoj L, Bourne DG. 2021. Coral probiotics: premise, promise, prospects. Annu Rev Anim Biosci 9:265–288. https://doi.org/10.1146/annurev-animal-090120-115444.
64. Nguyen MTHD, Liu M, Thomas T. 2014. Ankyrin-repeat proteins from sponge symbionts modulate amoebal phagocytosis. Mol Ecol 23:1635–1645. https://doi.org/10.1111/mec.12384.
65. Karimi E, Ramos M, Gonçalves JMS, Xavier JR, Reis MP, Costa R. 2017. Comparative metagenomics reveals the distinctive adaptive features of the Spongia officinalis endosymbiotic consortium. Front Microbiol 8:2499. https://doi.org/10.3389/fmicb.2017.02499.
66. Li J, Mahajan A, Tsai MD. 2006. Ankyrin repeat: a unique motif mediating protein-protein interactions. Biochemistry 45:15168–15178. https://doi.org/10.1021/bi062188q.
67. Lamb JR, Tugendreich S, Hieter P. 1995. Tetratrico peptide repeat interactions: to TPR or not to TPR? Trends Biochem Sci 20:257–259. https://doi.org/10.1016/S0968-0004(00)89037-4.
68. Goebl M, Yanagida M. 1991. The TPR snap helix: a novel protein repeat motif from mitosis to transcription. Trends Biochem Sci 16:173–177. https://doi.org/10.1016/0968-0004(91)90070-c.
69. Li D, Roberts R. 2001. WD-repeat proteins: structure characteristics, biological function, and their involvement in human diseases. Cell Mol Life Sci 58:2085–2097. https://doi.org/10.1007/pl00000838.
70. Jahn MT, Arkhipova K, Markert SM, Stigloher C, Lachnit T, Pita L, Kupczok A, Ribes M, Stengel ST, Rosenstiel P, Dutilh BE, Hentschel U. 2019. A phage protein aids bacterial symbionts in eukaryote immune evasion. Cell Host Microbe 26:542–550.e5. https://doi.org/10.1016/j.chom.2019.08.019.
71. Karimi E, Slaby BM, Soares AR, Blom J, Hentschel U, Costa R. 2018. Metagenomic binning reveals versatile nutrient cycling and distinct adaptive features in alphaproteobacterial symbionts of marine sponges. FEMS Microbiol Ecol https://doi.org/10.1093/femsec/fiy074.
72. Engelberts JP, Robbins SJ, de Goeij JM, Aranda M, Bell SC, Webster NS. 2020. Characterization of a sponge microbiome using an integrative genome-centric approach. ISME J 14:1100–1110. https://doi.org/10.1038/s41396-020-0591-9.
73. Botté ES, Nielsen S, Abdul Wahab MA, Webster J, Robbins S, Thomas T, Webster NS. 2019. Changes in the metabolic potential of the sponge microbiome under ocean acidification. Nat Commun 10:4134. https://doi.org/10.1038/s41467-019-12156-y.
74. Stringlis IA, Zamioudis C, Berendsen RL, Bakker PAHM, Pieterse CMJ. 2019. Type III secretion system of beneficial rhizobacteria Pseudomonas simiae WCS417 and Pseudomonas defensor WCS374. Front Microbiol 10:1631. https://doi.org/10.3389/fmicb.2019.01631.
75. Juhas M, Crook DW, Hood DW. 2008. Type IV secretion systems: tools of bacterial horizontal gene transfer and virulence. Cell Microbiol 10:2377–2386. https://doi.org/10.1111/j.1462-5822.2008.01187.x.
76. Lin L, Lezan E, Schmidt A, Basler M. 2019. Abundance of bacterial Type VI secretion system components measured by targeted proteomics. Nat Commun 10:2584. https://doi.org/10.1038/s41467-019-10466-9.
77. Cianciotto NP, White RC. 2017. Expanding role of type II secretion in bacterial pathogenesis and beyond. Infect Immun 85:e00014-17. https://doi.org/10.1128/IAI.00014-17.
78. Schöner TA, Gassel S, Osawa A, Tobias NJ, Okuno Y, Sakakibara Y, Shindo K, Sandmann G, Bode HB. 2016. Aryl polyenes, a highly abundant class of bacterial natural products, are functionally related to antioxidative carotenoids. Chembiochem 17:247–253. https://doi.org/10.1002/cbic.201500474.
79. Singh RP, Kothari R, Egan S. 2017. Exploring the complexity of macroalgal-bacterial interactions through interkingdom signalling system, p 301–315. *In* Systems biology of marine ecosystems. Springer, Berlin, Germany.
80. Sztajer H, Szafranski SP, Tomasch J, Reck M, Nimtz M, Rohde M, Wagner-Döbler I. 2014. Cross-feeding and interkingdom communication in dual-species biofilms of Streptococcus mutans and Candida albicans. ISME J 8:2256–2271. https://doi.org/10.1038/ismej.2014.73.
81. Santos H, Carmo FL, Duarte G, Dini-Andreote F, Castro CB, Rosado AS, Van Elsas JD, Peixoto RS. 2014. Climate change affects key nitrogen-fixing bacterial populations on coral reefs. ISME J 8:2272–2279. https://doi.org/10.1038/ismej.2014.70.
82. Welsh RM, Rosales SM, Zaneveld JR, Payet JP, Mcminds R, Hubbs SL, Thurber RLV. 2017. Alien vs. predator: bacterial challenge alters coral microbiomes unless controlled by Halobacteriovorax predators. PeerJ 5:e3315. https://doi.org/10.7717/peerj.3315.
83. Blockley A, Elliott DR, Roberts AP, Sweet M. 2017. Symbiotic microbes from marine invertebrates: driving a new era of natural product drug discovery. Diversity 9:49. https://doi.org/10.3390/d9040049.
84. Nguyen-Kim H, Bouvier T, Bouvier C, Doan-Nhu H, Nguyen-Ngoc L, Rochelle-Newall E, Baudoux AC, Desnues C, Reynaud S, Ferrier-Pages C, Bettarel Y. 2014. High occurrence of viruses in the mucus layer of scleractinian corals. Environ Microbiol Rep 6:675–682. https://doi.org/10.1111/1758-2229.12185.
85. Reynolds D, Thomas T. 2016. Evolution and function of eukaryotic-like proteins from sponge symbionts. Mol Ecol 25:5242–5253. https://doi.org/10.1111/mec.13812.
86. Silva SG, Blom J, Keller-Costa T, Costa R. 2019. Comparative genomics reveals complex natural product biosynthesis capacities and carbon metabolism across host-associated and free-living Aquimarina (Bacteroidetes, Flavobacteriaceae) species. Environ Microbiol 21:4002–4019. https://doi.org/10.1111/1462-2920.14747.
87. Tandon K, Chiang PW, Chen WM, Tang SL. 2018. Draft genome sequence of Endozoicomonas acroporae strain Acr-14T, isolated from Acropora

coral. Genome Announc 6:e01576-17. https://doi.org/10.1128/genomeA.01576-17.
88. Roder C, Bayer T, Aranda M, Kruse M, Voolstra CR. 2015. Microbiome structure of the fungid coral Ctenactis echinata aligns with environmental differences. Mol Ecol 24:3501–3511. https://doi.org/10.1111/mec.13251.
89. Ziegler M, Grupstra CGB, Barreto MM, Eaton M, BaOmar J, Zubier K, Al-Sofyani A, Turki AJ, Ormond R, Voolstra CR. 2019. Coral bacterial community structure responds to environmental change in a host-specific manner. Nat Commun 10:3092. https://doi.org/10.1038/s41467-019-10969-5.
90. Shnit-Orland M, Sivan A, Kushmaro A. 2012. Antibacterial activity of Pseudoalteromonas in the coral holobiont. Microb Ecol 64:851–859. https://doi.org/10.1007/s00248-012-0086-y.
91. Ushijima B, Videau P, Poscablo D, Stengel JW, Beurmann S, Burger AH, Aeby GS, Callahan SM. 2016. Mutation of the toxR or mshA genes from Vibrio coralliilyticus strain OCN014 reduces infection of the coral Acropora cytherea. Environ Microbiol 18:4055–4067. https://doi.org/10.1111/1462-2920.13428.
92. Weynberg KD, Voolstra CR, Neave MJ, Buerger P, Van Oppen MJH. 2016. From cholera to corals: viruses as drivers of virulence in a major coral bacterial pathogen. Sci Rep 5:17889. https://doi.org/10.1038/srep17889.
93. Fang Z, Sampson SL, Warren RM, Gey Van Pittius NC, Newton-Foot M. 2015. Iron acquisition strategies in mycobacteria. Tuberculosis 95:123–130. https://doi.org/10.1016/j.tube.2015.01.004.
94. Isaac DT, Laguna RK, Valtz N, Isberg RR. 2015. MavN is a Legionella pneumophila vacuole-associated protein required for efficient iron acquisition during intracellular growth. Proc Natl Acad Sci U S A 112:E5208–E5217. https://doi.org/10.1073/pnas.1511389112.
95. Holmstrom C, Kjelleberg S. 2006. Marine Pseudoalteromonas species are associated with higher organisms and produce biologically active extracellular agents. FEMS Microbiol Ecol 30:285–293. https://doi.org/10.1111/j.1574-6941.1999.tb00656.x.
96. Tebben J, Tapiolas DM, Motti CA, Abrego D, Negri AP, Blackall LL, Steinberg PD, Harder T. 2011. Induction of larval metamorphosis of the coral Acropora millepora by tetrabromopyrrole isolated from a Pseudoalteromonas bacterium. PLoS One 6:e19082. https://doi.org/10.1371/journal.pone.0019082.
97. Sneed JM, Sharp KH, Ritchie KB, Paul VJ. 2014. The chemical cue tetrabromopyrrole from a biofilm bacterium induces settlement of multiple Caribbean corals. Proc R Soc B 281:20133086. https://doi.org/10.1098/rspb.2013.3086.
98. Eichhorn E, Van Der Ploeg JR, Kertesz MA, Leisinger T. 1997. Characterization of α-ketoglutarate-dependent taurine dioxygenase from Escherichia coli. J Biol Chem 272:23031–23036. https://doi.org/10.1074/jbc.272.37.23031.
99. Desriac F, Defer D, Bourgougnon N, Brillet B, Le Chevalier P, Fleury Y. 2010. Bacteriocin as weapons in the marine animal-associated bacteria warfare: inventory and potential applications as an aquaculture probiotic. Mar Drugs 8:1153–1177. https://doi.org/10.3390/md8041153.
100. Hols P, Ledesma-García L, Gabant P, Mignolet J. 2019. Mobilization of microbiota commensals and their bacteriocins for therapeutics. Trends Microbiol 27:690–702. https://doi.org/10.1016/j.tim.2019.03.007.
101. Cimermancic P, Medema MH, Claesen J, Kurita K, Wieland Brown LC, Mavrommatis K, Pati A, Godfrey PA, Koehrsen M, Clardy J, Birren BW, Takano E, Sali A, Linington RG, Fischbach MA. 2014. Insights into secondary metabolism from a global analysis of prokaryotic biosynthetic gene clusters. Cell 158:412–421. https://doi.org/10.1016/j.cell.2014.06.034.
102. Jaspers C, Fraune S, Arnold AE, Miller DJ, Bosch TCG, Voolstra CR. 2019. Resolving structure and function of metaorganisms through a holistic framework combining reductionist and integrative approaches. Zoology (Jena) 133:81–87. https://doi.org/10.1016/j.zool.2019.02.007.
103. Schloss PD, Westcott SL, Ryabin T, Hall JR, Hartmann M, Hollister EB, Lesniewski RA, Oakley BB, Parks DH, Robinson CJ, Sahl JW, Stres B, Thallinger GG, Van Horn DJ, Weber CF. 2009. Introducing mothur: open-source, platform-independent, community-supported software for describing and comparing microbial communities. Appl Environ Microbiol 75:7537–7541. https://doi.org/10.1128/AEM.01541-09.
104. Quast C, Pruesse E, Yilmaz P, Gerken J, Schweer T, Yarza P, Peplies J, Glöckner FO. 2013. The SILVA ribosomal RNA gene database project: improved data processing and web-based tools. Nucleic Acids Res 41:D590–D596. https://doi.org/10.1093/nar/gks1219.
105. Evans J, Sheneman L, Foster J. 2006. Relaxed neighbor joining: a fast distance-based phylogenetic tree construction method. J Mol Evol 62:785–792. https://doi.org/10.1007/s00239-005-0176-2.
106. Saitou N, Nei M. 1987. The neighbor-joining method: a new method for reconstructing phylogenetic trees. Mol Biol Evol 4:406–425. https://doi.org/10.1093/oxfordjournals.molbev.a040454.
107. Sayers EW, Barrett T, Benson DA, Bryant SH, Canese K, Chetvernin V, Church DM, Dicuccio M, Edgar R, Federhen S, Feolo M, Geer LY, Helmberg W, Kapustin Y, Landsman D, Lipman DJ, Madden TL, Maglott DR, Miller V, Mizrachi L, Ostell J, Pruitt KD, Schuler GD, Sequeira E, Sherry ST, Shumway M, Sirotkin K, Souvorov A, Starchenko G, Tatusova TA, Wagner L, Yaschenko E, Ye J. 2009. Database resources of the National Center for Biotechnology Information. Nucleic Acids Res 37:D5–D15. https://doi.org/10.1093/nar/gkn741.
108. Letunic I, Bork P. 2019. Interactive Tree Of Life (iTOL) v4: recent updates and new developments. Nucleic Acids Res 47:W256–W259. https://doi.org/10.1093/nar/gkz239.
109. Chen IMA, Chu K, Palaniappan K, Pillay M, Ratner A, Huang J, Huntemann M, Varghese N, White JR, Seshadri R, Smirnova T, Kirton E, Jungbluth SP, Woyke T, Eloe-Fadrosh EA, Ivanova NN, Kyrpides NC. 2019. IMG/M v.5.0: an integrated data management and comparative analysis system for microbial genomes and microbiomes. Nucleic Acids Res 47:D666–D677. https://doi.org/10.1093/nar/gky901.
110. Overbeek R, Olson R, Pusch GD, Olsen GJ, Davis JJ, Disz T, Edwards RA, Gerdes S, Parrello B, Shukla M, Vonstein V, Wattam AR, Xia F, Stevens R. 2014. The SEED and the Rapid Annotation of microbial genomes using Subsystems Technology (RAST). Nucleic Acids Res 42:D206–D214. https://doi.org/10.1093/nar/gkt1226.
111. Wu S, Zhu Z, Fu L, Niu B, Li W. 2011. WebMGA: a customizable web server for fast metagenomic sequence analysis. BMC Genomics 12:444. https://doi.org/10.1186/1471-2164-12-444.
112. Hammer Ø, Harper DAT, Ryan PD. 2001. Past: paleontological statistics software package for education and data analysis. Palaeontol Electron 4:178.
113. Blin K, Shaw S, Steinke K, Villebro R, Ziemert N, Lee SY, Medema MH, Weber T. 2019. AntiSMASH 5.0: updates to the secondary metabolite genome mining pipeline. Nucleic Acids Res 47:W81–W87. https://doi.org/10.1093/nar/gkz310.